

1

Project	IEEE 802.16 Broadband Wireless Access Working Group < http://ieee802.org/16 >	
Title	IEEE 802.16m Evaluation Methodology Document (EMD)	
Date Submitted	2009-01-15	
Source(s)	Editor: Roshni Srinivasan, Intel Corporation roshni.m.srinivasan@intel.com Jeff Zhuang, Motorola (Section 3) jeff.zhuang@motorola.com Louay Jalloul, Beceem Communications (Section 4) jalloul@beceem.com Robert Novak, Nortel Networks (Section 5,6,7,8) rnovak@nortel.com Jeongho Park, Samsung Electronics (Section 10) jeongho.jh.park@samsung.com	
Re:	Evaluation Methodology for P802.16m-Advanced Air Interface	
Abstract	This document is the approved baseline 802.16m Evaluation Methodology. As directed by TGm, this document is a revision to IEEE 802.16m-08/004r4 according to the comment resolution conducted by TGm in Session #59.	
Purpose	Revised evaluation methodology for the P802.16m draft.	
Notice	<i>This document does not represent the agreed views of the IEEE 802.16 Working Group or any of its subgroups.</i> It represents only the views of the participants listed in the “Source(s)” field above. It is offered as a basis for discussion. It is not binding on the contributor(s), who reserve(s) the right to add, amend or withdraw material contained herein.	
Release	The contributor grants a free, irrevocable license to the IEEE to incorporate material contained in this contribution, and any modifications thereof, in the creation of an IEEE Standards publication; to copyright in the IEEE’s name any IEEE Standards publication even though it may include portions of this contribution; and at the IEEE’s sole discretion to permit others to reproduce in whole or in part the resulting IEEE Standards publication. The contributor also acknowledges and accepts that this contribution may be made public by IEEE 802.16.	
Patent Policy	The contributor is familiar with the IEEE-SA Patent Policy and Procedures: < http://standards.ieee.org/guides/bylaws/sect6-7.html#6 > and < http://standards.ieee.org/guides/opman/sect6.html#6.3 >. Further information is located at < http://standards.ieee.org/board/pat/pat-material.html > and < http://standards.ieee.org/board/pat >.	

Table of Contents

1	1.	Introduction.....	21
2	2.	System Simulation Requirements	22
3	2.1.	Antenna Characteristics	22
4	2.1.1.	BS Antenna	22
5	2.1.1.1.	BS Antenna Pattern	22
6	2.1.1.2.	BS Antenna Orientation	23
7	2.1.2.	MS Antenna	23
8	2.2.	Simulation Assumptions.....	24
9	2.3.	Test Scenarios	27
10	2.4.	Reference System Calibration	29
11	2.4.1.	Base Station Model.....	29
12	2.4.2.	Mobile Station Model	30
13	2.4.3.	OFDMA Parameters	30
14	3.	Channel Models.....	31
15	3.1.	Introduction	31
16	3.1.1.	General Considerations (Informative).....	32
17	3.1.2.	Overview of Channel Modeling Methodology (Informative).....	32
18	3.1.3.	Calibration Model (Informative)	34
19	3.1.4.	System Level Channel Modeling Considerations (Informative).....	35
20	3.2.	System Level Channel Model	36
21	3.2.1.	Spatial Channel Modeling.....	37
22	3.2.2.	Radio Environment and Propagation Scenarios	38
23	3.2.3.	Path Loss.....	39
24	3.2.3.1.	Urban Macrocell (Optional).....	40
25	3.2.3.2.	Suburban Macrocell (Optional).....	40
26	3.2.3.3.	Urban Microcell (Optional).....	40
27	3.2.3.4.	Indoor Small Office (Optional)	42
28	3.2.3.5.	Indoor Hot Spot (Optional).....	42
29	3.2.3.6.	Outdoor to Indoor (Optional).....	42
30	3.2.3.7.	Open Rural Macrocell (Optional).....	43
31	3.2.3.8.	Path Loss Model for Baseline Test Scenario (Mandatory)	43
32	3.2.4.	Shadowing Factor.....	44
33	3.2.5.	Cluster-Delay-Line Models	45
34	3.2.5.1.	Urban Macrocell (Optional).....	47
35	3.2.5.2.	Suburban Macrocell (Optional).....	48
36	3.2.5.3.	Urban Microcell (Optional).....	49
37	3.2.5.4.	Indoor Small Office (Optional)	50
38	3.2.5.5.	Indoor Hotspot (Optional)	50
39	3.2.5.6.	Outdoor to Indoor (Optional).....	52
40	3.2.5.7.	Rural Macrocell (Optional).....	52
41	3.2.6.	Channel Type and Velocity Mix	53
42	3.2.7.	Doppler Spectrum for Stationary Users.....	53
43	3.2.8.	Generation of Spatial Channels.....	53
44	3.2.9.	Channel Model for Baseline Test Scenario (Mandatory).....	58
45	3.3.	Link Level Channel Model.....	60
46	3.3.1.	Link Level Channel Model for Baseline MBSFN Test Scenario (Mandatory).....	61
47	4.	Link-to-System Mapping.....	65
48	4.1.	Background of PHY Abstraction	65
49	4.2.	Dynamic PHY Abstraction Methodology	65
50	4.3.	Mutual Information Based Effective SINR Mapping.....	67
51	4.3.1.	Received Bit Mutual Information Rate (RBIR) ESM (Mandatory).....	68
52	4.3.1.1.	RBIR Mapping for a SISO/SIMO System	68
53	4.3.1.2.	RBIR Mapping for a Linear MIMO Receiver	70

1	4.3.1.3.	RBIR Mapping for the Maximum-Likelihood (ML) MIMO Receiver	70
2	4.3.2.	Mean Mutual Information per Bit (MMIB) ESM	74
3	4.3.2.1.	MIB Mapping for SISO Systems	75
4	4.3.2.2.	MIMO Receiver Abstraction	79
5	4.3.2.3.	MIMO ML Receiver Abstraction	80
6	4.3.3.	Exponential ESM (EESM)	81
7	4.4.	Per-tone SINR Computation	82
8	4.4.1.	Per-tone Post Processing SINR for SISO	82
9	4.4.2.	Per-tone Post Processing SINR for SIMO with MRC	82
10	4.4.3.	Per-tone Post Processing SINR for MIMO STBC with MRC	83
11	4.4.4.	Per-Tone Post Processing SINR Calculation for Spatial Multiplexing	85
12	4.4.5.	Interference Aware PHY Abstraction	86
13	4.4.6.	Practical Transmitter/Receiver Impairments	86
14	4.4.7.	Channel Estimation Errors	86
15	4.4.7.1.	SISO Channel Estimation Error Modeling	87
16	4.4.7.2.	SIMO Channel Estimation Error Modeling	87
17	4.4.7.3.	2x2 MIMO Channel Estimation Error Modeling	88
18	4.4.8.	Interference Unaware Modeling	89
19	4.4.9.	Error Vector Magnitude	90
20	4.5.	Deriving Packet Error Rate from Block Error Rate	91
21	4.6.	PHY Abstraction for H-ARQ	91
22	4.6.1.	Baseline Modeling for HARQ	91
23	4.6.2.	Chase Combining	91
24	4.6.3.	Incremental Redundancy (IR)	92
25	4.7.	PHY Abstraction for Repetition Coding	94
26	5.	Link Adaptation	94
27	5.1.	Adaptive Modulation and Coding	94
28	5.1.1.	Link Adaptation with HARQ	94
29	5.2.	Channel Quality Feedback	95
30	5.2.1.	Channel Quality Feedback Delay and Availability	95
31	5.2.2.	Channel Quality Feedback Error	95
32	6.	HARQ	95
33	6.1.	HARQ Acknowledgement	96
34	7.	Scheduling	96
35	7.1.	DL Scheduler	97
36	7.2.	UL Scheduler	97
37	8.	Handover	97
38	8.1.	System Simulation with Mobility	97
39	8.1.1.	Single Moving MS Model	98
40	8.1.1.1.	Trajectories	98
41	8.1.1.1.1.	Trajectory 1	98
42	8.1.1.1.2.	Trajectory 2	98
43	8.1.1.1.3.	Trajectory 3	99
44	8.1.1.2.	10 Cell Topology	100
45	8.1.1.3.	Handover Evaluation Procedure	100
46	8.1.2.	Multiple Moving MS Model	101
47	8.1.2.1.	Trajectories	101
48	8.1.2.2.	19 Cell Topology	102
49	8.1.2.3.	Handover Evaluation Procedure	102
50	8.2.	Handover Performance Metrics	102
51	8.2.1.	Radio Layer Latency	103
52	8.2.2.	Network Entry and Connection Setup Time	103
53	8.2.3.	Handover Interruption Time	103
54	8.2.4.	Data Loss	104
55	8.2.5.	Handover Failure Rate	104
56	9.	Power Management (Informative)	104

1	9.1.	Formulation for IDLE to ACTIVE_STATE Transition Latency.....	104
2	9.1.1.	Device-initiated IDLE to ACTIVE_STATE Transition	105
3	9.1.2.	Network-initiated IDLE to ACTIVE_STATE Transition	105
4	9.1.3.	IDLE to ACTIVE_STATE Transition Latency.....	105
5	9.2.	Procedure for Evaluation of IDLE to ACTIVE_STATE Transition Latency	105
6	10.	Traffic Models.....	106
7	10.1.	Web Browsing (HTTP) Traffic Model	107
8	10.1.1.	HTTP and TCP Interactions for DL HTTP Traffic	110
9	10.1.2.	HTTP and TCP Interactions for UL HTTP Traffic	110
10	10.2.	File Transfer Protocol Model	110
11	10.3.	Speech Source Model (VoIP)	112
12	10.3.1.	Basic Voice Model	112
13	10.3.2.	VoIP Traffic Model Parameters	115
14	10.4.	Near Real Time Video Streaming Model	116
15	10.5.	Video Telephony Model	118
16	10.6.	Gaming Traffic Model.....	119
17	10.7.	Email Traffic Model	120
18	10.8.	Traffic Mixes.....	122
19	11.	Simulation Procedure and Flow	123
20	12.	Interference Modeling	124
21	13.	Performance Metrics	125
22	13.1.	Introduction	125
23	13.1.1.	Single User Performance Metrics	125
24	13.1.1.1.	Link Budget and Coverage Range (Noise Limited) - Single-Cell Consideration.....	125
25	13.1.1.2.	SINR Coverage – Interference Limited Multi-cell Consideration.....	128
26	13.1.1.3.	Data Rate Coverage – Interference Limited Multi-cell Consideration	128
27	13.1.2.	Multi-User Performance Metrics	128
28	13.2.	Definitions of Performance Metrics	129
29	13.2.1.	Throughput Performance Metrics	129
30	13.2.1.1.	Average Data Throughput for User u	130
31	13.2.1.2.	Average Per-User Data Throughput	130
32	13.2.1.3.	Sector Data Throughput.....	130
33	13.2.1.4.	Average Packet Call Throughput for User u	130
34	13.2.1.5.	Average Per-User Packet Call Throughput.....	131
35	13.2.1.6.	The Histogram of Users' Average Packet Call Throughput	131
36	13.2.1.7.	Throughput Outage	131
37	13.2.1.8.	Cell Edge User Throughput.....	131
38	13.2.2.	Performance Metrics for Delay Sensitive Applications	131
39	13.2.2.1.	Packet Delay	131
40	13.2.2.2.	The CDF of Packet Delay per User.....	131
41	13.2.2.3.	X%-tile Packet delay per User.....	132
42	13.2.2.4.	The CDF of X%-tile Packet Delays	132
43	13.2.2.5.	The Y%-tile of X%-tile Packet Delays	132
44	13.2.2.6.	User Average Packet Delay	132
45	13.2.2.7.	CDF of Users' Average Packet Delay	132
46	13.2.2.8.	Packet Loss Ratio	132
47	13.2.3.	System Level Metrics for Unicast Transmission.....	132
48	13.2.3.1.	System Data Throughput	132
49	13.2.3.2.	Spectral Efficiency	133
50	13.2.3.3.	CDF of SINR.....	133
51	13.2.3.4.	Histogram of MCS	133
52	13.2.3.5.	Application Capacity	133
53	13.2.3.6.	System Outage.....	134
54	13.2.3.7.	Coverage and Capacity Trade-off Plot.....	134
55	13.2.4.	System Level Metrics for Multicast Broadcast Service.....	134
56	13.2.4.1.	Maximum MBS Data Rate.....	134

1	13.2.4.2.	Coverage versus Data Rate Trade-off	134
2	13.2.4.3.	Impact of Multicast/Broadcast Resource Size on Unicast Throughput	134
3	13.3.	Fairness Criteria	134
4	13.3.1.	Moderately Fair Solution	135
5	13.3.2.	Short Term Fairness Indication	135
6	14.	Relay Evaluation Methodology	135
7	14.1.	Test Scenarios	136
8	14.1.1.	Above Rooftop RS Scenario	136
9	14.1.1.1.	Two Relays per Sector Scenario	137
10	14.1.2.	Below Rooftop RS Scenario	138
11	14.1.3.	Manhattan deployment scenario	140
12	14.2.	Basic Parameters	143
13	14.3.	Channel Models	146
14	14.3.1.	Pathloss Models	146
15	14.3.1.1.	ART RS Scenario	146
16	14.3.1.1.1.	BS-MS and RS-MS links	146
17	14.3.1.1.2.	BS-RS and RS-RS links	146
18	14.3.1.2.	BRT RS Scenario	147
19	14.3.1.2.1.	BS-MS link	148
20	14.3.1.2.2.	BS-RS link	148
21	14.3.1.2.3.	RS-MS link	149
22	14.3.1.2.4.	RS-RS link	150
23	14.3.1.2.5.	Comparison of Pathloss Models	150
24	14.3.1.3.	Manhattan deployment scenario (optional)	151
25	14.3.1.3.1.	BS-MS and RS-MS links	152
26	14.3.1.3.2.	BS-RS and RS-RS links	152
27	14.3.2.	Spatial channel models	152
28	14.3.2.1.	ART RS scenario	152
29	14.3.2.1.1.	BS-MS and RS-MS links	153
30	14.3.2.1.2.	BS-RS and RS-RS links	153
31	14.3.2.2.	BRT RS scenario	154
32	14.3.2.2.1.	BS-MS and RS-MS links	154
33	14.3.2.2.2.	RS-MS links	154
34	14.3.2.2.3.	RS-RS links	154
35	14.3.2.3.	Manhattan deployment scenario (optional)	154
36	14.3.2.3.1.	BS-MS and RS-MS links	155
37	14.3.2.3.2.	BS-RS and RS-RS links	155
38	14.3.3.	Shadowing models	155
39	14.3.4.	Summary	159
40	14.4.	Relaying Model	162
41	14.5.	Simulation Procedure and Flow	163
42	14.6.	MS Association	164
43	14.7.	Scheduling	164
44	14.7.1.	Frame partitioning	164
45	14.7.2.	Distributed scheduling	165
46	14.7.3.	Centralized scheduling	165
47	14.7.4.	Relay HARQ	165
48	14.8.	Performance metrics	165
49	14.8.1.	System performance metrics	166
50	14.8.1.1.	Spectral efficiency and aggregate sector throughput	166
51	14.8.1.2.	Combined coverage and capacity index	166
52	14.8.2.	Relay specific performance metrics	166
53	14.8.2.1.	Relay link overhead percentage	166
54	14.8.2.2.	Relay link average SE	167
55	14.8.2.3.	Relay link PER	167
56	15.	Template for Reporting Results	167

1	Appendix A: Spatial Correlation Calculation	169
2	Appendix B: Polarized Antenna	171
3	Appendix C: LOS Option with a K-factor	173
4	Appendix D: Antenna Gain Imbalance and Coupling	174
5	Appendix E: WINNER Primary Model Description	175
6	Appendix F: Generic Proportionally Fair Scheduler for OFDMA	177
7	Appendix G: 19 Cell Wrap Around Implementation	179
8	G-1. Multi-Cell Layout	179
9	G-2. Obtaining virtual MS locations	180
10	G-3. Determination of serving cell/sector for each MS in a wrap-around multi-cell network	180
11	Appendix H: Path Loss Calculations	182
12	Appendix I: Modeling Control Overhead and Signalling (Informative)	184
13	I-1. Overhead Channels	184
14	I-1.1. Dynamic Simulation of the Downlink Overhead Channels	184
15	I-1.2. Uplink Modeling in Downlink System Simulation	185
16	I-1.3. Signaling Errors	185
17	Appendix J: Transmit Power and EVM	186
18	Appendix K: TCP Modeling (Informative)	188
19	K-1. TCP Session Establishment and Release	188
20	K-2. TCP Slow Start Modeling	189
21	Appendix L: Trace Based Model for Streaming Video (Informative)	192
22	Appendix M: FCC Spectral Mask (Informative)	194
23	Appendix N: Per-tone Post Processing SINR for MISO and MIMO with CDD (Informative)	195
24	Appendix O: Updated HTTP Traffic Model (Informative)	196
25	Appendix P: Derivations and Details for RBIR Metric (Informative)	198
26	P-1. Derivation of the AVE and VAR for RBIR	198
27	P-2. Search for the Optimal 'a' Value	198
28	P-3. Search for the Optimal Values of p_1 and p_2	199

1	Index of Tables	
2	Table 1: System-level simulation assumptions for the downlink	25
3	Table 2: System-level simulation assumptions for the uplink	27
4	Table 3: Test scenarios	28
5	Table 4: BS equipment model	29
6	Table 5: MS equipment model	30
7	Table 6: OFDMA air interface parameters	31
8	Table 7: LOS probabilities for mixed LOS/NLOS scenario	41
9	Table 8: Standard deviation of shadow fading distribution	44
10	Table 9: Sub-cluster model used for some taps in spatial TDL or CDL model	47
11	Table 10: Urban macrocell CDL (XPR = 5 dB)	48
12	Table 11: Bad urban macrocell CDL (XPR = 5 dB)	48
13	Table 12: Suburban macrocell CDL (XPR = 5.5 dB)	49
14	Table 13: Urban microcell CDL (LOS) (XPR = 9.5 dB)	49
15	Table 14: Urban microcell CDL (NLOS) (XPR = 7.5 dB)	49
16	Table 15: Bad urban microcell CDL (NLOS) (XPR = 7.5 dB)	50
17	Table 16: Indoor small office (NLOS) (XPR = 10 dB)	50
18	Table 17: Indoor hotspot CDL (LOS) (XPR = 11dB)	51
19	Table 18: Indoor hotspot CDL (NLOS) (XPR = 11dB)	52
20	Table 19: Outdoor to indoor CDL (NLOS) (XPR = 8 dB)	52
21	Table 20: Rural macrocell CDL (LOS) (XPR = 7dB)	52
22	Table 21: Rural macrocell CDL (NLOS) (XPR = 7dB)	53
23	Table 22: ITU power delay profiles	59
24	Table 23: Modified ITU profiles for wideband systems	60
25	Table 24: MBSFN Channel Profiles for Wideband Systems	64
26	Table 25: SINR to RBIR mapping	69
27	Table 26: Mean and variance for symbol level LLR	72
28	Table 27: Values for parameter a	73
29	Table 28: Values of p_1 and p_2 for SM with Vertical Encoding	74
30	Table 29: Numerical approximations for MIB mappings	77
31	Table 30: Parameters for Gaussian cumulative approximation	79
32	Table 31: Numerical approximation for 16QAM 2x2 SM	81
33	Table 32: Numerical approximation for 64 QAM 2x2 SM	81
34	Table 33: Modes and parameters for channel estimation model*	89
35	Table 34: HTTP traffic parameters	109
36	Table 35: FTP traffic parameters	111
37	Table 36: Information on various vocoders	113
38	Table 37: VoIP packet calculation for AMR and G.729	115
39	Table 38: VoIP traffic model parameters specification	115
40	Table 39: Detailed description of the VoIP traffic model for IPv4	116
41	Table 40: Near real time video streaming traffic model parameters	118
42	Table 41: Video telephony traffic model	118
43	Table 42: FPS internet gaming traffic model	120
44	Table 43: Email traffic parameters	122
45	Table 44: Traffic mixes	123
46	Table 45: Link budget template	127
47	Table 46: Moderately fair criterion CDF	135
48	Table 47: Test Scenarios	143
49	Table 48: BS Equipment Model	144
50	Table 49: RS Equipment Model	146
51	Table 50: Pathloss models for the ART Relay Scenario	146
52	Table 51: Path loss models for BRT RS Scenario	148
53	Table 52: Pathloss models for the Manhattan deployment scenario	151
54	Table 53: Spatial channel models for the ART RS scenario	152
55	Table 54: WINNER B5a CDL channel model parameters	153

1	Table 55: WINNER B5a CDL channel model for clusters	153
2	Table 56: Spatial Channel Models for the BRT RS Scenario	154
3	Table 57: Spatial channel models for the Manhattan deployment scenario	154
4	Table 58: Shadowing standard deviation.....	156
5	Table 59: Correlation distance for shadowing.....	157
6	Table 60: Shadow fading correlation in ART RS scenario	157
7	Table 61: Shadow Fading Correlation in BRT RS Scenario	158
8	Table 62: Shadow fading correlation in the Manhattan deployment scenario.....	158
9	Table 63: Summary of pathloss and channel models	162
10	Table 64: Evaluation report.....	168
11	Table 65: Value of Δ_k	169
12	Table 66: Signaling errors.....	185
13	Table 67: Reference parameters for transmit power calibration	186
14	Table 68: MPEG4 video library	192
15	Table 69: FCC spectral mask.....	194
16	Table 70: HTTP parameters for updated model.	197

1	Index of Figures	
2	Figure 1 : Simulation components.....	21
3	Figure 2: Antenna pattern for 3-sector cells.....	22
4	Figure 3 : Antenna bearing orientation diagram.....	23
5	Figure 4: Geometry of street sections used for microcellular NLOS path loss model.....	41
6	Figure 5: Shadowing factor grid example showing interpolation.....	45
7	Figure 6: The MIMO channel model angle parameters.....	54
8	Figure 7: PHY link-to-system mapping procedure.....	66
9	Figure 8: Computational procedure for MIESM method.....	68
10	Figure 9: Bit Interleaved coded modulation system.....	75
11	Figure 10: BLER (\log_{10} scale) mappings for MMIB from AWGN performance results.....	79
12	Figure 11: PHY abstraction simulation procedure for average interference knowledge.....	90
13	Figure 12: ML-based parameter update after transmission.....	92
14	Figure 13: Trajectory 1.....	98
15	Figure 14: Trajectory 2.....	99
16	Figure 15: Trajectory 3.....	99
17	Figure 16: 10 Cell topology.....	100
18	Figure 17: 19 cell abbreviated example of MS movement in a wrap around topology *.....	102
19	Figure 18: HTTP traffic pattern.....	107
20	Figure 19: HTTP traffic profiles.....	110
21	Figure 20: FTP traffic patterns.....	111
22	Figure 21: FTP traffic profiles.....	112
23	Figure 22: Typical phone conversation profile.....	112
24	Figure 23: 2-state voice activity Markov model.....	113
25	Figure 24: Video streaming traffic model.....	116
26	Figure 25: Email traffic model.....	121
27	Figure 26: Throughput metrics measurement points.....	129
28	Figure 27: Above Rooftop RS Scenario.....	137
29	Figure 28: Cell structure for two ART RSs per sector.....	138
30	Figure 29: ART Deployment scenario with two RS & default RS placement angle (26^0).....	138
31	Figure 30: BRT RS Scenario.....	139
32	Figure 31: BRT RS Deployment Scenario.....	140
33	Figure 32: Manhattan deployment scenario propagation conditions.....	140
34	Figure 33: Manhattan deployment scenario with 1 BRT RS per sector.....	141
35	Figure 34: Manhattan deployment scenario with 2 BRT RSs per sector.....	142
36	Figure 35: Manhattan deployment scenario with 3 BRT RSs per sector.....	142
37	Figure 36: BRT RS Pathloss Models.....	151
38	Figure 37: Multi-cell layout and wrap around example.....	180
39	Figure 38: Antenna orientations for a sectorized system in wrap around simulation *.....	181
40	Figure 39: TCP connection establishment and release on the downlink.....	188
41	Figure 40: TCP connection establishment and release on the uplink.....	189
42	Figure 41: TCP slow start process.....	191

1 Abbreviations and Acronyms

2

3GPP	3G Partnership Project
3GPP2	3G Partnership Project 2
AAS	Adaptive Antenna System also Advanced Antenna System
ACK	Acknowledge
AES	Advanced Encryption Standard
AG	Absolute Grant
AMC	Adaptive Modulation and Coding
A-MIMO	Adaptive Multiple Input Multiple Output (Antenna)
AMS	Adaptive MIMO Switching
AoA	Angle of Arrival
AoD	Angle of Departure
ARQ	Automatic Repeat reQuest
ART	Above Rooftop
AS	Azimuth Spread
ASA	Azimuth Spread Arrival
ASD	Azimuth Spread Departure
ASN	Access Service Network
ASP	Application Service Provider
BE	Best Effort
BRT	Below Rooftop
CC	Chase Combining (also Convolutional Code)
CCI	Co-Channel Interference
CCM	Counter with Cipher-block chaining Message authentication code
CDF	Cumulative Distribution Function
CDL	Clustered Delay Line
CINR	Carrier to Interference + Noise Ratio
CMAC	block Cipher-based Message Authentication Code
CP	Cyclic Prefix
CQI	Channel Quality Indicator
CSN	Connectivity Service Network
CSTD	Cyclic Shift Transmit Diversity
CTC	Convolutional Turbo Code
DL	Downlink
DOCSIS	Data Over Cable Service Interface Specification
DSL	Digital Subscriber Line
DVB	Digital Video Broadcast
EAP	Extensible Authentication Protocol
EESM	Exponential Effective SIR Mapping
EIRP	Effective Isotropic Radiated Power
ErtVR	Extended Real-Time Variable Rate

EVM	Error Vector Magnitude
FBSS	Fast Base Station Switch
FCH	Frame Control Header
FDD	Frequency Division Duplex
FD-FDD	Full Duplex - Frequency Division Duplex
FFT	Fast Fourier Transform
FTP	File Transfer Protocol
FUSC	Fully Used Sub-Channel
HARQ	Hybrid Automatic Repeat reQuest
HD-FDD	Half Duplex – Frequency Division Duplex
HHO	Hard Handover
HMAC	keyed Hash Message Authentication Code
HO	Handover
HTTP	Hyper Text Transfer Protocol
IE	Information Element
IEFT	Internet Engineering Task Force
IFFT	Inverse Fast Fourier Transform
IR	Incremental Redundancy
ISI	Inter-Symbol Interference
LDPC	Low-Density-Parity-Check
LOS	Line of Sight
MAC	Media Access Control
MAI	Multiple Access Interference
MAN	Metropolitan Area Network
MAP	Media Access Protocol
MBS	Multicast and Broadcast Service
MCS	Modulation and Coding Scheme
MDHO	Macro Diversity Hand Over
MIMO	Multiple Input Multiple Output (Antenna)
MMS	Multimedia Message Service
MPC	Multipath Component
MPLS	Multi-Protocol Label Switching
MS	Mobile Station
MSO	Multi-Services Operator
NACK	Not Acknowledge
NAP	Network Access Provider
NLOS	Non Line-of-Sight
NRM	Network Reference Model
nrtPS	Non-Real-Time Polling Service
NSP	Network Service Provider
OFDM	Orthogonal Frequency Division Multiplex
OFDMA	Orthogonal Frequency Division Multiple Access

PER	Packet Error Rate
PF	Proportional Fair (Scheduler)
PKM	Public Key Management
PUSC	Partially Used Sub-Channel
QAM	Quadrature Amplitude Modulation
QPSK	Quadrature Phase Shift Keying
RG	Relative Grant
RMS	Root Mean Square
RR	Round Robin (Scheduler)
RRI	Reverse Rate Indicator
RS	Relay Station
RTG	Receive/transmit Transition Gap
rtPS	Real-Time Polling Service
RUIM	Removable User Identify Module
SCM	Spatial Channel Model
SDMA	Space (or Spatial) Division Multiple Access
SF	Spreading Factor
SN	Single Frequency Network
SGSN	Serving GPRS Support Node
SHO	Soft Handover
SIM	Subscriber Identify Module
SINR	Signal to Interference + Noise Ratio
SISO	Single Input Single Output (Antenna)
SLA	Service Level Agreement
SM	Spatial Multiplexing
SMS	Short Message Service
SNR	Signal to Noise Ratio
S-OFDMA	Scalable Orthogonal Frequency Division Multiple Access
SS	Subscriber Station
STC	Space Time Coding
TDD	Time Division Duplex
TDL	Tapped Delay Line
TEK	Traffic Encryption Key
TTG	Transmit/receive Transition Gap
TTI	Transmission Time Interval
TU	Typical Urban (as in channel model)
UE	User Equipment
UGS	Unsolicited Grant Service
UL	Uplink
UMTS	Universal Mobile Telephone System
VoIP	Voice over Internet Protocol
VPN	Virtual Private Network

VSF	Variable Spreading Factor
WiFi	Wireless Fidelity
WAP	Wireless Application Protocol
WiBro	Wireless Broadband (Service)
WiMAX	Worldwide Interoperability for Microwave Access

References

- [1] IST-4-027756 WINNER II, D 5.10.2, "Spectrum requirements for systems beyond IMT-2000", March 2007.
- [2] A. F. Molisch, "Wireless Communications", IEEE-Press Wiley, 2005.
- [3] V. Erceg, et al., "Channel models for fixed wireless applications", IEEE 802.16.3c-01/29r4, July 2001.
- [4] Recommendation ITU-R M.1225, "Guidelines for evaluation of radio transmission technologies for IMT-2000", 1997.
- [5] 3GPP-3GPP2 Spatial Channel Ad-hoc Group, "Spatial Channel Model Text Description," V7.0, August 2003.
- [6] 3GPP TR 25.996, "Spatial channel model for Multiple Input Multiple Output (MIMO) Simulations", June 2007.
- [7] G. Calcev, D. Chizhik, B. Goransson, S. Howard, H. Huang, A. Kogiantis, A. F. Molisch, A. L. Moustakas, D. Reed and H. Xu, "A Wideband Spatial Channel Model for System-Wide Simulations", IEEE Transactions Vehicular Technology, vol. 56, pp. 389-403, March 2007.
- [8] Daniel S. Baum et al, "An Interim Channel Model for Beyond-3G Systems – Extending the 3GPP Spatial Channel Model (SCM)", Proceedings of the IEEE VTC, May 2005.
- [9] A. F. Molisch, H. Asplund, R. Heddergott, M. Steinbauer, and T. Zwick, "The COST259 directional channel model – I. overview and methodology," IEEE Transactions on Wireless Communications, vol. 5, pp. 3421–3433, December 2006.
- [10] H. Asplund, A. A. Glazunov, A. F. Molisch, K. I. Pedersen, and M. Steinbauer, "The COST259 directional channel model II - macrocells," IEEE Transactions on Wireless Communications, vol. 5, pp. 3434–3450, December 2006.
- [11] L. Correia (ed.), "Flexible Personalized Wireless Communications", Wiley, 2001.
- [12] A. F. Molisch and H. Hofstetter, "The COST273 Channel Model," in "Mobile Broadband Multimedia Networks ", (L. Correia, ed.), Academic Press, 2006.
- [13] IST-WINNER II Deliverable D1.1.1 v1.0, "WINNER II Interim Channel Models", December 2006.
- [14] M. Steinbauer, A. F. Molisch, and E. Bonek, "The double-directional radio channel," IEEE Antennas and Propagation Magazine, pp. 51–63, August 2001.
- [15] G. J. Foschini and M. J. Gans, "On limits of wireless communications in a fading environment when using multiple antennas," Wireless Personal Communications, vol. 6, pp. 311–335, February 1998.
- [16] P. Almers, et al., "Survey of channel and radio propagation models for wireless MIMO systems," Eurasip Journal on Wireless Communication and Networking, January 2007.

- [17] T-S Chu, L.J. Greenstein, "A quantification of link budget differences between the cellular and PCS bands", IEEE Transactions on Vehicular Technology Vol. 48, No.1, pp. 60-65, January 1999.
- [18] "Digital mobile radio towards future generation systems", COST Action 231 Final Report, EUR 18957, 1999.
- [19] D. Parsons, "The Mobile Radio Propagation Channel", Chapter 4, pp. 88, Pentech Press, 1992.
- [20] Y. Oda, K. Tsunekawa, M. Hata, "Advanced LOS path-loss model in microcellular mobile communications", IEEE Trans AP-51, pp. 952-956, May 2003.
- [21] "Universal Mobile Telecommunications System (UMTS); Selection procedures for the choice of radio transmission technologies of the UMTS (UMTS 30.03 version 3.2.0)", ETSI technical report TR 101 112 v3.2.0, April 1998.
- [22] W.C. Jakes "Microwave mobile communications", Wiley, New York, 1974.
- [23] M. Patzold, "Mobile Fading Channels", John Wiley, 2002.
- [24] 3GPP, R1-061001, Ericsson, "LTE Channel Models and link simulations", March 2006.
- [25] Source code for a MATLAB/ANSI-C implementation of the WINNER Phase I Channel Model, https://www.ist-winner.org/phase_model.html, August 2006.
- [26] Y. Leiba, Y. Segal, Z. Hadad and I. Kitroser, "Coverage capacity simulations for OFDMA PHY in ITU-T channel models", IEEE C802.16d-03/78r1, November 2003.
- [27] Y. Leiba, I. Kitroser, Y. Segal and Z. Hadad, "Coverage simulation for OFDMA PHY mode", IEEE C802.16e-03/22r1, November 2003.
- [28] Sony, Intel, "TGn Sync TGn Proposal MAC Simulation Methodology", IEEE 802.11-04/895r2, November 2004.
- [29] A. Poloni, S. Valle, "Time Correlated Packet Errors in MAC Simulations", IEEE Contribution, 802.11-04-0064-00-000n, January 2004.
- [30] J. Gilbert et al., "Unified Black Box PHY Abstraction Methodology", IEEE 802.11-04/0218r1, March 2004.
- [31] 3GPP TR 25.892 V2.0.0 "Feasibility Study for OFDM for UTRAN enhancement", http://www.3gpp.org/ftp/tsg_ran/tsg_ran/TSGR_24/Docs/PDF/RP-040221.pdf, June 2004.
- [32] WG5 Evaluation Ad-hoc Group, "1x EV-DV Evaluation Methodology – Addendum (V6)," July 2001.
- [33] Ericsson, "System level evaluation of OFDM- further considerations", TSG-RAN WG1 #35, R1-031303, November 2003.
- [34] Nortel, "Effective SIR Computation for OFDM System-Level Simulations," TSG-RAN WG1 #35, R1-031370, November 2003.

- [35] Nortel, "OFDM Exponential Effective SIR Mapping Validation, EESM Simulation Results for System-Level Performance Evaluations," 3GPP TSG-RAN-1/TSG-RAN-4 Ad-Hoc, R1-040089, January 2004.
- [36] K. Brueninghaus et al., "Link performance models for system level simulations of broadband radio access," IEEE PIMRC, September 2005.
- [37] L. Wan, et al, "A fading insensitive performance metric for a unified link quality model" Proceedings of IEEE WCNC, Vol.4, pp. 2110-2114, April 2006.
- [38] DoCoMo, Ericsson, Fujitsu, Mitsubishi Electric, NEC, Panasonic, Sharp, Toshiba Corporation, "Link adaptation schemes for single antenna transmissions in the DL", 3GPP TSG-RAN WG1, R1-060987, March 2006.
- [39] G. Caire, "Bit-Interleaved Coded Modulation", IEEE Transactions on Information Theory, Vol. 44, No.3, May 1998.
- [40] J. Kim, et al., "Reverse Link Hybrid ARQ: Link Error Prediction Methodology Based on Convex Metric", Lucent Technologies, 3GPP2 TSG-C WG3 20030401-020, April 2003.
- [41] S. Tsai and A. Soong, "Effective-SNR Mapping for Modeling Frame Error Rates in Multiple-State Channels", 3GPP2-C30-20030429-010, April 2003.
- [42] IEEE P 802.20-PD-09 Version 1.0, "802.20 Evaluation Criteria – version 1.0," September 2005.
- [43] P. Barford and M. Crovella, "Generating Representative Web Workloads for Network and Server Performance Evaluation" In Proc. ACM SIGMETRICS International Conference on Measurement and Modeling of Computer Systems, pp. 151-160, July 1998.
- [44] S. Deng. "Empirical Model of WWW Document Arrivals at Access Link." In Proceedings of the 1996 IEEE International Conference on Communication, June 1996.
- [45] R. Fielding, J. Gettys, J. C. Mogul, H. Frystik, L. Masinter, P. Leach, and T. Berners-Lee, "Hypertext Transfer Protocol - HTTP/1.1", RFC 2616, HTTP Working Group, <ftp://ftp.ietf.org/rfc2616.txt>, June 1999.
- [46] B. Krishnamurthy and M. Arlitt, "PRO-COW: Protocol Compliance on the Web", Technical Report 990803-05-TM, AT&T Labs, <http://www.research.att.com/~bala/papers/procow-1.ps.gz>, August 1999.
- [47] B. Krishnamurthy and C. E. Wills, "Analyzing Factors That Influence End-to-End Web Performance", Computer Networks: The International Journal of Computer and Telecommunications Networking, Volume 33 , Issue 1-6, pp. 17-32, June 2000.
- [48] H. K. Choe, J. O. Limb, "A Behavioral Model of Web Traffic", Proceedings of the seventh International Conference on Network Protocols, 1999, pp. 327-334, November 1999.
- [49] F. D. Smith, F. H. Campos, K. Jeffay, D. Ott, "What TCP/IP Protocol Headers Can Tell Us About the Web", Proc. 2001 ACM SIGMETRICS International

- 1 Conference on Measurement and Modeling of Computer Systems, pp. 245-256,
2 June 2001.
- 3 [50] "cdma2000 Evaluation Methodology (V6)", 3GPP2/TSG-C30-20061204-062A
4 December 2006.
- 5 [51] J. Cao, W. S. Cleveland, D. Lin, D. X. Sun., "On the Non-stationarity of Internet
6 Traffic", Proc. ACM SIGMETRICS 2001, pp. 102-112, 2001.
- 7 [52] K. C. Claffy and S. McCreary, "Internet measurement and data analysis: passive
8 and active measurement", <http://www.caida.org/outreach/papers/Nae/4hansen.html>,
9 1999.
- 10 [53] "HTTP and FTP Traffic Model for 1xEV-DV Simulations", 3GPP2-TSGC5, 2001.
- 11 [54] "LTE physical layer framework for performance verification, Orange, China
12 Mobile", KPN, NTT DoCoMo, Sprint, T-Mobile, Vodafone, Telecom Italia, 3GPP
13 TSG-RAN1 #48 R1-070674, February 2007.
- 14 [55] WINNER Project, IST-2003-507581 WINNER D1.3 version 1.0, "Final usage
15 scenarios", June 2005.
- 16 [56] "User Equipment Radio Transmission and Reception (FDD)", 3GPP TS 25.101
17 v7.7.0, March 2007.
- 18 [57] Motorola, "Cubic Metric in 3GPP-LTE", 3GPP TSG RAN WG1, R1-060023,
19 January 2006.
- 20 [58] <http://www-tnk.ee.tu-berlin.de/research/trace/ltvt.html>.
- 21 [59] F. Fitzek and M. Reisslein, "MPEG-4 and H.263 traces for network performance
22 evaluation (extended version)", Technical Report TKN-00-06, Technical University
23 Berlin, Dept. of Electrical Eng., October 2000.
- 24 [60] W. R. Stevens, "TCP/IP Illustrated, Vol. 1", Addison-Wesley Professional
25 Computing Series, 1994.
- 26 [61] IEEE Std. 802.16-2004: IEEE Standard for Local and metropolitan area networks
27 – Part 16: Air Interface for Fixed Broadband Wireless Access Systems, June 2004.
- 28 [62] IEEE Std. 802.16e-2005, IEEE Standard for Local and metropolitan area
29 networks – Part 16: Air Interface for Fixed and Mobile Broadband Wireless Access
30 Systems – Amendment 2: Physical and Medium Access Control Layers for
31 Combined Fixed and Mobile Operation in Licensed Bands, and IEEE Std. 802.16-
32 2004/Cor1-2005, Corrigendum 1, December 2005.
- 33 [63] "Next Generation Mobile Networks Radio Access Performance Evaluation
34 Methodology", [www.Ngmn-cooperation.com/docs/NGMN_Evaluation_Methodology](http://www.Ngmn-cooperation.com/docs/NGMN_Evaluation_Methodology_V1.2.pdf)
35 V1.2.pdf, June 2007.
- 36 [64] FCC regulations: <http://www.hallikainen.com/FccRules/2007/27/53/>,
37 http://www.access.gpo.gov/nara/cfr/waisidx_06/47cfr27_06.html (see 27.53
38 emission limits), October 2007.
- 39 [65] UMTS Forum, 3G Offered Traffic Report, June 2003.

- [66] ITU-R M.2072, "World mobile telecommunication market forecast", November 2006.
- [67] B. H. Kim, and Y. Hur, "Application Traffic Model for WiMAX Simulation," POSDATA, Ltd., April 2007.
- [68] L. A. Dabbish, R. E. Kraut, S. Fussell and S. Kiesler, "Understanding Email Use: Predicting Action on a Message," Proceedings of the ACM Conference on Human Factors in Computing Systems (CHI'05), NY: ACM Press, pp.691-700, April 2005.
- [69] V. Bolotin, Y. Levy, and D. Liu," Characterizing Data Connection and Messages by Mixtures of Distributions on Logarithmic Scale", Proceedings of ITC '99, vol. 3a & 3b, pp. 887-894, June 1999.
- [70] G. Brasche and B. Walke, " Concepts Services, and Protocols of the New GSM Phase 2+ General Packet Radio Service, IEEE Communications Magazine, August 1997.
- [71] M. S. Borella," Source Models of Network Game Traffic", Computer Communications, 23 (4), pp. 403-410, February 2000.
- [72] P. Monogioudis and A. Kogiantis, "Wideband Extension of the ITU profiles with desired spaced-frequency correlation", IEEE C802.16m-07/181, September 2007.
- [73] L. Jalloul, "On the Expected Value of the Received Bit Information Rate", IEEE C802.16m-07/195, September 2007.
- [74] "Mobile WiMAX – Part 1: A Technical Overview and Performance Evaluation", WiMAX Forum, February, 2006.
- [75] B. Kim, "Application traffic model," http://www.flyvo.com/archive/Posdata-application_traffic_model.pdf, 2007.
- [76] "ComScore Media Metrix Releases January Top 50 Web Rankings and Analysis", <http://www.comscore.com/press/release.asp?press=1214>, February 2007.
- [77] H. Zheng et al., "Link Performance Abstraction for ML Receivers based on RBIR Metrics," IEEE C802.16m-08/119, March 2008.
- [78] K. Sayana et al., "Link Performance Abstraction based on Mean Mutual Information per Bit (MMIB) of the LLR Channel," IEEE C802.16m-07/97 and C802.16m-07/142r1, September 2007.
- [79] K. Sayana et al., "Channel Estimation Modeling for System Simulations," IEEE C802.16m-07/208r4, Atlanta, Georgia, November 2007.
- [80] T. Lestable et al., "Enhanced Approximation for RBIR PHY Abstraction in TGm", IEEE C802.16m-08/067r4, March 2008.
- [81] "Multi-hop System Evaluation Methodology (Channel Model and Performance Metrics)", IEEE 802.16j-06/013r3, February 2007.
- [82] IST-4-027756 WINNER II, D1.1.2 v1.2, "WINNER II Channel Models", <https://www.ist-winner.org/>, September 2007.

- 1 [83] IST-2003-507581 WINNER, D5.4 v. 1.4, "Final Report on Link Level and System
2 Level Channel Models", <https://www.ist-winner.org/>, November 2005.
- 3 [84] Draft New Report ITU-R M.[IMT.EVAL]: Guidelines for evaluation of radio
4 interface technologies for IMT-Advanced (Doc ITU-R 5/69), October 2008.
5

1 Editor's Notes

2 This document is the approved baseline 802.16m Evaluation Methodology. It is a
3 revision to IEEE 802.16m-08/004r4 based on change requests approved by TGm in
4 Session #59, January 2009.

5
6 IEEE 802.16m-08/004 was developed from IEEE 802.16m-07/037r2 through comment
7 resolution in Session #53. IEEE 802.16m-08/004r1, IEEE 802.16m-08/004r2, 802.16m-
8 08/004r3 and 802.16m-08/004r4 are revisions based on approved change requests in
9 Session #54, Session #55, Session #57 and Session #58 respectively.

10
11 IEEE 802.16m-07/037r2 was developed from C802.16m-07/080r3 by the evaluation
12 methodology ad-hoc groups in TGm through harmonization of contributions and
13 resolution of comments in TGm sessions #48, #49, #50, #51 and #52.

14
15

1. Introduction

A great deal can be learned about an air interface by analyzing its fundamental performance in a link-level setting which consists of one base station and one mobile terminal. This link-level analysis can provide information on the system's fundamental performance metrics. The actual performance, in real-world settings, where multiple base stations are deployed in a service area and operating in the presence of a large number of active mobile users, can only be evaluated through system-level analysis. The extension of the link-level analysis methods to a system-level analysis may start with adding multiple users in a single-cell setting. This technique is generally straightforward and provides a mechanism for initial understanding of the multiple-access characteristics of the system.

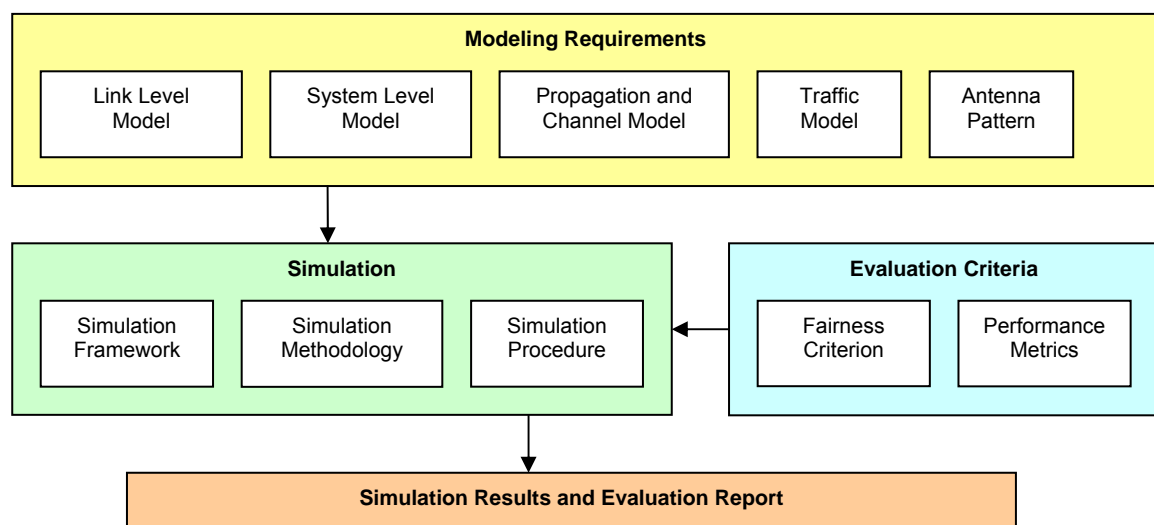


Figure 1 : Simulation components

Since system level results vary considerably with different propagation and interference environments, as well as with the number and distribution of users within the cells, it is important that the assumptions and parameters used in the analysis be reported carefully lest the quoted network-level performance be misleading.

The objective of this evaluation methodology is to define link-level and system-level simulation models and associated parameters that shall be used in the evaluation and comparison of technology proposals for IEEE 802.16m. Proponents of any technology proposal using this methodology shall follow the evaluation methods defined in this document and report the results using the metrics defined in this document. The methods provided in this evaluation methodology document may be extended or enhanced in order to align with IMT.EVAL[84] or to further evaluate specific proposals not covered by this document.

1 Evaluation of system performance of a mobile broadband wireless access technology
 2 requires system simulation that accurately captures the dynamics of a multipath fading
 3 environment and the architecture of the air-interface. The main simulation components
 4 are illustrated in Figure 1.

5 2. System Simulation Requirements

6 2.1. Antenna Characteristics

7 This section specifies the antenna characteristics, e.g. antenna pattern, orientation, etc.
 8 for antennas at the BS and the MS.

9 2.1.1. BS Antenna

10 2.1.1.1. BS Antenna Pattern



12
13
14
15 **Figure 2: Antenna pattern for 3-sector cells**

15 The antenna pattern used for each BS sector is specified as

$$16 \quad A(\theta) = -\min \left[12 \left(\frac{\theta}{\theta_{3\text{dB}}} \right)^2, A_m \right] \quad (1)$$

17 where $A(\theta)$ is the antenna gain in dBi in the direction θ , $-180^\circ \leq \theta \leq 180^\circ$, and $\min [.]$
 18 denotes the minimum function, $\theta_{3\text{dB}}$ is the 3 dB beamwidth (corresponding to

$\theta_{3dB} = 70^\circ$), and $A_m = 20$ dB is the maximum attenuation. Figure 2 shows the BS antenna pattern for 3 sector cells to be used in system level simulations.

A similar pattern will be used for elevation in simulations that need it. In this case the antenna pattern will be given by:

$$A_e(\phi) = -\min \left[12 \left(\frac{\phi}{\phi_{3dB}} \right)^2, A_m \right] \quad (2)$$

where $A_e(\phi)$ is the antenna gain in dBi in the elevation direction ϕ , $-90^\circ \leq \phi \leq 90^\circ$. ϕ_{3dB} is the elevation 3 dB value, and it may be assumed to be 15° , unless stated otherwise.

The combined antenna pattern at angles off the cardinal axes is computed as $A(\theta) + A_e(\phi)$.

2.1.1.2. BS Antenna Orientation

The antenna bearing is defined as the angle between the main antenna lobe center and a line directed due east given in degrees. The bearing angle increases in a clockwise direction. Figure 3 shows the hexagonal cell and its three sectors with the antenna bearing orientation proposed for the simulations. The center directions of the main antenna lobe in each sector point to the corresponding side of the hexagon.

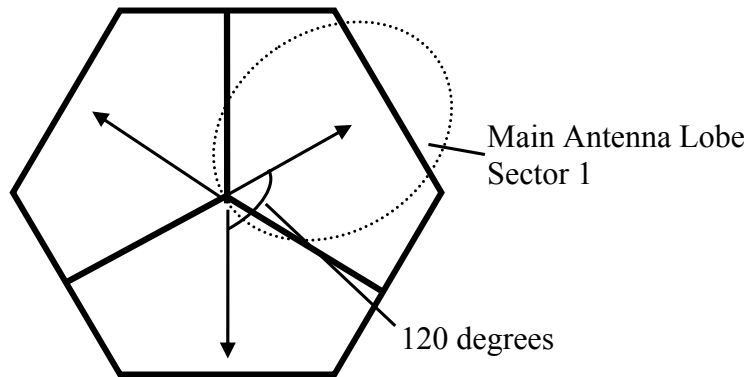


Figure 3 : Antenna bearing orientation diagram.

A uniform linear antenna array is assumed at the BS with an inter-element spacing of 4 wavelengths. For cross-polarized antennas, an antenna array with an inter-element spacing of 4 wavelengths is assumed with two co-located dual polarized elements and XPD as defined in the CDL tables of Section 3.2.5.

2.1.2. MS Antenna

The MS antenna is assumed to be omni directional.

A uniform linear antenna array is assumed at the MS with an inter-element spacing of 1/2 wavelength. For cross-polarized antennas, an antenna array with an inter-element spacing of 1/2 wavelength is assumed with two co-located dual polarized elements and XPD as defined in the CDL tables of Section 3.2.5.

2.2. Simulation Assumptions

The purpose of this section is to outline simulation assumptions that proponents will need to provide in order to facilitate independent assessment of their proposals. The current tables for downlink and uplink simulation assumptions are templates that may be extended for a complete description of simulation assumptions. Baseline simulation assumptions are specified for calibration of system-level performance of the reference system as defined by the 802.16m system requirement document. Additional or different simulation assumptions may be used in the evaluation of an 802.16m system proposal. These assumptions may also be used sometimes in reference system simulations, especially for ensuring a fair comparison with the proposal. In this case, sufficient details of the additional/different assumptions need to be provided by proponents to allow independent verification.

Topic	Description	Baseline Simulation Assumptions	Proposal Specific Assumptions (To be provided by Proponent)
Basic modulation	Modulation schemes for data and control	QPSK, 16QAM, 64QAM	
Duplexing scheme	TDD, HD-FDD or FD-FDD	TDD	
Subchannelization	Subcarrier permutation	PUSC	
Resource Allocation Granularity	Smallest unit of resource allocation	PUSC: Non-STC: 1 slot, STC: 2 slots (1 slot = 1 subchannel x 2 OFDMA symbols)	
Downlink Pilot Structure	Pilot structure, density etc.	Specific to PUSC subchannelization scheme	
Multi-antenna Transmission Format	Multi-antenna configuration and transmission scheme	MIMO 2x2 (Adaptive MIMO Switching Matrix A & Matrix B) Beamforming (2x2)	
Receiver Structure	MMSE/ML/MRC/ Interference Cancellation	MMSE (Matrix B data zone) MRC (MAP, Matrix A data zone)	
Data Channel Coding	Channel coding schemes	Convolutional Turbo Coding (CTC)	

Control Channel Coding	Channel coding schemes and block sizes	Convolutional Turbo Coding (CTC), Convolutional Coding (CC) for FCH only	
Scheduling	Demonstrate performance / fairness criteria in accordance to traffic mix	Proportional fairness for full buffer data only *, 10 active users per sector, fixed control overhead of 6 symbols, 22 symbols for data, 5 partitions of 66 slots each, latency timescale 1.5s	
Link Adaptation	Modulation and Coding Schemes (MCS), CQI feedback delay / error	QPSK(1/2) with repetition 1/2/4/6, QPSK(3/4), 16QAM(1/2), 16QAM(3/4), 64QAM(1/2), 64QAM(2/3), 64QAM(3/4) 64QAM(5/6), CQI feedback delay of 3 frames, error free CQI feedback **	
Link to System Mapping	EESM/MI	MI (RBIR) ***	
HARQ	Chase combining/ incremental redundancy, synchronous/asynchronous, adaptive/non-adaptive ACK/NACK delay, Maximum number of retransmissions, retransmission delay	Chase combining asynchronous, non-adaptive, 1 frame ACK/NACK delay, ACK/NACK error, maximum 4 HARQ retransmissions, minimum retransmission delay 2 frames****	
Power Control	Subcarrier power allocation	Equal power per subcarrier	
Interference Model	Co-channel interference model, fading model for interferers, number of major interferers, threshold, receiver interference awareness	Average interference on used tones in PHY abstraction (Refer to Section 4.4.8)	
Frequency Reuse	Frequency reuse pattern	3 Sectors with frequency reuse of 1 *****	
Control Signaling	Message/signaling format, overheads	Compressed MAP with sub-maps	

Table 1: System-level simulation assumptions for the downlink

* Details of PF scheduler implementation are given in Appendix F.

** Refer to Section 5.2

*** EESM may be used for liaison with NGMN after beta values are calibrated.

**** HARQ retransmission shall occur no earlier than the third frame after the previous transmission.

***** All technical proposals shall use frequency reuse factor of 1. A coverage vs. capacity trade-off, as defined in Section 13.2.3.7 shall be shown for all 802.16m technical proposals evaluating other reuse schemes (e.g., frequency reuse of 3).

1

Topic	Description	Baseline Simulation Assumptions	Proposal Specific Assumptions (To be filled by Proponent)
Basic Modulation	Modulation schemes for data and control	QPSK, 16QAM	
Duplexing Scheme	TDD, HD-FDD or FD-FDD	TDD	
Subchannelization	Subcarrier permutation	PUSC	
Resource Allocation Granularity	Smallest unit of resource allocation	PUSC: 1 slot, (1 slot = 1 subchannel x 3 OFDMA symbols)	
Uplink Pilot Structure	Pilot structure, density etc.	Specific to PUSC subchannelization scheme	
Multi-antenna Transmission Format	Multi-antenna configuration and transmission scheme	Collaborative SM for two MS with single antenna	
Receiver Structure	MMSE/ML Interference cancellation	MMSE	
Data Channel Coding	Channel coding schemes	Convolutional Turbo Coding (CTC)	
Control Channel Coding	Channel coding schemes	CDMA Codes (PUSC 2 symbols) for initial ranging and handover, CDMA Codes (PUSC 1 symbol) for periodic ranging and bandwidth request, CQICH (6 bits)	
Scheduling	Demonstrate performance / fairness criteria in accordance to traffic mix	Proportional fairness for full buffer data only *, 10 active users per sector, fixed control overhead of 3 symbols, 15 symbols for data, 5 partitions of 35 slots each, latency timescale 1.5s	
Link Adaptation	Modulation and Coding Schemes (MCS)	QPSK(1/2) with repetition 1/2/4/6, QPSK(3/4), 16QAM(1/2), 16QAM(3/4)	
Link to System Mapping	EESM/MI	MI(RBIR) **	

HARQ	Chase combining/ incremental redundancy, synchronous asynchronous, adaptive/non-adaptive ACK/NACK delay, maximum number of retransmissions, retransmission delay	Chase combining asynchronous, non-adaptive, ACK/NACK delay N/A, ACK/NACK error, maximum 4 HARQ retransmissions, minimum retransmission delay 2 frames***	
Power Control	Open loop / closed loop		
Interference Model	Co-channel interference model, fading model for interferers, number of major interferers, threshold, receiver interference awareness	Average interference on used tones in PHY abstraction (Refer to Section 4.4.8)	
Frequency Reuse	Frequency reuse pattern	3 Sectors with frequency reuse of 1 ****	
Control Signaling	Message/signaling format, overheads	Initial ranging, periodic ranging, handover ranging, bandwidth request, fast feedback/CQI channel, sounding	

Table 2: System-level simulation assumptions for the uplink

* Details of PF scheduler implementation are given in Appendix F.

** EESM may be used for liaison with NGMN after beta values are calibrated.

*** HARQ retransmission shall occur no earlier than the third frame after the previous transmission.

**** All technical proposals shall use frequency reuse factor of 1. A coverage vs. capacity trade-off, as defined in Section 13.2.3.7 shall be shown for all 802.16m technical proposals evaluating other reuse schemes (e.g., frequency reuse of 3).

2.3. Test Scenarios

The following table summarizes the test environments and associated assumptions and parameters that are required for system level simulations. SRD Requirements must be met for TDD and FDD. Proponents are required to present performance results for the baseline configuration as defined in Table 3.

Case 1: Baseline Configuration, uncorrelated antennas at both BS and MS

Case 2: Baseline Configuration, uncorrelated antennas at MS, correlated antennas at BS (Section 3.2.9)

Test scenarios for evaluation of IMT-Advanced candidate radio interface technologies are defined in [84].

Scenario/ Parameters	Baseline Configuration (Calibration & SRD) TDD and FDD	NGMN Configuration TDD and FDD	Urban Macrocell TDD and FDD
Requirement	Mandatory	Optional *	Optional
Site-to-Site Distance	1.5 km	0.5 km	1 km
Carrier Frequency	2.5 GHz	2.5 GHz	2.5 GHz
Operating Bandwidth	10 MHz for TDD / 10 MHz per UL and DL for FDD	10 MHz for TDD / 10 MHz per UL and DL for FDD	10 MHz for TDD / 10 MHz per UL and DL for FDD
BS Height	32 m	32 m	32 m
BS Tx Power per sector	46 dBm	46 dBm	46 dBm
MS Tx Power	23 dBm	23 dBm	23 dBm
MS Height	1.5 m	1.5 m	1.5 m
Penetration Loss	10 dB	20 dB	10 dB
Path Loss Model	Loss (dB) = $130.19 + 37.6 \log_{10}(R)$ (R in km) **	Loss (dB) = $130.19 + 37.6 \log_{10}(R)$ (R in km) **	Refer to Section 3.2.3.1
Lognormal Shadowing Std. Dev.	8 dB	8 dB	8 dB
Correlation Distance for Shadowing	50m	50m	50m
Mobility	0-120 km/hr	0-120 km/hr	0-120 km/hr
Channel Mix	ITU Ped B 3 km/hr – 60% ITU Veh A 30 km/hr – 30% ITU Veh A 120 km/hr – 10% (Refer to Section 3.2.9 ***)	Low Mobility: 3km/hr UL: Typical Urban, DL: SCM-C Mixed Mobility: ITU Ped B 3 km/hr – 60% ITU Veh A 30 km/hr – 30% ITU Veh A 120 km/hr – 10% (Refer to Section 3.2.9 ***)	3 km/hr – 60% 30 km/hr – 30% 120 km/hr – 10%
Spatial Channel Model	ITU with spatial correlation (Refer to Section 3.2.9 ***)	Low Mobility: 3km/hr SCM, Mixed Mobility: ITU with spatial correlation (Refer to Section 3.2.9 ***)	Urban Macrocell CDL (Refer to Table 9 in Section 3.2.5.1) with spatial correlation (Appendix A)
Error Vector Magnitude (EVM)	30 dB	N/A	30 dB

Table 3: Test scenarios

* Used for liaison with NGMN

** Refer to Section 3.2.3.8

*** Wideband extension to the ITU Power Delay Profiles in Table 23 must be used.

2.4. Reference System Calibration

The purpose of this section is to provide guidelines for simulation parameters that proponents will need to use in order to evaluate performance gains of their proposals relative to the reference system as defined in the 802.16m requirements document. The purpose of calibration is to ensure that, under a set of common assumptions and models, the simulator platforms that will be used by various proponents can produce results that are similar.

2.4.1. Base Station Model

Parameter	Description	Value
P_{BS}	MAX transmit power per sector/carrier	46 dBm @ 10 MHz bandwidth
H_{BS}	Base station height	32m
G_{BS}	Gain (boresight)	17 dBi
S	Number of sectors	3
θ_{BS}	3-dB beamwidth	$S = 3 : \theta_{BS} = 70^0$
G_{FB}	Front-to-back power ratio	20 dB
M_{TX}	Number of transmit antennas	2
M_{RX}	Number of receive antennas	2
d_{BS}	BS antenna spacing	4λ
NF_{BS}	Noise figure	5 dB
HW_{BS}^*	Cable loss	2 dB

Table 4: BS equipment model

* Implementation loss must be justified and accounted for separately.

2.4.2. Mobile Station Model

Parameter	Description	Value
P_{SS}	RMS transmit power/per SS	23 dBm
H_{SS}	Subscriber station height	1.5 m
G_{SS}	Gain (boresight)	0 dBi
$\{\theta_{SS}\}, G(\{\theta_{SS}\})$	Gain as a function of Angle-of-arrival	Omni
N_{TX}	Number of transmit antennas	1
N_{RX}	Number of receive antennas	2
d_{SS}	SS antenna spacing	$\lambda / 2$
NF_{SS}	Noise figure	7 dB
HW_{SS}^*	Cable Loss	0 dB

Table 5: MS equipment model

* Implementation loss must be justified and accounted for separately.

2.4.3. OFDMA Parameters

Parameter	Description	Value : 802.16e Reference System	Value: 802.16m
f_c	Carrier frequency	2.5 GHz	
BW	Total bandwidth	10 MHz	
N_{FFT}	Number of points in full FFT	1024	
F_s	Sampling frequency	11.2 MHz	
Δ_f	Subcarrier spacing	10.9375 kHz	
$T_o = 1 / \Delta_f$	OFDMA symbol duration without cyclic prefix	91.43 us	

CP	Cyclic prefix length (fraction of T_o)	1/8	
T_s	OFDMA symbol duration with cyclic prefix	102.86 us for CP=1/8	
T_F	Frame length	5 ms	
N_F	Number of OFDMA symbols in frame	47	
R_{DL-UL}	Ratio of DL to UL (TDD mode)	Full buffer data only: 29 symbols: 18 symbols VoIP only: DL to UL ratio suitably chosen to support bidirectional VoIP	
T_{duplex}	Duplex time	TTG: 296 PS for 10 MHz RTG: 168 PS for 10 MHz $PS = 4 / F_s$	
DL_{Perm}	DL permutation type	PUSC	
UL_{Perm}	UL permutation type	PUSC	

Table 6: OFDMA air interface parameters

3. Channel Models

3.1. Introduction

Channel models suitable for evaluation of 802.16m system proposals are described in this section, wherein the model considers parameters specific to 802.16m including bandwidths, operating frequencies, cell scenario (environment, cell radius, etc), and multi-antenna configurations. Both system level and link level models are described in detail with a purpose of fulfilling the needs to conduct effective link- and system-level simulations that can generate trustworthy and verifiable results to assess performance related to the 802.16m system requirements.

Section 3.1.1, Section 3.1.2, Section 3.1.3 and Section 3.1.4 are informative only. The detailed specifications of system and link level models are in section 3.2. Section 3.2.9 describes the channel model to be used for calibration and baseline simulations as defined in the test scenarios in Table 3.

Channel models for evaluation of IMT-Advanced candidate radio interface technologies are defined in [84]. Mandatory channel model parameters for evaluation of radio interface technologies for the scenarios Indoor Hotspot, Urban Micro-cell, Urban Macro-cell, and Rural Macro-cell are contained in the Primary Module of IMT-Advanced channel model [84].

3.1.1. General Considerations (Informative)

The channel models defined in this document are to provide sufficient details for the purpose of evaluating the system proposals to 802.16m. Since 802.16m is also targeting IMT-Advanced, the system requirements, deployment scenario, and operational bandwidth and frequency of a future IMT-advanced system should also be considered.

In the ITU-R recommendation ITU-R M.1645 the framework for systems beyond IMT-2000 (IMT-Advanced) envisions data rates of up to 1Gbps for nomadic/local area wireless access, and up to 100 Mbps for mobile access. As a reference, the European WINNER project has devised a method for determining spectrum requirements for IMT-Advanced, and their conclusions are given in [1]. In that report it is stated that in order to achieve the above performance targets of IMT-Advanced, sufficiently wide bandwidth and possibly multiple such wideband RF channels may be needed. Candidate bands for IMT-Advanced are to be considered in 2007 at the WRC-07 conference. When considering candidate bands, the WINNER report further suggests that the utilization of bands above 3 GHz may be necessary, but these bands could present significant technical challenges if used for wide area mobile access, due to the increase in path loss with frequency.

The terrain environment in which 802.16m systems may be deployed (i.e., outdoor, indoor, macro-, micro-, and pico-cell, etc.) dictates the channel modeling, affecting not only parameters but also the model itself. Therefore, channel modeling needs to consider various radio environments and propagation scenarios in which 802.16m system may be deployed.

3.1.2. Overview of Channel Modeling Methodology (Informative)

The channel behavior is described by its long-term and short-term fading characteristics where the former often depends on the geometrical location of a user in a wireless network and the latter defines the time-variant spatial channels.

In general, there are two ways of modeling a channel: *deterministic* and *stochastic* [2]. The deterministic category encompasses all models that describe the propagation channel for a specific transmitter location, receiver location, and environment. Deterministic channel models are site-specific, as they clearly depend on the location of transmitter, receiver, and the properties of the environment. They are therefore most suitable for network planning and deployment.

In many cases, it is not possible or desirable to model the propagation channel in a specific environment. Especially for system testing and evaluation, it is more appropriate to consider channels that reflect “typical”, “best case”, and “worst case” propagation scenarios. A stochastic channel model thus prescribes *statistics* of the channel impulse responses (or their equivalents), and during the actual simulation, impulse responses are generated as *realizations* according to those statistics.

For a simulation-based study, stochastic channel modeling is more suitable. Almost all the existing channels models are stochastic ones, such as the SUI model proposed for IEEE 802.16d [3], the ITU model for IMT-2000 [4], the 3GPP SCM model [5][6][7] and

SCME (Spatial Channel Model Extensions) model [8], the COST 259 model [9][10][11], the COST 273 model[12], and the WINNER model[13].

Essential to the evaluation of multiple-antenna techniques, which are envisioned to be a key enabling technology for 802.16m and IMT-Advanced, is the modeling of MIMO channels that can be represented as double-directional channels [15] or as vector (or matrix) channels[14]. The former representation is more related to the physical propagation effects, while the latter is more on the “mathematical” effect of the channel on the system [16]. The double-directional model is a physical model in which the channel is constructed from summing over multiple waves or rays. Thus it can also be referred to as a “ray-based model”. The vector or matrix channel is a mathematical or analytical model in which the space-time channel as seen by the receiver is constructed mathematically, assuming certain system and antenna parameters. In this approach, the channel coefficients are correlated random process in both space and time, where the correlation is defined mathematically.

A realization of a *double-directional channel* is characterized by its double-directional impulse response. It consists of N propagation waves between the transmitter and the receiver sites. Each wave is delayed in accordance to its excess-delay τ_ℓ , weighted with the proper complex amplitude $a_\ell e^{j\phi_\ell}$. Note that the amplitude is a two-by-two matrix, since it describes the vertical and horizontal polarizations and the cross-polarization; neglecting a third possible polarization direction is admissible in macro- and microcells. Finally, the waves are characterized by their Angle of Departure (AoD) $\Omega_{T,\ell}$ and Angle of Arrival (AoA) $\Omega_{R,\ell}$.^{*} The channel impulse response matrix \underline{h} , describing horizontal and vertical polarization is then

$$\underline{h}(t, \tau, \Omega_T, \Omega_R) = \sum_{\ell=1}^N \underline{h}_\ell(t, \tau, \Omega_T, \Omega_R) = \sum_{\ell=1}^N \underline{a}_\ell e^{j\phi_\ell} \delta(\tau - \tau_\ell) \delta(\Omega - \Omega_{T,\ell}) \delta(\Psi - \Omega_{R,\ell}) \quad (3)$$

The number of waves N can become very large if all possible paths are taken into account; in the limit, the sum has to be replaced by an integral. For practical purposes, waves that are significantly weaker than the considered noise level can be neglected. Furthermore, waves with similar AoDs, AoAs, and delays can also be merged into “effective” paths, known also as taps.

In general, all multipath parameters in the channel impulse response, $\tau_\ell, \Omega_{R,\ell}, \Omega_{T,\ell}, \underline{a}_\ell$, and $e^{j\phi_\ell}$ will depend on the absolute time t ; also the set of waves or multipath components (MPCs) contributing to the propagation will vary, $N \rightarrow N(t)$. The variations with time can occur both because of movements of scatterers, and movement of the mobile station or MS (the BS is assumed fixed).

A mathematical wideband *matrix* channel response describes the channel from a transmit to a receive antenna array. It is characterized by a matrix \underline{H} whose elements

^{*}We stress that the (double-directional) channel is reciprocal. While the directions of multipath components at the base station and at the mobile station are different, the directions at one link end for the transmit case and the receive case must be identical. When we talk in the following about AoAs and AoDs, we refer to the directions at two different link ends.

H_{ij} are the (non-directional) impulse responses from the j -th transmit to the i -th receive antenna element. They can be computed for any antenna constellation as

$$H_{i,j} = h(\tau, \vec{x}_{R,i}, \vec{x}_{T,j}) = \sum_{\ell=1}^N \vec{g}_R(\Omega_R) \cdot \underline{h}(\tau_\ell, \Omega_{R,\ell}, \Omega_{T,\ell}) \cdot \vec{g}_T(\Omega_T) \cdot e^{j\langle \vec{k}(\varphi_{R,\ell}) \vec{x}_{R,i} \rangle} e^{j\langle \vec{k}(\varphi_{T,\ell}) \vec{x}_{T,j} \rangle}, \quad (4)$$

where \vec{x}_R and \vec{x}_T are the vectors of the chosen element-position measured from an arbitrary but fixed reference points $\vec{x}_{R,0}$ and $\vec{x}_{T,0}$ (e.g., the centers of the arrays) and \vec{k} is the wave vector so that

$$\langle \vec{k}(\Omega) \cdot \vec{x} \rangle = \frac{2\pi}{\lambda} (x \cos \vartheta \cos \varphi + y \cos \vartheta \sin \varphi + z \sin \vartheta). \quad (5)$$

where ϑ and φ denote elevation and azimuth, respectively. The functions $\vec{g}_R(\Omega_R)$ and $\vec{g}_T(\Omega_T)$ are the antenna patterns at transmitter and receiver, respectively, where the two entries of the vector \vec{g} describe the antenna pattern for horizontal and vertical polarization.

3.1.3. Calibration Model (Informative)

A link level channel model is used mainly for calibrating point-to-point MIMO link performance at various SINR points of interest, with extensions to multiple links in the case of interference. Note that any particular link level channel does not contain the information of large-scale fading or how often a particular kind of link condition occurs in a wireless system.

A link level channel can be naturally developed as a typical representation of a propagation scenario under a particular system setting (e.g., a macrocell outdoor system with a representative BS and MS antenna configuration). A link-level channel modeling methodology should be consistent with the system level modeling methodology.

Conventional Tapped Delay Line (TDL) models, such as the three-tap ones used for the IEEE 802.16d SUI TDL [3] and the six-tap ITU models for IMT-2000 [4], need to be extended to include the spatial channel modeling to capture the relationship among all the channels between multiple transmit and receive antennas. For example, SCME models [8] define TDLs where each tap consists of multiple rays in the space that can be further grouped into 3 or 4 mid-taps. WINNER II clustered delay line (CDL) models [13] for systems beyond-3G also defined delay line model with additional angular information specified for each tap.

A few important observations need to be considered:

1. The six-tap ITU models were developed for 5 MHz bandwidth channels, and as the bandwidth increases, the resolution in the delay domain increases so that more taps are required for higher bandwidth channel models. Each resolvable tap consists of a number of multipath components so that the tap fades as the mobile moves. As bandwidth increases there will be fewer multipath components per resolvable tap so that the fading characteristics of the taps are likely to change. The tap fading is likely to become more Ricean in nature (i.e., increasing

1 K-factor with bandwidth) and the Doppler spectrum will not have the classic
2 “bathtub” shape. This also means that the coherence times or distances for the
3 tap fading will most likely be longer for higher bandwidths. The above
4 observation suggests that measurement data under bandwidths up to 100MHz
5 needs to be collected and analyzed to obtain the appropriate channel statistics
6 which may vary according to transmission bandwidth.
7

- 8 2. The model should be flexible to incorporate various antenna effects such as the
9 potential antenna gain imbalance, antenna coupling, and polarization. Ideally the
10 model would include both azimuth and elevation angle (i.e., antenna tilt).

11 **3.1.4. System Level Channel Modeling Considerations (Informative)**

12 System level simulation is a tool widely used to understand and assess the overall
13 system performance. In system-level modeling, all possible link conditions are modeled
14 along with their occurrence probability. System models include additionally the large-
15 scale location-dependent propagation parameters such as path loss and shadowing, as
16 well as the relationship among multiple point-to-point links.

17 Channel models that allow effective and efficient system level simulations are of
18 particular interest in the evaluation methodology discussion. In a typical system level
19 simulation, the geometry of a wireless deployment is first defined (e.g., typically a
20 cellular topology is assumed), based on which the long-term fading behaviors and large-
21 scale parameters are derived. After that, the short-term time-variant spatial fading
22 channels are generated.

23 As mentioned previously, there are in general two types of methodologies to generate
24 short-term fading channels. The first is a physical model in which the channel is
25 constructed from summing over multiple rays that are parameterized according to the
26 geometrics. The physical modeling is independent of the antenna configuration, which
27 means that the actual mathematical channel perceived by a receiver will need to further
28 incorporate the antenna configuration, traveling speed, velocity, and so on.

29 As an example of a physical model, the 3GPP SCM model [5] has been widely used in
30 system simulation. It models the physical propagation environment using paths and
31 sub-paths with randomly specified angles, delays, phases, and powers. The MIMO
32 channel coefficients for simulation are derived after defining the antenna configuration
33 and array orientation at both MS and BS. Time-variation is realized after defining MS
34 travel direction and speed. Other ray-based channel models for system level simulation
35 include, but not limited to, SCME [8] and WINNER channel model [13]. The ray-based
36 physical models are powerful as they are independent from any particular assumption of
37 antenna configurations.

38 The other modeling methodology is mathematical or analytical modeling in which the
39 space-time channel as seen by the receiver is constructed mathematically, assuming
40 certain system and antenna parameters. In this method, the channel coefficients are
41 correlated random process in both space and time, where the correlation is defined
42 mathematically.

Mathematical modeling tries to analytically model the statistical behavior of a channel, represented by probability distributions and power profiles of delays and angles. On the other hand, in a ray-based modeling, the statistical behavior is satisfied through the summation of multiple rays with random parameters. The two approaches can be viewed as two different simulation implementations, especially if they are based on the same probability distributions and power profiles. The system performance results are expected to be very close with both models.

Both approaches could be considered for system simulation purpose. A few important considerations for system simulations are:

- *Simulation run-time.* A system level simulation typically involves the generation of spatial channels from a MS position to multiple base stations (e.g., 19 cells or 57 sectors in a three-sector cellular network). Multi-user scheduling is also commonly simulated, in which the channel conditions of multiple MSs (e.g., 10, 20, or more) are required in the scheduler to determine how to distribute resources among them. Therefore, it is important if a model can result in the reduction of run-time without sacrificing the truthfulness to reality.
- *Consistency with link-level models.* Link level models should reflect particular (e.g., typical) link conditions experienced in various propagation scenarios. A link level study relies on the system level model to understand the likelihood of the particular link condition, while system level study sometimes relies on the link-level study results in order to model the actual link performance.
- *Comparison of results and statistical convergence.* A channel model should facilitate comparison of system study results from independent sources. A channel model should ensure the statistical behavior of a channel to converge quickly without having to run a larger number of realizations (run-time concern). As an example, if a model defines some second order statistics as random variables themselves (e.g., angular spread, delay spread, etc.), the simulation may require more realizations and thus longer time to get convergence.

3.2. System Level Channel Model

This section focuses on the system-level simulation procedure and parameters for modeling the long- and short-term behavior of spatial channels between a MS and one or more BSs. The procedure and all the required parameters for the purposes of simulation will be described in sufficient detail.

For assumptions and parameters related to test scenarios, as required in system level simulation, refer to Section 2 of this evaluation methodology document. The deployment parameters include, among others, cell radius and topology, BS transmission power, BS antenna pattern, orientation, height, gain, and front-to-back ratio, MS transmission power, MS antenna pattern, height, and gain.

Once the deployment parameters are specified, a system level simulation typically involves the random drop of users in a radio environment of interest. The set of users

comprises of a specified mix of different speeds and channel scenarios. Then, the long-term parameters of the link between a set of BS and a MS, such as path loss and shadowing factor, are generated. The short-term time-varying spatial fading channel coefficients are generated in the final step. Typically, multiple links between an MS and multiple BSs are needed, among which there are multiple desired links (at least one) and multiple interference links. The shadowing factor of these links can be correlated.

Following the introduction of the general approach to spatial channel modeling, the remaining subsections will define the channel modeling procedure and parameters, as well as channel scenarios and speed mix recommended for system simulation.

3.2.1. Spatial Channel Modeling

The general modeling approach is based on the geometry of a network layout. The large-scale parameters such as path loss and shadowing factor are generated according to the geometric positions of the BS and MS. Then the statistical channel behavior is defined by some distribution functions of delay and angle and also by the power delay and angular profiles. Typically, an exponential power delay profile and Laplacian power angular profile are assumed with the function completely defined once the RMS delay spread and angular spread (both Angle of Departure (AoD) and Angle of Arrival (AoA)) are specified. The RMS delay and angular spread parameters can be random variables themselves, with a mean and deviation as in SCM. The RMS delay and angular spread can be mutually correlated, together with other large-scale parameters such as shadowing factors.

According to the exact profile and distribution functions defined by the particular RMS delay and angular spread values, a finite number of channels taps are generated randomly with a per-tap delay, mean power, mean AoA and AoD, and RMS angular spread. They are defined in a way such that the overall power profile and distribution function are satisfied. Each tap is the contribution of a number of rays (plane waves) arriving at the same time (or roughly the same time), with each ray having its own amplitude, AoA, and AoD.

The number of taps and their delay and angles may be randomly defined, but a reduced-complexity model can specify the delays, mean powers, and angles of the channel taps in a pre-determined manner when typical values are often chosen. Similar to the well-known TDL version of the WSSUS (Wide-Sense Stationary Uncorrelated Scattering) model, where the power delay profile is fixed, a “spatial” TDL reduced-complexity model additionally defines the spatial information such as per-tap mean AoA, AoD, and per-tap angular spread (thus the power angular profile). Spatial TDL models are also referred to as Cluster Delay Line or CDL models as each tap is modeled as the effect of a cluster of rays arriving at about the same time. Each tap suffers from fading in space and over time. The spatial fading process will satisfy a pre-determined power angular profile. Due to the simplicity of reduced complexity modeling, it is recommended for system level simulation.

The actual realization of a time-varying spatial channel can be performed in two ways:

- Ray-based: The channel coefficient between each transmit and receive antenna pair is the summation of all rays at each tap and at each time instant, according

to the antenna configuration, gain pattern, and the amplitude, AoA, AoD of each ray. The temporal channel variation depends on the traveling speed and direction relative to the AoA/AoD of each ray.

- Correlation based: The antenna correlation for each tap is computed first according the per-tap mean AoA/AoD, per-tap power angular profile, and antenna configuration parameters (e.g., spacing, polarization, etc.). The per-tap Doppler spectrum depends on the traveling speed and direction relative to the mean per-tap AoA/AoD, as well as the per-tap power angular profile. The MIMO channel coefficients at each tap can then be generated mathematically by transforming typically the i.i.d. Gaussian random variables according to the antenna correlation and the temporal correlation (correspondingly the particular Doppler spectrum). The approach of pre-calculating and storing all the correlations and time-varying fading processes may also be used in system simulation.

Correlation based method should be used as the mandatory baseline channel modeling approach.

3.2.2. Radio Environment and Propagation Scenarios

The terrain or radio environment, such as indoor, urban, or suburban, dictates the radio propagation behavior. Even in similar terrain environments, there may be different propagation behavior or scenarios.

For the simulation of IEEE 802.16m systems, the following test scenarios are defined:

1. **Urban Macrocell (Optional)**: In a typical urban Macrocell, a mobile station is located outdoors at street level with a fixed base station clearly above surrounding building heights. As for propagation conditions, non- or obstructed line-of-sight is a common case, since street level is often reached by a single diffraction over the rooftop. The building blocks can form either a regular Manhattan type of grid, or have more irregular locations. Typical building heights in urban environments are over four floors. Buildings height and density in typical urban macrocell are mostly homogenous. As a variant, the *optional bad urban macrocell* describes cities with buildings with distinctly inhomogeneous building heights or densities. The inhomogeneities in city structures can be the result of, for example, large water areas separating the built-up areas, or the high-rise skyscrapers in an otherwise typical urban environment. Increased delay and angular dispersion can also be caused by mountains surrounding the city. The base station is typically located above the average rooftop level, but within its coverage range there can also be several high-rise buildings exceeding the base station height. From the modeling point of view this differs from typical urban macrocell by an additional far scatterer cluster.
2. **Suburban Macrocell (Optional)**: In suburban macrocells, base stations are located well above the rooftops to allow wide area coverage, and mobile stations are outdoors at street level. Buildings are typically low residential detached houses with one or two floors, or blocks of flats with a few floors. Occasional open areas such as parks or playgrounds between the houses make the

environment rather open. Streets do not form urban-like regular strict grid structure. Vegetation is modest.

3. **Urban Microcell (Optional):** In the urban microcell scenario, the heights of both the antenna at the BS and that at the MS are assumed to be well below the tops of surrounding buildings. Both antennas are assumed to be outdoors in an area where streets are laid out in a Manhattan-like grid. The streets in the coverage area are classified as “the main street”, where there is LOS from all locations to the BS, with the possible exception of cases in which LOS is temporarily blocked by traffic (e.g. trucks and busses) on the street. Streets that intersect the main street are referred to as perpendicular streets, and those that run parallel to it are referred to as parallel streets. This scenario is defined for both LOS and NLOS cases. Cell shapes are defined by the surrounding buildings, and energy reaches NLOS streets as a result of propagation around corners, through buildings, and between them. The *optional Bad Urban Microcell* scenarios are identical in layout to Urban Microcell scenarios. However, propagation characteristics are such that multipath energy from distant objects can be received at some locations. This energy can be clustered or distinct, has significant power (up to within a few dB of the earliest received energy), and exhibits long excess delays. Such situations typically occur when there are clear radio paths across open areas, such as large squares, parks or bodies of water.
4. **Indoor Small Office (Optional):** This scenario investigates isolated cells for home or small office coverage. In a typical small office environment, there are multiple floors and multiple rooms or areas.
5. **Outdoor to Indoor (Optional):** This scenario is the combination of an outdoor and an indoor scenario such as **urban microcell** and **indoor small office**. In this particular combination, the MS antenna height is assumed to be at 1 – 2 m (plus the floor height), and the BS antenna height below roof-top, at 5 - 15 m depending on the height of surrounding buildings (typically over four floors high).
6. **Indoor Hotspot (Optional):** This scenario concentrates on the propagation conditions in a hotspot in the urban scenario with much higher traffic as in conference halls, shopping malls and teaching halls. The indoor hotspot scenario is also different from the indoor office scenario due to building structures.
7. **Open Rural Macrocell (Optional):** In rural open area, there is low building density; the height of the BS antenna is much higher than the average building height. Depending on terrain, morphology and vegetation, LOS conditions might exist in most of the coverage area.

3.2.3. Path Loss

The path loss model depends on the propagation scenario. For example, in a macrocell environment, the COST-231 modified Hata model [18] is well known and widely used for systems with a carrier frequency less than or equal to 2.5 GHz. The Erceg-Greenstein model [3] was proposed in IEEE 802.16a for carrier frequencies up to 3.5 GHz. Extensions to these path loss models to carrier frequencies above 3.5 GHz are also proposed in the WINNER model [13].

For the evaluation of IEEE 802.16m systems, the following path loss models are specified:

3.2.3.1. Urban Macrocell (Optional)

With default BS and MS heights of 32m and 1.5m respectively, and as derived in Appendix H, the modified COST 231 Hata path loss model for the urban macrocell at carrier frequency f [GHz] ($2 < f < 6$) is given by

$$PL_{urban_macro} [dB] = 35.2 + 35 \log_{10}(d) + 26 \log_{10}(f/2) \quad (6)$$

where d in meters is the distance from the transmitter to the receiver.

3.2.3.2. Suburban Macrocell (Optional)

With default BS and MS heights of 32m and 1.5m respectively, and as shown in Appendix H, the modified COST 231 Hata path loss model for the suburban microcell at carrier frequency f [GHz] ($2 < f < 6$) is given by

$$PL_{suburban_macro} [dB] = PL_{urban_macro} - 2[1.5528 + \log_{10}(f)]^2 - 5.4 \quad (7)$$

3.2.3.3. Urban Microcell (Optional)

LOS case:

With default BS and MS heights of 12.5m and 1.5m respectively, and as shown in Appendix H the path loss model for the urban microcell with LOS [20] at carrier frequency f [GHz] is given by

$$PL_{urban_micro_LOS} [dB] = 32.4418 + 20 \log_{10}(f) + 20 \log_{10}(d) + 0.0174d + 20 \log_{10}(\max(0.013d/f, 1)) \quad (8)$$

where d in meters is the distance from the transmitter to the receiver.

NLOS Case:

With default BS and MS heights of 12.5m and 1.5m respectively, and as shown in Appendix H, the path loss model for the urban microcell with NLOS [20] at carrier frequency f in GHz is given by

$$PL_{urban_micro_NLOS} [dB] = \min(PL_{over_the_rooftop}, PL_{Berg}) \quad (9)$$

Where

$$PL_{over_the_rooftop} = 24 + 45 \log_{10}(r_{Eu} + 20) \quad (10)$$

$$PL_{Berg} = 32.4418 + 20 \log_{10}(f) + 20 \log_{10}(d_n) + 20 \log_{10}(\max(R/r_{bp}, 1)) + 20 \log_{10}(R) + 0.0174R \quad (11)$$

$$r_{bp} = \min\{76.67f, r_0\},$$

and

$R = \sum_{j=1}^n r_{j-1}$ is the distance along streets between transmitter and receiver.

The distance r_j is the length of the street between nodes j and $j+1$ (there are $n+1$ nodes in total) and r_{Eu} is the Euclidean distance in meters from the transmitter to the receiver.

The distance d_n is the illusory distance and it is defined by the recursive expression:

$$\begin{aligned} k_j &= k_{j-1} + d_j q_{j-1} \\ d_j &= k_j r_{j-1} + d_{j-1} \end{aligned} \quad (12)$$

with $k_0 = 1$, $d_0 = 0$ and $q_j(\theta_j) = \left(\frac{|\theta_j|}{90}\right)^{1.5}$

where θ_j is the angle between streets at junction j .

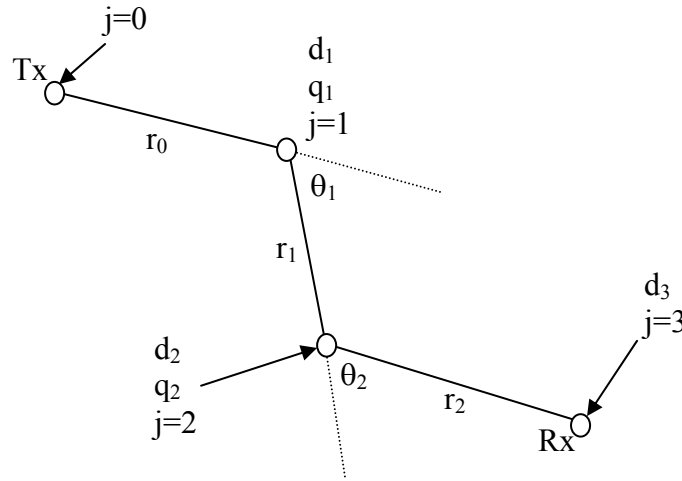


Figure 4: Geometry of street sections used for microcellular NLOS path loss model

Since the path loss defined above requires additional street layout information in addition to just the BS-MS distance as typically specified in system simulation, in order to make it possible to derive the path loss based on the BS-MS distance, the following assumption on street layout should be used:

- Street intersection angle: 90 degree
- Segment length: 50m
- Number of street segments: $\text{round}[d/[(\text{SQRT}(2)*\text{segment_length})]]$, where d is the distance between transmitter and receiver

For propagation scenarios that describe both LOS and NLOS situations, simulations should use a random mix of LOS and NLOS scenarios with the probability of selecting a LOS scenario given in Table 7.

Propagation Scenario	Probability of LOS as a function of distance d (m)
Urban Microcell	$P_{LOS} = 1 \quad d \leq 15m$
	$1 - \left(1 - (1.56 - 0.48 \log_{10}(d))^3\right)^{1/3} \quad d > 15m$
Indoor Hotspot	$P_{LOS} = 1 \quad d \leq 10m$
	$e^{[-(d-10)/45]} \quad d > 10m$
Rural	$P_{LOS} = e^{(-d/1000)}$

Table 7: LOS probabilities for mixed LOS/NLOS scenario

3.2.3.4. Indoor Small Office (Optional)

The WINNER model [13] defines the following model for NLOS case under the condition of $3 \text{ m} < d < 100 \text{ m}$, $h_{\text{BS}} = h_{\text{MS}} = 1 \sim 2.5 \text{ m}$,

NLOS (Room to Corridor):

$$PL(\text{dB}) = 43.8 + 36.8 \log_{10}(d[\text{m}]) + 20 \log_{10}(f[\text{GHz}]/5.0) \quad (13)$$

NLOS (through-wall):

$$PL(\text{dB}) = 46.4 + 20 \log_{10}(d[\text{m}]) + 5n_w + 20 \log_{10}(f[\text{GHz}]/5.0) \quad (\text{Light Wall}) \quad (14)$$

$$PL(\text{dB}) = 46.4 + 20 \log_{10}(d[\text{m}]) + 12n_w + 20 \log_{10}(f[\text{GHz}]/5.0) \quad (\text{Heavy Wall}) \quad (15)$$

where n_w is the number of walls between BS and MS. It is assumed that there is one light wall every 3m and one heavy wall every 30 m. [†]

3.2.3.5. Indoor Hot Spot (Optional)

LOS case ($20 \text{ m} < d < 60 \text{ m}$, $h_{\text{BS}} = h_{\text{MS}} = 1 \sim 2.5 \text{ m}$)

$$PL(\text{dB}) = 49.3 + 11.8 \log_{10}(d[\text{m}]) + 20 \log_{10}(f[\text{GHz}]/5.0) \quad (16)$$

NLOS case ($20 \text{ m} < d < 80 \text{ m}$, $h_{\text{BS}} = h_{\text{MS}} = 1 \sim 2.5 \text{ m}$)

$$PL(\text{dB}) = 25.5 + 43.3 \log_{10}(d[\text{m}]) + 20 \log_{10}(f[\text{GHz}]/5.0) \quad (17)$$

The probability of selecting a LOS scenario is given in Table 7[†]

3.2.3.6. Outdoor to Indoor (Optional)

The WINNER model [13] defines the following path loss model for the NLOS case.

$$PL(\text{dB}) = PL_b + PL_{\text{tw}} + PL_{\text{in}} \quad (18)$$

Where $PL_b = PL_{\text{B1}}(d_{\text{out}} + d_{\text{in}})$, $PL_{\text{tw}} = 14 + 15(1 - \cos(\theta))^2$, $PL_{\text{in}} = 0.5 d_{\text{in}}$
 $3 \text{ m} < d_{\text{out}} + d_{\text{in}} < 1000 \text{ m}$, $h_{\text{BS}} = 12.5 \text{ m}$, $h_{\text{MS}} = 3n_{\text{Fl}} + 1.5 \text{ m}$, $n_{\text{Fl}} = 2$.

PL_{B1} is path-loss of urban-micro cell (a function with the input distance of $d_{\text{out}} + d_{\text{in}}$), d_{out} is the distance between the outside terminal and closest point of the wall to the inside terminal, d_{in} is the distance from wall to the inside terminal, θ is the angle between the outdoor path and the normal of the wall. n_{Fl} is the number of the floor (the ground floor is assigned the number 1).

For simulation purposes, the default value of $\theta = 45$ degree can be used. Additionally, the path loss of the outdoor portion follows the NLOS case. [†]

[†] The models (including the parameters in respective CDL models defined later) are currently aligned with IMT.EVAL, but will be adjusted if needed in order to fully align with the final model adopted in IMT.EVAL once available. All parameter values need to be defined for simulation.

3.2.3.7. Open Rural Macrocell (Optional)

According to the recent experimental result of the WINNER model [13], the path loss is

LOS:

$$PL(dB) = 44.2 + 21.5 \log_{10}(d[m]) + 20 * \log_{10}(f[GHz]/5.0) \quad 20m < d < d_{BP} \quad (19)$$

$$PL(dB) = 10.5 + 40.0 \log_{10}(d[m]) - 18.5 \log_{10}(h_{BS}[m]) - 18.5 \log_{10}(h_{ms}[m]) + 1.5 \log_{10}(f[GHz]/5.0) \quad d > d_{BP} \quad (20)$$

NLOS:

$$PL(dB) = 55.4 + 25.1 * \log_{10}(d[m]) + 21.3 * \log_{10}(f[GHz]/5.0) - 0.13(h_{BS}[m] - 25) \log_{10}(\frac{d}{d_0}) - 0.9(h_{ms}[m] - 1.5) \quad (21)$$

Where d = distance

$$d_{BP} = 4 \cdot h_{ms} \cdot h_{BS} \cdot f / c$$

h_{BS} = the height of the base station

h_{ms} = the height of the mobile station

f = the centre-frequency (GHz)

c = the velocity of light in vacuum (m/s)

σ = standard deviation

d_0 = 100 meter (the reference distance)

The probability of selecting a LOS scenario is given in Table 7.†

3.2.3.8. Path Loss Model for Baseline Test Scenario (Mandatory)

This model [4] is applicable for the test scenarios in urban and suburban areas outside the high rise core where the buildings are of nearly uniform height.

$$PL(dB) = 40(1 - 4 \times 10^{-3} h_{BS}) \log_{10}(R) - 18 \log_{10}(h_{BS}) + 21 \log_{10}(f) + 80 \quad (22)$$

Where R in kilometers is the distance from the transmitter to the receiver, f is the carrier frequency in MHz and h_{BS} is the base station antenna height above rooftop.

If the base station antenna height is fixed at 15 meters above the average rooftop and a carrier frequency of 2 GHz, the path loss formula reduces to

$$PL(dB) = 128.1 + 37.6 \log_{10}(R) \quad (23)$$

Applying a frequency correction factor $21 \log_{10}(2.5/2)$ for operation at 2.5 GHz, the path loss can be calculated as

$$PL(dB) = 130.19 + 37.6 \log_{10}(R) \quad (24)$$

3.2.4. Shadowing Factor

The shadowing factor (SF) has a log-normal distribution and a standard deviation defined in the following table based on the WINNER parameters [13], for different scenarios.[‡]

Propagation Scenario	Standard Deviation of Shadow Fading
Urban macrocell	8 dB
Suburban macrocell	8 dB
Urban microcell	NLOS: 4 dB, LOS 3 dB
Indoor Small Office	NLOS (Room to Corridor) 4 dB, NLOS (through-wall) 6 dB (light wall), 8 dB (heavy-wall)
Indoor Hot Spot	LOS 1.5 dB, NLOS 1.1 dB
Outdoor to indoor	7 dB
Open Rural Macrocell	NLOS: 8 dB, LOS: 6 dB

Table 8: Standard deviation of shadow fading distribution

The site-to-site shadowing correlation is 0.5. The SF of closely positioned MSs is typically observed similar or correlated. Therefore, the SF can be obtained via interpolation in the following way.

For each base station, a uniformly spaced grid is generated using the pre-defined de-correlation distance as shown in Figure 5. Each node $S_{n,l}$ on the grid represents the shadowing factor corresponding to base station l at the geographic location n with (x, y) coordinate. All nodes $\{S_{n,0}, \dots, S_{n,L}\}$, where L represents the set of base stations in the simulation, correspond to a single geographical location n in a simulated system. The distance between closest nodes, D_{cor} , in the grid is the pre-defined de-correlation distance (e.g. 50 meters).

For a mobile location, either from a random drop or a result of mobility, the shadowing factor from the mobile to a base station l should be calculated by interpolating the shadowing factors of the closest four nodes, $S_{0,l}, S_{3,l}$ for the corresponding base station l in Figure 5. Specifically, the shadowing factor $g_{k,l}$ at a location corresponding to base station l is determined by

$$SF(g_{k,l}) = \left(\sqrt{1 - \frac{x_{pos}}{D_{cor}}} \right) \left[S_{0,l} \sqrt{\frac{y_{pos}}{D_{cor}}} + S_{3,l} \left(\sqrt{1 - \frac{y_{pos}}{D_{cor}}} \right) \right] + \left[S_{1,l} \sqrt{\frac{y_{pos}}{D_{cor}}} + S_{2,l} \left(\sqrt{1 - \frac{y_{pos}}{D_{cor}}} \right) \right] \sqrt{\frac{x_{pos}}{D_{cor}}} \quad (25)$$

Note that the linear interpolation above guarantees smooth change of shadowing factors around the nodes on the grid, and moving from one square to another square. Additionally, the linear interpolation above guarantees the same standard deviation of shadowing factors at all points in the simulated system.

[‡] The values chosen for the shadowing factor are currently aligned with IMT.EVAL, but they will be adjusted if needed to completely align with the final model adopted in IMT.EVAL.

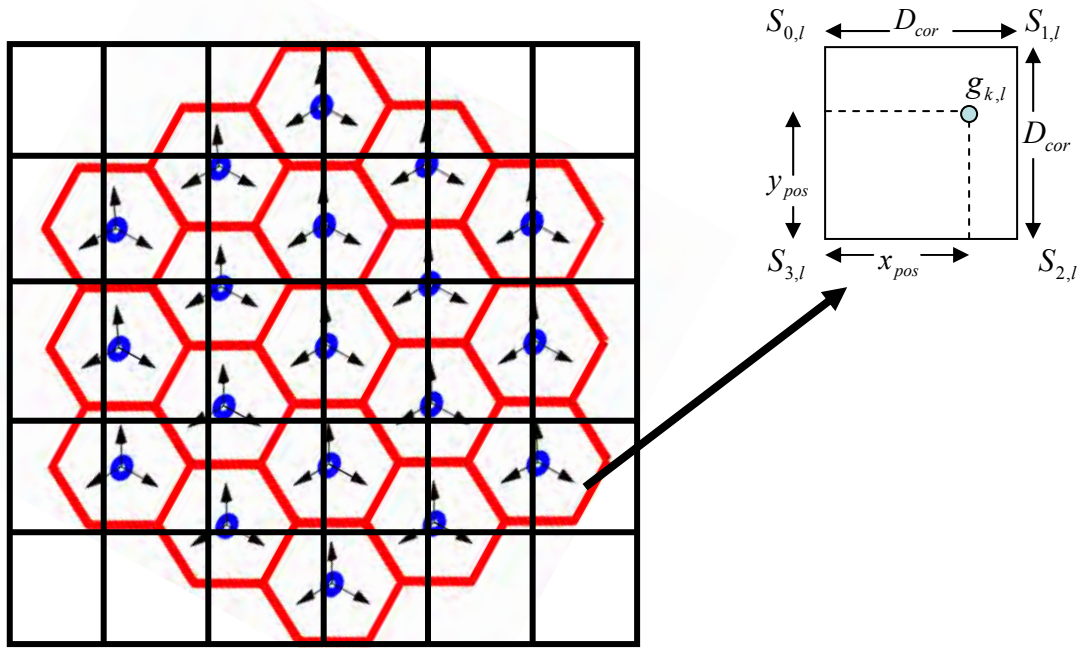


Figure 5: Shadowing factor grid example showing interpolation

The shadow fading $SB_{n,lB}$ at the nodes is modeled as a Gaussian distributed random variable with zero mean and standard deviation σ as defined in Table 8. The shadow fading component is expressed as the weighted sum of a common component, Z_n , to all cell sites, and an independent component, Z_l , from each cell site. In other words, Z_n is generated based on local shadowing point at the node coordinates (e.g. related to a mobile station location), and Z_l is generated based on local shadowing point for a given base station. The shadow fading value between node n and base station l is $SB_{n,lB} = aZ_n + bZ_l$. Typical values for a and b are $a^2 = b^2 = 1/2$. That is, the correlation is 0.5 between sectors from different cells and 1.0 between sectors of the same cell. Once the shadow fading values at the grid nodes have been determined according to the preceding procedure, the interpolation of equation (25) can be carried out according to each mobile location or along the mobile trajectory for handoff simulations during one drop.

3.2.5. Cluster-Delay-Line Models

The CDL models as referred in the WINNER report define tap delayed line models for the power delay profile with additional spatial information such as per-tap mean AoA, AoD, and per-tap angular spread (thus the power angular profile). The CDL models can be deemed as a spatial extension of the TDL model with the number of taps (clusters), their delays and powers, the mean AoA and AoD of each cluster, and the arrival and departure angular spread (AS). So they offer well-defined radio channels with fixed parameters to obtain comparable simulation results with relatively non-complicated channel models. Note that the word “cluster” is used in “clustered delay lines” in a way

that deviates from its commonly accepted definition in the scientific literature. Clusters are either defined as (i) groups of multipath components (MPCs) whose large-scale characteristics change in a similar way (e.g., as the MS moves over large distances, the relative AoAs, AoDs, and delays of the MPCs within one cluster do not change, or (ii) as groups of MPCs with similar delays, AoAs, and AoDs. For the latter definition, it is important to notice the difference between clusters and multipath groups. i.e., a number of MPCs that are indistinguishable to a RX because of limited resolution are different from a cluster. A cluster consists usually of several multipath groups with similar delays and angles, and is surrounded (in the delay-angle plane) by areas of no "significant" power. For a receiver with very low angular/delay resolution, it might happen that each cluster contains only a single multipath group, or even that a multipath group contains several clusters. Consequently, the MPCs belonging to a cluster do not change, even as the resolution of the measurement device becomes finer and finer; while the MPCs belonging to a multipath group change as the resolution becomes finer.

As discussed in Section 3.1, the use of fixed values for delay and mean AoA/AoD makes the CDL model a simplification, as it does not account for the (experimentally observed) random variations of delay spread, angular spread, etc. This might have significant consequences for the absolute and even relative performance of various systems. While the model is suitable for the purposes of standardization, it is not recommended for scholarly investigations.

For each propagation scenario, the corresponding CDL model is given in one of the following subsections. It includes power delay profile and the corresponding per-tap power angular profile. Note that the AoA and AoD values given in the following tables are the mean AoA/AoD of each cluster (i.e., tap or path). The mean power of each tap and its delay is also given. The ray power is 1/20 of the mean tap power (i.e., -13 dB).

In a CDL model, each tap may be simulated via generating 20 equal-power rays with fixed offset angles, as suggested in WINNER. The offset angles are the same as those defined in SCM and they are specified in a way such that by adjusting the interval between these equal-power rays a Laplacian power angular profile can be approximated. Note that the offset angles are the deviation from the mean AoA/AoD (Refer to Table 65 in Appendix A for the offset). In the case when a ray of dominant power exists, the cluster has 20+1 rays. This dominant ray has a zero angle offset. The departure and arrival rays are coupled randomly.

CDL models also allow for the generation of spatial correlation mathematically, which can be used directly to generate the matrix channel coefficients. The spatial correlation for each tap can be derived from the mean AoA/AoD and the Laplacian power angular profile with the specified angular spread. Per-tap correlation can also be derived numerically based on the 20 equal-power rays used to approximate the Laplacian power angular profile.

Most of the taps have a single delay. In case a tap has three delays values, these correspond to sub-clusters as defined in the table below[§]:

Sub-cluster #	Mapping to Rays	Fractional Power	Delay Offset (ns)
1	1,2,3,4,5,6,7,8,19,20	10/20	0
2	9,10,11,12,17,18	6/20	5
3	13,14,15,16	4/20	10

Table 9: Sub-cluster model used for some taps in spatial TDL or CDL model

The sub-cluster can be easily simulated with a ray-based model. But when a spatial correlation is computed in the correlation-based implementation, the three sub-taps should be approximated to have the same correlation. $AS_{BS} AS_{MS}$

The cross polarization ratio XPR_V is the power ratio of vertical-to-vertical polarized component to vertical-to-horizontal polarized component, XPR_H is the power ratio of horizontal-to-horizontal polarized component to horizontal-to-vertical polarized component. It is assumed that $XPR_V = XPR_H = XPR$ and the cross polarization ratios are assumed the same for all clusters (i.e., taps). A reference cross polarized antenna configuration is also defined in order to derive spatial correlation, in which case the BS antenna element is assumed to be 45-deg cross-polarized and the MS antenna element is 90-deg cross-polarized, as assumed in Appendix B.

3.2.5.1. Urban Macrocell (Optional)

Cluster #	Delay [ns]			Power [dB]			AoD [°]	AoA [°]	Ray power [dB]	Cluster $AS_{BS} = 2^\circ$	Cluster $AS_{MS} = 15^\circ$
1	0			-6.4			11	61	-19.5		
2	60			-3.4			-8	44	-16.4		
3	75			-2.0			-6	-34	-15.0		
4	145	150	155	-3.0	-5.2	-7.0	0	0	-13.0		
5	150			-1.9			6	33	-14.9		
6	190			-3.4			8	-44	-16.4		
7	220	225	230	-3.4	-5.6	-7.4	-12	-67	-13.4		
8	335			-4.6			-9	52	-17.7		
9	370			-7.8			-12	-67	-20.8		
10	430			-7.8			-12	-67	-20.8		
11	510			-9.3			13	-73	-22.3		
12	685			-12.0			15	-83	-25.0		
13	725			-8.5			-12	-70	-21.5		

[§] It must be noted that the power delay profiles provided for different test scenarios may not represent channels that are normalized in terms of power.

14	735	-13.2	-15	87	-26.2		
15	800	-11.2	-14	80	-24.2		
16	960	-20.8	19	109	-33.8		
17	1020	-14.5	-16	91	-27.5		
18	1100	-11.7	15	-82	-24.7		
19	1210	-17.2	18	99	-30.2		
20	1845	-16.7	17	98	-29.7		

Table 10: Urban macrocell CDL (XPR = 5 dB)

Cluster #	Delay [ns]			Power [dB]			AoD [°]	AoA [°]	Ray power [dB]	Cluster AS _{BS} = 2°	Cluster AS _{MS} = 15°
1	0			-4.7			-10	61	-17.7		
2	0	5	10	-3	-5.2	-7	0	0	-13		
3	10			-7.2			12	-75	-20.2		
4	10			-6.3			-11	-70	-19.3		
5	30	35	40	-4.8	-7	-8.8	-12	76	-14.8		
6	50			-3.7			-9	53	-16.7		
7	80			-7.4			-12	76	-20.4		
8	110			-7.2			12	-75	-20.2		
9	155			-9.6			14	-87	-22.7		
10	165			-5.2			-10	64	-18.3		
11	165			-6.3			11	70	-19.3		
12	250			-8.9			14	83	-21.9		
13	280			-8.5			13	-81	-21.5		
14	440			-8.4			13	-81	-21.4		
15	490			-8.5			-13	81	-21.5		
16	525			-5			10	62	-18		
17	665			-10.9			15	92	-23.9		
18	685			-10.9			15	92	-24		
19	4800			-9.7			-135	25	-22.7		
20	7100			-13			80	40	-26		

Table 11: Bad urban macrocell CDL (XPR = 5 dB)

3.2.5.2. Suburban Macrocell (Optional)

Cluster #	Delay [ns]			Power [dB]			AoD [°]	AoA [°]	Ray power [dB]	Cluster AS _{BS} = 2°	Cluster AS _{MS} = 10°
1	0	5	10	-3.0	-5.2	-7.0	0	0	-13.0		
2	25			-7.5			13	-71	-20.5		
3	35			-10.5			-15	-84	-23.5		
4	35			-3.2			-8	46	-16.2		
5	45	50	55	-6.1	-8.3	-10.1	12	-66	-16.1		

6	65	-14.0	-17	-97	-27.0		
7	65	-6.4	12	-66	-19.4		
8	75	-3.1	-8	-46	-16.1		
9	145	-4.6	-10	-56	-17.6		
10	160	-8.0	-13	73	-21.0		
11	195	-7.2	12	70	-20.2		
12	200	-3.1	8	-46	-16.1		
13	205	-9.5	14	-80	-22.5		
14	770	-22.4	22	123	-35.4		

Table 12: Suburban macrocell CDL (XPR = 5.5 dB)

3.2.5.3. Urban Microcell (Optional)

In the LOS model Ricean K-factor is 3.3 dB, which corresponds to 20m distance between Tx and Rx.

Cluster #	Delay [ns]			Power [dB]			AoD [°]	AoA [°]	Ray power [dB]		Cluster ASD = 3°	Cluster AS _{MS} = 18°
1	0			0.0			0	0	-0.31 [*]	-24.7 ^{**}		
2	30	35	40	-10.5	-12.7	-14.5	5	45	-20.5			
3	55			-14.8			8	63	-27.8			
4	60	65	70	-13.6	-15.8	-17.6	8	-69	-23.6			
5	105			-13.9			7	61	-26.9			
6	115			-17.8			8	-69	-30.8			
7	250			-19.6			-9	-73	-32.6			
8	460			-31.4			11	92	-44.4			

Table 13: Urban microcell CDL (LOS) (XPR = 9.5 dB)

* Power of dominant ray,

** Power of each other ray

Cluster #	Delay [ns]			Power [dB]			AoD [°]	AoA [°]	Ray power [dB]	Cluster AS _{BS} = 10°	Cluster AS _{MS} = 22°
1	0			-1.0			8	-20	-14.0		
2	90	95	100	-3.0	-5.2	-7.0	0	0	-13.0		
3	100	105	110	-3.9	-6.1	-7.9	-24	57	-13.9		
4	115			-8.1			-24	-55	-21.1		
5	230			-8.6			-24	57	-21.6		
6	240			-11.7			29	67	-24.7		
7	245			-12.0			29	-68	-25.0		
8	285			-12.9			30	70	-25.9		
9	390			-19.6			-37	-86	-32.6		
10	430			-23.9			41	-95	-36.9		
11	460			-22.1			-39	-92	-35.1		
12	505			-25.6			-42	-99	-38.6		
13	515			-23.3			-40	94	-36.4		
14	595			-32.2			47	111	-45.2		
15	600			-31.7			47	110	-44.7		
16	615			-29.9			46	-107	-42.9		

Table 14: Urban microcell CDL (NLOS) (XPR = 7.5 dB)

1 Bad Urban Microcell (Optional)

Cluster #	Delay [ns]			Power [dB]			AoD [°]	AoA [°]	Ray power [dB]	Cluster AS _{BS} = 3°	Cluster AS _{MS} = 5°
1	0	5	10	-3.0	-5.2	-7.0	0	0	-13.0		
2	25	30	35	-3.4	-5.6	-7.3	-14	31	-13.4		
3	25			-1.7			-13	30	-14.7		
4	35			-1.9			-14	31	-14.9		
5	45			-2.2			15	-34	-15.2		
6	70			-5.0			22	51	-18.0		
7	70			-3.6			19	44	-16.6		
8	90			-3.8			-19	-45	-16.8		
9	155			-6.4			-25	-58	-19.4		
10	170			-2.7			-17	-38	-15.7		
11	180			-7.5			-27	-63	-20.5		
12	395			-16.5			-41	93	-29.5		
13	1600			-5.7			-110	15	-18.7		
14	2800			-7.7			75	-25	-20.7		

Table 15: Bad urban microcell CDL (NLOS) (XPR = 7.5 dB)

4 3.2.5.4. Indoor Small Office (Optional)

5 Only NLOS condition is given below.

Cluster #	Delay [ns]			Power [dB]			AoD [°]	AoA [°]	Ray power [dB]	Cluster AS _{BS} = 5°	Cluster AS _{MS} = 5°
1	0	5	10	-3.0	-5.2	-7.0	0	0	-13.0		
2	5			-4.0			59	-55	-17.0		
3	20			-4.7			-64	-59	-17.7		
4	25			-9.0			89	-82	-22.0		
5	30			-8.0			83	-77	-21.0		
6	30	35	40	-4.0	-6.2	-8.0	-67	62	-14.0		
7	35			-1.1			32	29	-14.2		
8	45			-5.2			-67	62	-18.2		
9	55			-9.5			-91	-84	-22.5		
10	65			-7.9			-83	77	-20.9		
11	75			-6.8			-77	-71	-19.8		
12	90			-14.8			-113	105	-27.8		
13	110			-12.8			-106	98	-25.8		
14	140			-14.1			111	-103	-27.2		
15	210			-26.7			-152	141	-39.7		
16	250			-32.5			-168	-156	-45.5		

Table 16: Indoor small office (NLOS) (XPR = 10 dB)

9 3.2.5.5. Indoor Hotspot (Optional)

10 The CDL parameters of LOS and NLOS condition are given below. In the LOS model
 11 Ricean K factor are 15.3 dB and 10.4 dB, respectively for the first and second clusters.
 12

Cluster #	Delay [ns]	Power [dB]	AoD [°]	AoA [°]	Ray power [dB]	
1	0	0	0	0	-0.1*	-28.4**
2	5	-3.4	7	-2	-3.7*	-27.1**
3	10	-9.2	0	-12	-22.2	
4	20	-18.9	7	13	-31.9	
5	30	-17.1	11	16	-30.1	
6	40	-16.3	-7	-34	-29.3	
7	50	-13.7	-60	-12	-26.7	
8	60	-16.3	-43	-17	-29.3	
9	70	-16.8	11	-59	-29.8	
10	80	-17.9	8	-78	-30.9	
11	90	-15.9	14	-65	-28.9	
12	100	-17.4	-1	-56	-30.4	
13	110	-25.8	-11	-57	-38.8	
14	120	-31.0	-129	-22	-44.0	
15	130	-33.4	-123	-12	-46.4	

Cluster AS_{BS} = 5°Cluster AS_{MS} = 8°

Table 17: Indoor hotspot CDL (LOS) (XPR = 11dB)

* Power of dominant ray,

** Power of each other ray

Cluster #	Delay [ns]	Power [dB]	AoD [°]	AoA [°]	Ray power [dB]
1	0	-6.9	2	2	-19.9
2	5	0	-2	9	-13.0
3	10	-0.7	-7	14	-13.7
4	15	-1.0	-3	-7	-14.0
5	20	-1.4	-1	-6	-14.4
6	25	-3.8	-5	-18	-16.8
7	30	-2.6	0	-3	-15.6
8	35	-0.2	-6	-3	-13.2
9	45	-3.6	-9	14	-16.6
10	55	-5.7	1	44	-18.7
11	65	-11.6	4	13	-24.6
12	75	-8.9	-5	65	-21.9
13	95	-7.3	-11	46	-20.3
14	115	-11.2	-4	35	-24.2
15	135	-13.5	-3	48	-26.5
16	155	-13.4	-7	41	-26.4
17	175	-12.2	8	7	-25.2

Cluster AS_{BS} = 5°Cluster AS_{MS} = 11°

18	195	-14.7	4	69	-27.7
19	215	-15.8	-11	133	-28.8

Table 18: Indoor hotspot CDL (NLOS) (XPR = 11dB)

3.2.5.6. Outdoor to Indoor (Optional)

Cluster #	Delay [ns]	Power [dB]	AoD [°]	AoA [°]	Ray power [dB]		
1	0	-7.7	29	102	-20.8	Cluster AS _{BS} = 5°	Cluster AS _{MS} = 8°
2	10 15 20	-3.0 -5.2 -7.0	0	0	-13.0		
3	20	-3.7	20	70	-16.7		
4	35	-3.0	-18	-64	-16.0		
5	35	-3.0	18	-63	-16.0		
6	50	-3.7	20	70	-16.7		
7	55 60 65	-5.4 -7.6 -9.4	29	100	-15.4		
8	140	-5.3	24	84	-18.3		
9	175	-7.6	29	100	-20.6		
10	190	-4.3	-21	76	-17.3		
11	220	-12.0	36	-126	-25.0		
12	585	-20.0	46	163	-33.0		

Table 19: Outdoor to indoor CDL (NLOS) (XPR = 8 dB)

3.2.5.7. Rural Macrocell (Optional)

The CDL parameters of LOS and NLOS condition are given below. In the LOS model Ricean K-factor is 13.7 dB.

Cluster #	Delay [ns]	Power [dB]	AoD [°]	AoA [°]	Ray power [dB]		
1	0	0.0	0	0	-0.02* -35.9**	Cluster AS _{BS} = 2°	Cluster AS _{MS} = 3°
2	40	-22.3	-95	189	-35.3		
3	40	-25.6	102	203	-38.6		
4	40 45 50	-23.1 -25.3 -27.1	-90	-179	-33.1		
5	40 45 50	-23.7 -25.9 -27.7	104	-208	-33.7		
6	60	-27.4	-105	210	-40.4		
7	115	-27.0	104	-208	-40.0		
8	135	-25.2	-101	-201	-38.2		
9	175	-30.1	110	-219	-43.1		
10	195	-32.5	114	228	-45.5		
11	215	-31.7	-113	-225	-44.7		
12	235	-33.9	-117	-233	-46.9		
13	235	-31.0	-112	223	-44.0		

Table 20: Rural macrocell CDL (LOS) (XPR = 7dB)

* Power of dominant ray,

** Power of each other ray

Cluster #	Delay [ns]			Power [dB]			AoD [°]	AoA [°]	Ray power [dB]	Cluster AS _{BS} = 2°	Cluster AS _{MS} = 3°
1	0	5	10	-3.0	-5.2	-7.0	0	0	-13.0		
2	0			-1.8			-8	28	-14.8		
3	5			-3.3			-10	38	-16.3		
4	10	15	20	-4.8	-7.0	-8.8	15	-55	-14.8		
5	20			-5.3			13	48	-18.3		
6	25			-7.1			15	-55	-20.1		
7	55			-9.0			-17	62	-22.0		
8	100			-4.2			-12	42	-17.2		
9	170			-12.4			20	-73	-25.4		
10	420			-26.5			29	107	-39.5		

Table 21: Rural macrocell CDL (NLOS) (XPR = 7dB)

3.2.6. Channel Type and Velocity Mix

In system level simulations, users may be associated with a set of different channel types and velocities. In such cases, a mix of user speeds and channel types is evaluated.

The channel types and mobility mixes corresponding to the required test scenarios are defined in Table 3.

3.2.7. Doppler Spectrum for Stationary Users

If the TX and the RX are stationary, and the channel at time t is to be computed, then each cluster is made of a number of coherent (fixed) rays N_c and a number of scattered (variable) rays N_s ($N_c + N_s$ = total number of rays per clusters).

The variable rays are ascribed a bell-shaped Doppler spectrum as described in [3]:

$$S(f) = \begin{cases} 1 - 1.72f_0^2 + 0.785f_0^4 & |f_0| \leq 1 \\ 0 & |f_0| > 1 \end{cases} \quad \text{where } f_0 = \frac{f}{f_m} \quad (26)$$

where f_m is the maximum Doppler rate (suggested value: 2 Hz in [3]). The fixed rays within a cluster share the same amplitude and phase, and their Doppler spectrum is a Dirac impulse at $f = 0$ Hz.

An alternative is to simply model the Doppler spectrum as a Jakes spectrum with 2 Hz Doppler frequency.

3.2.8. Generation of Spatial Channels

The following procedure describes the simulation procedure based on the spatial TDL or CDL models. In the correlation based implementation, the spatial and temporal

correlation need to be derived first before generating the channel coefficients. In the ray-based approach, the time-variant matrix channels are constructed from all the rays.

Step 1: Choose a propagation scenario (e.g. Urban Macro, Suburban Macro etc.). After dropping a user, determine the various distance and orientation parameters.

The placement of the MS with respect to each BS is to be determined according to the cell layout. From this placement, the distance between the MS and the BS (d) and the LOS directions with respect to the BS and MS (θ_{BS} and θ_{MS} respectively) can be determined. Note that θ_{BS} and θ_{MS} are defined relative to the broadside directions. The MS antenna array orientations (Ω_{MS}), are i.i.d., drawn from a uniform 0 to 360 degree distribution.

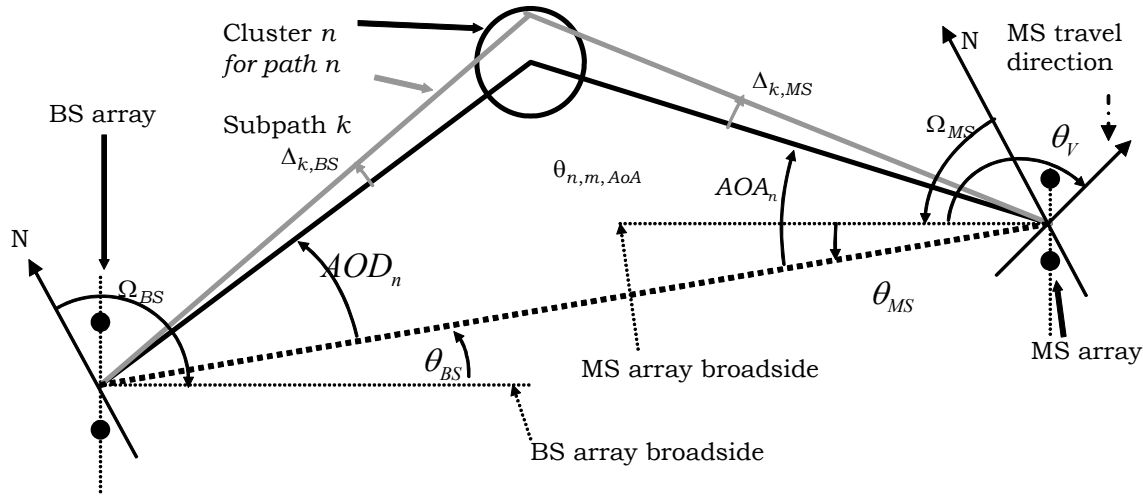


Figure 6: The MIMO channel model angle parameters

Step 2: Calculate the bulk path loss associated with the BS to MS distance.

Step 3: Determine the Shadowing Factor (SF).

The SF is randomly generated from a log-normal distribution with a pre-specified standard deviation. Generate the SF according to Section 3.2.4

If a ray-based implementation is being used, skip steps 4, 6 and 7.

Step 4: Calculate the per-tap spatial correlation matrix based on per-tap $AS_{BS, path}$ at the BS and the per-tap $AS_{MS, path}$ at the MS, both of which are specified in the reduced complexity models specified in 3.2.5. The spatial correlation also depends on the BS/MS antenna configurations (a random broadside direction, number and spacing of antennas, polarization, etc.)

Once the per-tap AS, mean AoA, and mean AoD are defined, the theoretical spatial correlation at both BS and MS can be derived, assuming Laplacian power angular

distribution. Assuming omni directional antennas at the BS and MS the antenna spatial correlations, the antenna spatial correlations between the p-th and q-th antenna at the BS and MS respectively, are

$$r_{n,BS}(p, q) = \int_{-\infty}^{\infty} f(\alpha) \exp \left\{ j \frac{2\pi d_{BS}}{\lambda} (p - q) \sin(AOD_n + \alpha) \right\} d\alpha$$

$$r_{n,MS}(p, q) = \int_{-\infty}^{\infty} f(\beta) \exp \left\{ j \frac{2\pi d_{MS}}{\lambda} (p - q) \sin(AOA_n + \beta) \right\} d\beta$$
(27)

where d_{BS} (d_{MS}) is the antenna spacing at BS (MS) and λ is the wavelength. α is the angular offset around the mean AoD at BS, and β is the angular offset around the mean AoA at MS. The PDF of angular offsets is

$$f(\alpha) = \frac{1}{\sqrt{2} AS_{BS, Path}} \exp \left\{ -\frac{\sqrt{2} |\alpha|}{AS_{BS, Path}} \right\}$$

$$f(\beta) = \frac{1}{\sqrt{2} AS_{MS, Path}} \exp \left\{ -\frac{\sqrt{2} |\beta|}{AS_{MS, Path}} \right\}$$
(28)

Note that $AS_{BS, path}$ and $AS_{MS, path}$ are specified in the reduced complexity models specified in 3.2.5. The above integration can be computed with two approaches (other alternatives may also exist). Refer to Appendix A for details. In summary, the first approach is to approximate the Laplacian PDF with 20 rays, after which the integration is reduced to a summation. The second approach is to compute the integration using a numerical method. The second approach is to compute the integration using the exact expression given in the Appendix A. Either using 20-ray approximation or exact expression, it is possible to quantize the AoA or AoD and then pre-compute the spatial correlation for each quantized AoA and AoD values. Using pre-stored correlation matrices may reduce the simulation run-time.

Denoting the spatial correlation matrix at BS and MS as $\mathbf{R}_{BS,n}$ and $\mathbf{R}_{MS,n}$, the per-tap spatial correlation is determined as

$$\mathbf{R}_n = \mathbf{R}_{BS,n} \otimes \mathbf{R}_{MS,n} \text{ (Kronecker product)}$$
(29)

In the case that the antenna elements are cross-polarization antennas, we denote the number of receive antennas by N and the number of transmit antennas by M. If cross-polarized antennas are present at the receiver, it is assumed that the N/2 receive antennas have the same polarization, while the remaining N/2 receive antennas have the orthogonal polarization. Likewise, if cross-polarized antennas are present at the transmitter, it is assumed that M/2 transmit antennas have the same polarization, while the remaining M/2 transmit antennas have orthogonal polarization. It is further assumed that the antenna arrays are composed of pairs of co-located antennas with orthogonal polarization. With these assumptions, the per-tap channel correlation is determined as

$$\mathbf{R}_n = \mathbf{R}_{BS,n} \otimes \mathbf{\Gamma} \otimes \mathbf{R}_{MS,n}$$
(30)

Where $R_{MS,n}$ is a $N \times N$ matrix if all the receive antennas have the same polarization, or a $(N/2) \times (N/2)$ matrix if the receive antennas are cross-polarized. Likewise, $R_{BS,n}$ is a $M \times M$ matrix if all the transmit antennas have the same polarization, or a $(M/2) \times (M/2)$ matrix if the transmit antennas are cross-polarized. Γ is a cross-polarization matrix based on the cross polarization defined in the CDL models. Γ is a 2×2 matrix if cross-polarized antennas are used at the transmitter or at the receiver. It is a 4×4 matrix if cross-polarized antennas are used at both the transmitter and the receiver. An example of how to derive Γ is given in Appendix B based on the assumption of a default antenna configuration with cross-polarized antennas at both the transmitter and the receiver. Γ is just a scalar equal to one if all antennas have the same polarization.

Step 5: Determine the antenna gains of the BS and MS paths as a function of their respective AoDs and AoAs. Calculate the per-tap average power with BS/MS antenna gain as

$$P_n^* = P_n \bullet G_{BS}(AOD_n + \theta_{BS}) \bullet G_{MS}(AOA_n + \theta_{MS}) \quad (31)$$

Step 6: Determine Doppler spectrum using *Jakes spectrum*. It is recognized that the use of a Jakes spectrum is self-inconsistent when a non-uniform power angular spectrum occurs at the mobile station. However, it is used in simulations to trade off between simulation complexity and model accuracy. Generating the time-varying fading process from a Doppler spectrum based on the traveling direction and mean AoA can be computationally expensive. The impact on the overall system level performance with this more accurate method may be small. This method will facilitate easy generation of such a time-varying process (e.g. offline generation).

Step 7: Generate time-variant MIMO channels with above-defined per-tap spatial correlations.

For each tap, generate $N \times M$ i.i.d. channels first that satisfies the specified Doppler spectrum H_{iid} (each tap is a $N \times M$ matrix) where N is the number of receive antennas and M is the number of transmit antennas.

To generate temporally correlated Gaussian process that satisfies a specific Doppler spectrum, one implementation method is to use the summation of equal-power sinusoids where their frequencies are calculated numerically using either Method of Exact Doppler Spread (MEDS) or L_2 -Norm Method (LNPM) [23]. Pre-computing the sinusoid frequencies for a set of quantized angle \mathcal{G}_n can be considered as a means to reduce simulation run time, comparing with computing the sinusoid frequencies on the fly. As an example, a non-Jakes Doppler spectrum can be simulated using the summation of 10 equal-power sinusoids with random phases, but their frequencies are defined as

$$f_{n,i} = f_{\max} \cos(\phi_{n,i}) \quad (32)$$

where

$$\phi_{n,i} = \mathcal{G}_n + AS_{MS,Path} * [-1.8157, -1.0775, -0.6456, -0.3392, -0.1015, 0.1015, 0.3392, 0.6456, 1.0775, 1.8157]$$

It is also possible to use more than 10 sinusoids where the angle spacing between equal power sub-rays is chosen to make sure that area under the Laplacian PDF (i.e., separated by the sub-rays) equal to $1/(N+1)$ where N is the number of sub-rays, i.e., for the positive side

$$\frac{1}{2} \left[\exp \left\{ -\frac{\sqrt{2}|\alpha_1|}{AS} \right\} - \exp \left\{ -\frac{\sqrt{2}|\alpha_2|}{AS} \right\} \right] = \frac{1}{N+1} \quad (33)$$

where α_1 and α_2 are two adjacent angles with an increasing order and for the first angle on the positive side assuming an even N is

$$\frac{1}{2} \left[1 - \exp \left\{ -\frac{\sqrt{2}|\alpha_1|}{AS} \right\} \right] = \frac{0.5}{N+1} \quad (34)$$

For $N=10$ and $AS=1$, the angles are $[\pm 1.2054 \quad \pm 0.7153 \quad \pm 0.4286 \quad \pm 0.2252 \quad \pm 0.0674]$. Note that due to finite quantization, the standard deviation of all the ten angles is not “1” any more, it is $C=0.6639$ instead. So scaling of $1/C$ must be used to compensate for the finite quantization.

Compute the correlated channel at each tap as

$$\mathbf{H}_n = \text{unvec} \left\{ R_n^{1/2} \text{vec}(H_{iid}) \right\} \quad (35)$$

where $\text{vec}(H)$ denotes the column-wise stacking of matrix H and unvec is the reverse operation. $R_n^{1/2}$ denotes the square-root of matrix R_n .

Step 8 (Ray-based method only, Skip for correlation-based implementation):
Generate time-variant MIMO channels.

For an N element linear BS array and a M element linear MS array, the channel coefficients for one of L multipath components are given by a $N \times M$ matrix of complex amplitudes. We denote the channel matrix for the n th multipath component ($n = 1, \dots, L$) as $\mathbf{H}_n(t)$. The (u,s) th component ($s = 1, \dots, N$, $u = 1, \dots, M$) of $\mathbf{H}_n(t)$ is given in the following, assuming polarized arrays (If polarization is not considered, the 2×2 polarization matrix can be replaced by scalar $\exp(\Phi_{n,m})$ and only vertically polarized field patterns applied)

$$h_{u,s,n}(t) = \sqrt{\frac{P_n \sigma_{SF}}{M}} \sum_{m=1}^M \begin{pmatrix} \left[\begin{array}{c} \chi_{BS}^{(v)}(\theta_{n,m,AoD}) \\ \chi_{BS}^{(h)}(\theta_{n,m,AoD}) \end{array} \right]^T \left[\begin{array}{cc} \exp(j\Phi_{n,m}^{(v,v)}) & \sqrt{r_{n1}} \exp(j\Phi_{n,m}^{(v,h)}) \\ \sqrt{r_{n2}} \exp(j\Phi_{n,m}^{(h,v)}) & \exp(j\Phi_{n,m}^{(h,h)}) \end{array} \right] \left[\begin{array}{c} \chi_{MS}^{(v)}(\theta_{n,m,AoA}) \\ \chi_{MS}^{(h)}(\theta_{n,m,AoA}) \end{array} \right] \\ \exp(jkd_s \sin(\theta_{n,m,AoD})) \times \exp(jkd_u \sin(\theta_{n,m,AoA})) \times \exp(jk\|\mathbf{v}\| \cos(\theta_{n,m,AoA} - \theta_v) t) \end{pmatrix} \times \quad (36)$$

where

P_n is the power of the n th path

σ_{SF}	is the lognormal shadow factor
M	is the number of subpaths per-path.
$\theta_{n,m,AoD}$	is equal to $(AoD_n + \alpha + \theta_{BS})$, where α is the angular offset around the mean AoD_n at BS (Refer to angular offsets in Appendix A).
$\theta_{n,m,AoA}$	is equal to $(AoA_n + \beta + \theta_{MS})$, where β is the angular offset around the mean AoA_n at MS (Refer to angular offsets in Appendix A).
j	is the square root of -1.
k	is the wave number $2\pi/\lambda$ where λ is the carrier wavelength in meters.
d_s	is the distance in meters from BS antenna element s from the reference ($s = 1$) antenna. For the reference antenna $s = 1$, $d_1=0$.
d_u	is the distance in meters from MS antenna element u from the reference ($u = 1$) antenna. For the reference antenna $u = 1$, $d_1=0$.
$\Phi_{n,m}$	is the phase of the m th subpath of the n th path.
$\ \mathbf{v}\ $	is the magnitude of the MS velocity vector.
θ_v	is the angle of the MS velocity vector with respect to the MS broadside.
$\chi_{BS}^{(v)}(\theta_{n,m,AoD})$	is the BS antenna complex response for the V-pol component.
$\chi_{BS}^{(h)}(\theta_{n,m,AoD})$	is the BS antenna complex response for the H-pol component.
$\chi_{MS}^{(v)}(\theta_{n,m,AoA})$	is the MS antenna complex response for the V-pol component.
$\chi_{MS}^{(h)}(\theta_{n,m,AoA})$	is the MS antenna complex response for the H-pol component.
r_{n1}	is the random variable representing the power ratio of waves of the n th path leaving the BS in the vertical direction and arriving at the MS in the horizontal direction (v-h) to those leaving in the vertical direction and arriving in the vertical direction (v-v).
r_{n2}	is the random variable representing the power ratio of waves of the n th path leaving the BS in the horizontal direction and arriving at the MS in the vertical direction (h-v) to those leaving in the vertical direction and arriving in the vertical direction (v-v).
$\Phi_{n,m}^{(x,y)}$	phase offset of the m th subpath of the n th path between the x component (either the horizontal h or vertical v) of the BS element and the y component (either the horizontal h or vertical v) of the MS element.]

Step 9: If a non-zero K -factor is to be enforced (i.e., $K \neq 0$), adjust the LOS path power. Refer to Appendix C for details.

Step 10: Introduce receive antenna gain imbalance or coupling, if needed. Refer to Appendix D for details.

3.2.9. Channel Model for Baseline Test Scenario (Mandatory)

In section 2.3, a baseline test scenario with a 2x2 antenna configuration is defined for calibrating system level simulators. A similar test scenario is also defined for liaising with NGMN.

A simplified correlation-based approach is used to implement the channel model for these test scenarios by determining a spatial correlation matrix for each user and applying the same correlation matrix for all the taps of the ITU TDL model [4].

Two types of spatial correlation are defined, assuming the Jakes Doppler spectrum for both cases:

Case 1: Uncorrelated antennas at both BS and MS

Case 2: Uncorrelated antennas at MS, correlated antennas at BS with the correlation (identical for all taps) derived as in Appendix-A according to the following assumptions:

- Mean AoD determined according to the MS-BS LOS direction, relative to the BS antenna array bore sight.
- Uniform linear antenna array at the BS with any number of elements and an inter-element spacing of 4 wavelengths for baseline 2x2 antenna configuration (refer to Table 1 and Table 2).
- Laplacian angular power profile at the BS with an angular spread of 3 degrees for baseline test scenario corresponding to 1.5 km site-to-site distance, and 15 degrees for the NGMN configuration with 0.5 km site-to-site distance (15 degrees is the same as the mean angular spread specified in 3GPP/3GPP2 SCM urban macrocell environment).

The two test scenarios and the methodology described in this section are also suitable to optionally simulate larger antenna configurations with any number of antennas at the BS and MS, different antenna spacing and angular spreads.

The default ITU channel models are described by their power delay profiles as they appear in Table 22.

Path Index	Pedestrian B		Vehicular A	
	Power (dB)	Delay (ns)	Power (dB)	Delay (ns)
1	-3.9179	0	-3.1426	0
2	-4.8175	200	-4.1420	310
3	-8.8174	800	-12.1396	710
4	-11.9179	1200	-13.1426	1090
5	-11.7198	2300	-18.1531	1730
6	-27.6955	3700	-23.0980	2510

Table 22: ITU power delay profiles

The modified power delay profiles [72] for the ITU channel models are specified in Table 23. Baseline channel models for a 10MHz system bandwidth as defined in Table 3 shall use these profiles. Table 23 provides the delays relative to the first path in nanoseconds and the relative power of each path compared to the strongest (similar to the default ITU models). The modified ITU Pedestrian B and Vehicular A channel models use 24 paths.

Path Index	Modified Pedestrian B		Modified Vehicular A	
	Power (dB)	Delay (ns)	Power (dB)	Delay (ns)
1	-1.175	0	-3.1031	0
2	0	40	-0.4166	50
3	-0.1729	70	0	90
4	-0.2113	120	-1.0065	130
5	-0.2661	210	-1.4083	270
6	-0.3963	250	-1.4436	300
7	-4.32	290	-1.5443	390
8	-1.1608	350	-4.0437	420
9	-10.4232	780	-16.6369	670
10	-5.7198	830	-14.3955	750
11	-3.4798	880	-4.9259	770
12	-4.1745	920	-16.516	800
13	-10.1101	1200	-9.2222	1040
14	-5.646	1250	-11.9058	1060
15	-10.0817	1310	-10.1378	1070
16	-9.4109	1350	-14.1861	1190
17	-13.9434	2290	-16.9901	1670
18	-9.1845	2350	-13.2515	1710
19	-5.5766	2380	-14.8881	1820
20	-7.6455	2400	-30.348	1840
21	-38.1923	3700	-19.5257	2480
22	-22.3097	3730	-19.0286	2500
23	-26.0472	3760	-38.1504	2540
24	-21.6155	3870	-20.7436	2620

Table 23: Modified ITU profiles for wideband systems

3.3. Link Level Channel Model

The link level channel model should be the same as the CDL channel model described in Section 3.2.

For various propagation scenarios, the corresponding CDL model can be directly used for link simulation, assuming the AoA and AoD are relative to the broadside direction of the receiver array, instead of assuming random orientation of the array in system simulations.

In the case of correlation-based implementation, the spatial correlation can be easily derived once the AoA/AoD is well defined based on either 20-ray approximation or numerical integration. The antenna configuration is assumed to either be a linear array, or a polarized antenna with XPD values defined in the CDL models. The antenna spacing in the linear array shall be of 4 wavelengths at the base station as specified in Section 3.2.9 for the mandatory test scenarios in Case 2 with correlated antennas, or it may be chosen as 0.5, 4 or 10 wavelengths for optional scenarios. The Doppler spectrum depends on traveling direction relative to the AoA. Instead of setting a random traveling direction which can vary from simulation to simulation, a worst case Jakes spectrum should be used.

3.3.1. Link Level Channel Model for Baseline MBSFN Test Scenario (Mandatory)

In a Multicast Broadcast Single Frequency Network (MBSFN), the same signal is transmitted from all BSs in the Single Frequency Network (SFN)-zone with symbol level synchronization. The signals from different BSs coherently combine at the MS to provide improved SNR. There is no interference in SFN since all BSs transmit the same desired signal. However, the effect of multipath is magnified due to the fact that signals from different BSs take different paths and experience different propagation delays. The propagation delays depend fundamentally on the Inter-Site Distance (ISD), which in turn is deployment specific. The other factor that would affect propagation delays is the location of the user. In system level simulations, each of the above mentioned effects can be factored in deriving the MBSFN channel model. However some modifications to the ITU power delay profiles are necessary for MBSFN link level simulation.

The default procedure to generate a MBSFN channel profile is to concatenate several ITU channel profiles, mimicking links from many BSs to a single MS as is the case with broadcast. The modified ITU Vehicular-A channel profile given in Table 23 is assumed as the base channel profile for the link between BS and MS. The location of the MS and those of the BSs are assumed to be known. A composite channel model for MBSFN in a 19 cell hexagonal layout is a concatenation of 19 modified Vehicular-A channel profiles, offset by appropriate propagation delays and scaled by the appropriate path loss powers. The basic system level simulation set up is used to derive the propagation delays.

Step 1: A standard system level simulation set up of 19 cells in a hexagonal grid layout is used. N users (the value of N must be large to get statistically stable values for the propagation delays) are dropped in the center cell, and for each user the values of received power from each cell are collected. The received power is computed as the difference of transmit power (43dBm) and the path loss plus penetration loss. The mandated path loss model is described in Section 3.2.3.8. The received energy is ordered from the largest to the smallest. For each of the N users, an index of cells ordered from the one that contributed to the most energy to the one that contributed to the least can be derived. Using the cell index, the values of the propagation delays (time it takes for the energy to travel from BS to MS) from each cell to the users can be computed.

Step 2: Using the ordered list computed in Step 1, the average propagation delays for the signal with the most energy at the MS, second most energy at the MS and so on so forth can be computed for all the 19 energy contributors. Another permitted variation is to limit the average propagation delay computation to the users in the cell edge i.e., users who are beyond the 95th percentile distance from the central cell. Using this average propagation delay, the average path loss from each cell can be computed by first finding the average distance (from $d = c \times t_p$), where c is the speed of light and t_p is the propagation delay, and then using the average distances in the path loss formula given in Section 3.2.3.8.

Step 3: The relative average propagation delays are computed by subtracting the smallest average propagation delay from the average propagation delays from each cell.

Step 4: The relative average path loss is computed by dividing the average path loss from each cell with the largest average path loss.

Step 5: The base channel model is replicated as many times as the number of the cells, offset by the relative propagation delays and then combined after scaling by the relative average path loss. If $\mathbf{h}(t) = [h_1(t) \ h_2(t-t_1) \ \cdots \ h_{L-1}(t-t_{L-1}) \ h_L(t-t_L)]$ is the base channel model and L is the number of multi-paths, then the concatenated matrix is given by

$$\mathbf{h}_{MBSFN}(t) = \sum_{n=1}^{19} \mathbf{h}(t - \delta_n) g_n$$

where δ_n is the relative average propagation delay of the n^{th} cell and g_n is the relative average path loss of the n^{th} cell. The base channel profiles given in Table 23 are mandatory and either of them can be used. It is recommended that the chosen base model used in the simulations is reported.

Step 6: Paths whose powers are less than a predetermined threshold are removed. The typical threshold value for the power is -30dB.

Step 7: The powers of the channel delay spread, $\mathbf{h}_{MBSFN}(t)$ are normalized.

A few example MBSFN channel delay profiles are presented in Table 24. The modified Vehicular A channel model was used as the base channel model and the propagation delay statistics were averaging across 20,000 users.

	ISD 1500m threshold = -30dB Carrier Frequency = 2.5GHz			ISD 5000m threshold = -30dB Carrier Frequency = 2.5GHz	
	Delay (ns)	Relative Power (dB)		Delay (ns)	Relative Power (dB)
1	0	-11.4490628		0	-11.3740582
2	179	-10.9084665		179	-10.833462
3	357	-8.3406372		357	-10.081528
4	536	-12.4633332		714	-14.0803359
5	714	-9.75337904		1070	-14.8582371
6	1070	-10.7559291		1250	-19.1945833
7	1250	-13.9563018		1610	-20.5965833
8	1430	-12.5029909		1790	-12.1561028
9	1610	-17.7370487		1960	-13.088364

10	1790	-15.1363444		2140	-12.3364301
11	1960	-22.2264545		2500	-14.8459521
12	2140	-16.3332827		2680	-22.4733333
13	2320	-23.8307264		2860	-17.1131391
14	2500	-17.2968504		3040	-21.4494854
15	2680	-17.1954007		3390	-14.8523521
16	2860	-16.0102646		3570	-13.8095188
17	3040	-24.1032045		3750	-14.3093888
18	3210	-23.0282251		4110	-18.3081967
19	3390	-22.457144		4290	-22.472301
20	3570	-18.5806309		4460	-18.0386208
21	3750	-18.0184926		4640	-23.4224441
22	3930	-22.7807536		5000	-24.8244441
23	4110	-18.5275394		5180	-21.7958355
24	4290	-21.9917747		5890	-24.4452598
25	4460	-18.8465526		6070	-26.7011941
26	4640	-23.4780931		7500	-19.6140022
27	4820	-18.6887037		7680	-19.0734059
28	5000	-20.6358428		7860	-18.321472
29	5180	-18.3215816		8210	-22.3202798
30	5360	-24.3514061		8570	-23.098181
31	5540	-19.8948111		8750	-27.4345273
32	5710	-23.1245407		9110	-28.8365273
33	5890	-19.4137505		9290	-25.8079187
34	6070	-21.2027588		10000	-28.4573429
35	6250	-21.2753119		10900	-22.2410927
36	6430	-22.3730786		11100	-21.7004964
37	6610	-21.9777622		11300	-20.9485625
38	6790	-21.569547		11600	-24.9473703
39	6960	-22.9610943		12000	-25.7252715
40	7140	-23.1938225		12700	-22.308965
41	7320	-24.6286689		12900	-22.9831694
42	7500	-24.3724159		13000	-22.2312354
43	7680	-27.727038		13400	-25.0013015
44	7860	-27.3749393		13800	-22.3834939
45	8210	-28.8094026		13900	-22.9928176
46				14100	-22.92716
47				14500	-21.8799534
48				14600	-24.1578138
49				14800	-22.0332653

50				15200	-26.2023184
51				15500	-22.7063434
52				15700	-24.1089393
53				15900	-24.0333418
54				16300	-25.4039075
55				16600	-24.1804962
56				16800	-24.7882738
57				17000	-24.1860396
58				17100	-25.3108767
59				17300	-23.2919693
60				17500	-25.0343227
61				17700	-29.4981878
62				17900	-27.7912713
63				18000	-26.0455696
64				18200	-24.0305013
65				18400	-24.1816707
66				18800	-24.7911385
67				18900	-25.6465326
68				19100	-24.1521644
69				19500	-29.8918585
70				19800	-28.1160842
71				20000	-24.4677523
72				20200	-24.3288341
73				20400	-23.3563092
74				20700	-27.1878413
75				20900	-28.3347599
76				21100	-25.0545844
77				21300	-25.5850098
78				21600	-25.9340901
79				21800	-26.3104614
80				22000	-26.007297
81				22500	-27.3900373
82				22700	-25.8394243
83				22900	-27.2724912
84				24100	-28.6710005
85				24300	-28.0417348
86				24500	-28.5688624

Table 24:MBSFN Channel Profiles for Wideband Systems.

4. Link-to-System Mapping

4.1. Background of PHY Abstraction

The objective of the physical layer (PHY) abstraction is to accurately predict link layer performance in a computationally simple way. The requirement for an abstraction stems from the fact that simulating the physical layer links between multiples BSs and MSs in a network/system simulator can be computationally prohibitive. The abstraction should be accurate, computationally simple, relatively independent of channel models, and extensible to interference models and multi-antenna processing.

In the past, system level simulations characterized the average system performance, which was useful in providing guidelines for system layout, frequency planning etc. For such simulations, the average performance of a system was quantified by using the topology and macro channel characteristics to compute a geometric (or average) SINR distribution across the cell. Each subscriber's geometric SINR was then mapped to the highest modulation and coding scheme (MCS), which could be supported based on link level SINR tables that capture fast fading statistics. The link level SINR-PER look-up tables served as the PHY abstraction for predicting average link layer performance. Examples of this static methodology may be found in [26], [27].

Current cellular systems designs are based on exploiting instantaneous channel conditions for performance enhancement. Channel dependent scheduling and adaptive coding and modulation are examples of channel-adaptive schemes employed to improve system performance. Therefore, current system level evaluation methodologies are based on explicitly modeling the dynamic system behavior by including fast fading models within the system level simulation. Here the system level simulation must support a PHY abstraction capability to accurately predict the instantaneous performance of the PHY link layer.

4.2. Dynamic PHY Abstraction Methodology

In system level simulations, an encoder packet may be transmitted over a time-frequency selective channel. For example, OFDM systems may experience frequency selective fading, and hence the channel gain of each sub-carrier may not be equal. In OFDM, the coded block is transmitted over several sub-carriers and the post-processing SINR values of the pre-decoded streams are thus non-uniform. Additionally, the channel gains of sub-carriers can be time selective, i.e. change in time due to the fading process and possible delays involved in H-ARQ re-transmissions. The result on a transmission of a large encoder packet is encoded symbols of unequal SINR ratios at the input of the decoder due to the selective channel response over the encoder packet transmission.

PHY abstraction methodology for predicting instantaneous link performance for OFDM systems has been an active area of research and has received considerable attention in the literature [28]-[37]. The role of a PHY abstraction method is to predict the coded block error rate (BLER) for a given received channel realization across the OFDM sub-carriers used to transmit the coded FEC block. In order to predict the coded performance, the post-processing SINR values at the input to the FEC decoder are

considered as input to the PHY abstraction mapping. As the link level curves are generated assuming a frequency flat channel response at given SINR, an effective SINR, $SINR_{eff}$ is required to accurately map the system level SINR onto the link level curves to determine the resulting BLER. This mapping is termed *effective SINR mapping (ESM)*. The ESM PHY abstraction is thus defined as compressing the vector of received SINR values to a single effective SINR value, which can then be further mapped to a BLER number as shown in Figure 7.

Several ESM approaches to predict the instantaneous link performance have been proposed in the literature. Examples include mean instantaneous capacity [28]-[30], exponential-effective SINR Mapping (EESM, [31], [33]-[35]) and Mutual Information Effective SINR Mapping (MIESM, [36], [37]). Within the class of MIESM there are two variants, one is based on the mutual information per received symbol normalized to yield the bit mutual information and the other directly computes the bit mutual information. Each of these PHY abstractions uses a different function to map the vector of SINR values to a single number. Given the instantaneous EESM SINR, mean capacity or mutual information effective SINR, the BLER for each MCS is calculated using a suitable mapping function.

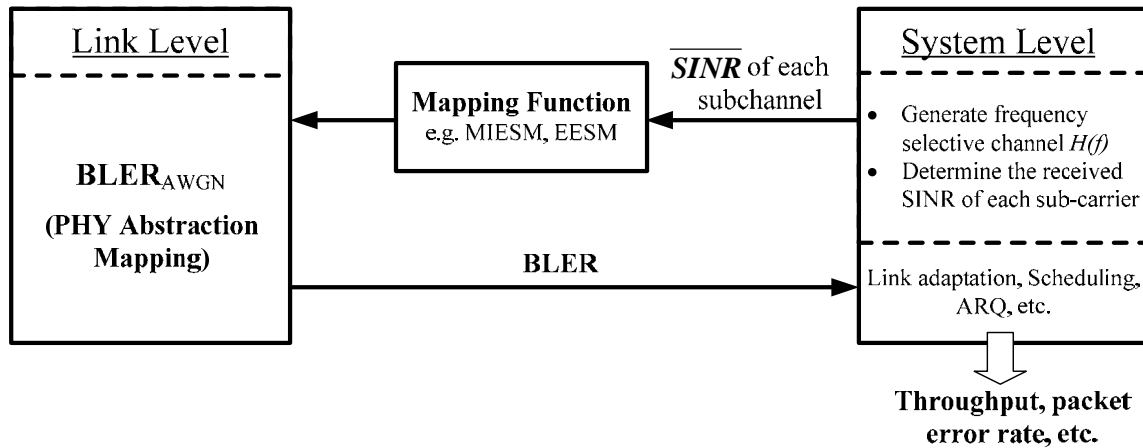


Figure 7: PHY link-to-system mapping procedure

Before diving into the details of the various PHY abstraction methods, the following notation is defined and used for the rest of the section:

Notation:

N : Number of sub-carriers used, i.e. the size of the FFT

n : is the index of a given sub-carrier, $n = 1, 2, \dots, N$

N_T : number of transmit antennas in a MIMO set-up,

N_R : number of receive antennas in a MIMO set-up,

M : size of the modulation constellation,

$m = \log_2 M$ is the number of bits per transmitted modulation symbol,

J : number of blocks in a packet,

\mathbf{H} : MIMO channel matrix with dimensions $N_R \times N_T$,

\mathbf{H}^H : denotes the conjugate transpose operation on the matrix \mathbf{H} ,
 $N(\mu, \sigma^2)$: denotes the Gaussian probability density function (pdf) with mean μ and
 variance σ^2 .

For all the ESM methods, the following system model for describing the MIMO relationship,

$$\mathbf{Y} = \mathbf{H}\mathbf{X} + \mathbf{U} \quad (37)$$

where \mathbf{Y} is the received signal vector from the N_R antennas, \mathbf{X} is the transmitted symbol stream which is a vector of dimensions $N_T \times 1$ (\mathbf{X} is just a scalar in the case of SISO/SIMO), and \mathbf{U} is the noise vector of dimensions $N_R \times 1$, modelled as zero-mean complex Gaussian.

In general, the ESM PHY abstraction methods can be described as follows,

$$SINR_{eff} = \Phi^{-1} \left\{ \frac{1}{N} \sum_{n=1}^N \Phi(SINR_n) \right\} \quad (38)$$

where $SINR_{eff}$ is the effective SINR, $SINR_n$ is the SINR in the n^{th} sub-carrier (or sub-carrier), N is the number of symbols in a coded block, or the number of sub-carriers used in an OFDM system and $\Phi(\bullet)$ is an invertible function.

In the case of the mutual information based ESM the function $\Phi(\bullet)$ is derived from the constrained capacity; while in the case of EESM, the function $\Phi(\bullet)$ is derived from the Chernoff bound on the probability of error. In the next three sections, we describe in detail these ESM methods.

4.3. Mutual Information Based Effective SINR Mapping

The accuracy of a mutual information-based metric depends on the equivalent channel over which this metric is defined. Capacity is the mutual information based on a Gaussian channel with Gaussian inputs. Modulation constrained capacity is the mutual information of a “symbol channel” (i.e. constrained by the input symbols from a complex set).

The computation of the mutual information per coded bit can be derived from the received symbol-level mutual information; this approach is termed received bit mutual information rate (RBIR). An alternative is a method that directly arrives at the bit-level mutual information; this method called mean mutual information per bit (MMIB).

A block diagram for the MIESM approaches is shown in Figure 8. Given a set of N received encoder symbol SINRs from the system level simulation, denoted as $SINR_1, SINR_2, SINR_3, \dots, SINR_N$, a mutual information metric is computed. Based on the computed MI-metric an equivalent SINR is obtained and used to look-up the BLER.

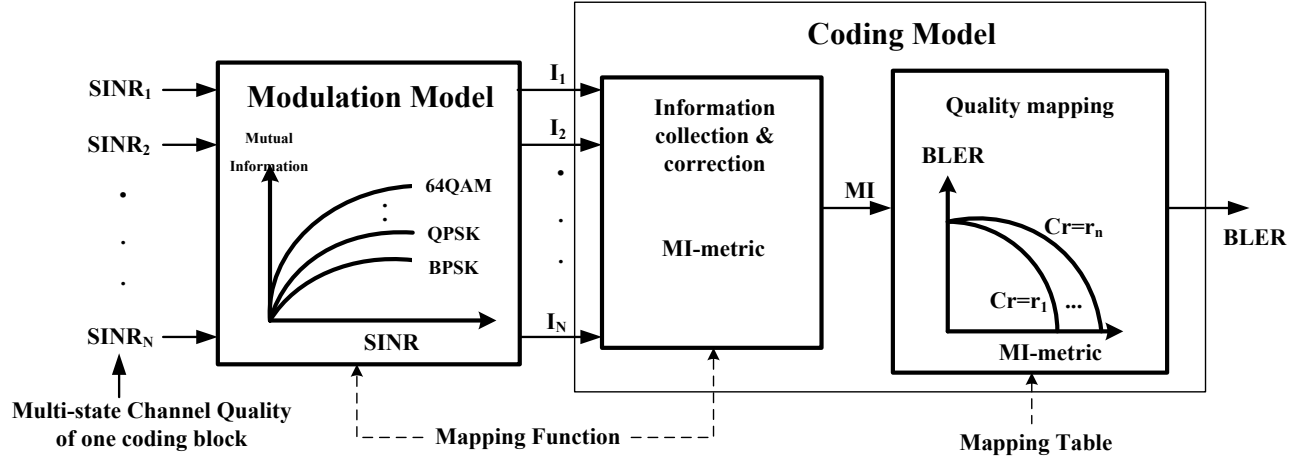


Figure 8: Computational procedure for MIESM method.

4.3.1. Received Bit Mutual Information Rate (RBIR) ESM (Mandatory)

In this section the RBIR ESM PHY abstraction method is described for SISO/SIMO as well as for MIMO under various receiver configurations^{**}.

4.3.1.1. RBIR Mapping for a SISO/SIMO System

For a SISO/SIMO system the symbol mutual information (SI) is given by

$$SI(SINR_n, m(n)) = \log_2 M - \frac{1}{M} \sum_{m=1}^M E_U \left\{ \log_2 \left(1 + \sum_{k=1, k \neq m}^M \exp \left[-\frac{|X_k - X_m + U|^2 - |U|^2}{(1/SINR_n)} \right] \right) \right\} \quad (39)$$

where \underline{U} is zero mean complex Gaussian with variance $1/(2SINR_n)$ per component, $SINR_n$ is the post-equalizer SINR at the n -th symbol or sub-carrier and $m(n)$ is the number of bits at the n -th symbol (or sub-carrier).

Assuming N sub-carriers are used to transmit a coded block, the normalized mutual information per received bit (RBIR) is given by

$$RBIR = \frac{\sum_{n=1}^N SI(SINR_n, m(n))}{\sum_{n=1}^N m(n)} \quad (40)$$

^{**} Details of the mathematical derivations are found in [77].

The symbol mutual information curves $SI(SINR, m)$ are generated once in the system simulator for each modulation order, and the RBIR values are stored as shown in Table 25 in 0.5dB SINR increments ranging from -20dB to 27dB.

We note that even though we refer to the coded block being carried over a set of sub-carriers, in general, the coded block may be carried over multiple dimensions, including the spatial dimensions available with MIMO. Also, note that in the above, the mutual information may be computed even with non-uniform modulation across the coded block. RBIR provides a direct relationship to the BLER that is dependent only on the AWGN link performance curves for a given code rate and is independent of the modulation scheme. This feature is useful in computing the PHY abstraction for cases where the coded block comprises of mixed modulation symbols.

	QPSK	16QAM	64QAM
SINR Span (dB)	[-20:0.5:27]	[-20:0.5:27]	[-20:0.5:27]
RBIR Value	[0.0072 0.0080 0.0090	[0.0036 0.0040 0.0045	[0.0024 0.0027 0.0030
	0.0101 0.0114 0.0127	0.0050 0.0057 0.0063	0.0034 0.0038 0.0043
	0.0143 0.0159 0.0179	0.0071 0.0080 0.0089	0.0047 0.0054 0.0060
	0.0200 0.0225 0.0251	0.0100 0.0112 0.0126	0.0067 0.0075 0.0084
	0.0282 0.0315 0.0352	0.0141 0.0158 0.0176	0.0094 0.0106 0.0117
	0.0394 0.0442 0.0493	0.0197 0.0221 0.0247	0.0132 0.0147 0.0165
	0.0551 0.0616 0.0688	0.0276 0.0308 0.0344	0.0184 0.0207 0.0229
	0.0767 0.0855 0.0953	0.0384 0.0428 0.0476	0.0257 0.0285 0.0319
	0.1061 0.1180 0.1311	0.0531 0.0590 0.0656	0.0354 0.0396 0.0437
	0.1456 0.1615 0.1788	0.0728 0.0808 0.0895	0.0488 0.0539 0.0599
	0.1978 0.2184 0.2407	0.0990 0.1094 0.1206	0.0660 0.0732 0.0805
	0.2650 0.2910 0.3190	0.1329 0.1461 0.1603	0.0890 0.0974 0.1073
	0.3489 0.3806 0.4141	0.1756 0.1920 0.2094	0.1172 0.1285 0.1398
	0.4493 0.4859 0.5239	0.2279 0.2474 0.2680	0.1525 0.1653 0.1795
	0.5628 0.6024 0.6422	0.2896 0.3122 0.3357	0.1937 0.2092 0.2247
	0.6817 0.7207 0.7584	0.3600 0.3852 0.4112	0.2415 0.2583 0.2763
	0.7944 0.8281 0.8592	0.4379 0.4653 0.4933	0.2942 0.3132 0.3321
	0.8872 0.9119 0.9331	0.5219 0.5509 0.5804	0.3519 0.3718 0.3924
	0.9507 0.9649 0.9760	0.6103 0.6403 0.6709	0.4131 0.4345 0.4558
	0.9842 0.9901 0.9942	0.7014 0.7317 0.7617	0.4778 0.4997 0.5223
	0.9968 0.9983 0.9992	0.7910 0.8193 0.8463	0.5448 0.5677 0.5907
	0.9997 0.9999 1.0000	0.8716 0.8949 0.9158	0.6141 0.6374 0.6611
	1.0000 1.0000 1.0000	0.9343 0.9501 0.9633	0.6848 0.7087 0.7325
	1.0000 1.0000 1.0000	0.9739 0.9821 0.9883	0.7564 0.7802 0.8036
	1.0000 1.0000 1.0000	0.9927 0.9957 0.9976	0.8269 0.8489 0.8708
	1.0000 1.0000 1.0000	0.9988 0.9994 0.9997	0.8904 0.9100 0.9262
	1.0000 1.0000 1.0000	0.9999 1.0000 1.0000	0.9425 0.9547 0.9668
	1.0000 1.0000 1.0000	1.0000 1.0000 1.0000	0.9732 0.9796 0.9840
	1.0000 1.0000 1.0000	1.0000 1.0000 1.0000	0.9883 0.9910 0.9937
	1.0000 1.0000 1.0000	1.0000 1.0000 1.0000	0.9954 0.9971 0.9983
	1.0000 1.0000 1.0000	1.0000 1.0000 1.0000	0.9995 0.9998 1.0000
	1.0000 1.0000]	1.0000 1.0000]	1.0000 1.0000]

Table 25: SINR to RBIR mapping

In order to derive the mapping between RBIR and BLER, the following steps may be considered:

1. Calculate the effective SINR (SINReff) based on RBIR and Table 25.
2. Reference the AWGN link performance curves to obtain the mapping between SINR and BLER.
3. Use the SINReff obtained in Step 1 and the mapping obtained in Step 2 to derive the mapping between SINReff and BLER.

4.3.1.2. RBIR Mapping for a Linear MIMO Receiver

With linear equalizers such as zero-forcing (ZF) and minimum mean-squared error (MMSE), each one of the N_T MIMO streams is treated as an equivalent SISO channel with SINRs given by the post combining SINRs of the linear receiver. The same procedure is applied to the case of MIMO Matrix A.

4.3.1.3. RBIR Mapping for the Maximum-Likelihood (ML) MIMO Receiver

The SI in equation (40) can now be rewritten as

$$SI = \frac{1}{M} \sum_{i=1}^M \int_{-\infty}^{\infty} p(LLR_i) \log_2 \frac{M}{1 + e^{-LLR_i}} dLLR_i \quad (41)$$

where $p(LLR_i)$ is the conditional pdf of the symbol-level log-likelihood ratio (LLR) of the i -th constellation point. The conditional pdf of symbol LLR for an ML receiver can be approximated as Gaussian. Note that RBIR PHY abstraction is based on the fixed relationship between the LLR distribution and BLER. Hence, a representative LLR distribution among M distributions is considered. Further, using the numerical integration method of [73], the mutual information per symbol in Equation (41) can be approximated [80] as

$$SI \approx \log_2(M) - \frac{1}{\log_e(2)} \cdot J$$

where $J = \left(\frac{J_A + J_B}{2} \right) + \left(\frac{J_A - J_B}{2} \right) \text{sign}(T - J_B) \quad T \approx 0.65,$

$$J_A = \sqrt{VAR} \left\{ \frac{-\eta}{2} \cdot \text{Erfc} \left(\frac{\eta}{\sqrt{2}} \right) + \frac{1}{\sqrt{2\pi}} \cdot e^{\left(\frac{-\eta^2}{2} \right)} \right\},$$

the coefficient of variation, $\eta = \frac{AVE}{\sqrt{VAR}},$,

$$J_B = \frac{2}{3} f(AVE) + \frac{1}{6} f(AVE + \sqrt{3VAR}) + \frac{1}{6} f(AVE - \sqrt{3VAR}),$$

$$f(x) = \log_e(1 + e^{-x}),$$

$$\text{sign}(x) = \begin{cases} +1, & x \geq 0 \\ -1, & x < 0 \end{cases}$$

From Equation (42), it can be seen that only the mean and variance of the LLR are needed to calculate the RBIR metric.

In this section both Vertical and Horizontal encoding are considered. As shown in Table 26 the mean, AVE and the variance, VAR, are computed as a function of an intermediate variable, γ_{dB} , defined as

$$\gamma_{dB} = 10 \log_{10} \left(\frac{d^2 |H_k|^2}{\sigma^2} \right),$$

where d is the minimum distance in the QAM constellation

$$d = \begin{cases} \sqrt{2}, & \text{for QPSK} \\ 2 / \sqrt{10}, & \text{for 16QAM} \\ 2 / \sqrt{42}, & \text{for 64QAM} \end{cases}$$

H_k is the k -th column vector of the channel matrix $\mathbf{H} = [H_1 \ H_2]$, and σ^2 is the variance of noise plus interference (assuming the interference is also spatially white). In Table 26 γ_{dB} is quantized to 0.5dB increments ranging from -20dB to 30dB.

A detailed derivation of the AVE and VAR as shown in Table 26 is given in Appendix P. A block size of 6 subchannels x 4 OFDMA symbols and the PUSC permutation are used.

γ_{dB} (dB)	[-20:0.5:30]				
AVE	[-0.4016	-0.4123	-0.4233	-0.4344	-0.4457
	-0.4571	-0.4687	-0.4804	-0.4922	-0.5041
	-0.5160	-0.5279	-0.5397	-0.5515	-0.5631
	-0.5745	-0.5856	-0.5962	-0.6065	-0.6161
	-0.6249	-0.6329	-0.6399	-0.6456	-0.6499
	-0.6524	-0.6530	-0.6513	-0.6470	-0.6396
	-0.6287	-0.6139	-0.5944	-0.5697	-0.5391
	-0.5018	-0.4567	-0.4031	-0.3396	-0.2650
	-0.1780	-0.0770	0.0398	0.1743	0.3286
	0.5051	0.7063	0.9352	1.1949	1.4889
	1.8211	2.1959	2.6179	3.0926	3.6259
	4.2245	4.896	5.6491	6.4933	7.4396
	8.5006	9.6904	11.0251	12.5229	14.2045
	16.0930	18.2146	20.5989	23.2784	26.2897
	29.6733	33.4750	37.7458	42.5431	47.9314
	53.9830	60.7788	68.4100	76.9786	86.5992
	97.4004	109.5263	123.1389	138.4197	155.5725
	174.8260	196.4366	220.6922	247.9159	278.4700
	312.7611	351.2455	394.4351	442.9043	497.2976
	558.3381	626.8372	703.7054	789.9640	886.7593
	995.3772]				
VAR	[0.2952	0.3003	0.3055	0.3108	0.3162
	0.3218	0.3276	0.3336	0.3400	0.3468

	0.3541	0.3620	0.3705	0.3800	0.3904
	0.4021	0.4152	0.4301	0.4471	0.4673
	0.4887	0.5143	0.5438	0.5779	0.6175
	0.6633	0.7164	0.7779	0.8491	0.9316
	1.0270	1.1373	1.2645	1.4112	1.5801
	1.7741	1.9967	2.2516	2.5430	2.8755
	3.2542	3.6849	4.1737	4.7277	5.3548
	6.0636	6.8644	7.7680	8.7895	9.9429
	11.2474	12.7253	14.4033	16.3140	18.4964
	20.9982	23.8761	27.1982	31.0450	35.5109
	40.7058	46.7560	53.8056	62.0176	71.5751
	82.6815	95.5627	110.4754	127.720	147.6512
	170.6826	197.2945	228.0421	263.5665	304.6084
	352.0229	406.7979	470.0740	543.1686	627.6030
	725.1343	837.7913	967.9172	1118.2180	1291.8186
	1492.3277	1723.9127	1991.3863	2300.3061	2657.0904
	3069.1507	3545.0462	4094.6610	4729.4092	5462.4720
	6309.0710	7286.7839	8415.9098	9719.8896	11225.7930
	12964.8798];				

Table 26: Mean and variance for symbol level LLR

For MIMO systems, the average, AVE and the variance, VAR are scaled as follows for both horizontal and vertical coding:

$$\begin{aligned}
 AVE_{Stream} &= a \times AVE, \quad VAR_{Stream} = VAR \quad \text{for QPSK, 16QAM} \\
 AVE_{Stream} &= a \times AVE, \quad VAR_{Stream} = 2 \times VAR \quad \text{for 64QAM}
 \end{aligned}
 \tag{43}$$

As seen from Table 27, the parameter a is referenced based on the channel condition number, k obtained through the Eigen value decomposition of the channel as

$$\begin{aligned}
 H^H H &= V \begin{bmatrix} \lambda_{\max} & 0 \\ 0 & \lambda_{\min} \end{bmatrix} V^H \Rightarrow k = \frac{\lambda_{\max}}{\lambda_{\min}} \\
 \lambda_{\min} dB &= 10 \log_{10}(\lambda_{\min} / \sigma^2)
 \end{aligned}
 \tag{44}$$

The parameter a in Equation (43) is optimized to minimize the difference between effective SINR and AWGN SINR for every definite BLER. The parameter 'a' has been found to be independent of power delay profiles and MIMO channel models. The search procedure used to obtain the parameter a is described in Appendix P. A block size of 6 subchannels x 4 OFDMA symbols and the PUSC permutation are used in the parameter search.

		QPSK 1/2	QPSK 3/4	16QAM 1/2	16QAM 3/4	64QAM 1/2	64QAM 2/3	64QAM 3/4	64QAM 5/6
$k < 10$ $\lambda_{\min} dB \leq -10$	1 st Stream	3.7500	2.7000	5.0000	3.4000	5.0000	5.0000	0.1000	2.1000
	2 nd Stream	5.0000	1.9000	5.0000	2.3000	5.0000	5.0000	0.1000	3.0000
$k < 10$ $-10 < \lambda_{\min} dB \leq 8$	1 st Stream	3.0000	4.9000	0.4000	1.8000	2.1000	2.1000	2.7000	0.9000
	2 nd Stream	2.9000	4.9000	0.1000	1.5111	3.8556	2.5000	2.5000	1.3000

	Stream								
$k < 10$ $\lambda_{\min} dB > 8$	1 st Stream	1.5000	1.0000	1.3200	2.1000	0.4300	1.1111	1.5000	5.0000
	2 nd Stream	1.5000	1.0000	2.0000	3.1000	0.4300	1.1000	1.6000	4.8000
$10 \leq k < 100$ $\lambda_{\min} dB \leq -10$	1 st Stream	2.8500	1.7000	1.0000	0.6778	5.0000	4.1000	3.5000	3.3000
	2 nd Stream	2.4000	1.7556	1.0000	0.8111	5.0000	2.7000	4.5000	3.4000
$10 \leq k < 100$ $-10 < \lambda_{\min} dB \leq 8$	1 st Stream	0.1500	0.8000	0.1000	1.0556	0.1000	1.1000	1.3000	1.5000
	2 nd Stream	0.4500	0.8000	0.0444	0.9889	0.1000	1.1889	1.2000	1.6000
$10 \leq k < 100$ $\lambda_{\min} dB > 8$	1 st Stream	1.5000	1.0000	1.1000	2.7000	2.1000	1.4000	1.3000	1.9000
	2 nd Stream	1.5000	1.0000	2.0000	1.4000	1.0889	1.3778	1.9000	1.4000
$k \geq 100$ $\lambda_{\min} dB \leq -10$	1 st Stream	0.7500	0.8667	0.3556	0.3889	0.5000	0.5222	0.6000	0.3000
	2 nd Stream	0.7500	0.8444	0.2778	0.2667	0.7000	0.3000	0.4000	0.5000
$k \geq 100$ $-10 < \lambda_{\min} dB \leq 8$	1 st Stream	0.1500	0.1000	0.9000	1.0444	0.6889	1.0333	1.0000	1.1000
	2 nd Stream	0.1500	0.1000	1.0000	1.5000	0.7444	1.1111	1.1000	1.0000
$k \geq 100$ $\lambda_{\min} dB > 8$	1 st Stream	1.5000	1.0000	1.0000	5.0000	5.0000	3.5667	1.2000	1.2000
	2 nd Stream	1.5000	1.0000	1.0000	5.0000	5.0000	4.1222	0.1000	2.0000

Table 27: Values for parameter a Horizontal Encoding:

For a 2x2 system using MIMO Matrix B and horizontal encoding, the conditional PDF of symbol LLR output is approximated as Gaussian for each of the two streams and is given by

$$\begin{aligned} p(LLR_1) &= N(AVE_{Stream1}, VAR_{Stream1}) \\ p(LLR_2) &= N(AVE_{Stream2}, VAR_{Stream2}) \end{aligned} \quad (45)$$

where $AVE_{Stream1}$, $AVE_{Stream2}$, $VAR_{Stream1}$ and $VAR_{Stream2}$ are obtained as shown in Equation (43). The symbol mutual information is then computed based on the approximation in equation (42) and substituted in equation (40) to compute the RBIR metric.

Vertical Encoding:

For a 2x2 system using MIMO Matrix B and vertical encoding, the distribution of the LLR from an ML receiver can be approximated as a Gaussian mixture. Thus, the PDF of LLR can be expressed as a weighted sum given by

$$p(LLR_{MIMO}) = p_1 \cdot N(AVE_{stream1}, VAR_{stream1}) + p_2 \cdot N(AVE_{stream2}, VAR_{stream2}) \quad (46)$$

where the parameters p_1 and p_2 are given in Table 28. Thus, SI is also a weighted sum of two SI values given by

$$SI = p_1 \cdot SI_{stream1} + p_2 \cdot SI_{stream2} \quad (47)$$

Note that $SI_{stream1}$ and $SI_{stream2}$ are computed based on Equation (42) and finally the SI of Equation (47) is substituted in Equation (40) to compute the RBIR metric.

		QPSK 1/2	QPSK 3/4	16QAM 1/2	16QAM 3/4	64QAM 1/2	64QAM 2/3	64QAM 3/4	64QAM 5/6
$k < 10$ $\lambda_{min} dB \leq -10$	p_1	0.5000	0.5000	0.5000	0.5000	0.5000	0.5000	0.5000	0.5000
	p_2	0.5000	0.5000	0.5000	0.5000	0.5000	0.5000	0.5000	0.5000
$k < 10$ $-10 < \lambda_{min} dB \leq 8$	p_1	0.5000	0.5000	0.5000	0.5000	0.5000	0.5000	0.5000	0.5000
	p_2	0.5000	0.5000	0.5000	0.5000	0.5000	0.5000	0.5000	0.5000
$k < 10$ $\lambda_{min} dB > 8$	p_1	0.5000	0.5000	0.5000	0.5000	0.5000	0.5000	0.5000	0.5000
	p_2	0.5000	0.5000	0.5000	0.5000	0.5000	0.5000	0.5000	0.5000
$10 \leq k < 100$ $\lambda_{min} dB \leq -10$	p_1	0.5088	0.5000	0.5000	0.5000	0.5000	0.5000	0.5000	0.4966
	p_2	0.4812	0.5000	0.5000	0.5000	0.5000	0.5000	0.5000	0.5034
$10 \leq k < 100$ $-10 < \lambda_{min} dB \leq 8$	p_1	0.5094	0.5000	0.4688	0.4900	0.5200	0.4688	0.5000	0.5000
	p_2	0.4906	0.5000	0.5312	0.5100	0.4800	0.5312	0.5000	0.5000
$10 \leq k < 100$ $\lambda_{min} dB > 8$	p_1	0.5218	0.5184	0.5625	0.5000	0.5000	0.5156	0.5000	0.5000
	p_2	0.4782	0.4816	0.4375	0.5000	0.5000	0.4844	0.5000	0.5000
$k \geq 100$ $\lambda_{min} dB \leq -10$	p_1	0.5000	0.5000	0.5538	0.5200	0.5000	0.5000	0.5222	0.5128
	p_2	0.5000	0.5000	0.4462	0.4800	0.5000	0.5000	0.4778	0.4872
$k \geq 100$ $-10 < \lambda_{min} dB \leq 8$	p_1	0.5000	0.5000	0.5469	0.5000	0.5178	0.5469	0.5000	0.5000
	p_2	0.5000	0.5000	0.4531	0.5000	0.4822	0.4531	0.5000	0.5000
$k \geq 100$ $\lambda_{min} dB > 8$	p_1	0.4922	0.5000	0.5312	0.5000	0.5000	0.5312	0.5000	0.5178
	p_2	0.5078	0.5000	0.4688	0.5000	0.5000	0.4688	0.5000	0.4822

Table 28: Values of p_1 and p_2 for SM with Vertical Encoding

The parameters p_1 and p_2 in Table 28 have been optimized to minimize the difference between effective SINR and AWGN SINR for every definite BLER. The procedure used to obtain the parameters p_1 and p_2 is described in Appendix P. A block size of 6 subchannels x 4 OFDMA symbols and the PUSC permutation are used in the parameter search.

4.3.2. Mean Mutual Information per Bit (MMIB) ESM

It is possible to obtain the mutual information per bit metric from the symbol channel by simply normalizing this constrained capacity (i.e. by dividing by the modulation order) as done in the RBIR method. Note, however that the symbol channel does not account for the constellation mapping, i.e. the mapping of bits to symbols in the constellation, thus it is invariable to different bit-to-symbol mappings. An alternative method is to define the mutual information on the bit channel itself, which we will refer to as the mutual information per coded Bit or MIB (or MMIB when a mean of multiple MIBs is involved). It is however possible that for certain constellation mappings (say Gray encoding) MMIB and RBIR functions may be similar.

More generally, given that our goal is to abstract the performance of the underlying binary code, the closest approximation to the actual decoder performance is obtained by defining an information channel at the coder-decoder level, i.e. defining the mutual information between bit input (into the QAM mapping) and LLR output (out of the LLR computing engine at the receiver), as shown in Figure 9. The concept of “bit channel” encompasses SIMO/MIMO channels and receivers. It is demonstrated that this definition will greatly simplify the PHY abstraction by moving away from an empirically adjusted model and introducing instead MIB functions of equivalent bit channels^{††}.

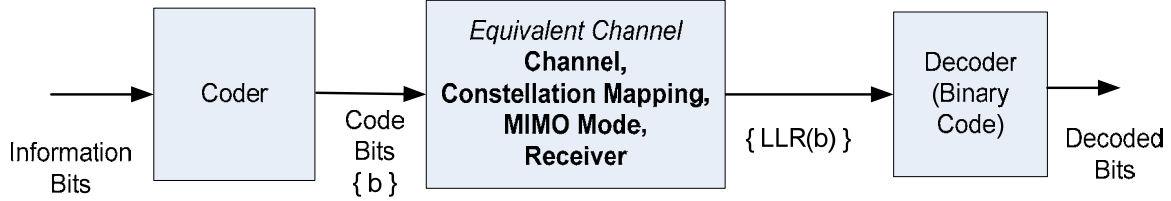


Figure 9: Bit Interleaved coded modulation system

In the bit channel of Figure 9, the task now is to define functions that capture the mutual information per bit. The following sections further develop an efficient approach for MIB computation by approximating the LLR PDF with a mixture of Gaussian PDFs. We will begin with the development of explicit functions for MIBs in SISO and later extend it to MIMO.

The concept of deriving mutual information between coded bits and their LLR values was also well known from work in MIESM for BPSK [41]. For BPSK, however, bit-level capacity is the same as symbol-level capacity.

4.3.2.1. MIB Mapping for SISO Systems

The mutual information (MI) of the coded bit is dependent on the actual constellation mapping. The MI of each bit-channel is obtained and averaged across the bits in a QAM symbol. After encoding (e.g. Turbo or CTC), a binary coded bit stream c_k is generated before QAM mapping. The QAM modulation can be represented as a labeling map $\mu: A \rightarrow X$, where A is the set of m -tuples, $m \in \{2, 4, 6\}$ to represent QPSK, 16 and 64-QAM, of binary bits and X is the constellation. Given the observation y_n corresponding to the n^{th} QAM symbol in a codeword, the demodulator computes the log-likelihood ratio (LLR) $LLR(b_{i,n})$ of the i^{th} bit comprising the symbol via the following expression (where the symbol index n is dropped for convenience)

$$LLR(b_i) = \ln \left(\frac{P(y | b_i = 1)}{P(y | b_i = 0)} \right) \quad (48)$$

When the coded block sizes are very large in a bit-interleaved coded modulation system, the bit interleaver effectively breaks up the memory of the modulator, and the

^{††} Additional details are found in [78].

system can be represented as a set of parallel independent bit-channels [39]. Conceptually, the entire encoding process can be represented as shown in Figure 9.

Due to the asymmetry of the modulation map, each bit location in the modulated symbol experiences a different 'equivalent' bit-channel. In the above model, each coded bit is randomly mapped (with probability $1/m$) to one of the m bit-channels. The mutual information of the equivalent channel can be expressed as:

$$I(b, LLR) = \frac{1}{m} \sum_{i=1}^m I(b_i, LLR(b_i)) \quad (49)$$

where $I(b_i, LLR(b_i))$ is the mutual information between input bit and output LLR for i^{th} bit in the modulation map. As can be seen, the bit LLR reflects the demodulation process to compute LLR, which was not reflected in the symbol-level MI and the RBIR defined above. This is the main difference between the bit- and symbol-level MI definitions.

More generally, however, the mean mutual information – computed by considering the observations over N symbols (or channel uses) – over the codeword may be computed as

$$M_I = \frac{1}{mN} \sum_{n=1}^N \sum_{i=1}^m I(b_i^{(n)}, LLR(b_i^{(n)})) \quad (50)$$

The mutual information function $I(b_i^{(n)}, LLR(b_i^{(n)}))$ is, of course, a function of the QAM symbol SINR, and so the mean mutual information M_I (MMIB) may be alternatively written as

$$M_I = \frac{1}{mN} \sum_{n=1}^N \sum_{i=1}^m I_{m, b_i^{(n)}}(SINR_n) = \frac{1}{N} \sum_{n=1}^N I_m(SINR_n) \quad (51)$$

The mean mutual information is dependent on the SINR on each modulation symbol (index n) and the code bit index i (or i -th bit channel), and varies with the constellation order m . Accordingly, the relationship $I_{m, b_i^{(n)}}(SINR)$ is required for each modulation type and component bit index in order to construct $I_m(SINR)$.^{‡‡}

For BPSK/QPSK, a closed form expression is given in [39]-[40], which is a non-linear function that can be approximated in polynomial form. For the particular case of BPSK/QPSK, the function would be the same as that obtained by defining the mutual information of a symbol channel (symbol channel is just a bit channel for BPSK).

For BPSK, conditional LLR PDF is Gaussian and the MIB can be expressed as

^{‡‡} Note that in the 802.16e specification, bit indexing typically proceeds from 0.

$$J(x) \approx \begin{cases} a_1 x^3 + b_1 x^2 + c_1 x, & \text{if } x \leq 1.6363 \\ 1 - \exp(a_2 x^3 + b_2 x^2 + c_2 x + d_2) & \text{if } 1.6363 \leq x \leq \infty \end{cases} \quad (52)$$

where $a_1 = -0.04210661$, $b_1 = 0.209252$ and $c_1 = -0.00640081$ for the first approximation, and where $a_2 = 0.00181492$, $b_2 = -0.142675$, $c_2 = -0.0822054$ and $d_2 = 0.0549608$ for the second approximation.

The inverse function needed for the effective SINR computation is given by

$$J^{-1}(y) \approx \begin{cases} a_3 y^2 + b_3 y + c_3 \sqrt{y}, & \text{if } 0 \leq y \leq 0.3646 \\ a_4 \log_e [b_4 (y-1)] + c_4 y & \text{if } 0.3646 < y \leq 1 \end{cases} \quad (53)$$

where $a_3 = 1.09542$, $b_3 = 0.214217$, $c_3 = 2.33727$, $a_4 = -0.706692$, $b_4 = -0.386013$, $c_4 = 1.75017$.

It can be shown that the LLR PDFs for any other modulation can be approximated as a mixture of Gaussian distributions that are non-overlapping at high SINR. It then follows that the corresponding MIB can be expressed as a sum of $J(\bullet)$ functions, i.e.

$$I_m(x) = \sum_{k=1}^K a_k J(c_k x) \quad \text{and} \quad \sum_{k=1}^K a_k = 1$$

We will use this parameterized function for expressing all non-linear MIB functions. The corresponding parameters themselves would be a function of the modulation.

The optimized functions for QPSK, 16-QAM and 64-QAM are given in Table 29.

MIB Function	Numerical Approximation
$I_2(\gamma)$ (QPSK)	$J(2\sqrt{\gamma})$ (<i>Exact</i>)
$I_4(\gamma)$ (16-QAM)	$\frac{1}{2}J(0.8\sqrt{\gamma}) + \frac{1}{4}J(2.17\sqrt{\gamma}) + \frac{1}{4}J(0.965\sqrt{\gamma})$
$I_6(\gamma)$ (64-QAM)	$\frac{1}{3}J(1.47\sqrt{\gamma}) + \frac{1}{3}J(0.529\sqrt{\gamma}) + \frac{1}{3}J(0.366\sqrt{\gamma})$

Table 29: Numerical approximations for MIB mappings

Once the MMIB is computed using equation (52) and Table 29 over a set of sub-carriers corresponding to coded symbols, a direct MMIB to BLER relationship can be used to obtain block error rate, without necessarily defining an effective SINR.

Lookup tables for the AWGN reference curves for different MCS levels can be used in order to map the MMIB to BLER. Another alternative is to approximate the reference curve with a parametric function. For example, we consider a Gaussian cumulative

model with 3 parameters which provides a close fit to the AWGN performance curve, parameterized as

$$y = \frac{a}{2} \left[1 - \operatorname{erf} \left(\frac{x-b}{\sqrt{2}c} \right) \right], \quad c \neq 0 \quad (54)$$

where a is the “transition height” of the error rate curve, b is the “transition center” and c is related to the “transition width” (transition width = $1.349c$) of the Gaussian cumulative distribution. The parameter a can be set to 1, and the mapping requires only two parameters, which are given for each MCS index in the table below. The accuracy of the curve fit with this model is verified with MCS modes supported in 802.16e as shown in Figure 10. This parameterization of AWGN reference considerably simplifies the storage and simulation requirements.

So, for each MCS the BLER is obtained as

$$BLER_{MCS} = \frac{1}{2} \left[1 - \operatorname{erf} \left(\frac{x-b_{MCS}}{\sqrt{2}c_{MCS}} \right) \right], \quad c \neq 0 \quad (55)$$

Figure 10 is a plot of the MMIB versus BLER for parameters based on the 802.16e system using 6 different MCSs with rates 1/2 and 3/4 on an AWGN channel. It can be seen from Figure 10 that, to a first-order approximation, the mapping from MMIB to BLER can be assumed independent of the QAM modulation type. However, since code performance is strongly dependent on code sizes and code rates, $BLER_{MCS}$ will not be independent of these parameters. Further, we can achieve an additional simplification.

With the above result, we can achieve the following simplification: We generalize the AWGN reference curves to be a function of the block size and coding rate (BCR) only, thus

$$BLER_{BCR} = \frac{1}{2} \left[1 - \operatorname{erf} \left(\frac{x-b_{BCR}}{\sqrt{2}c_{BCR}} \right) \right], \quad c \neq 0 \quad (56)$$

With this simplification, only two parameters need to be stored for each supported BCR.

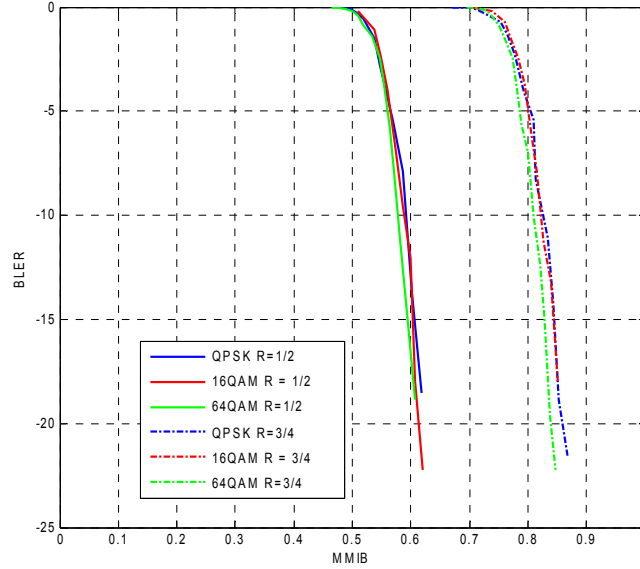
Note: The choice of this particular MMIB to BLER mapping is due to the underlying physical interpretation. The parameter b is closely related to the binary code rate and will be equal to the code rate for an ideally designed code. Similarly, parameter c represented the rate of fall of the curve and is also related to the block size.

Table 30 shows the parameters based on the performance in a static AWGN channel.

BCR Index	Code Rate	Information Word Length	Code Word Length (bits)	b_{BCR}	c_{BCR}
-----------	-----------	-------------------------	-------------------------	-----------	-----------

		(bits)			
1	1/2	432	864	0.5512	0.0307
2	1/2	480	960	0.5512	0.0307
3	3/4	432	576	0.7863	0.03375
4	2/3	384	576	0.7082	0.0300
5	5/6	480	576	0.8565	0.02622

Table 30: Parameters for Gaussian cumulative approximation

Figure 10: BLER (\log_{10} scale) mappings for MMIB from AWGN performance results

4.3.2.2. MIMO Receiver Abstraction

With linear receivers like MMSE, each one of the N_T MIMO streams is treated as an equivalent SISO channel with SINRs given by post combining SINRs of the linear receiver. For vertically encoded SM, the MIB can be obtained as

$$M_I = \frac{1}{NN_T} \sum_{n=1}^N \sum_{k=1}^{N_T} I_m(\gamma_{nk})$$

and

$$BLER = B_{BCR}(M_I)$$

where γ_{nk} is the post combining SINR of the k -th layer on the n -th sub-carrier, N_T is the number of transmit antennas, N is the total number of coded sub-carriers, and the mapping functions $I_m(\cdot)$ and $B_{BCR}(\cdot)$ are defined in sections on SISO for each BCR. Note that the block size should correspond to the total codeword size of the N_T streams.

4.3.2.3. MIMO ML Receiver Abstraction

MMIB can be evaluated for an ML receiver. In this section, we summarize the ML receiver abstraction to optimally compute MIB with the ML receiver using mixture Gaussian models for LLR PDFs.

With vertical encoding, a codeword is transmitted on both the streams. In this case, for the purpose of code performance prediction, a single MIB metric is sufficient, which is the average MIB of the two streams. This section describes the computation of this metric for each modulation.

1) Obtain the Eigen value decomposition of the equivalent channel matrix

$$H^H H = V D V^H \quad (58)$$

such that D is a diagonal matrix given by

$$D = \begin{pmatrix} \lambda_{\max} & 0 \\ 0 & \lambda_{\min} \end{pmatrix} \quad (59)$$

where

$$\begin{aligned} \lambda_{\min} &= \text{Minimum Eigen Value} \\ \lambda_{\max} &= \text{Maximum Eigen Value} \end{aligned} \quad (60)$$

2) From the decomposition obtain the 3rd parameter

$$p_a = \text{Eigen mode subspace power distribution} = \min\{p, 1-p\}$$

$$\text{where } |V| \cdot |V| = \begin{pmatrix} p & 1-p \\ 1-p & p \end{pmatrix}, \quad 0 \leq p \leq 1 \quad (61)$$

where $|V|$ denotes the matrix after taking element-wise absolute values, and \cdot represents the operation of element-wise multiplication.

3) Obtain the following array of conditional means sorted in ascending order

$$\begin{aligned} \gamma = \text{sort}_{asc} \{ & \lambda_{\max} p_a + \lambda_{\min} (1-p_a), \lambda_{\min} p_a + \lambda_{\max} (1-p_a), \\ & \lambda_{\max} (1-2\sqrt{p_a(1-p_a)}) + \lambda_{\min} (1+2\sqrt{p_a(1-p_a)}) \} \end{aligned} \quad (62)$$

4)

i) For QPSK, the MMIB of the MIMO symbol is

$$I_2^{(2 \times 2)}(\lambda_{\min}, \lambda_{\max}, P_a) = \frac{1}{2} J(a\sqrt{\gamma(1)}) + \frac{1}{2} J(b\sqrt{\gamma(2)}), \quad a = 0.85, b = 1.19 \quad (63)$$

where $I_m^{(2 \times 2)}(\cdot)$ is the 2x2 SM MI function for modulation level m .

ii) For 16QAM and 64QAM, the 2x2 SM MI mapping is modeled as

$$I_m^{(2 \times 2)}(\lambda_{\min}, \lambda_{\max}, p_a) = \frac{1}{3} \left[J(a_m \sqrt{\gamma(1)}) + J(b_m \sqrt{\gamma(2)}) + J(c_m \sqrt{\gamma(3)}) \right] \quad (64)$$

where a_m , b_m and c_m are the parameters which are listed in Table 31 and Table 32 for each SINR and condition number ($\kappa = \lambda_{\max} / \lambda_{\min}$) partition.

16 QAM	$1 < \kappa \leq 10$	$10 < \kappa \leq 100$	$\kappa > 100$
$-10dB < \lambda_{\min, dB} < 8dB$	$a = 0.48, b = 0.27$ $c = 0.69$	$a = 0.40, b = 0.21$ $c = 0.56$	$a = 0.32, b = 0.13$ $c = 0.37$
$\lambda_{\min, dB} > 8dB$	$a = 0.35, b = 0.43$ $c = 0.59$	$a = 0.37, b = 0.33$ $c = 100$	$a = 0.42, b = 0.11$ $c = 100$

Table 31: Numerical approximation for 16QAM 2x2 SM

64 QAM	$1 < \kappa \leq 10$	$10 < \kappa \leq 100$	$\kappa > 100$
$-10dB < \lambda_{\min, dB} < 8dB$	$a = 0.23, b = 0.16$ $c = 0.59$	$a = 0.12, b = 0.12$ $c = 0.38$	$a = 0.08, b = 0.07$ $c = 0.17$
$\lambda_{\min} > 8dB$	$a = 0.20, b = 0.21$ $c = 0.62$	$a = 0.22, b = 0.13$ $c = 100$	$a = 0.24, b = 0.08$ $c = 100$

Table 32: Numerical approximation for 64 QAM 2x2 SM

where $\lambda_{\min, dB} = 10 \log_{10}(\lambda_{\min})$.

The MMIB of the channel realization is given by

$$M_I^{(2 \times 2)} = \frac{1}{N} \sum_{i=1}^N I_m^{(2 \times 2)}(\lambda_{\min}(\mathbf{H}_i), \lambda_{\max}(\mathbf{H}_i), p_a(\mathbf{H}_i)) \quad (65)$$

where \mathbf{H}_i is the $N_R \times 2$ channel matrix on the i -th sub-carrier.

The MMIB to BLER mapping is similar to that of SISO as in section 4.3.2.1. The code size should correspond to the total codeword size on the two streams.

4.3.3. Exponential ESM (EESM)

The EESM abstraction method is given by

$$SINR_{eff} = -\beta \ln \left(\frac{1}{N} \sum_{n=1}^N \exp \left(-\frac{SINR_n}{\beta} \right) \right) \quad (66)$$

where β is a value for optimization/adjustment that depends on the MCS and the encoding block length. A table of these β values shall be provided once the numerology has been decided.

4.4. Per-tone SINR Computation

All PHY abstraction metrics are computed as a function of post-processing per-tone SINR values across the coded block at the input to the decoder. The post-processing per-tone SINR is therefore dependent on the transmitter/receiver algorithm used to modulate/demodulate the symbols.

4.4.1. Per-tone Post Processing SINR for SISO

As an illustration of how the post-processing per-tone SINR values can be computed, we first consider the simple case of a single-input-single output (SISO) system with a matched filter receiver. Without loss of generality, let the target user/sector be denoted by the index 0. The received signal at the n -th sub-carrier for the target user is calculated as:

$$Y^{(0)}(n) = \sqrt{P_{tx}^{(0)} P_{loss}^{(0)}} H^{(0)}(n) X^{(0)}(n) + \sum_{j=1}^{N_I} \sqrt{P_{tx}^{(j)} P_{loss}^{(j)}} H^{(j)}(n) X^{(j)}(n) + U^{(0)}(n) \quad (67)$$

where

N_I is the number of interferers,

$P_{tx}^{(j)}$ is the total transmit power from j -th BS (per sector) or MS,

$P_{loss}^{(j)}$ is the distance dependent path loss including shadowing and antenna gain/loss and cable losses from the j -th sector or MS, $P_{loss}^{(j)}$ (is a linear term) that is smaller or equal to unity,

$H^{(j)}(n)$ is the channel gain for the desired MS for the n -th sub-carrier and j -th user/sector,

$X^{(j)}(n)$ is the transmitted symbols by the j -th user/sector on the n -th sub-carrier,

$U^{(0)}(n)$ is the receiver thermal noise, modeled as AWGN noise with zero mean and variance σ^2 .

Using a matched filter receiver, given by $H^{(0)}(n)^* Y^{(0)}(n)$, the post-processing SINR may be expressed as

$$SINR^{(0)}(n) = \frac{P_{tx}^{(0)} P_{loss}^{(0)} |H^{(0)}(n)|^2}{\sigma^2 + \sum_{j=1}^{N_I} P_{tx}^{(j)} P_{loss}^{(j)} |H^{(j)}(n)|^2} \quad (68)$$

4.4.2. Per-tone Post Processing SINR for SIMO with MRC

In order to obtain the per tone post processing SINR for the SIMO with MRC, we consider a 1 transmit and N_R receive antennas system. The received signal at the n -th sub-carrier in the r -th receive antenna is expressed as

$$Y_r^{(0)}(n) = \sqrt{P_{tx}^{(0)} P_{loss}^{(0)}} H_r^{(0)}(n) X^{(0)}(n) + \sum_{j=1}^{N_I} \sqrt{P_{tx}^{(j)} P_{loss}^{(j)}} H_r^{(j)}(n) X^{(j)}(n) + U_r^{(0)}(n) \quad (69)$$

After MRC process, the post-processing SINR of the desired user for the n -th sub-carrier is given as

$$SINR^{(0)}(n) = \frac{P_{tx}^{(0)} P_{loss}^{(0)} \left(\sum_{r=0}^{N_R-1} |H_r^{(0)}(n)|^2 \right)^2}{\left(\sum_{r=0}^{N_R-1} |H_r^{(0)}(n)|^2 \right) \sigma^2 + \sum_{j=1}^{N_I} P_{tx}^{(j)} P_{loss}^{(j)} \left| \sum_{r=0}^{N_R-1} H_r^{(0)}(n)^* H_r^{(j)}(n) \right|^2} \quad (70)$$

4.4.3. Per-tone Post Processing SINR for MIMO STBC with MRC

In order to obtain the per tone post processing SINR for the MIMO STBC (matrix A), we consider a 2 transmit and N_R receive antennas system. The interferers are divided into the set with STBC and the set with non-STBC because interference statistics are different from each other. The received signal at the n -th sub-carrier in the 1st and the 2nd STBC symbol interval are expressed as

$$\begin{aligned} Y_r^{(0)}(n, 0) &= \sum_{j \in STBCset} \sqrt{P_{tx}^{(j)} P_{loss}^{(j)}} \left(H_{0,r}^{(j)}(n) X_0^{(j)}(n, 0) - H_{1,r}^{(j)}(n) X_0^{(j)}(n, 1)^* \right) + \\ &\quad \sum_{j \notin STBCset} \sum_{t=0}^{N_T^{(j)}-1} \sqrt{P_{tx}^{(j)} P_{loss}^{(j)}} H_{t,r}^{(j)}(n) X_t^{(j)}(n, 0) + U_r^{(0)}(n, 0), \\ Y_r^{(0)}(n, 1) &= \sum_{j \in STBCset} \sqrt{P_{tx}^{(j)} P_{loss}^{(j)}} \left(H_{0,r}^{(j)}(n) X_0^{(j)}(n, 1) + H_{1,r}^{(j)}(n) X_0^{(j)}(n, 0)^* \right) + \\ &\quad \sum_{j \notin STBCset} \sum_{t=0}^{N_T^{(j)}-1} \sqrt{P_{tx}^{(j)} P_{loss}^{(j)}} H_{t,r}^{(j)}(n) X_t^{(j)}(n, 1) + U_r^{(0)}(n, 1), \end{aligned} \quad (71)$$

where

$STBCset$, is a set for transmit with MIMO STBC. The index 0 is for the desired user and others are for interferers that transmit with MIMO STBC, and includes the interferers who transmit with MIMO STBC,

r is the received antenna index,

t is the transmit antenna index,

$N_T^{(j)}$ is the number of transmitting antennas for the j -th interferer with non-STBC transmission,

$Y_r^{(0)}(n, i)$ is the received signal in the i -th STBC symbol interval for the target user, $i = 0, 1$,

$X_t^{(j)}(n, i)$ is the transmitted symbol in the i -th STBC symbol interval, $i = 0, 1$,

1 In the case of non-STBC, if we define transmitted symbol vector
2 $X^{(j)}(n) \triangleq [X^{(j)}(n,0)^T, X^{(j)}(n,1)^T]^T$ (where $X^{(j)}(n,i) \triangleq [X_0^{(j)}(n,i), \dots, X_{N_T^{(j)}-1}^{(j)}(n,i)]^T$), covariance
3 of vectors $X^{(j)}(n)$ are $\sigma_j^2 I_{2N_T^{(j)} \times 2N_T^{(j)}}$ $j \notin STBCset$
4 In the case of STBC, $X_0^{(j)}(n,0) = X_1^{(j)}(n,1)^*$, $X_1^{(j)}(n,0) = -X_0^{(j)}(n,1)^*$ and the covariance of
5 symbol vector $X^{(j)}(n,0)$ is $\sigma_j^2 I_{2 \times 2}$ $j \in STBCset$,
6 $H_{t,r}^{(j)}(n)$ is the channel gain between the t -th transmit and the r -th receive antenna, and
7 is assumed to be static for two STBC symbols,
8 $U_r^{(0)}(n,i)$ is the receiver thermal noise in the i -th STBC symbol interval, $i = 0,1$, and
9 modeled as AWGN noise with zero mean and variance σ^2 .

10
11 The 1st and the 2nd STBC symbols are obtained through the following processes as
12

$$\begin{aligned} \hat{X}_0^{(0)}(n,0) &= \sum_{r=0}^{N_R-1} \left(H_{0,r}^{(0)*}(n) Y_r^{(0)}(n,0) + H_{1,r}^{(0)}(n) Y_r^{(0)}(n,1)^* \right) \\ \hat{X}_1^{(0)}(n,0) &= \sum_{r=0}^{N_R-1} \left(H_{1,r}^{(0)}(n)^* Y_r^{(0)}(n,0) - H_{0,r}^{(0)}(n) Y_r^{(0)}(n,1)^* \right) \end{aligned} \quad (72)$$

14 After decoding process of STBC, the post-processing SINR of the desired user for the
15 n -th sub-carrier SINR is given as

$$SINR^{(0)}(n) = \frac{P_s}{P_N + P_{I_NonSTBC} + P_{I_STBC}} \quad (73)$$

17 where

$$P_s = P_{tx}^{(0)} P_{loss}^{(0)} \sigma_0^2 \left(\sum_{t=0}^1 \sum_{r=0}^{N_R-1} |H_{t,r}^{(0)}(n)|^2 \right)^2,$$

$$P_N = \left(\sum_{t=0}^1 \sum_{r=0}^{N_R-1} |H_{t,r}^{(0)}(n)|^2 \right) \sigma^2,$$

$$P_{I_NonSTBC} = \sum_{\substack{j \neq 0, \\ j \notin STBCset}} P_{tx}^{(j)} P_{loss}^{(j)} \sigma_j^2 \left(\sum_{t=0}^{N_T^{(j)}-1} \left| \sum_{r=0}^{N_R-1} H_{0,r}^{(0)}(n)^* H_{t,r}^{(j)}(n) \right|^2 + \sum_{t=0}^{N_T^{(j)}-1} \left| \sum_{r=0}^{N_R-1} H_{1,r}^{(0)}(n) H_{t,r}^{(j)}(n)^* \right|^2 \right), \text{ and}$$

$$P_{I_STBC} = \sum_{\substack{j \neq 0, \\ j \in STBCset}} P_{tx}^{(j)} P_{loss}^{(j)} \sigma_j^2 \left(\left| \sum_{r=0}^{N_R-1} H_{0,r}^{(0)}(n)^* H_{0,r}^{(j)}(n) + H_{1,r}^{(0)}(n) H_{1,r}^{(j)}(n)^* \right|^2 + \left| \sum_{r=0}^{N_R-1} H_{1,r}^{(0)}(n) H_{0,r}^{(j)}(n)^* - H_{0,r}^{(0)}(n)^* H_{1,r}^{(j)}(n) \right|^2 \right).$$

4.4.4. Per-Tone Post Processing SINR Calculation for Spatial Multiplexing

A linear minimum mean square error (MMSE) receiver will be used as baseline receiver for the matrix B in the system level simulation methodology.

To illustrate the per-tone post processing SINR calculation for a MIMO system based on a linear MMSE receiver, we assume an N_T transmit and N_R receive antennas. Since these calculations are illustrative, for the sake of simplicity, we assume that N_T spatial streams are transmitted and $N_R \geq N_T$. We also assume that interferers and the desired signal use the same MIMO scheme for transmission. The simplified signal model is described as follows:

$$\underline{Y}^{(0)}(n) = \sqrt{P_{tx}^{(0)} P_{loss}^{(0)}} \underline{H}^{(0)}(n) \underline{X}^{(0)}(n) + \sum_{j=1}^{N_I} \sqrt{P_{tx}^{(j)} P_{loss}^{(j)}} \underline{H}^{(j)}(n) \underline{X}^{(j)}(n) + \underline{U}^{(0)} \quad (74)$$

where

$\underline{Y}^{(0)}(n)$ is a $N_R \times 1$ dimensional received signal vector at the desired MS for the n -th sub-carrier,

$\underline{H}^{(j)}(n)$ is the $N_R \times N_T$ channel gain matrix between the desired user and the interfering BS for the n -th sub-carrier,

$\underline{X}^{(0)}(n)$ and $\underline{X}^{(j)}(n)$ are the data modulation vectors ($N_T \times 1$) of the desired MS and the j -th interfering MS, with covariances $\sigma_0^2 \underline{I}$ and $\sigma_j^2 \underline{I}$ $j=1,2,\dots,N_I$, respectively, and

$\underline{U}^{(0)}$ is modeled as zero mean AWGN noise vector with covariance $\sigma^2 \underline{I}$, \underline{I} is the $N_R \times N_R$ identity matrix.

A linear MMSE receiver is used to demodulate the transmitted signal vector, thus

$$\underline{X}^{(0)}(n) = \underline{W}^*(n) \underline{Y}^{(0)}(n) \quad (75)$$

Here, the MMSE weights $\underline{W}(n)$ ($N_R \times N_T$ matrix) are specified as

$$\underline{W}(n) = \left(\sigma_0^2 P_{tx}^{(0)} P_{loss}^{(0)} \underline{H}^{(0)}(n) \underline{H}^{(0)*}(n) + \tilde{\sigma}^2 \right)^{-1} \sigma_0^2 \sqrt{P_{tx}^{(0)} P_{loss}^{(0)}} \underline{H}^{(0)}(n) \quad (76)$$

where $(.)^*$ is the Hermitian operator and $\tilde{\sigma}^2 = \sigma^2 \underline{I} + \sum_{j=1}^{N_I} \sigma_j^2 P_{tx}^{(j)} P_{loss}^{(j)} \underline{H}^{(j)}(n) \underline{H}^{(j)*}(n)$

The post-processing SINR can be computed by defining the following two expressions:

$D(n) = \text{diag} \left[W^*(n) \sqrt{P_{tx}^{(0)} P_{loss}^{(0)}} \underline{H}^{(0)}(n) \right]$ which denotes the desired signal component

and $I_{self}(n) = W^*(n) \sqrt{P_{tx}^{(0)} P_{loss}^{(0)}} \underline{H}^{(0)}(n) - D(n)$ which is the self interference between MIMO streams.

The post-processing SINR of the desired MS for n -th sub-carrier and the k -th MIMO stream is thus given as:

$$SINR_k^{(0)}(n) = \frac{\text{diag} \left[\sigma_0^2 D(n) D^*(n) \right]_{kk}}{\text{diag} \left[\sigma^2 W^*(n) W(n) + \sigma_0^2 I_{self} I_{self}^* + \sum_{j=1}^{N_I} P_{tx}^{(j)} P_{loss}^{(j)} \sigma_j^2 W^*(n) \underline{H}^{(j)}(n) \underline{H}^{(j)*}(n) W(n) \right]_{kk}} \quad (77)$$

4.4.5. Interference Aware PHY Abstraction

Proponents should provide justification of assumptions related to knowledge of interference statistics used in system level simulations.

4.4.6. Practical Transmitter/Receiver Impairments

The evaluation methodology should account for practical transmitter and receiver impairments and implementation losses.

4.4.7. Channel Estimation Errors

The evaluation methodology should account for losses resulting from channel estimation errors. Proponents should provide the description of the assumed channel estimation scheme as well as link level simulation results justifying the loss model by comparing performance with known channel versus performance with estimated channel.

An example of how to model to channel estimation error is described in the following steps^{§§}:

Step 1: The channel estimation MSE is modeled as

$$MSE = aE_s + (1/B)b\sigma^2 \quad (78)$$

where a, b are parameters that represent asymptotic interpolation error and noise gain respectively. B represents the power boosting of pilot over data. E_s and σ^2 are the average total signal power and average interference plus noise power.

^{§§} Details of the mathematical derivations leading up to channel estimation modeling are shown in [79].

1 **Step 2:** Obtain Post Processing SNRs for a given transmission mode and receiver type
 2 as follows

3 4.4.7.1. SISO Channel Estimation Error Modeling

4 The per subcarrier SNR is modeled as

$$5 \quad SNR_i = \frac{|H_i|^2}{aE_s + [1 + (1/B)b]\sigma^2} \quad (79)$$

6 where H_i is the channel on subcarrier i . E_s and σ^2 are the average total signal power
 7 and average interference plus noise power.

8 4.4.7.2. SIMO Channel Estimation Error Modeling

9 For the single stream 1x2 SIMO case, the received data signal is given by

$$10 \quad \begin{aligned} \begin{bmatrix} y_1 \\ y_2 \end{bmatrix} &= \begin{bmatrix} h_{11} \\ h_{21} \end{bmatrix} s_1 + \begin{bmatrix} I_1 \\ I_2 \end{bmatrix} + \begin{bmatrix} w_1 \\ w_2 \end{bmatrix} \\ &= \begin{bmatrix} h_{11} \\ h_{21} \end{bmatrix} s_1 + \begin{bmatrix} n_1 \\ n_2 \end{bmatrix} \end{aligned} \quad (80)$$

11 where I_i, w_i are the interference and noise components on the i -th receive antenna and
 12 $n_i = I_i + w_i$ is the total interference plus noise. Here, $E[|h_{ij}|^2] = E_s$, the signal power, and
 13 $E[|s_1|^2] = 1$ to retain normalization of the total transmit power at 1. With channel
 14 estimation, it can be modified as

$$15 \quad \begin{aligned} \begin{bmatrix} y_1 \\ y_2 \end{bmatrix} &= \begin{bmatrix} \hat{h}_{11} \\ \hat{h}_{21} \end{bmatrix} s_1 + \begin{bmatrix} e_{11} \\ e_{21} \end{bmatrix} s_1 + \begin{bmatrix} n_1 \\ n_2 \end{bmatrix} \\ &= \begin{bmatrix} \hat{h}_{11} \\ \hat{h}_{21} \end{bmatrix} s_1 + \begin{bmatrix} e_{11}s_1 + n_1 \\ e_{21}s_1 + n_2 \end{bmatrix} \\ &= \begin{bmatrix} \hat{h}_{11} \\ \hat{h}_{21} \end{bmatrix} s_1 + \begin{bmatrix} n_1^{ce} \\ n_2^{ce} \end{bmatrix} \\ &\triangleq \begin{bmatrix} h_{11} \\ h_{21} \end{bmatrix} s_1 + \begin{bmatrix} n_1^{ce} \\ n_2^{ce} \end{bmatrix} \end{aligned} \quad (81)$$

16 We then have

$$17 \quad \sigma_{ce,i}^2 = E[|n_i^{ce}|^2] = MSE_{1,i} + \sigma_i^2 \quad (82)$$

18 where σ_i^2 is the total interference plus noise power on receive antenna i , and $\sigma_{ce,i}^2$ is
 19 now the effective combined noise variance to be used in the MRC combining equations

after appropriate scaling. MSE_{n_t, n_r} is the MSE on transmit antenna N_T and receive antenna N_R .

4.4.7.3. 2x2 MIMO Channel Estimation Error Modeling

Here we provide modified signal expressions with channel estimation. They can be adapted to general $N_R \times N_T$ MIMO configuration. The received signal on data sub-carriers is given by

$$\begin{aligned} \begin{bmatrix} y_1 \\ y_2 \end{bmatrix} &= \begin{bmatrix} h_{11} & h_{12} \\ h_{21} & h_{22} \end{bmatrix} \begin{bmatrix} s_1 \\ s_2 \end{bmatrix} + \begin{bmatrix} I_1 \\ I_2 \end{bmatrix} + \begin{bmatrix} w_1 \\ w_2 \end{bmatrix} \\ &= \begin{bmatrix} \hat{h}_{11} & \hat{h}_{12} \\ \hat{h}_{21} & \hat{h}_{22} \end{bmatrix} \begin{bmatrix} s_1 \\ s_2 \end{bmatrix} + \begin{bmatrix} n_1 \\ n_2 \end{bmatrix} \end{aligned} \quad (83)$$

where $E[|h_{ij}|^2] = E_s$. Further $E[|s_1|^2] = E[|s_2|^2] = 1/2$ to normalize the total transmit power (i.e. the sum of the transmit power over both antennas) to 1. Note that this does provide an implicit pilot boosting, since pilots are transmitted in SISO mode on each antenna, but this factor is recognized in the derivation which follows. With channel estimation, the above expression can be modified to

$$\begin{aligned} \begin{bmatrix} y_1 \\ y_2 \end{bmatrix} &= \begin{bmatrix} \hat{h}_{11} & \hat{h}_{12} \\ \hat{h}_{21} & \hat{h}_{22} \end{bmatrix} \begin{bmatrix} s_1 \\ s_2 \end{bmatrix} + \begin{bmatrix} e_{11} & e_{12} \\ e_{21} & e_{22} \end{bmatrix} \begin{bmatrix} s_1 \\ s_2 \end{bmatrix} + \begin{bmatrix} n_1 \\ n_2 \end{bmatrix} \\ &= \begin{bmatrix} \hat{h}_{11} & \hat{h}_{12} \\ \hat{h}_{21} & \hat{h}_{22} \end{bmatrix} \begin{bmatrix} s_1 \\ s_2 \end{bmatrix} + \begin{bmatrix} e_{11}s_1 + e_{12}s_2 + n_1 \\ e_{21}s_1 + e_{22}s_2 + n_2 \end{bmatrix} \\ &= \begin{bmatrix} \hat{h}_{11} & \hat{h}_{12} \\ \hat{h}_{21} & \hat{h}_{22} \end{bmatrix} \begin{bmatrix} s_1 \\ s_2 \end{bmatrix} + \begin{bmatrix} n_1^{ce} \\ n_2^{ce} \end{bmatrix} \\ &\triangleq \begin{bmatrix} h_{11} & h_{12} \\ h_{21} & h_{22} \end{bmatrix} \begin{bmatrix} s_1 \\ s_2 \end{bmatrix} + \begin{bmatrix} n_1^{ce} \\ n_2^{ce} \end{bmatrix} \end{aligned} \quad (84)$$

which separates the known component of signal and the error due to channel estimation. Further, the last expression neglects the minor degradation in received signal component, since the loss of performance can primarily be attributed to the increase in effective noise variance. We have

$$\sigma_{ce,i}^2 = E[|n_i^{ce}|^2] = \frac{1}{2} MSE_{1,i} + \frac{1}{2} MSE_{2,i} + \sigma_i^2 \quad (85)$$

σ_i^2 is the total interference plus noise power on receive antenna i . MSE could potentially be different on the different transmit antennas with time processing or if different pilot patterns are used, but typically can be assumed to be the same. Further, the above equation assumes transmit power is split equally among transmit streams. More generally it is

$$\sigma_{ce,i}^2 = E[|n_i^{ce}|^2] = E[|s_1|^2] \times MSE_{1,i} + E[|s_2|^2] \times MSE_{2,i} + \sigma_i^2 \quad (86)$$

With the above modified signal model, the approach is then similar to that with ideal channel estimation. The post processing SNRs are computed starting from this model and then input to link abstraction methods.

Filter Design Set	Permutation/MIMO Mode/Pilot Pattern	Channel	Model Parameters		
			SNR Range [-3 5] dB	SNR Range [5 20] dB	SNR Range [20 30] dB
1	PUSC	ITU Ped-B 3km/hr	[0.027,0.1]	[8.7e-4,0.19]	[7.5e-5,0.26]
2	PUSC	ITU Veh-A 30km/hr	[0.019,0.1]	[1.6e-3,0.17]	[1.5e-4,0.30]
3	PUSC	ITU Veh-A 120km/hr	[0.03,0.1]	[2.1e-3,0.23]	[1.7e-4,0.38]
4	PUSC-STC Zone	ITU Ped-B 3km/hr	[0.05, 0.16]	[1.9e-3,0.34]	[1.7e-4 0.47]
5	PUSC-STC Zone	ITU Veh-A 30km/hr	[0..039, 0.158]	[3e-3, 0.29]	[0.45e-3,0.52]
6	PUSC-STC Zone	ITU Veh-A 120km/hr	[0.54 0.157]	[5e-3,0.38]	[0.66e-3,0.71]

Table 33: Modes and parameters for channel estimation model*

*MMSE over a grid of 1 cluster x 4 symbols is assumed

When system level results are provided in a contribution with channel estimation schemes turned on, it would be sufficient to provide the parameters as shown in Table 33. Different filter designs could correspond to different permutation modes like PUSC, AMC, different pilot patterns like common pilots or dedicated pilots, SNRs, Doppler, channels etc. The parameterization can be implementation dependent and is recommended to be provided with the simulation results when channel estimation is used. Though they are specific to individual implementations, they have enough information to harmonize or calibrate results.

The parameters can be derived for each filter design set (i.e., a fixed channel estimation filters) by

1. Running the channel estimator at a set of SNRs.
2. Storing the MSE of channel estimation at each of these SNRs.
3. Performing a simple linear least squares curve fit to this data.

The parameters can be obtained from link simulations with channel estimation.

4.4.8. Interference Unaware Modeling

In the previous sections we assumed that the receiver has knowledge of interference power per sub-carrier when computing the post-processing SINR. In practice, the per-sub-carrier interference power is unknown at the decoder. Therefore, the per-sub-carrier

SINR is modified by averaging the interference power across the set of sub-carriers used.

As seen from Figure 11, the interference plus noise in the post processing SINR equation are averaged over all the occupied sub-carriers. Thus, the per-tone signal-to-average interference plus noise (SAINR) is calculated and used as input to the PHY abstraction. This method of accounting for the effect of practical interference knowledge applies to all transmitter/receiver configurations.

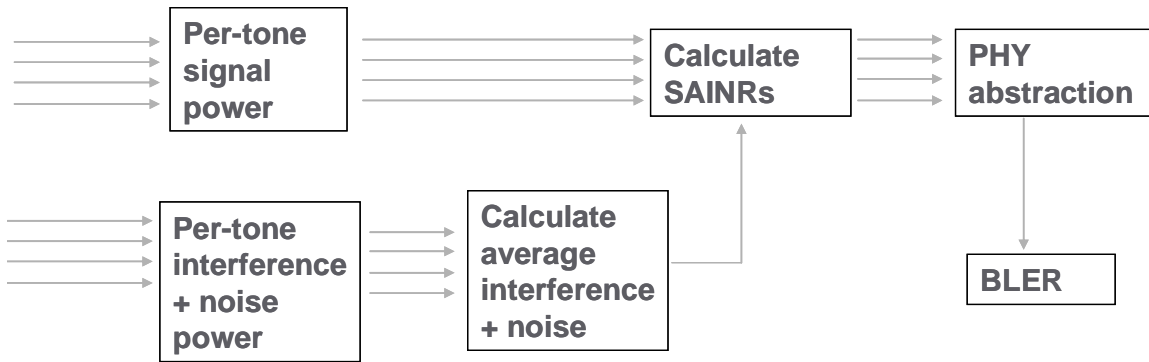


Figure 11: PHY abstraction simulation procedure for average interference knowledge

4.4.9. Error Vector Magnitude

The model of the received signal in Equation (69) ignored the non-idealities of the transmitted waveform. Appendix J includes a discussion on the typical effects of peak-to-average power reduction (PAPR) methods and their impact on the transmitted waveform quality, captured in terms of a quantity termed error vector magnitude (EVM). Thus, in the case of evaluating PAPR ratio reduction methods, the EVM component should be included in the per-tone SINR computation. The transmitted waveform is thus composed of the desired signal plus an error signal whose power is proportional to the transmitted signal power. Thus, an EVM term should be added by including an additional interferer using the same channel matrix as the target user and transmit power lower by EVM than the user's transmit power, i.e. $10^{-EVM/10} P_{tx}^{(0)}$.

Taking into account the effect of EVM, the per-tone SINR for the SISO case as an example becomes

$$SINR^0(n) = \frac{\sigma_0^2 P_{tx}^{(0)} P_{loss}^{(0)} |H^{(0)}(n)|^2}{\sigma^2 + \sum_{j=1}^{N_i} \sigma_j^2 P_{tx}^{(j)} P_{loss}^{(j)} |H^{(j)}(n)|^2 + 10^{-EVM/10} \cdot \sigma_0^2 \cdot P_{tx}^{(0)} P_{loss}^{(0)} |H^{(0)}(n)|^2} \quad (87)$$

where the EVM value is defined in Table 3.

4.5. Deriving Packet Error Rate from Block Error Rate

A packet comprises several FEC blocks. The packet error rate (PER) is the probability that an error occurs in at least one of FEC blocks comprising the packet. The PHY abstraction predicts the link performance, in terms of BLER, for a coded FEC block. Here we need to extrapolate the PER given the predicted BLER. If a packet is comprised of J blocks and the predicted BLERs are given by $BLER_1, BLER_2, \dots, BLER_J$, then assuming that the block errors events are independent, the PER is given as

$$PER = 1 - \prod_{j=1}^J (1 - BLER_j) \quad (88)$$

4.6. PHY Abstraction for H-ARQ

PHY abstraction of H-ARQ depends on the H-ARQ method. Similar to the non-HARQ PHY abstraction, proponents should provide the additional parameters required for the H-ARQ coding and retransmission schemes. This section summarizes the methods that are generally applicable to all PHY abstraction approaches with H-ARQ. Specifically, the approaches are similar for all bit-based mutual information-based abstraction techniques (MMIB, RBIR). For convenience, we will just refer to these metrics as MI in this section.

4.6.1. Baseline Modeling for HARQ

The following abstraction is proposed as baseline:

- For Chase combining (CC): The SINR values of the corresponding sub-carriers are summed across retransmissions, and these combined SINR values will be fed into the PHY abstraction.
- For Incremental redundancy (IR): The transmission and retransmissions are regarded as a single codeword, and all the SINR values are fed into the PHY abstraction. In practice, some partial repetition occurs, when part of the coded information is repeated in subsequent retransmissions.

For methods combining CC and IR the second approach is preferred but should be justified by link level simulations.

4.6.2. Chase Combining

The post-processing SINR in this case can be obtained as the sum of the SINRs from the first transmission and subsequent retransmissions, and thus the post-combining mutual information metric is given by

$$M_I = \frac{1}{N} \sum_{n=1}^N I_m \left(\sum_{j=1}^q \gamma_{nj} \right) \quad (89)$$

where q is the number of transmissions, $I_m(\cdot)$ is the MI function for modulation order ' m ' and γ_{nj} is the n -th symbol SINR during j -th retransmission. The mutual information metric can then be input to the AWGN reference characterized by the ' b ' and ' c ' parameters (as used in section [78]).

Similarly, the effective SINR for EESM in the case of Chase combining is given by

$$\gamma_{eff} = -\beta \ln \left(\frac{1}{N} \sum_{n=1}^N \exp \left(-\frac{\sum_{j=1}^q \gamma_{nj}}{\beta} \right) \right) \quad (90)$$

where γ_{eff} is the effective SINR after q transmissions that is input to the AWGN reference to compute the BLER.

4.6.3. Incremental Redundancy (IR)

With no repetition of coded bits, the performance of the decoder at each stage is that corresponding to a binary code with the modified equivalent code rate and code size as illustrated in Figure 12 for MI based approaches.

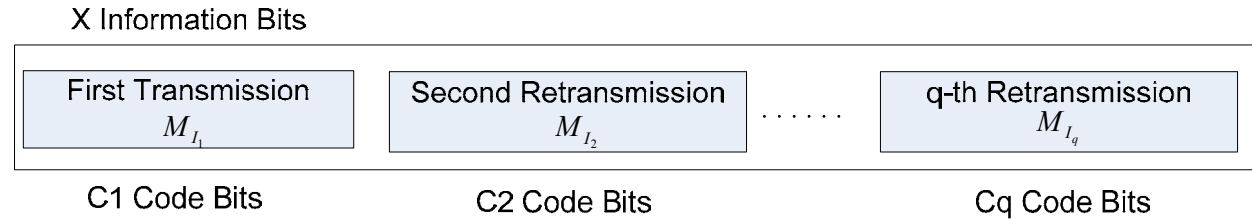


Figure 12: MI-based parameter update after transmission

The required input parameters for AWGN mapping function are given below

$$\begin{aligned} R_{eff} &= \frac{X}{\sum_{i=1}^q C_i} \\ L_{eff} &= \sum_{i=1}^q C_i \\ M_{I_{IR,q}} &= \frac{\sum_{i=1}^q C_i M_{I_i}}{\sum_{i=1}^q C_i} \end{aligned} \quad (91)$$

where R_{eff} , L_{eff} and $M_{I_{IR,q}}$ are the effective code rate, block size and mutual information after q retransmissions, respectively.

In practice, due to finite granularity in IR implementation, partial repetition of coded bits is possible. Depending on the rate matching algorithm used, every H-ARQ transmission could have a set of new parity bits and other bits that are repeated. Accumulating the mutual information is appropriate as long as new parity bits are transmitted in every symbol. Otherwise, the receiver combines the demodulation symbols or, more typically, the LLRs. In this section, we consider a rate-matching approach that does pure IR transmissions and involves coded bit repetitions once all the coded bits from a base code rate are exhausted.

To handle this general case, we consider a retransmission including a set of N_{NR} new coded bits and a set of N_R coded bits repeated from pervious transmissions. Further, we assume that there are N_{pre} coded bits that are not re-transmitted in this re-transmission. The averaged mutual information per bit from previous transmissions is $M_{I_{old}}$. The averaged mutual information per bit in this re-transmissions is \bar{I}_b .

We can then compute an updated mutual information metric after this retransmission as follows

$$M_{I_{new}} = \frac{N_{pre} \cdot M_{I_{old}} + N_{NR} \cdot \bar{I}_b + N_R \cdot f_1\left(f_1^{-1}(M_{I_{old}}) + f_1^{-1}(\bar{I}_b)\right)}{N_{pre} + N_{NR} + N_R} \quad (92)$$

where $f_1(\cdot)$ is a mapping from bit SINR to MI. If the modulation is constant across retransmissions, $f_1(\cdot)$ should be the MI function corresponding to that modulation. Otherwise, it is recommended to use the MI function corresponding QPSK. When the number of retransmissions is greater than one, Equation (92) is used recursively.

The BLER can be obtained by looking up the AWGN MI to BLER relationship corresponding to the modified effective code rate and code size, which are given by

$$R_{eff} = \frac{X}{N_{pre} + N_{NR} + N_R} \quad (93)$$

$$L_{eff} = N_{pre} + N_{NR} + N_R$$

A code rate-code size parameterized relationship for b and c parameters in the AWGN reference (Refer to Section 4.3.2), is recommended to cover the new and many possible BCR combinations with IR. Such a relationship can be obtained by expressing the b and c parameters as simple 2-dimensional parameterized functions of block size and code rate as follows, which could further reduce storage requirements and streamline simulation methodology,

$$\begin{aligned} b &= f(R, L) = R + f'(R, L) \\ c &= g(R, L) \end{aligned} \quad (94)$$

where R is the code rate (e.g. 1/2) and L is the block size (e.g. 500 bits).

For EESM, if the modulation does not change in retransmission, the effective SINR for k -th transmission can be calculated as follows:

$$SINR_{eff}^1 = -\beta \ln \left(\frac{1}{|U_1|} \sum_{n \in U_1} \exp \left(-\frac{SINR_{n,1}}{\beta} \right) \right)$$

1 and (95)

$$SINR_{eff}^k = -\beta \ln \left(\frac{1}{|U_k|} \left(\sum_{n \in U_{k-1}} \exp \left(-\frac{1}{\beta} (SINR_{eff}^{k-1} + I_{n,k} SINR_{n,k}) \right) + \sum_{n \in V_k, n \notin U_{k-1}} \exp \left(-\frac{SINR_{n,k}}{\beta} \right) \right) \right)$$

2 where $SINR_{eff}^k$ is k -th transmission's effective SINR, $SINR_{n,k}$ is k -th transmission's post
 3 processed SINR for bit index n , V_k is the set of indices where a coded bit was
 4 transmitted on k -th transmission, $I_{i,k}$ is an indicator function for codeword bit index i for
 5 the set V_k , ($I_{i,k} = 0$ for $i \notin V_k$, and $I_{i,k} = 1$ for $i \in V_k$), and U_k is the unique bit indices
 6 transmitted up to transmission k , $U_k = \bigcup_{j=1}^k V_j$. The choice of β 's is TBD.

7 4.7. PHY Abstraction for Repetition Coding

8 The SINR values of the sub-carriers are summed across repetition number, and these
 9 combined SINR values will be fed into the PHY abstraction.

10 5. Link Adaptation

11
 12 Link adaptation can enhance system performance by optimizing resource allocation in
 13 varying channel conditions. System level simulations should include adaptation of the
 14 modulation and coding schemes, according to link conditions.

15
 16 The purpose of this section is to provide guidelines for link adaptation in system
 17 evaluations. The use of link adaptation is left to the proponent as it may not pertain to all
 18 system configurations. The link adaptation algorithms implemented in system level
 19 simulations are left to Individual proponents for each proposal. Proponents should
 20 specify link adaptation algorithms including power, MIMO rank, and MCS adaptation per
 21 resource block.

22 5.1. Adaptive Modulation and Coding

23 The evaluation methodology assumes that adaptive modulation and coding with various
 24 modulation schemes and channel coding rates is applied to packet data transmissions.
 25 In the case of MIMO, different modulation schemes and coding rates may be applied to
 26 different streams.

27 5.1.1. Link Adaptation with HARQ

28 The link adaptation algorithm should be optimized to maximize the performance at the
 29 end of the HARQ process (e.g. maximize the average throughput under constraint on
 30 the delay and PER, or maximize number of users per service).

5.2. Channel Quality Feedback

A Channel Quality Indicator (CQI) channel is utilized to provide channel-state information from the user terminals to the base station scheduler. Relevant channel-state information can be fed back. For example, Physical CINR, effective CINR, MIMO mode selection and frequency selective sub-channel selection may be included in CQI feedback. Some implementations may use other methods, such as channel sounding, to provide accurate channel measurements. CQI feedback granularity and its impact may also be considered. Proponents should describe the CQI feedback type and assumptions of how the information is obtained.

5.2.1. Channel Quality Feedback Delay and Availability

Channel quality feedback delay accounts for the latency associated with the measurement of channel at the receiver, the decoding of the feedback channel, and the lead-time between the scheduling decision and actual transmission. The delay in reception of the channel quality feedback shall be modeled to accurately predict system performance.

Channel quality feedback may not be available every frame due to system constraints such as limited feedback overhead or intermittent bursts. The availability of the channel quality feedback shall be modeled in the system simulations.

The proponents should indicate the assumptions of channel quality feedback delay and availability for system proposals.

5.2.2. Channel Quality Feedback Error

System simulation performance should include channel quality feedback error by modeling appropriate consequences, such as misinterpretation of feedback or erasure.

The proposals shall describe if CQI estimation errors are taken into account and how those errors are modeled.

6. HARQ

The Hybrid ARQ (HARQ) protocol should be implemented in system simulations. Multiple parallel HARQ streams may be present in each frame, and each stream may be associated with a different packet transmission, where a HARQ stream is an encoder packet transaction pending, i.e., a HARQ packet has been transmitted but has not been acknowledged. Different MIMO configurations may also have an impact on the HARQ implementation.

Each HARQ transmission results in one of the following outcomes: successful decoding of the packet, unsuccessful decoding of the packet transmission requiring further re-transmission, or unsuccessful decoding of the packet transmission after maximum number of re-transmissions resulting in packet error. The effective SINR for packet transmissions after one or more HARQ transmissions used in system simulations is determined according to the PHY abstraction in Section 4.7.

1 When HARQ is enabled, retransmissions are modeled based on the HARQ option
2 chosen. For example, HARQ can be configured as synchronous/asynchronous with
3 adaptive/non-adaptive modulation and coding schemes for Chase combining or
4 incremental redundancy operation. Synchronous HARQ may include synchronous
5 HARQ acknowledgement and/or synchronous HARQ retransmissions. Synchronous
6 HARQ acknowledgement means that the HARQ transmitter side expects the HARQ
7 acknowledgments at a known delay after the HARQ transmission. Synchronous HARQ
8 retransmission means that the HARQ receiver side expects the HARQ retransmissions
9 at known times. In the case of asynchronous HARQ, the acknowledgement and/or
10 retransmission may not occur at known times. Adaptive H-ARQ, in which the
11 parameters of the retransmission (e.g. power, MCS) are changed according to channel
12 conditions reported by the MS may be considered. In the case of non-adaptive HARQ,
13 the parameters of the retransmission are not changed according to channel conditions.
14

15 The HARQ model and type shall be specified with chosen parameters, such as
16 maximum number of retransmissions, minimum retransmission delay, incremental
17 redundancy, Chase combining, etc. HARQ overhead (associated control) should be
18 accounted for in the system simulations on both the uplink and downlink

19 **6.1. HARQ Acknowledgement**

20 The HARQ acknowledgment is used to indicate whether or not a packet transmission
21 was successfully received.
22

23 Modeling of HARQ requires waiting for HARQ acknowledgment after each transmission,
24 prior to proceeding to the next HARQ transmission. The HARQ acknowledgment delay
25 should include the processing time which includes, decoding of the traffic packet, CRC
26 check, and preparation of acknowledgment transmissions. The amount of delay is
27 determined by the system proposal.
28

29 Misinterpretation, missed detection, or false detection of the HARQ acknowledgment
30 message results in transmission (frame or encoder packet) error or duplicate
31 transmission. Proponents of each system proposal shall justify the system performance
32 in the presence of error of the HARQ acknowledgment.

33 **7. Scheduling**

34 The scheduler allocates system resources for different packet transmissions according
35 to a set of scheduling metrics, which can be different for different traffic types. The same
36 scheduling algorithm shall be used for all simulation runs. System performance
37 evaluation and comparison require that fairness be preserved or at least known in order
38 to promote comparisons. On the other hand it is clear that various scheduling
39 approaches will have different performance and overhead impacts and will need to be
40 aligned. The owner(s) of any proposal to be standardized should also describe the
41 scheduling algorithm used for performance evaluation, along with assumptions on
42 feedback. The scheduling will be done with consideration of the reported metric where
43 the reported metric may include CQI and other information. The scheduler shall

1 calculate the available resources after accounting for all control channel overhead and
2 protocol overhead.

3 **7.1. DL Scheduler**

4 For the baseline simulation, a generic proportionally fair scheduler shall be used for the
5 full-buffer traffic model. The generic proportionally fair scheduler is defined in Appendix
6 F.

7
8 In the general deployment case, the MAC scheduler should be capable of handling a
9 traffic mix of different QoS service classes that are enabled by the air interface. The
10 proponent may present additional results with a more sophisticated scheduler other
11 than proportionally fair scheduler and shall describe the scheduler algorithm in detail.

12 **7.2. UL Scheduler**

13 The UL scheduler is very similar to DL Scheduler. The UL scheduler maintains the
14 request-grant status of various uplink service flows. Bandwidth requests arriving from
15 various uplink service flows at the BS will be granted in a similar fashion as the downlink
16 traffic.

17 **8. Handover**

18 The system simulation defined elsewhere in the document deals with throughput,
19 spectral efficiency, and latency. User experience in a mobile broadband wireless system
20 is also influenced by the performance of handover. This section focuses on the methods
21 to study the performance of handover which affects the end-users experience.
22 Proponents of system proposals specifically relating to handover should provide
23 performance evaluations according to this section.

24 For parameters such as cell size, DL&UL transmit powers, number of users in a cell,
25 traffic models, and channel models; the simulation follows the simulation methodology
26 defined elsewhere in the document. In this document, only intra-radio access
27 technology handover is considered; inter-radio access technology handover is not
28 considered.

29
30 The handover procedure consists of cell reselection via scanning, handover decision
31 and initiation, and network entry including synchronization and ranging with a target BS.

32
33 Latency is a key metric to evaluate and compare various handover schemes as it has
34 direct impact on application performance perceived by a user. Total handover latency is
35 decomposed into several latency elements. Further, data loss rate and unsuccessful
36 handover rate are important metrics.

38 **8.1. System Simulation with Mobility**

39 Two possible simulation models for mobility related performance are given in this
40 section. The first is a reduced complexity model that considers a single MS moving
41 along one of three trajectories with all other users at fixed locations, and a second

simulation model that considers all mobiles in the system moving along random trajectories.

8.1.1. Single Moving MS Model

For simplicity, one moving MS and multiple fixed MSs can be modeled as a baseline for the mobility simulations. The mobility related performance metrics shall be computed only for this moving terminal. The mobility mix for MSs is specified in the test scenarios of Section 2.3. The speed of the single moving MS is selected from the speed(s) specified in the mobility mix of the test scenario.

The trajectory of the moving MS can be chosen from the trajectories given in following section.

8.1.1.1. Trajectories

The movement of the single moving MS is constrained to one of the trajectories defined in this section. More detailed and realistic mobility models may be considered.

8.1.1.1.1. Trajectory 1

In this trajectory, the MS moves from Cell 1 to Cell 2 along the arrow shown in Figure 13. The trajectory starts from the center of Cell 1 to the center of Cell 2 while passing through the midpoint of the sector boundaries as shown in Figure 13. The purpose of this trajectory is to evaluate handover performance in a scenario where the signal strength from the serving sector continuously decreases whereas the signal strength from the target sector continuously increases.

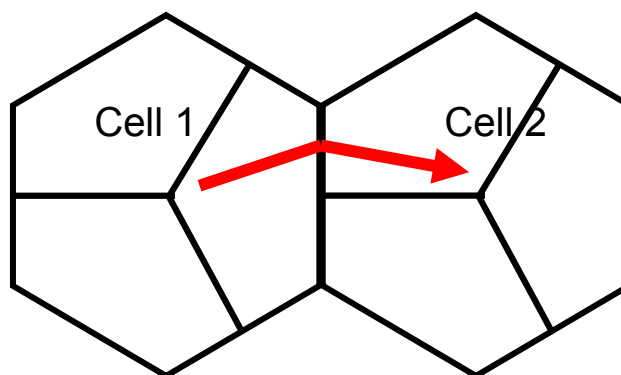


Figure 13: Trajectory 1

8.1.1.1.2. Trajectory 2

In this trajectory, the single moving MS moves from Cell 1 to Cell 2 along the arrow shown in Figure 14. The MS moves along the sector boundary between Cell 1 and Cell 2 until the midpoint of the cell boundary between Cell 1 and Cell 2. The purpose of this

- 1 trajectory is to evaluate handover performance when the MS moves along the boundary
2 of two adjacent sectors.

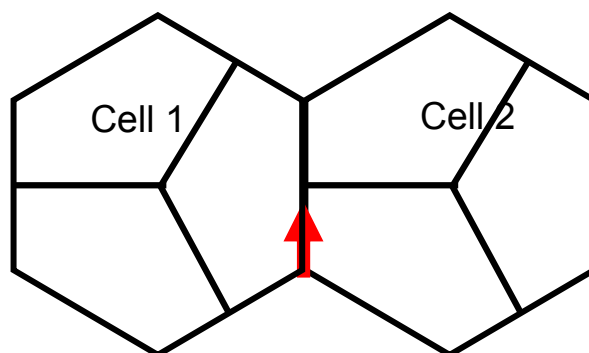


Figure 14: Trajectory 2

8.1.1.1.3. Trajectory 3

In this trajectory, the single moving MS moves from Cell 2 to Cell 1 along the arrow shown in Figure 15. The MS starts from the center of Cell 2, moves along the boundary of two adjacent sectors of Cell 2 and towards the center of the Cell 1. The purpose of this trajectory is to evaluate a handover performance in the scenario where the MS traverses multiple sector boundaries.

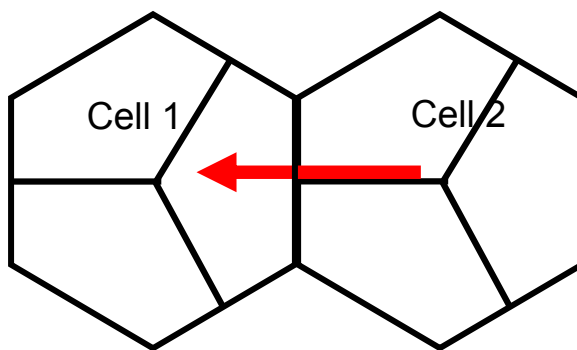


Figure 15: Trajectory 3

8.1.1.2. 10 Cell Topology

As a reduced complexity option, a 10 cell topology may be used for handover evaluation with a single moving MS. In the 10 cell topology, both serving and target cells should have one tier of neighboring cells as interferers shown in Figure 16.

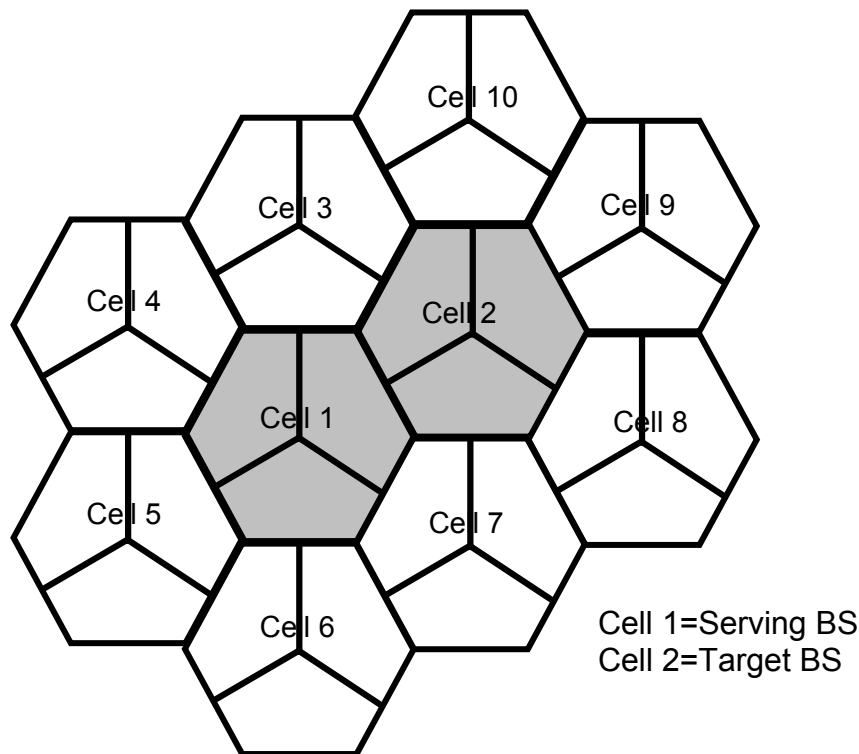


Figure 16: 10 Cell topology

8.1.1.3. Handover Evaluation Procedure

1. The system may be modeled using the 10 cell topology as illustrated in Figure 16 for the evaluation of handover performance. Each cell has three sectors and frequency reuse is modeled by planning frequency allocations in different sectors in the network.
2. N MSs are dropped independently with uniform distribution across the cell area. Different load levels in the network are simulated by changing the number of MSs and the traffic generated.
3. Path loss, shadow fading and fast fading models for each MS should be consistent with the models defined in Section 3. Fading signal and fading interference are computed from each mobile station into each sector and from each sector to each mobile for each simulation interval.

4. In the single MS model, the trajectories defined in Section 8.1.1.1 should be used to model the movement of a single MS associated with the center cell. The locations of all other MSs are assumed to be fixed and the serving sector for the fixed MSs does not change for the duration of the drop.
5. Path loss, shadow fading and fast fading are updated based on location and velocity of a moving MS. As the MS moves along the specified trajectory, the target sector is chosen according to the metric used to perform handover.
6. Traffic generated by the MSs should be according to the mixes specified in Table 44 in Section 10.7. The moving MS may be assigned one of the traffic types in the chosen traffic mix to analyze the effect of handover on the performance of the assigned traffic application. Traffic from the fixed MSs constitutes background load. Start times for each traffic type for each user should be randomized as specified in the traffic model being simulated.
7. Statistics related to handover metrics are collected for the moving MS only.
8. Packets are not blocked when they arrive into the system (i.e. queue depths are infinite). Packets are scheduled with a packet scheduler using the required fairness metric. Channel quality feedback delay, PDU errors are modeled and packets are retransmitted as necessary. The HARQ process is modeled by explicitly rescheduling a packet as part of the current packet call after a specified HARQ feedback delay period.
9. Sequences of simulation are run, each with a different random seed. For a given drop the simulation is run for this duration, and then the process is repeated with the MSs dropped at new random locations. A sufficient number of drops are simulated to ensure convergence in the system performance metrics.

8.1.2. Multiple Moving MS Model

In this model, multiple moving MSs are uniformly placed over the simulation environment and given a random trajectory and speed. The parameters selected remain in effect until a drop is completed.

8.1.2.1. Trajectories

Each MS is assigned an angle of trajectory at the beginning of a call. The assigned angle is picked from a uniform distribution across the range of 0-359 degrees in one degree increments. The angle of zero degrees points directly North in the simulation environment. Movement of the MS is established by selecting a random speed for the users according to profiles in Section 2.3 such that the population of MS users meets the desired percentages. The MS remains at the selected random speed and direction for the duration of the simulation drop. When a MS crosses a wrap around boundary point within the simulation space, the MS will wrap around to the associated segment

identified within Appendix G, continuing to keep the same speed and trajectory. Figure 17 depicts an example of the movement process for a 19-cell system.

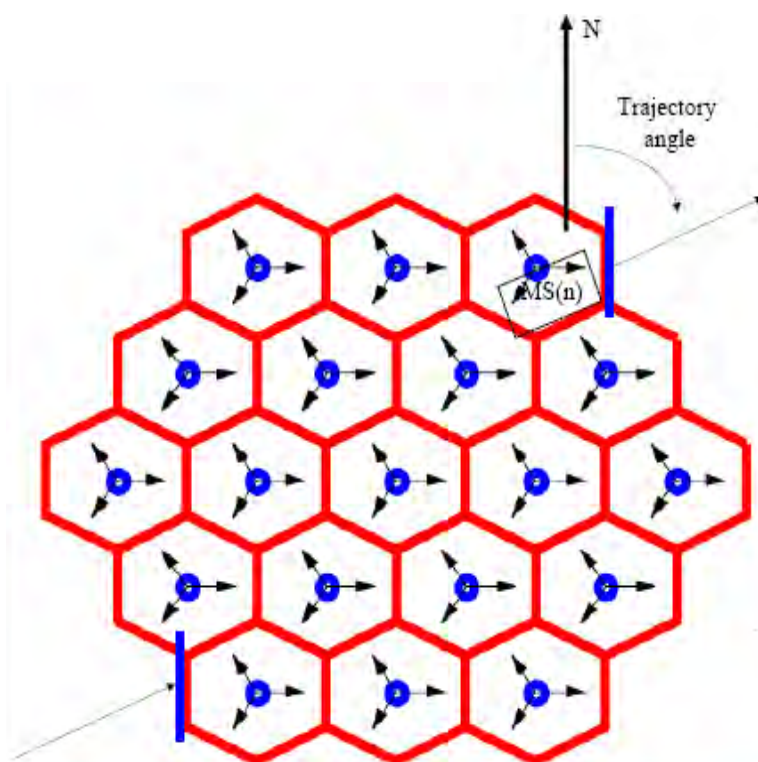


Figure 17: 19 cell abbreviated example of MS movement in a wrap around topology *

* Blue lines denote paired wrap around boundary segments

8.1.2.2. 19 Cell Topology

The 19 cell topology with wrap around can be used for handover evaluation with multiple moving MSs. The details of this topology can be found in Appendix G.

8.1.2.3. Handover Evaluation Procedure

For the 19 cell topology with wrap around defined for the multiple moving MS model, the simulation procedure outlined in Section 11 should be followed. In step 7 of this procedure, for the purposes of simulating handover performance, it may additionally be assumed that an MS is initially connected to a specific serving sector(s). As the MS moves along the trajectory described in Section 8.1.2.1, the target sector or diversity set is chosen according to the metric used to perform handover.

8.2. Handover Performance Metrics

The following parameters should be collected in order to evaluate the performance of different handover schemes. These statistics defined in this section should be collected

in relation to the occurrence of handovers. A CDF of each metric may be generated to evaluate a probability that the corresponding metric exceeds a certain value.

For a simulation run, we assume:

- The total number of successful handovers occurred during the simulation time = $N_{HO_success}$
- The total number of failed handover during the simulation time = N_{HO_fail}
- The total number of handover attempts during the simulation time = $N_{attempt}$, where $N_{attempt} = N_{HO_success} + N_{HO_fail}$

8.2.1. Radio Layer Latency

This value measures the delay between the time instance $T_{1,i}$ that an MS transmits a serving BS its commitment to HO (for a hard handover (HHO), this is the time that the MS disconnects from the serving BS) and the time instance $T_{2,i}$ that the MS successfully achieves PHY layer synchronization at the target BS (i.e., frequency and DL timing synchronization) due to handover occurrence i . The exact thresholds for successful PHY synchronization are for further study. For this metric, the average radio latency will be measured as

$$\text{Average Radio Layer Latency} = \frac{\sum_{i=1}^{N_{HO_success}} (T_{2,i} - T_{1,i})}{N_{HO_success}} \quad (96)$$

8.2.2. Network Entry and Connection Setup Time

This value represents the delay between an MS's radio layer synchronization at $T_{2,i}$, and the start of transmission of first data packet from the target BS at $T_{3,i}$ due to handover occurrence i . In the case of the reference system, this consists of ranging, UL resource request processes (contention or non-contention based), negotiation of capabilities, registration, DL packet coordination and a path switching time. The transmission error rate of MAC messages associated with network entry can be modeled dynamically or with a fixed value (e.g., 1%). A path switching time, as a simulation input parameter, may vary depending on network architecture.

$$\text{Average Network Entry and Connection Setup Time} = \frac{\sum_{i=1}^{N_{HO_success}} (T_{3,i} - T_{2,i})}{N_{HO_success}} \quad (97)$$

8.2.3. Handover Interruption Time

Handover interruption time represents the time duration that an MS cannot receive service from any BS during a handover. It is defined as the time interval from when the MS disconnects from the serving BS to the start of transmission of first data packet from the target BS.

8.2.4. Data Loss

This value represents the number of lost bits during the handover processes. This document uses DL data loss to evaluate the data loss performance of the air link. $D_{RX,i}$ and $D_{TX,i}$ denotes the number of received bits by the MS and the number of total bits transmitted by the serving and the target BSs during the MS performs handover occurrence i , respectively. Traffic profiles used for the simulation experiments to compare different handover schemes need to be identical.

$$\text{Data Loss} = \frac{\sum_{i=1}^{N_{HO_success}} (D_{TX,i} - D_{RX,i})}{N_{HO_success}} \quad (98)$$

8.2.5. Handover Failure Rate

This value represents the ratio of failed handover to total handover attempts. Handover failure occurs if handover is executed while the reception conditions are inadequate on either the DL or the UL such that the mobile would have to go to a network entry state.

$$\text{Handover Failure Rate} = \frac{N_{HO_fail}}{N_{attempt}} \quad (99)$$

9. Power Management (Informative)

The implementation of an idle state is proposed to be used in the IEEE 802.16m broadband wireless system to conserve battery power of mobile devices when a call session is not active. A mobile device returns to active state whenever required, e.g., when there is incoming data for the said device. IDLE to ACTIVE_STATE transition latency is a key metric to evaluate and compare various proposals related to IDLE to ACTIVE_STATE transition schemes as this latency has direct impact on application performance experienced by a user.

The IDLE to ACTIVE_STATE transition latency requirement is specified in the IEEE 802.16m Requirements document. According to this document, the IDLE to ACTIVE_STATE transition latency is defined as the time it takes for a device to go from an idle state (fully authenticated/registered and monitoring the control channel) to when it begins exchanging data with the network on a traffic channel.

IDLE to ACTIVE_STATE transition latency has several components as formulated in Section 9.1. Section 9.2 provides a simulation procedure to evaluate IDLE to ACTIVE_STATE transition latency. Proponents of system proposals specifically relating to IDLE to ACTIVE_STATE transition should evaluate performance according to this section.

9.1. Formulation for IDLE to ACTIVE_STATE Transition Latency

The IDLE to ACTIVE_STATE transition may be initiated either by the device or by the network. The first case is referred to as device-initiated IDLE to ACTIVE_STATE

transition and the second case is referred to as network-initiated IDLE to ACTIVE_STATE transition. The components of the IDLE to ACTIVE_STATE transition latency are described in the following sub-sections.

9.1.1. Device-initiated IDLE to ACTIVE_STATE Transition

The steps involved during device-initiated IDLE to ACTIVE_STATE transition are as follows:

1. Ranging
2. Network re-entry

During the ranging process the device adjusts its transmission parameters. During the network re-entry [61] service flows, CIDs, and other connection related states are established for the said device. The successful completion of the network re-entry process can be indicated by using appropriate network re-entry success message or other signaling mechanisms.

9.1.2. Network-initiated IDLE to ACTIVE_STATE Transition

The steps involved during network-initiated IDLE to ACTIVE_STATE transition are as follows:

1. Transmission of paging indication
2. Ranging
3. Network re-entry

During the transmission of the paging indication, the BSs in the paging area of the said idle mode device transmit a paging indication message containing the identification information of the said idle mode device. This step is completed when the said idle mode device successfully receives the paging indication. The measurement of IDLE to ACTIVE_STATE transition latency starts from the time when the said device receives paging indication through a paging message (i.e., not including the paging period). The ranging and network re-entry procedures are as defined in Section 9.1.1.

9.1.3. IDLE to ACTIVE_STATE Transition Latency

The IDLE to ACTIVE_STATE transition latency, τ_d is defined as follows.

$$\tau_d = T_r + T_e \quad (100)$$

where T_r and T_e are the times required to execute ranging and network re-entry, respectively.

9.2. Procedure for Evaluation of IDLE to ACTIVE_STATE Transition Latency

1. An idle mode device that is synchronized to the downlink channel, fully registered and authenticated with the network is considered as the candidate device to receive the paging indication using a paging message. In addition, it is considered that the said candidate device in idle mode is residing in the same paging group (PG) and IP subnet after entering into idle operation. This eliminates the need for evaluating the effect of backbone messages on the IDLE to ACTIVE_STATE transition latency.

1 The IDLE to ACTIVE_STATE transition latency shall be evaluated for device-
2 initiated IDLE to ACTIVE_STATE transition as well as network-initiated IDLE to
3 ACTIVE_STATE transition.
4

- 5 2. The system is modeled using the cell topology as defined in Section 8.1.1.2 and
6 each cell has three sectors. Frequency reuse is modeled by planning frequency
7 allocations in different sectors in the network.
8
- 9 3. N MSs are dropped independently with uniform distribution across the cell area.
10 Different load levels in the network are simulated by changing the number of MSs
11 and the traffic generated.
12
- 13 4. Path loss, shadow fading and fast fading models for each MS should be
14 consistent with the models defined in Section 3. Fading signal and fading
15 interference are computed from each mobile station into each sector and from
16 each sector to each mobile for each simulation interval.
17
- 18 5. It is considered that the device performing IDLE to ACTIVE_STATE transition is
19 stationary and may be located anywhere in the center cell with uniform
20 probability. The IDLE to ACTIVE_STATE transition is triggered by the MAC layer
21 of the device in case of device-initiated IDLE to ACTIVE_STATE transition. In the
22 case of network-initiated IDLE to ACTIVE_STATE transition, the IDLE to
23 ACTIVE_STATE transition is triggered by the MAC layer of the BSs in the paging
24 group of the device.
25
- 26 6. Traffic generated by the MSs in the fixed locations should be according to the
27 mixes specified in Table 44 in Section 10.7 and this traffic constitutes
28 background load.
29
- 30 7. Statistics of IDLE to ACTIVE_STATE transition latency are measured at different
31 locations of the center cell. A weighted sum of these measurements is used to
32 determine the mean value of the IDLE to ACTIVE_STATE transition latency.
33
- 34 8. Packets are not blocked when they arrive into the system (i.e. queue depths are
35 infinite). Packets are scheduled with a packet scheduler using the required
36 fairness metric.
37

38 Sequences of simulation are run, each with a different random seed. A sufficient
39 number of runs are simulated to ensure convergence in the performance metrics.

40 10. Traffic Models

41 This section describes traffic models in detail. A major objective of system simulations is
42 to provide an operator with a view of the maximum number of active users that can be
43 supported for a given service under a specified configuration at a given coverage level.
44

Modeling of User Arrival Process: Typically all users are not active at a given time and even the active users might not register for the same service. In order to avoid different user registration and demand models, the objective of the proposed simulation model is restricted to evaluate the performance with the users that are maintaining a session with transmission activity. This model can be used to determine the number of such registered users that can be supported. This document does not address the arrival process of such registered users, i.e. it does not address the statistics of subscribers that register and become active.

The traffic generated by a service should be accurately modeled in order to evaluate the performance of a system. This may be a time consuming exercise. Traffic modeling can be simplified, as explained below, by not modeling the user arrival process and assuming full queue traffic which is considered as the baseline. Modeling non-full-queue traffic is also discussed in the subsections that follow.

Full Queue Model: In the full queue user traffic model, all the users in the system always have data to send or receive. In other words, there is always a constant amount of data that needs to be transferred, in contrast to bursts of data that follow an arrival process. This model allows the assessment of the spectral efficiency of the system independent of actual user traffic distribution type. A user is in outage if residual PER after HARQ retransmissions exceeds 1%.

In the following sections, we will concentrate on traffic generation only for the non-full queue case. In addition, the interaction of the generated traffic with the higher layer protocol stack such as TCP is not fully included here. Instead, we will provide references to documents which provide the detailed TCP transport layer implementation and its interaction with the various traffic models.

The models described in this section shall be used for evaluating 802.16m proposals. Optionally, for liaison with NGMN, statistical traffic models and associated parameters defined in [63] or its latest revision may be used for system performance evaluation.

10.1. Web Browsing (HTTP) Traffic Model

HTTP traffic characteristics are governed by the structure of the web pages on the World Wide Web (WWW), and the nature of human interaction. The nature of human interaction with the WWW causes the HTTP traffic to have a bursty profile, where the HTTP traffic is characterized by ON/OFF periods as shown in Figure 18.

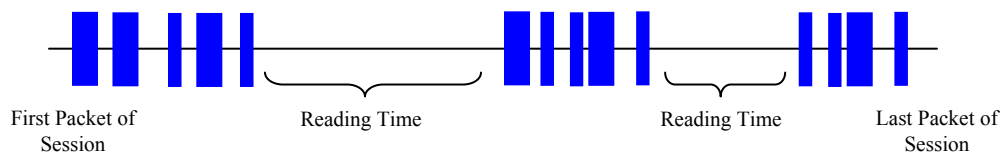


Figure 18: HTTP traffic pattern

The ON periods represent the sequence of packets in which the web page is being transferred from source to destination; while the OFF periods represent the time the user spends reading the webpage before transitioning to another page. This time is also known as Reading Time [43][44].

The amount of information passed from the source to destination during the ON period is governed by the web page structure. A webpage is usually composed of a main object and several embedded objects. The size of the main object, in addition to the number and size of the embedded objects define the amount of traffic passed from source to destination.

In summary, the HTTP traffic model is defined by the following parameters:

S_M : Size of main object in page

N_d : Number of embedded objects in a page

S_E : Size of an embedded object in page

D_{pc} : Reading time

T_p : Parsing time for the main page

In addition to the model parameters, HTTP traffic behavior is also dependent on the HTTP version used. Currently HTTP 1.0 and HTTP 1.1 are widely used by servers and browsers [45]-[48]. In HTTP 1.0, also known as burst mode transfer, a distinct TCP connection is used for each object in the page, thereby facilitating simultaneous transfer of objects. The maximum number of simultaneous TCP connections is configurable, with most browsers using a maximum of 4 simultaneous TCP connections. In HTTP/1.1, also known as persistent mode transfer, all objects are transferred serially over a single persistent TCP connection. Table 34 provides the model parameters for HTTP traffic.

Component	Distribution	Parameters	PDF
Main object size (S_M)	Truncated Lognormal	Mean = 10710 bytes SD = 25032 bytes Min = 100 bytes Max = 2 Mbytes (before truncation)	$f_x = \frac{1}{\sqrt{2\pi}\sigma x} \exp\left[-\frac{(\ln x - \mu)^2}{2\sigma^2}\right], x \geq 0$ $\sigma = 1.37, \mu = 8.37$ if $x > \max$ or $x < \min$, discard and generate a new value for x
Embedded object size (S_E)	Truncated Lognormal	Mean = 7758 bytes SD = 126168 bytes Min = 50 bytes Max = 2 Mbytes (before truncation)	$f_x = \frac{1}{\sqrt{2\pi}\sigma x} \exp\left[-\frac{(\ln x - \mu)^2}{2\sigma^2}\right], x \geq 0$ $\sigma = 2.36, \mu = 6.17$ if $x > \max$ or $x < \min$, discard and generate a new value for x

Number of embedded objects per page (Nd)	Truncated Pareto	Mean = 5.64 Max. = 53 (before truncation)	$f_x = \frac{\alpha k}{x^{\alpha+1}}, k \leq x < m$ $f_x = \left(\frac{k}{m} \right)^{\alpha}, x = m$ $\alpha = 1.1, k = 2, m = 55$ <p>Subtract k from the generated random value to obtain Nd</p> <p>if $x > \max$, discard and regenerate a new value for x</p>
Reading time (Dpc)	Exponential	Mean = 30 sec	$f_x = \lambda e^{-\lambda x}, x \geq 0$ $\lambda = 0.033$
Parsing time (Tp)	Exponential	Mean = 0.13 sec	$f_x = \lambda e^{-\lambda x}, x \geq 0$ $\lambda = 7.69$

Table 34: HTTP traffic parameters

To request an HTTP session, the client sends an HTTP request packet, which has a constant size of 350 bytes. From the statistics presented in the literature, a 50%-50% distribution of HTTP versions between HTTP 1.0 and HTTP 1.1 has been found to closely approximate web browsing traffic in the internet [49].

Further studies also showed that the maximum transmit unit (MTU) sizes most common to in the internet are 576 bytes and 1500 bytes (including the TCP header) with a distribution of 24% and 76% respectively. Thus, the web traffic generation process can be described as in Figure 19.

A user is defined in outage for HTTP service if the average packet call throughput is less than the minimum average throughput requirement of 128 kbps. The system outage requirement is such that no more than 2% of users can be in outage. The air link PER of MAC SDUs for HTTP traffic should be not be greater than 1%.

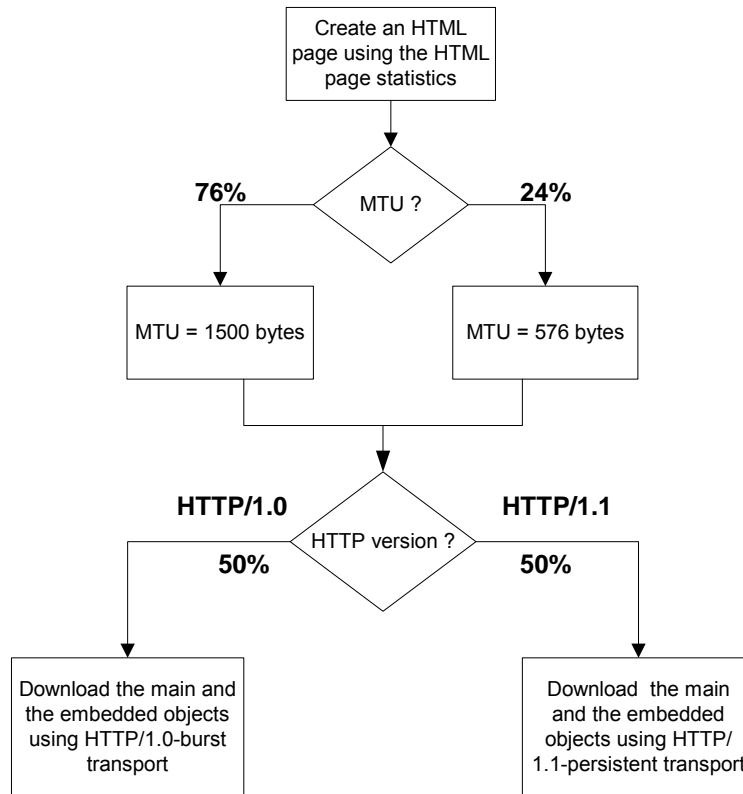


Figure 19: HTTP traffic profiles

10.1.1. HTTP and TCP Interactions for DL HTTP Traffic

Two versions of the HTTP protocol, HTTP/1.0 and HTTP/1.1, are widely used by servers and browsers. Users shall specify 50% HTTP/1.0 and 50% HTTP/1.1 for HTTP traffic. For people who have to model the actual interaction between HTTP traffic and the underlying TCP connection, refer to 4.1.3.2, 4.2.4.3 of [50] for details.

10.1.2. HTTP and TCP Interactions for UL HTTP Traffic

HTTP/1.1 is used for UL HTTP traffic. For details regarding the modeling of the interaction between HTTP traffic and the underlying TCP connection, refer to 4.2.4.1, 4.2.4.2 of [50].

10.2. File Transfer Protocol Model

File transfer traffic is characterized by a session consisting of a sequence of file transfers, separated reading times. Reading time is defined as the time between end of transfer of the first file and the transfer request for the next file. The packet call size is therefore equivalent to the file size and the packet call inter-arrival time is the reading time. A typical FTP session is shown in Figure 20.

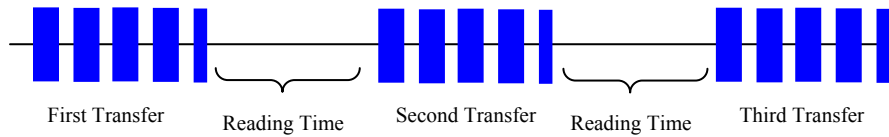


Figure 20: FTP traffic patterns

Table 35 provides the model parameters for FTP traffic that includes file downloads as well as uploads [51]-[52]. In the case of file uploads, the arrival of new users is Poisson distributed and each user transfers a single file before leaving the network.

The FTP traffic generation process is described in Figure 21. Based on the results on packet size distribution, 76% of the files are transferred using an MTU size of 1500 bytes and 24% of the files are transferred using an MTU size of 576 bytes. Note that these two packet sizes also include a 40 byte IP packet header and this header overhead for the appropriate number of packets must be added to the file sizes calculated from the statistical distributions in Table 35 or each file transfer a new TCP connection is used whose initial congestion window size is 1 segment.

A user is defined in outage for FTP service if the average packet call throughput is less than the minimum average throughput requirement of 128 kbps. The system outage requirement is such that no more than 2% of users can be in outage. The air link PER of MAC SDUs for FTP traffic should be not be greater than 1%.

Component	Distribution	Parameters	PDF
File size (S)	Truncated Lognormal	Mean = 2 Mbytes SD = 0.722 Mbytes Max = 5 Mbytes	$f_x = \frac{1}{\sqrt{2\pi}\sigma} \exp\left[-\frac{(\ln x - \mu)^2}{2\sigma^2}\right], x \geq 0$ $\sigma = 0.35, \mu = 14.45$ <p>if $x > \text{max}$ or $x < \text{min}$, discard and generate a new value for x</p>
Reading time (D_{pc})	Exponential	Mean = 180 sec.	$f_x = \lambda e^{-\lambda x}, x \geq 0$ $\lambda = 0.006$

Table 35: FTP traffic parameters

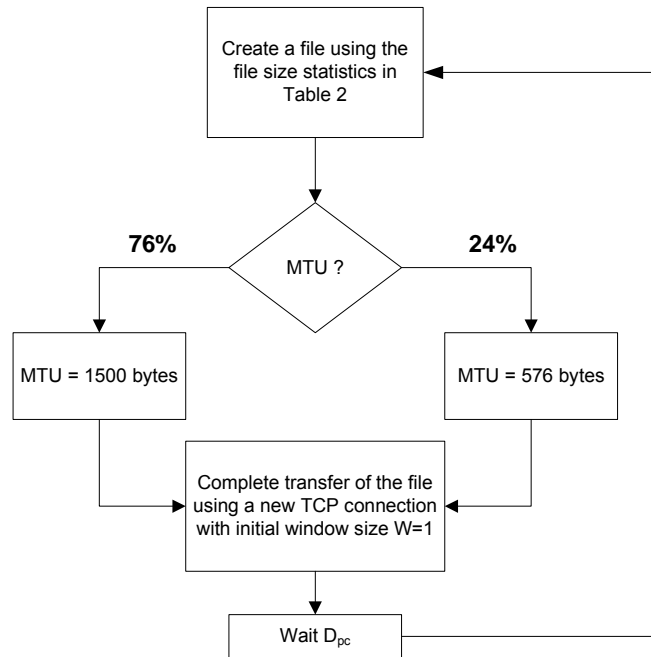


Figure 21: FTP traffic profiles

10.3. Speech Source Model (VoIP)

VoIP refers to real-time delivery of voice packet across networks using the Internet protocols. A VoIP session is defined as the entire user call time and VoIP session occurs during the whole simulation period.

There are a variety of encoding schemes for voice (i.e., G.711, G.722, G.722.1, G.723.1, G.728, G.729, and AMR) that result in different bandwidth requirements. Including the protocol overhead, it is very common for a VoIP call to require between 5 Kbps and 64 Kbps of bi-directional bandwidth.

10.3.1. Basic Voice Model

A typical phone conversation is marked by periods of active talking / talk spurts (ON periods) interleaved by silence / listening periods (or OFF periods) as shown in Figure 22.

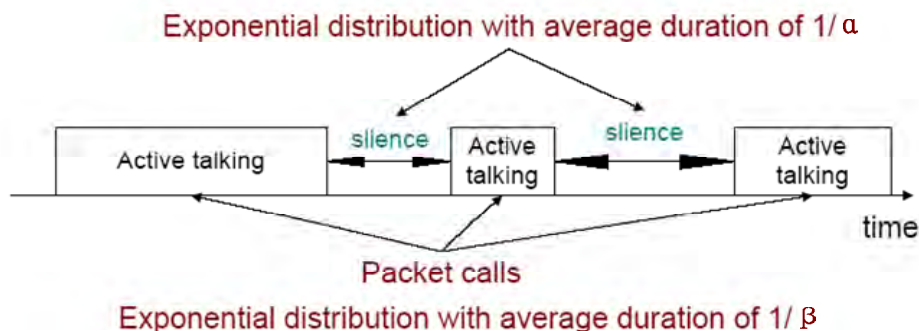


Figure 22: Typical phone conversation profile

Consider the simple 2-state voice activity Markov model shown in Figure 23 [54].

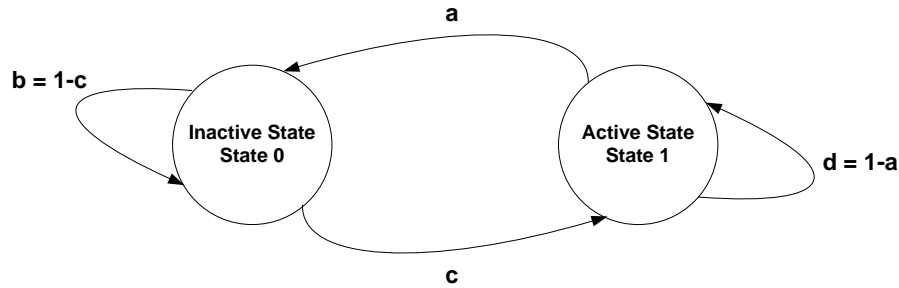


Figure 23: 2-state voice activity Markov model

In the model, the conditional probability of transitioning from state 1 (the active speech state) to state 0 (the inactive or silent state) while in state 1 is equal to a , while the conditional probability of transitioning from state 0 to state 1 while in state 0 is c . The model is assumed to be updated at the speech encoder frame rate $R=1/T$, where T is the encoder frame duration (typically, 20 ms). Packets are generated at time intervals $iT + \tau$, where τ is the network packet arrival delay jitter, and i is the encoder frame index. During the active state, packets of fixed sizes are generated at these time intervals, while the model is updated at regular frame intervals. The size of packet and the rate at which the packets are sent depends on the corresponding voice codecs and compression schemes. Table 36 provides information on some common vocoders.

Vocoder	EVRC	AMR	GSM 6.10	G.711	G.723.1		G.729A
Source Bit rate [Kb/s]	0.8/2/4/8.55	4.75-12.2	13	64	5.3	6.3	8
Frame duration [ms]	20	20	20	10	30	30	10
Information bits per frame	16/40/80/171	95-244	260	640	159	189	80

Table 36: Information on various vocoders

Among the various vocoders in Table 36, a simplified AMR (Adaptive Multi-Rate) audio data compression model can be used to simplify the VoIP modeling process. AMR is optimized for speech coding and was adopted as the standard speech codec by 3GPP and widely used in GSM. The original AMR codec uses link adaptation to select from one of eight different bit rates based on link conditions. If the radio condition is bad, source coding is reduced (less bits to represent speech) and channel coding (stronger FEC) is increased. This improves the quality and robustness of the network condition while sacrificing some voice clarity. In the simplified version in this document, link adaptation has been disabled and the full rate of 12.2 kbps is used in the active state. This model captures the worst case scenario.

Table 37 shows the VoIP packet size calculation for simplified AMR operation with or without header compression when using IPv4 or IPv6. In the table, the MAC CRC of 4

bytes for ARQ is not included and only CRC for HARQ is included because the ARQ process can be assumed to be disabled for VoIP services.

To calculate the total packet size, MAC headers and CRC need to be accounted for (example: there are 6 bytes of MAC header and 2 bytes of HARQ CRC in IEEE 802.16e reference system). Without header compression, an AMR payload of 33 bytes is generated in the active state every $20 + \tau$ ms and an AMR payload of 7 bytes is generated in the inactive state every $160 + \tau$ ms. Assuming IPv4 and uncompressed headers, the resulting VoIP packet size is 81 bytes in the active mode and 55 bytes in the inactive mode.

The voice capacity assumes a 12.2 kbps codec with a 50% activity factor such that the percentage of users in outage is less than 2% where a user is defined to have experienced voice outage if more than 2% of the VoIP packets are dropped, erased or not delivered successfully to the user within the delay bound of 50 ms.

The packet delay is defined based on the 98th percentile of the CDF of all individual users' 98th percentiles of packet delay (i.e., the 98th percentile of the packet delay CDF first determined for each user and then the 98th percentile of the CDF that describes the 98th percentiles of the individual user delay is obtained).

Description	AMR without Header Compression IPv4/IPv6	AMR with Header Compression IPv4/IPv6	G.729 without Header Compression IPv4/IPv6	G.729 with Header Compression IPv4/IPv6
Voice Payload (20 ms aggregation interval)	7 bytes for inactive 33 bytes for active	7 bytes for inactive 33 bytes for active	0 bytes for inactive 20 bytes for active	0 bytes for inactive 20 bytes for active
Protocol Headers (including UDP checksum)	40 bytes / 60 bytes	3 bytes / 5 bytes	40 bytes / 60 bytes	3 bytes / 5 bytes
RTP	12 bytes		12 bytes	
UDP	8 bytes		8 bytes	
IPv4 / IPv6	20 bytes / 40 bytes		20 bytes / 40 bytes	
802.16e Generic MAC Header	6 bytes	6 bytes	6 bytes	6 bytes
802.16e CRC for HARQ	2 bytes	2 bytes	2 bytes	2 bytes

Total VoIP packet size	55 bytes/ 75 bytes for inactive 81 bytes / 101 bytes for active	18 bytes/ 20 bytes for inactive 44 bytes / 46 bytes for active	0 bytes for inactive 68 bytes/ 88 bytes for active	0 bytes for inactive 31 bytes/ 33 bytes for active
------------------------	--	---	--	--

Table 37: VoIP packet calculation for AMR and G.729

VoIP capacity is measured in Active Users/MHz/Sector. It is the minimum of the calculated capacity for either link direction divided by the effective bandwidth in the respective link direction. In other words, the effective bandwidth is the operating bandwidth normalized appropriately considering the uplink/downlink ratio.

10.3.2. VoIP Traffic Model Parameters

During each call (each session), a VoIP user will be in the Active or Inactive state. The duration of each state is exponentially distributed. In the Active/Inactive state, packets of fixed sizes will be generated at intervals of $iT + \tau$ seconds, where T is the VoIP frame interval of 20 ms, τ is the DL network delay jitter and i is the VoIP frame index. For the UL, τ is equal to 0. As the range of the delay jitter is limited to 120 ms, the model may be implemented by generating packets at times $iT + \tau'$ seconds, where $\tau' = \tau + 80$ ms and is always positive. The air interface delay is the time elapsed from the packet arrival time ($iT + \tau'$) to successful reception and decoding of the packet. Table 38 specifies the distributions and parameters associated with the VoIP traffic model.

Component	Distribution	Parameters	PDF
Active/Inactive state duration	Exponential	Mean = 1.25 second	$f_x = \lambda e^{-\lambda x}, x \geq 0$ $\lambda = 1 / \text{Mean}$
Probability of state transition	N/A	0.016	N/A
Packet arrival delay jitter (Downlink only)	Laplacian	$\beta = 5.11 \text{ ms}$	$f_x = \frac{1}{2\beta} e^{\frac{- x }{\beta}},$ $-80 \text{ ms} \leq \tau \leq 80 \text{ ms}$

Table 38: VoIP traffic model parameters specification

Link adaptation of AMR codec is disabled in order to evaluate performance under worst case, and to simplify the voice traffic model.

During the inactive state, we have chosen to generate comfort noise with smaller packet sizes at regular intervals instead of no packet transmission. This simplified model does not include a feature called hangover, which generates additional seven frames at the same rate as speech to ensure the correct estimation of comfort noise parameters at the receiver side even if there is a silence period at the end of a talk spurt (ON state),

and after the hangover period, a SID_FIRST frame is sent. The voice traffic model specifies only one rate during the ON state (talk spurt) of the AMR codec (12.2 kbps) and another rate for the comfort noise (SID_UPDATE) during the OFF state of the AMR codec. SID_UPDATE frames are generated every 8th frame during the silence period.

Table 39 provides the relevant parameters of the VoIP traffic that shall be assumed in the simulations. The details of the corresponding traffic model are described below:

Parameter	Characterization
Codec	RTP AMR 12.2, Source rate 12.2 kbps
Encoder frame length	20 ms
Voice activity factor (VAF)	50%
Payload	Active: 33 bytes (Octet alignment mode)Inactive: 7 bytes SID packet every 160 ms during silence
Protocol Overhead with compressed header	RTP/UDP/IP (including UDP check sum): 3 bytes 802.16 Generic MAC Header: 6 bytes CRC for HARQ: 2 bytes
Total voice payload on air interface	Active: 44 bytes Inactive: 18 bytes

Table 39: Detailed description of the VoIP traffic model for IPv4

10.4. Near Real Time Video Streaming Model

This section describes a model for streaming video traffic for DL direction. Figure 24 illustrates the steady state of video streaming traffic from the network as observed by the base station. Call setup latency and overhead are not considered in this model.

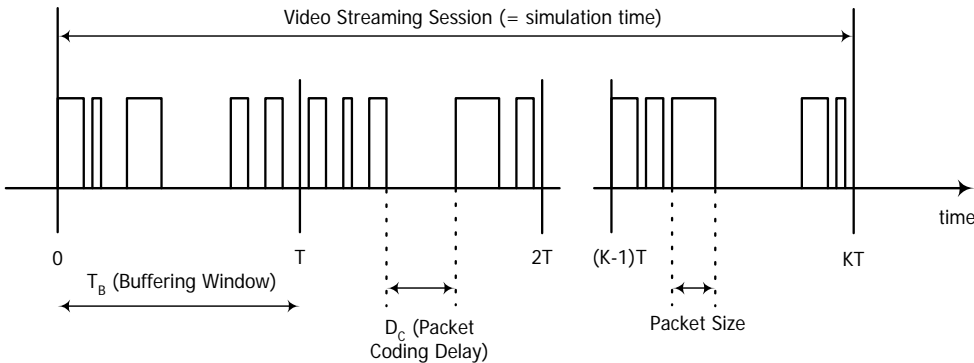


Figure 24: Video streaming traffic model

Each frame of video data arrives at a regular interval T . Each frame can be treated as a packet call and there will be zero OFF duration within a session. Within each frame (packet call), packets (or datagrams) arrive randomly and the packet sizes are random as well.

To counter the jittering effect caused by the random packet arrival rate within a frame at the MS, the MS uses a de-jitter buffer window to guarantee a continuous display of video streaming data. The de-jitter buffer window for video streaming service is 5 seconds. At the beginning of the simulation, the MS de-jitter buffer shall be full with video data. During simulation, data is leaked out of this buffer at the source video data rate and filled as DL traffic reaches the MS from the BS. As a performance criterion, the simulation shall record the length of time, if any, during which the de-jitter buffer runs dry.

The packet sizes and packet inter-arrival rate can be found in when using a source rate of 64 kbps. Table 40 lists the parameters for the video streaming model.

Component	Distribution	Parameters	PDF
Inter-arrival time between the beginning of each frame	Deterministic	100 ms (Based on 10 frames per second)	
Number of packets (slices) in a frame	Deterministic	8 packets per frame	
Packet (slice) size	Truncated Pareto	Mean =100 bytes, Max = 250 bytes (before truncation)	$f_x = \frac{\alpha k^\alpha}{x^{\alpha+1}}, k \leq x < m$ $f_x = \left(\frac{k}{m}\right)^\alpha, x = m$ $\alpha = 1.2, k = 40\text{bytes}, m = 250\text{bytes}$ <p>if $x > \max$, discard and regenerate a new value for x</p>
Inter-arrival time between packets (slices) in a frame	Truncated Pareto	Mean=6 ms, Max=12.5 ms (before truncation)	$f_x = \frac{\alpha k^\alpha}{x^{\alpha+1}}, k \leq x < m$ $f_x = \left(\frac{k}{m}\right)^\alpha, x = m$ $\alpha = 1.2, k = 2.5\text{ms}, m = 12.5\text{ms}$ <p>if $x > \max$, discard and regenerate a</p>

			new value for x
--	--	--	-----------------

Table 40: Near real time video streaming traffic model parameters

It must be noted that additional network protocol overhead, such as IP, TCP/UDP headers should be added to each packet (slice) generated by the video streaming model described in Table 40.

A user is defined in outage for streaming video service if the 98th percentile video frame delay is larger than 5 seconds. The system outage requirement is such that no more than 2% of users can be in outage.

Parameter	Value
Service	Video Telephony
Video Codec	MPEG-4
Protocols	UDP
Scene Length (sec)	Session duration
Direction	Bi-direction (DL and UL)
Frames/sec	25 frames/sec
GOP	N=12, M=3
Display size	176x144
Color depth (bit)	8
Video Quality	Medium
Mean BW	110 kbps
I frame size (byte)	Weibull($\alpha = 5.15$, $\beta = 863$), shift=3949, $\mu = 4742$, $\sigma = 178$, min=4034, max=5184
P frame size (byte)	Lognormal($\mu = 259$, $\sigma = 134$), min=100, max=1663
B frame size (byte)	Lognormal($\mu = 147$, $\sigma = 74$), min=35, max=882

Table 41: Video telephony traffic model

10.5. Video Telephony Model

Based on the compression efficiency and market acceptance as described in the section 10.4, MPEG 4 has been selected for the video codec. The estimated values for the parameters to model a video stream vary from one trace to another. For parameters

associated with the statistical distributions, the estimates depend strongly on the dimensions of the captured frames. For the video telephony traffic model, medium quality of an Office Cam trace is used and the trace library is available at [58]. For the traffic model, two different qualities for the video have been considered; high and medium quality. For the medium quality encoding the quantization parameters for all three frame types were fixed at 10, and for the high quality encoding the quantization parameters for all three frame types were fixed at 4 [59].

The scene length for the video telephony is assumed to be the entire application session since the background or the main subject may not be so dynamic.

10.6. Gaming Traffic Model

Gaming is a rapidly growing application embedded into communication devices, and thus wireless gaming needs to be considered. Games in different genre, such as First Person Shooter (FPS), Role Play Game (RPG), etc., show dramatic different traffic behaviors. FPS model is recommended to represent the gaming traffic model in this document because it posts additional requirements to the system performance, such as real time delay with irregular traffic arrivals.

FPS is a genre of video games. It is a good representation of the modern Massively Multiplayer Online (MMO) game. Due to the nature of the FPS game, it has stringent network delay requirement. For the FPS game, if the client to server to client round trip delay (i.e., ping time, or end to end delay) is below 150 ms, the delay is considered excellent. When the delay is between 150 ms to 200 ms, the delay is noticeable especially to the experienced player. It is considered good or playable. When ping time is beyond 200 ms, the delay becomes intolerable.

This end to end delay budget can be broken down into internet delay, server processing delay, cellular network delay, air interface delay, and client processing delay, etc. Let the IP packet delay be the time that the IP packet entering the MAC SDU buffer to the time that the IP packet is received by the receiver and reassembled into IP packet. The IP packet delay is typically budgeted as 50 ms to meet the 200 ms end to end delay. A gamer is considered in outage if 10% of its packet delay is either lost or delayed beyond the budget, i.e., 50 ms. The system outage requirement is such that no more than 2% of users can be in outage.

The FPS traffic can be modeled by the Largest Extreme Value distribution. The starting time of a network gaming mobile is uniformly distributed between 0 and 40 ms to simulate the random timing relationship between client traffic packet arrival and reverse link frame boundary. The parameters of initial packet arrival time, the packet inter arrival time, and the packet sizes are illustrated in Table 42.

Component	Distribution		Parameters		PDF
	DL	UL	DL	UL	
Initial packet arrival	Uniform	Uniform	a = 0, b = 40 ms	a=0, b=40 ms	$f(x) = \frac{1}{b-a} \quad a \leq x \leq b$
Packet arrival time	Extreme	Extreme	a = 50 ms, b = 4.5 ms	a = 40 ms, b = 6 ms	$f(x) = \frac{1}{b} e^{-\frac{x-a}{b}} e^{-e^{-\frac{x-a}{b}}}, b > 0$ $[X = \lfloor a - b \ln(-\ln Y) \rfloor]$ $Y \in U(0,1)$
Packet size	Extreme	Extreme	a = 330 bytes, b = 82 bytes	a = 45 bytes, b = 5.7 bytes	$f(x) = \frac{1}{b} e^{-\frac{x-a}{b}} e^{-e^{-\frac{x-a}{b}}}, b > 0$ $X = \lfloor a - b \ln(-\ln Y) \rfloor + 2^*$, $Y \in U(0,1)$

Table 42: FPS internet gaming traffic model

* A compressed UDP header of 2 bytes has been accounted for in the packet size.

10.7. Email Traffic Model

Email is an important application that constitutes a high percentage of internet traffic. Email application traffic is included in the UMTS Forum 3G traffic models and ITU R M.2072 [65], [66].

Interactions between email servers and clients are governed by email protocols. The three most common email protocols are POP, IMAP and MAPI. Most email software operates under one of these (and many products support more than one) protocols. The Post Office Protocol (currently in version 3, hence POP3) allows email client software to retrieve email from a remote server. The Internet Message Access Protocol (now in version 4 or IMAP4) allows a local email client to access email messages that reside on a remote server. The Messaging Application Programming Interface (MAPI) is a proprietary email protocol of Microsoft that can be used by Outlook to communicate with Microsoft Exchange Server. It provides somewhat similar but more functionality than an IMAP protocol.

The email traffic model in this section considers both POP3 and MAPI since these protocols generate different traffic patterns. To model POP3, an FTP model can be used, and an email transaction with MAPI protocol can be modeled with multiple MAPI segment transactions in series. Each MAPI fragment is transmitted using the TCP protocol and segmented into smaller segments again based on the TCP configuration. A maximum MAPI fragment size of 16896 bytes has been found so far, and this information is indicated in the first packet of a MAPI fragment. Outlook finishes all the TCP ACK packet transmission for the current MAPI segment and the Exchange server

waits for the MAPI fragment completion indication packet before sending the next one. The last packet in the MAPI fragment sets the "PUSH" bit in the TCP packet to transmit all of the packets in the TCP buffer to the application layer at the receiver side [67].

Email traffic can be characterized by ON/OFF states. During the ON-state an email could be transmitted or received, and during the OFF-state a client is writing or reading an email. Figure 25 depicts a simplified email traffic pattern.

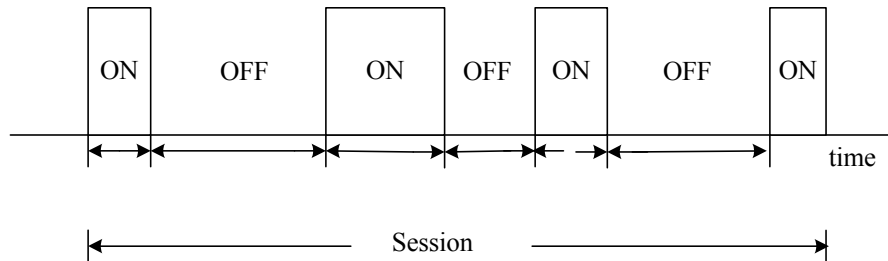


Figure 25: Email traffic model

The parameters for the email traffic model are summarized in Table 43 [67]- [69], [70], [71].

Parameter	Distribution	Parameters	PDF
E-Mail Protocol	N/A	POP3, MAPI	N/A
E-Mail Average Header Size (Bytes)	Deterministic	1 K	N/A
Number of email receive	Lognormal	Mean = 30 Standard Deviation = 17	$f_x = \frac{1}{x\sigma\sqrt{2\pi}} \exp\left[-\frac{(\ln(x) - \mu)^2}{2\sigma^2}\right]$ $x \geq 0$ $\sigma = 3.262, \mu = 0.5277$
Number of email send	Lognormal	Mean = 14 Standard Deviation = 12	$f_x = \frac{1}{x\sigma\sqrt{2\pi}} \exp\left[-\frac{(\ln(x) - \mu)^2}{2\sigma^2}\right]$ $x \geq 0$ $\sigma = 2.364, \mu = 0.742$
Email reading time (sec)	Pareto	$\alpha = 1.1, k = 2, m = 65$, mean = 60, maximum = 63	$f_x = \frac{\alpha k^\alpha}{x^{\alpha+1}}, k \leq x < m$ $f_x = \left(\frac{k}{m}\right)^\alpha, x = m$
Email writing time (sec)	Pareto	$\alpha = 1.1, k = 2, m = 125$, mean = 120, maximum = 123	$f_x = \frac{\alpha k^\alpha}{x^{\alpha+1}}, k \leq x < m$ $f_x = \left(\frac{k}{m}\right)^\alpha, x = m$
Size of email receive/send without attachment	Cauchy	median $\mu = 22.7$ Kbytes, 90%-tile = 80Kbytes	$f_x = \frac{A}{\pi((x - \mu)^2 + 1)}$, A is selected to satisfy 90%-tile

(Kbytes)			value
Size of email receive/send with attachment (Kbytes)	Cauchy	median $\mu = 227$ Kbytes , 90%-tile = 800 Kbytes	$f_x = \frac{A}{\pi((x-\mu)^2 + 1)}$, A is selected to satisfy 90%-tile value
Ratio of email with attachment	Deterministic	Without attachment: 80% With attachment: 20%	N/A

Table 43: Email traffic parameters

10.8. Traffic Mixes

A mobile broadband wireless system is expected to support a mix of simultaneous traffic types. There can be different types of usage scenarios (multi-service v. single-type), different types of devices (notebook PCs, vs. PDAs or smart phones), different usage levels (intense vs. light) and different delay/latency requirements (real-time vs. best-effort).

The previous sections are primarily concerned with the traffic models for each of the potential traffic types. As discussed in the previous section, these models are based on statistical analysis of measured traffic that yielded some invariant patterns that are not very dependant on the specific system. It is more difficult to describe a similar invariant mix of traffic types since these tend to depend more heavily on the type of system and the actual deployment mix of user device types.

In the context of system performance evaluation, the specific traffic-mix chosen should emphasize different aspects of the system performance, e.g. sustained throughput for file downloads v. faster response times for interactive applications.

Table 44 contains traffic mixes that should be used in system evaluations. For system level simulation purposes, “traffic mix” refers to the percentage of users in the system generating a particular type of traffic. In this context, each user is assumed to be generating only one type of traffic, recognizing that in an actual network a single user’s terminal could support multiple applications and generate several types of traffic simultaneously.

Mandatory traffic mixes (full buffer data only and VoIP only) shall be required for the evaluation of performance metrics as defined in the 802.16m requirements. For proposals that target improvements in performance metrics related to optional traffic mixes, the proponents should provide simulation results based on the corresponding traffic mixes. The NGMN traffic mix as specified in [63] or a later revision may be used for liaison with NGMN. The following table specifies mandatory and optional traffic mixes required for 802.16m system performance evaluation:

	VoIP	FTP	HTTP	NRTV	Gaming	VT	Full Buffer	Email	Mandatory/Optional
VoIP only	100% * (#users = N_v *)	0%	0%	0%	0%	0%	0%	0%	Mandatory

Full Buffer Data only	0%	0%	0%	0%	0%	0%	100%, 10 users per sector	0%	Mandatory
NGMN Traffic Mix	30%	10%	20%	20%	20%	0%	0%	0%	Optional
FTP only	0%	100%	0%	0%	0%	0%	0%	0%	Optional
HTTP only	0%	0%	100%	0%	0%	0%	0%	0%	Optional
NRTV only	0%	0%	0%	100%	0%	0%	0%	0%	Optional
Gaming only	0%	0%	0%	0%	100%	0%	0%	0%	Optional
VT only	0%	0%	0%	0%	0%	100%	0%	0%	Optional
Email only	0%	0%	0%	0%	0%	0%	0%	100%	Optional
VoIP & Full Buffer Mix 1	0.5 of N_v	0%	0%	0%	0%	0%	10 users per sector	0%	Optional
VoIP & Full Buffer Mix 2	0.75 of N_v	0%	0%	0%	0%	0%	10 users per sector	0%	Optional

Table 44: Traffic mixes

* N_v is the system voice capacity that satisfies outage criteria at system and user level

11. Simulation Procedure and Flow

A nineteen cell network topology with wrap-around (as shown in Appendix G) shall be used as the baseline network topology for all system-level simulations.

1. The system is modeled as a network of 7 clusters. Each cluster has 19 hexagonal cells with six cells in the first tier and twelve cells in the second tier surrounding the central cell of each cluster. Each cell has three sectors. Frequency reuse is modeled by planning frequency allocations in different sectors in the network.
2. MSs are dropped independently with uniform distribution throughout the system. Each mobile corresponds to an active user session that runs for the duration of the drop.
3. Mobiles are randomly assigned channel models. Depending on the simulation, these may be in support of a desired channel model mix, or separate statistical realizations of a single type of channel model.
4. MSs are dropped according to the specified traffic mix.
5. For sectors belonging to the center cluster, sector assignment to an MS is based on the received power at an MS from all potential serving sectors. The sector with best path to MS, taking into account slow fading characteristics (path loss, shadowing, and antenna gains) is chosen as the serving sector.

6. Mobile stations are randomly dropped over the 57 sectors such that each sector has the required numbers of users. Although users may be in regions supporting handover each user is assigned to only one sector for counting purposes. All sectors of the system shall continue accepting users until the desired fixed number of users per sector is achieved everywhere. Users dropped within 35 meters of a sector antenna shall be redropped. MS locations for six wrapping clusters are the same as the center cluster.
7. For simulations that do not involve handover performance evaluation, the location of each MS remains unchanged during a drop, and the speed of an MS is only used to determine the Doppler effect of fast fading. Additionally, the MS is assumed to remain attached to the same BS for the duration of the drop.
8. Fading signal and fading interference are computed from each mobile station into each sector and from each sector to each mobile for each simulation interval.
9. Packets are not blocked when they arrive into the system (i.e. queue depths are infinite). Users with a required traffic class shall be modeled according to the traffic models defined in this document. Start times for each traffic type for each user should be randomized as specified in the traffic model being simulated.
10. Packets are scheduled with a packet scheduler using the required fairness metric. Channel quality feedback delay, PDU errors are modeled and packets are retransmitted as necessary. The HARQ process is modeled by explicitly rescheduling a packet as part of the current packet call after a specified HARQ feedback delay period.
11. Simulation time is chosen to ensure convergence in user performance metrics. For a given drop the simulation is run for this duration, and then the process is repeated with the MSs dropped at new random locations. A sufficient number of drops are simulated to ensure convergence in the system performance metrics.
12. Performance statistics are collected for MSs in all cells according to the output matrix requirements.
13. All 57 sectors in the system shall be dynamically simulated.

12. Interference Modeling

The reuse of frequencies through planned allocation enables a cellular system to increase capacity with a limited number of channels. The interference model due to frequency reuse should accurately represent the time-frequency selective nature of OFDMA interference. The channel matrices for the desired and interfering signals shall be generated according to the models in Section 3 which account for the pathloss, BS antenna gain, shadowing, and fast fading variations. For simplicity, the same fast fading channel model but a different realization shall be assigned to each link between

an MS & all BSs in the network. This time-frequency modeling can create significant computational complexity in network simulations. To reduce complexity, pathloss and shadowing are calculated to determine the I_{strong} strongest interferers. The strongest interferers are modeled as spatially correlated processes and their channel matrices include pathloss, BS antenna gain, shadowing and fast fading components. The remaining I_{weak} interferers are modeled as spatially white spectrally flat processes. It has been shown that this modeling procedure results in negligible loss in performance.

The procedure for downlink simulations is summarized below:

1. Determine the pathloss, BS antenna gain, and shadowing from all interfering sectors to MS.
2. Rank the interfering sectors in order of received power (based on pathloss, BS antenna gain, and shadowing).
3. Model the channels of the strongest (I_{strong}) interferers as described in Section 3. The channel matrices of the strongest interfering sectors account for the pathloss, BS antenna gain, shadowing, and fast fading variations. For downlink baseline simulations with Matrix A and Matrix B, the value of I_{strong} shall be set to 8.
4. Model the remaining sectors as spatially white Gaussian noise processes whose variances are based on a spectrally flat Rayleigh fading process. The power of the Rayleigh fading process includes the effects of pathloss, BS antenna gain, and shadowing. The fading processes for all links between MS and BS are assumed to be independent, and the Doppler rate is determined by the speed of the mobile. At any instant in time, the total received interference power is the summation of the receive power from of all weak interferers. Hence, the interference power is varying in time during a simulation drop.

13. Performance Metrics

13.1. Introduction

Performance metrics may be classified as single-user performance metrics or multi-user performance metrics.

13.1.1. Single User Performance Metrics

13.1.1.1. Link Budget and Coverage Range (Noise Limited) - Single-Cell Consideration

Link budget evaluation is a well known method for initial system planning that needs to be carried out for BS to MS links. Although a link budget can be calculated separately for each link, it is the combination of the links that determines the performance of the system as a whole. The parameters to be used needs to be agreed upon after obtaining consensus. Using the margins in the link budget, the expected signal to noise

Item	Downlink	Uplink
System Configuration		
Carrier frequency/Total channel bandwidth	GHz/MHz	GHz/MHz
BS/MS heights	M	m
Test environment	Indoor, outdoor vehicular, etc.	Indoor, outdoor vehicular, etc.
Channel type	Control channel/ Traffic channel	Control channel/ Traffic channel
Area coverage	%	%
Test service	Data (rate)/ VoIP (rate)	Data (rate)/ VoIP (rate)
Chosen modulation and coding scheme (explicitly state the use of repetition coding)	-	-
Total channel bandwidth	MHz	MHz
Multipath channel class (characterization of both temporal and spatial properties, e.g., ITU VehA with fixed spatial correlation)	-	-
Mobile speed	km/h	km/h
Transmitter		
(a) Number of transmit antennas	-	-
(b) Maximum transmitter power per antenna	dBm	dBm
(c) Transmit backoff	dB	dB
(d) Transmit power per antenna = (b) - (c)	dBm	dBm
(d1) Total transmit power per sector = function (a) & (d)	dBm	dBm
(e) Transmitter antenna gain	dBi	dBi
(e1) Transmitter array gain (depends on transmitter array configurations and technologies such as adaptive beam forming, CDD (Cyclic delay diversity), etc.)	dB	dB
(e2) Control channel power boosting gain	dB	dB
(e3) Data carrier power loss due to pilot/control boosting	dB	dB
(f) Cable, connector, combiner, body losses (enumerate sources)	dB	dB
(g) Transmitter control EIRP = (d1) + (e) + (e1) + (e2) - (f) Data EIRP = (d1) + (e) + (e1) - (e3) - (f)	dBm	dBm
Receiver		
(h) Number of receive antennas	-	-

(i)	Receiver antenna gain	dBi	dBi
(j)	Cable, connector, body losses	dB	dB
(k)	Receiver noise figure	dB	dB
(l)	Thermal noise density	-174 dBm/Hz	-174 dBm/Hz
(m)	Receiver interference density	dBm/Hz	dBm/Hz
(n)	Total noise plus interference density = $10 \log (10^{(l)/10} + 10^{(m)/10})$	dBm/Hz	dBm/Hz
(o)	Occupied channel bandwidth (for meeting the requirements of the test service)	Hz	Hz
(p)	Effective noise power = (n) + (k) + $10 \log((o))$	dBm	dBm
(q)	Required SNR (AWGN 1-branch sensitivity)	dB	dB
(r)	Receiver implementation margin	dB	dB
(r1)	Fast fading margin (include scheduler gain)	dB	dB
(r2)	HARQ gain	dB	dB
(r3)	Handover gain	dB	dB
(r4)	BS/MS diversity gain	dB	dB
(s)	Receiver sensitivity = (p) + (q) + (j) + (r) + (r1) - (r2) - (r3) - (r4)	dBm	dBm
(t)	Hardware link budget = (g) + (i) - (s)	dB	dB
Calculation of Available Pathloss			
(u)	Lognormal shadow fading std deviation	dB	dB
(v)	Shadow fading margin (function of the area coverage and (u))	dB	dB
(w)	Penetration margin	dB	dB
(w1)	Other gains	dB	dB
(x)	Available path loss = (t) - (v) - (w) + (w1)	dB	dB
Range/coverage Efficiency Calculation			
(y)	Maximum range (according to the selected carrier frequency, BS/MS antenna heights, and test environment – Refer to System Configuration section of the link budget)	M	m
(z)	Coverage Efficiency ($\pi (v)^2$)	sq m/site	sq m/site

Table 45: Link budget template

ratio can be evaluated at given distances. Using these results, the noise limited range can be evaluated for the system.

The link budget template, as shown in Table 45, is adopted from ITU-R recommendation M.1225 [4] with additional entries and some modifications to reflect

different system operation and characteristics that may be exploited or considered in 802.16m but are not accounted for in the M.1225 document [4]. It must be noted that the link budget should be evaluated separately for control and data channels.

Coverage range is defined as the maximum radial distance to meet a certain percentage of area coverage (x%) with a signal to noise ratio above a certain threshold (target SINR) over y% of time, assuming no interference signals are present. It is proposed that x be 99 and y be 95.

13.1.1.2. SINR Coverage – Interference Limited Multi-cell Consideration

The SINR coverage is defined as the percentage area of a cell where the average SINR experienced by a stationary user is larger than a certain threshold (target SINR).

13.1.1.3. Data Rate Coverage – Interference Limited Multi-cell Consideration

The percentage area for which a user is able to transmit/receive successfully at a specified mean data rate using single-user analysis mentioned above. No delay requirement is considered here.

13.1.2. Multi-User Performance Metrics

Although a user may be covered for a certain percentage area (e.g. 99%) for a given service, when multiple users are in a sector/BS, the resources (time, frequency, power) are to be shared among the users. It can be expected that a user's average data rate may be reduced by a factor of N when there are N active users (assuming resources are equally shared and no multi-user diversity gain), compared to a single user rate.

For example, assume that there is a system, where a shared channel with a peak rate of 2 Mbps can serve 99% of the area. Consider the scenario where a particular user wants to obtain a video streaming service at 2 Mbps. This user may be able to obtain the service if no other user gets any service during the whole video session (which may extend for more than an hour). Therefore, in this example although 99% area is covered for the video service, this service is not a viable service for the operator and the evaluation of coverage needs to be coupled with the evaluation of capacity in order to reflect viable service solutions. Coverage performance assessment must be coupled with capacity (# of MSs), to obtain a viable metric.

The users having poor channel quality may be provided more resources so that they would get equal service from the cellular operator. This could adversely impact the total cell throughput. Thus, there is a trade-off between coverage and capacity. Any measure of capacity should be provided with the associated coverage. .

Since an operator should be able to provide the service to multiple users at the same time, an increase in the area coverage itself does not give an operator the ability to offer a given service. Therefore, the number of users that can be supported under a given coverage captures actual coverage performance for a given service from a viability point of view.

The suggested performance metric is the number of admissible users (capacity), parameterized by the service (R_{min}), and the coverage (allowable outage probability).

13.2. Definitions of Performance Metrics

It is assumed that simulation statistics are collected from sectors belonging to the test cell(s) of the 19-cell deployment scenario. Collected statistics will be traffic-type (thus traffic mix) dependent.

In this section, we provide a definition for various metrics collected in simulation runs. For a simulation run, we assume:

- 1] Simulation time per drop = T_{sim}
 - 2] Number of simulation drops = D
 - 3] Total number of users in sector(s) of interest = N_{sub}
 - 4] Number of packet calls for user $u = p_u$
- Number of packets in i^{th} packet call = $q_{i,u}$

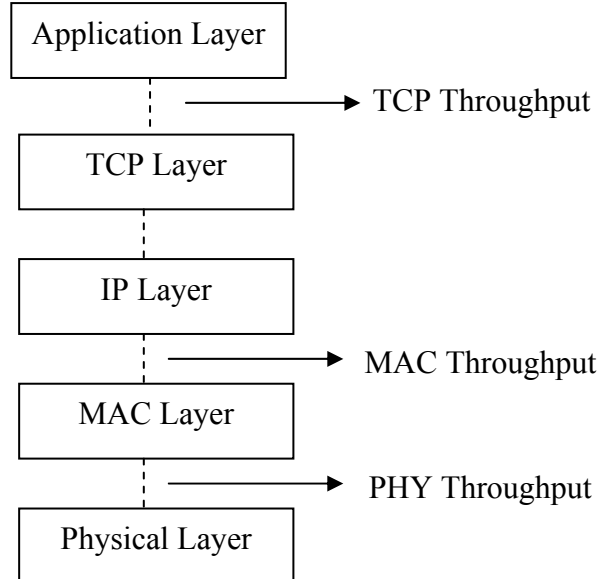


Figure 26: Throughput metrics measurement points

13.2.1. Throughput Performance Metrics

For evaluating downlink (uplink) throughput, only packets on the downlink (uplink) are considered in the calculations. Downlink and uplink throughputs are denoted by upper case DL and UL respectively (example: R_u^{DL}, R_u^{UL}). The current metrics are given per a single simulation drop.

The throughput metrics below shall be measured at the following layers:

- PHY Layer
- MAC Layer
- TCP Layer

The throughput for those layers is measured at the points identified in Figure 26, where throughput refers to the payload throughput without overhead.

13.2.1.1. Average Data Throughput for User u

The data throughput of a user is defined as the ratio of the number of information bits that the user successfully received divided by the amount of the total simulation time. If user u has $p_u^{DL(UL)}$ downlink (uplink) packet calls, with $q_{i,u}^{DL(UL)}$ packets for the i^{th} downlink (uplink) packet call, and $b_{j,i,u}$ bits for the j^{th} packet; then the average user throughput for user u is

$$R_u^{DL(UL)} = \frac{\sum_{i=1}^{p_u^{DL(UL)}} \sum_{j=1}^{q_{i,u}^{DL(UL)}} b_{j,i,u}}{T_{Sim}} \quad (101)$$

13.2.1.2. Average Per-User Data Throughput

The average per-user data throughput is defined as the sum of the average data throughput of each user in the system as defined in Section 13.2.1.1, divided by the total number of users in the system.

13.2.1.3. Sector Data Throughput

Assuming N_{sub} users in sector of interest, and u^{th} user where $u \in N_{sub}$ has throughput $R_u^{DL(UL)}$, then DL or UL sector data throughput is :

$$R_{sec}^{DL(UL)} = \sum_{u=1}^{N_{sub}} R_u^{DL(UL)} \quad (102)$$

13.2.1.4. Average Packet Call Throughput for User u

Packet call throughput is the total bits per packet call divided by total packet call duration. If user u has $p_u^{DL(UL)}$ downlink (uplink) packet calls, with $q_{i,u}^{DL(UL)}$ packets for the i^{th} downlink (uplink) packet call, and $b_{j,i,u}$ bits for the j^{th} packet; then the average packet call throughput is

$$R_u^{pc,DL(UL)} = \frac{1}{p_u^{DL(UL)}} \left(\sum_{i=1}^{p_u^{DL(UL)}} \frac{\sum_{j=1}^{q_{i,u}^{DL(UL)}} b_{j,i,u}}{(T_{i,u}^{end,DL(UL)} - T_{i,u}^{start,DL(UL)})} \right) \quad (103)$$

where $T_{i,u}^{start,DL(UL)}$ defines the time instant at which the transmission of first packet of the i^{th} downlink (uplink) packet call for user u starts and $T_{i,u}^{end,DL(UL)}$ defines the time

instant at which the last packet of the i^{th} downlink (uplink) packet call for user u is received.

13.2.1.5. Average Per-User Packet Call Throughput

The average per-user packet call throughput is defined as the sum of the average packet call throughput of each user in the system as defined in Section 13.2.1.4, divided by the total number of users in the system.

13.2.1.6. The Histogram of Users' Average Packet Call Throughput

The histogram will display the distribution of the downlink (uplink) average packet call throughput observed at the MS (BS) for the subscribed users.

13.2.1.7. Throughput Outage

Throughput outage ($O_{thpt}(R_{min})$) is defined as the percentage of users with data rate R_u^{DL} , less than a predefined minimum rate R_{min} .

13.2.1.8. Cell Edge User Throughput

The cell edge user throughput is defined as the 5th percentile point of the CDF of users' average packet call throughput.

13.2.2. Performance Metrics for Delay Sensitive Applications

For evaluating downlink (uplink) delay, only packets on the downlink (uplink) are considered in the calculations. Downlink and uplink delays are denoted by upper case DL and UL respectively (example: D_u^{DL}, D_u^{UL}).

13.2.2.1. Packet Delay

Assuming the j^{th} packet of the i^{th} packet call destined for user u arrives at the BS (SS) at time $T_{j,i,u}^{arr,DL(UL)}$ and is delivered to the MS (BS) MAC-SAP at time $T_{j,i,u}^{dep,DL(UL)}$, the packet delay is defined as

$$Delay_{j,i,u}^{DL(UL)} = T_{j,i,u}^{dep,DL(UL)} - T_{j,i,u}^{arr,DL(UL)} \quad (104)$$

Packets that are dropped or erased may or may not be included in the analysis of packet delays depending on the traffic model specifications. For example, in modeling traffic from delay sensitive applications, packets may be dropped if packet transmissions are not completed within a specified delay bound. The impact of such dropped packets can be captured in the packet loss rate.

13.2.2.2. The CDF of Packet Delay per User

CDF of the packet delay per user provides a basis in which maximum latency, x%-tile, average latency as well as jitter can be derived.

13.2.2.3. X%-tile Packet delay per User

The x%-tile packet delay is simply the packet delay value for which x% of packets have delay below this value.

13.2.2.4. The CDF of X%-tile Packet Delays

The CDF of x%-tiles of packet latencies is used in determining the y%-tile latency of the x%-tile per user packet delays.

13.2.2.5. The Y%-tile of X%-tile Packet Delays

The y%-tile is the latency number in which y% of per user x%-tile packet latencies are below this number. This latency number can be used as a measure of latency performance for delay sensitive traffic. A possible criteria for VoIP, for example, is that the 98th %-tile of the 98%-tile of packet latencies per user is 50ms.

13.2.2.6. User Average Packet Delay

The average packet delay is defined as the average interval between packets originated at the source station (either MS or BS) and received at the destination station (either BS or MS) in a system for a given packet call duration. The average packet delay for user u , $D_u^{avg,DL(UL)}$ is given by:

$$D_u^{avg,DL(UL)} = \frac{\sum_{i=1}^{P_u} \sum_{j=1}^{q_{i,u}} (T_{j,i,u}^{dep,DL(UL)} - T_{j,i,u}^{arr,DL(UL)})}{\sum_{i=1}^{P_u} q_{i,u}} \quad (105)$$

13.2.2.7. CDF of Users' Average Packet Delay

The CDF will reflect the cumulative distribution of the average packet delay observed by all users.

13.2.2.8. Packet Loss Ratio

The packet loss ratio per user is defined as

$$Packet\ Loss\ Ratio = 1 - \frac{Total\ Number\ of\ Successfully\ Delivered\ Packets}{Total\ Number\ of\ Packets} \quad (106)$$

where the total number of packets includes packets that were transmitted over the air interface and packets that were dropped prior to transmission.

13.2.3. System Level Metrics for Unicast Transmission

13.2.3.1. System Data Throughput

The data throughput of a BS is defined as the number of information bits per second that a site can successfully deliver or receive via the air interface using the scheduling algorithms.

13.2.3.2. Spectral Efficiency

Both physical layer spectral efficiency and MAC layer spectral efficiency should be evaluated. Physical layer spectral efficiency should represent the system throughput measured at the interface from the physical layer to the MAC layer, thus including physical layer overhead but excluding MAC and upper layer protocols overhead. MAC layer spectral efficiency should represent the system throughput measured at the interface from the MAC layer to the upper layers, thus including both physical layer and MAC protocol overhead. Typical Layer 1 and Layer 2 overheads are described in Appendix I.

The MAC efficiency of the system should be evaluated by dividing the MAC layer spectral efficiency by the physical layer spectral efficiency.

The average cell/sector spectral efficiency is defined as

$$r = \frac{R}{BW_{eff}} \quad (107)$$

Where R is the aggregate cell/sector throughput, BW_{eff} is the effective channel bandwidth. The effective channel bandwidth is defined as

$$BW_{eff} = BW \times TR \quad (108)$$

where BW is the used channel bandwidth, and TR is time ratio of the link. For example, for FDD system TR is 1, and for TDD system with DL:UL=2:1, TR is 2/3 for DL and 1/3 for UL, respectively.

13.2.3.3. CDF of SINR

For uplink simulations, this is defined as the cumulative distribution function (CDF) for the signal to interference and noise ratio (SINR) observed by the BS for each MS on the uplink. For downlink simulations, this is defined as the CDF for the SINR observed by each MS on the downlink. This metric allows for a comparison between different reuse scenarios, network loading conditions, smart antenna algorithms, resource allocation and power control schemes, etc.

13.2.3.4. Histogram of MCS

This histogram will display the distribution of MCS for all subscribed users.

13.2.3.5. Application Capacity

Application capacity (C_{app}) is defined as the maximum number of application users that the system can support without exceeding the maximum allowed outage probability.

13.2.3.6. System Outage

System outage is defined as when the number of users experiencing outage exceeds 2% of the total number of users. The user outage criterion is defined based on the application of interest in Section 10.

13.2.3.7. Coverage and Capacity Trade-off Plot

In order to evaluate the coverage and capacity trade-off, system level simulation shall provide a plot of the x% coverage data rate versus sector throughput. The default value of x is 95%.

13.2.4. System Level Metrics for Multicast Broadcast Service

In order to evaluate the performance of multicast broadcast services, two cases should be considered. The first case consists of all 57 sectors transmitting the same MBS service. In the second case, which is used to evaluate the performance at the MBS zone edge, only the centre cell and the first tier of cells are transmitting the same MBS service. The remaining cells are either transmitting unicast data or a different MBS service. In both cases, the self interference due to effective channel delay exceeding cyclic prefix should be modeled. Both cases should be evaluated with the performance metrics given in the following subsections.

13.2.4.1. Maximum MBS Data Rate

The maximum MBS data rate is defined as the maximum data rate for 95% coverage with a target packet error rate of 1%.

13.2.4.2. Coverage versus Data Rate Trade-off

The coverage versus data rate trade-off can be evaluated through a plot of the coverage percentage versus the data rate for a target packet error rate of 1%.

13.2.4.3. Impact of Multicast/Broadcast Resource Size on Unicast Throughput

As the MBS resource size increases, the impact on unicast throughput should be provided. Given the total resource budget, the impact of multicast/broadcast resource size on unicast throughput can be evaluated through a plot of the unicast throughput versus the multicast/broadcast throughput for 95% coverage with a target PER of 1%.

13.3. Fairness Criteria

It may be an objective to have uniform service coverage resulting in a fair service offering for best effort traffic. A measure of fairness under the best effort assumption is important in assessing how well the system solutions perform.

The fairness is evaluated by determining the normalized cumulative distribution function (CDF) of the per user throughput. The CDF is to be tested against a predetermined fairness criterion under several specified traffic conditions. The same scheduling algorithm shall be used for all simulation runs. That is, the scheduling algorithm is not to be optimized for runs with different traffic mixes. The owner(s) of any proposal should also describe the scheduling algorithm used for simulation.

Let $T_{\text{put}}[k]$ be the throughput for user k . For a packet call, let $T_{\text{put}}[k]$ be defined as the average packet call throughput for user k as defined in Section 13.2.1.4. The normalized throughput with respect to the average user throughput for user k , $\tilde{T}_{\text{put}}[k]$ is given by

$$\tilde{T}_{\text{put}}[k] = \frac{T_{\text{put}}[k]}{\text{avg}_i T_{\text{put}}[i]} \quad (109)$$

13.3.1. Moderately Fair Solution

The CDF of the normalized throughputs with respect to the average user throughput for all users is determined. This CDF shall lie to the right of the curve given by the three points in Table 46.

Normalized Throughput w.r.t average user throughput	CDF
0.1	0.1
0.2	0.2
0.5	0.5

Table 46: Moderately fair criterion CDF

13.3.2. Short Term Fairness Indication

During the simulation, the following short-term fairness indicator should be computed and recorded every τ ms (τ is suggested to be 20 or 40):

$$F(t) = \frac{\left| \sum_{i \in A} \hat{T}_i(t) \right|^2}{|A| \sum_{i \in A} \hat{T}_i^2(t)} \quad (110)$$

where $\hat{T}_i(t)$ is the amount of service received by the i th user in time interval $[t, t + \tau)$, A is the set of users with nonzero buffers in $[t, t + \tau)$, and $|A|$ is the cardinality of A . The minimum of $F(t)$ during the simulation time, defined as $F_{\min} = \min_{t \in \{0, \tau, 2\tau, 3\tau, \dots, T_{\text{sim}}\}} F(t)$, can serve as an indication of how much fairness is maintained all the time. It must be noted that the fairness indicator is valid only if all users have equal service requirements.

14. Relay Evaluation Methodology

This section captures the required changes and extensions to the methodology described earlier in this document to evaluate and compare relay proposals. It is

1 assumed that the recommendations made in the other sections of this document apply
2 to the evaluation of relay except in those cases where it is explicitly stated in this
3 section.

4 **14.1. Test Scenarios**

5 Three basic scenarios with Relay Stations (RS) are defined for the purpose of system
6 level simulations:

- 7 • Above Rooftop (ART) RS scenario
 - 8 ○ Two relays per sector
- 9 • Below Rooftop (BRT) RS scenario
 - 10 ○ Six relays per sector (1.5 km BS site-to-site distance)
 - 11 ○ TBD relays per sector (3.0 km BS site-to-site distance)
- 12 • Manhattan deployment scenario (Optional)

13
14 Proponents can define additional test scenarios in order to highlight specific
15 performance gains, such as capacity, coverage, throughput, in specific deployment
16 scenarios as long as the scenario is described in sufficient detail to allow simulations to
17 be recreated by others. Detailed descriptions of these scenarios are given in Sections
18 14.1.1, 14.1.2 and 14.1.3.

19
20 In the ART and BRT scenarios, cells are partitioned into three sectors, as is specified in
21 Section 2. Many of the parameters and procedures previously specified in this
22 document are used. In this section we specify the modifications and additions to these
23 procedures required to support relay simulation studies.

24 **14.1.1. Above Rooftop RS Scenario**

25 The ART RS scenario as shown in Figure 27 assumes that the BS and RS are located
26 above rooftop (ART) while the MSs are located below rooftop (BRT).
27

28 The basic system level parameters describing characteristics (equipment models) of the
29 BS, RS and MS are provided in Section 0. The channel models for system level
30 simulations of all possible links (BS-RS, BS-MS, RS-MS and RS-RS) are defined in
31 Section 14.3 of this document. Note that the parameters proposed in Section 0 and
32 14.3 do not depend on the number of RSs per sector. Meanwhile, it is obvious that
33 simulation results may significantly depend on the positions of RSs inside the cell. The
34 default positions of the RSs inside the cell and their antenna configurations have to be
35 specified for calibration of simulation results. Section 14.1.1.1 provides nominal
36 positions for RSs which are suggested to be used for system level simulation.
37

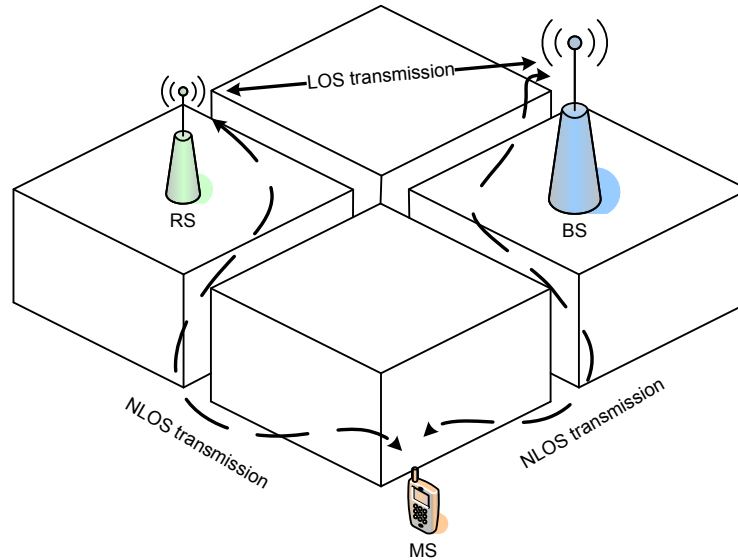


Figure 27: Above Rooftop RS Scenario

In both ART RS scenarios a directional narrow-beam donor antenna is used at the RSs for the BS-RS link. These antennas are pointed directly to the BS. For RS-MS communication the RS uses omni-directional antennas. For more details on BS and RS antenna parameters refer to Section 14.2.

In ART scenarios, the relay link is modeled as a static link. See Section 14.5 for the modeling procedure for static links.

14.1.1.1. Two Relays per Sector Scenario

In this scenario two RSs are deployed in each sector. The positions of the relays are determined by the BS-RS distance r and the angle φ between the boresight direction of the BS sector antenna and the LOS to the RS (refer to Figure 28). By default the distance r is equal to 3/8 of the site-to-site distance and the angle φ is 260° . A value of 300° may optionally be used. Note that specified recommended values of r and φ are currently aligned for DL spatial multiplexing of relay links assuming that the BS is equipped with 2 or 4 antenna elements and antenna spacing of 4 wavelengths. The optional parameters are aligned with the case when no beamforming and spatial multiplexing techniques are applied. The defined values for r and φ are not obligatory and may be changed for other simulation scenarios, but in this case their values must be specified by the proponents. The particular choice may be justified by specific BS antenna system parameters (i.e., antenna spacing and number of antenna elements) and used signal processing techniques. For instance, the angles may be selected to reduce the amount of interference from neighboring cells or to increase the performance of spatially multiplexed relay links for a given BS antenna configuration.

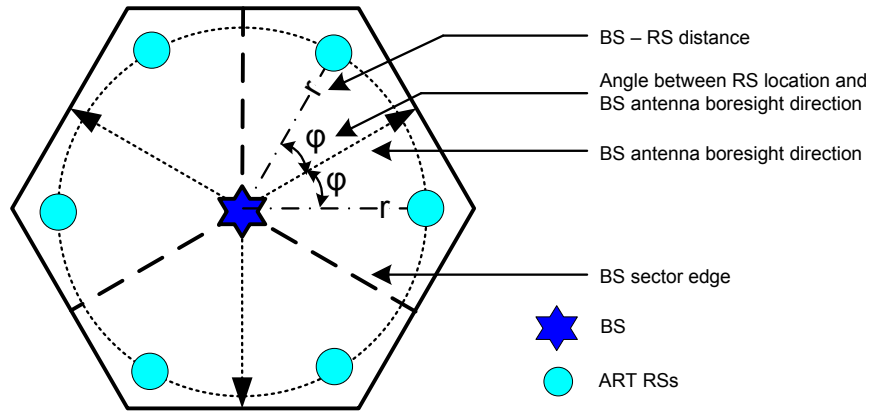


Figure 28: Cell structure for two ART RSs per sector

Figure 29 illustrates the deployment scenario with two ART RSs per sector for the RS placement angle of 26° in a 19 cell topology.

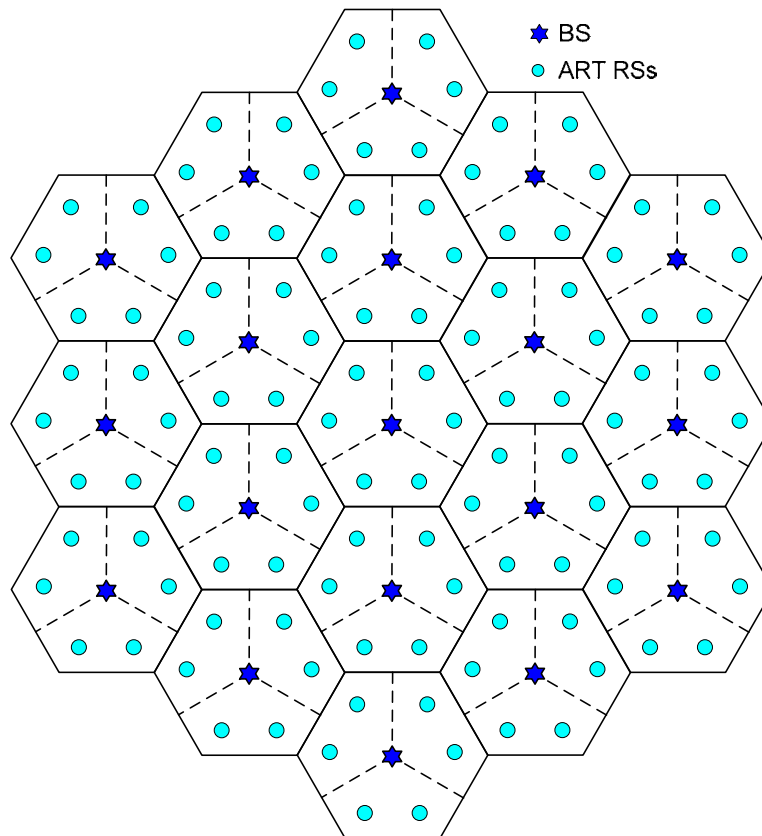


Figure 29: ART Deployment scenario with two RS & default RS placement angle (26°)

14.1.2. Below Rooftop RS Scenario

In this scenario the BS is located above rooftop (ART) while the RS and MS are located below rooftop (BRT), see Figure 30.

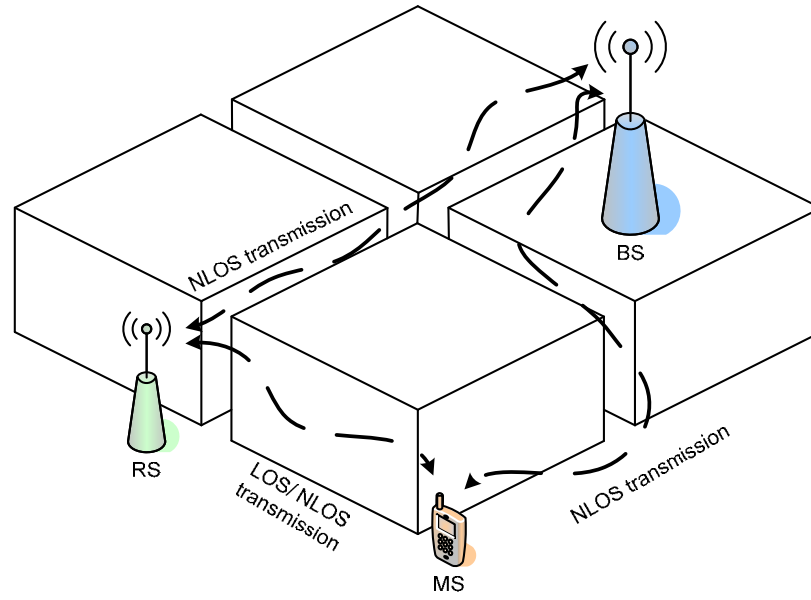


Figure 30: BRT RS Scenario

In the BRT scenario, the number of RSs deployed in each sector is increased to six. The reason for increasing the number of RSs is the more severe propagation characteristics of the BS-RS links and the reduced coverage area of the BRT RS in comparison to the ART RS scenarios of Section 14.1.1. The other difference from the ART scenario is in the type of the RS antenna configuration used for the BS-RS link. Since the BRT RSs are deployed below the rooftop, the probability of having LOS between the BS and RS is reduced. For this reason the BRT RS scenario assumes omni-directional antennas for both relay (BS-RS) and access links (RS-MS). The RS antenna array broadside is assumed to be aligned with the LOS direction to the BS. The basic RS parameters for the BRT RS scenario are provided in Section 14.2.

Figure 31 shows the deployment of BRT RSs with six relays per sector for a 19 cell topology. The deployment resembles the hexagonal RS grid with smaller cell sizes (mini-cells) overlayed by the hexagonal BS grid. As it can be seen from Figure 31, one of the RSs in each BS sector is geographically located in the neighboring cell.

Note that hexagonal BRT RSs deployment is not obligatory and may be changed for other simulation scenarios, but in this case location of BRT RSs must be specified by the proponents. The particular choice may be justified by specific BS antenna system parameters (i.e., antenna spacing and number of antenna elements) and used signal processing techniques. For instance, the angles may be selected to reduce the amount of interference from neighboring cells or to increase the performance of spatially multiplexed relay links for a given BS antenna configuration.

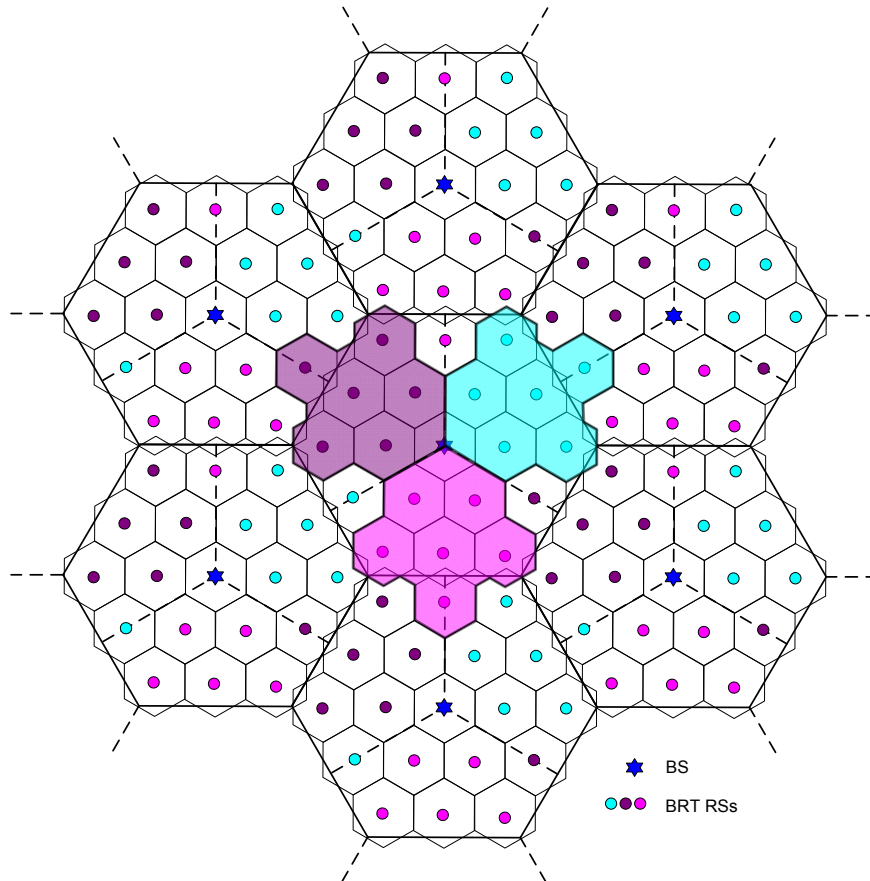


Figure 31: BRT RS Deployment Scenario

In BRT scenarios, the relay link is modeled as a dynamic link. See Section 14.5 for the modeling procedure for dynamic links.

14.1.3. Manhattan deployment scenario

In this scenario the BS/RS/MS are located below rooftop (see Figure 32).

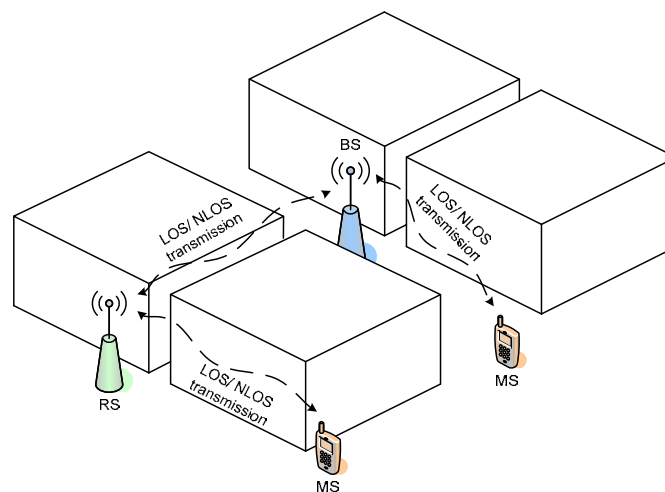


Figure 32: Manhattan deployment scenario propagation conditions

Manhattan grid network deployment complements the hexagonal deployments modeled by the ART and BRT test scenarios. The deployment is adapted to the square street raster. In this scenario employing BRT RSs provides additional coverage in the streets that are out of the BS coverage area. This scenario assumes a specific BS equipment model whose parameters are aligned with the specific signal propagation environment which exists in a Manhattan grid deployment. The BS is placed BRT in a street intersection and has 4 sectors with directional antennas towards the streets, creating four main axes. The RSs are equipped with directional antennas pointing to the direction of the relay link source (the BS for the first tier RSs) and are placed on the main axes. They also have small directional antennas for the access links, such to illuminate the streets perpendicular to the main axes.

Different variants of the deployment of the BSs and the RSs can be used for evaluation of Manhattan grid network deployment. Figure 33, Figure 34 and Figure 35 show some realistic scenarios.

Figure 33 shows single cell of the Manhattan deployment scenario with one relay per BS sector.

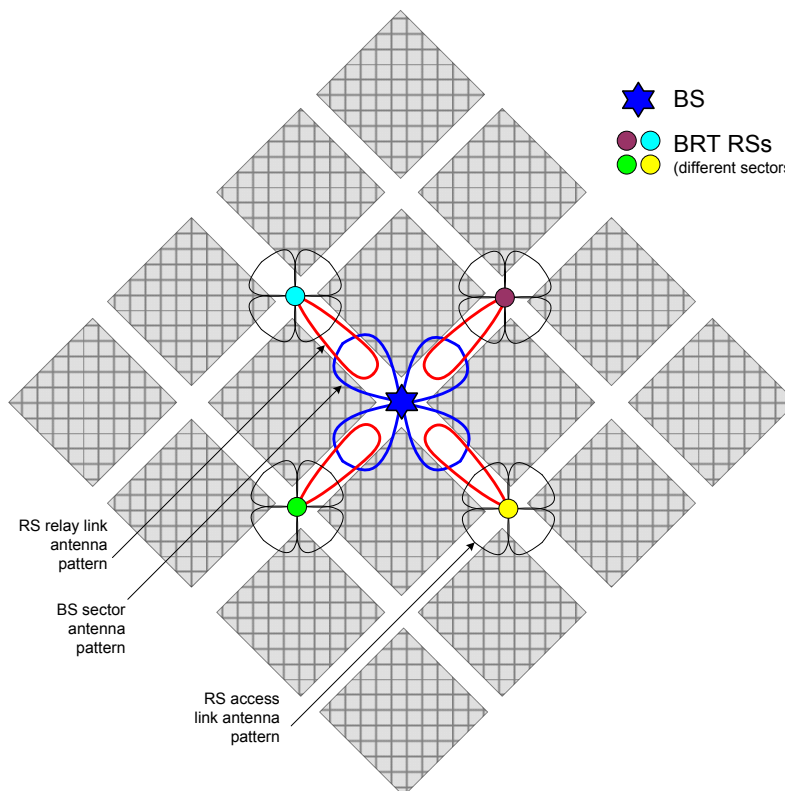


Figure 33: Manhattan deployment scenario with 1 BRT RS per sector

Figure 34 shows single cell of the Manhattan deployment scenario with two relays per BS sector.

1

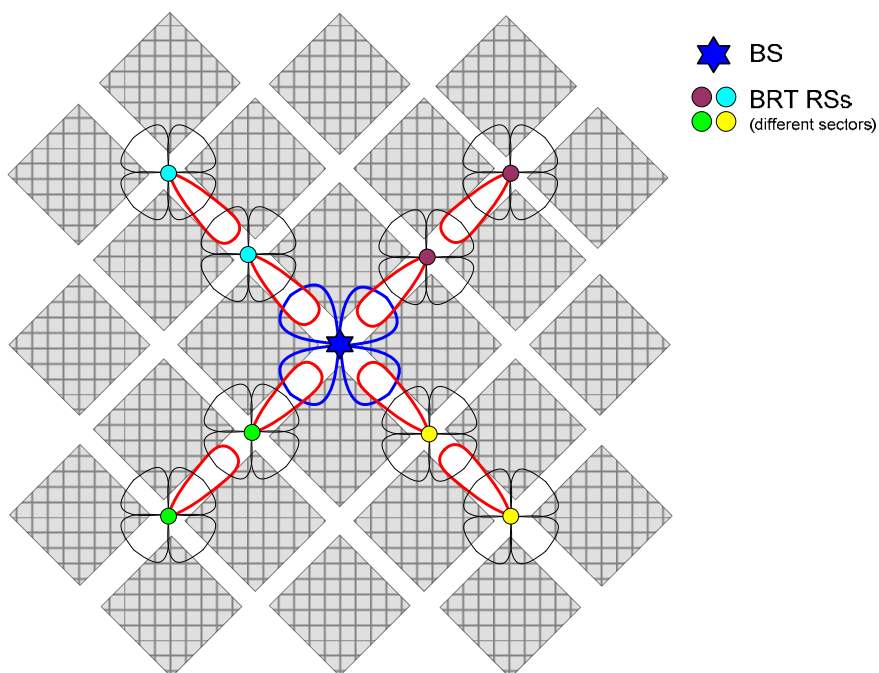


Figure 34: Manhattan deployment scenario with 2 BRT RSs per sector

Figure 35 shows single cell of the Manhattan deployment scenario with three relays per BS sector.

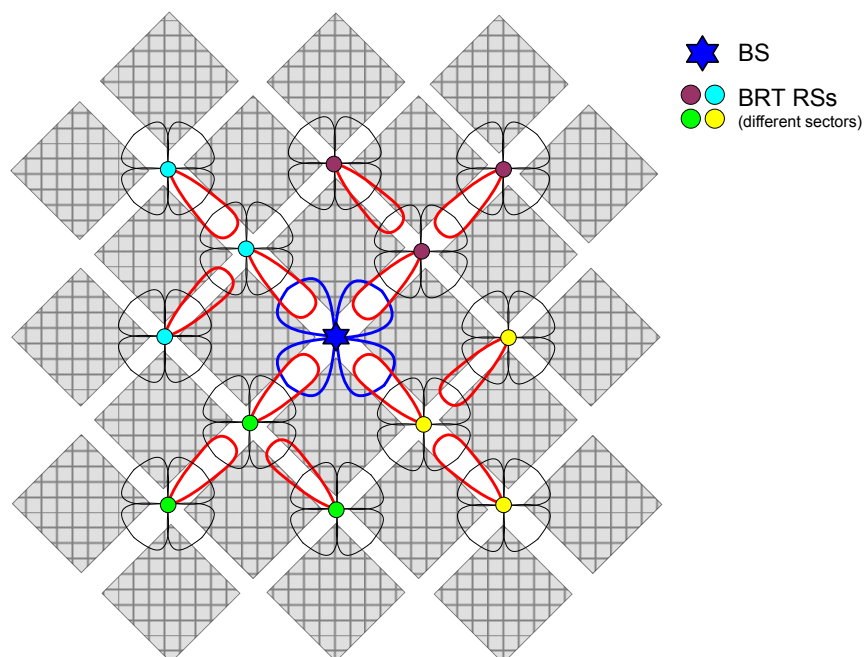
2
3
4
5
6
7

Figure 35: Manhattan deployment scenario with 3 BRT RSs per sector

More detailed parameters of the Manhattan grid deployment, such as typical network sizes, multi-cell structure and others are FFS.

8
9
10
11
12

1 14.2. Basic Parameters

Scenario/ parameters	ART RS scenario	BRT RS scenario	Manhattan deployment scenario
Carrier Frequency	Refer to Baseline configuration (Table 3)		
Operating Bandwidth	Refer to Baseline configuration (Table 3)		
Frequency Reuse	1x3x1 (required)*		
Number of RS per sector	2**	6 (1.5 km site-to-site distance) 6-12 (3.0 km site-to-site distance)	1,2,3
BS Site-to-site distance	1.5km (mandatory) 3.0km (optional)	1.5 km (mandatory) 3.0 km (optional)	TBD
RS placement distance (r)	2 RSs per sector – 3/8 of site-to-site distance	6 RSs per sector – symmetrical positioning (hexagonal)	TBD
RS placement angle (φ)	2 RSs per sector - 26° (Default); 30° (Optional)	6 RSs per sector – symmetrical positioning (hexagonal)	TBD
MS mobility	Refer to Baseline configuration (Table 3)		

Table 47: Test Scenarios

* In a frequency reuse pattern of $N \times S \times K$, the network is divided into clusters of N cells (each cell in the cluster has a different frequency allocations), S sectors per cell, and K different frequency allocations per cell.

**Two RSs per sector are recommend here because the other parameters(e.g. RS placement distance, RS placement angle) are dependant on the number of RS.

Parameter	Value	
	ART RS and BRT RS scenario	Manhattan deployment scenario (optional)
BS Tx Power per sector	Refer to Table 4	46 dBm (Refer to Table 4)
		36 dBm (optional)
Base station antenna height	Refer to Table 4	12.5m
Number of transmit antennas per sector	2 (Mandatory) 4 (Optional)	
Number of receive antennas per sector	2 (Mandatory) 4 (Optional)	
Number of sectors	Refer to Table 4	4 (oriented along the streets)
Antenna gain (boresight)	Refer to Table 4	TBD
Antenna 3-dB beamwidth	Refer to Table 4	TBD
Antenna front-to-back power ratio	30 dB (Mandatory) 20 dB (Optional) (Refer to Table 4)	TBD
Antenna spacing	4 λ (Mandatory) (Refer to Table 4) 0.5 λ (Optional)	
Noise figure	Refer to Table 4	
Cable loss	Refer to Table 4	

Table 48: BS Equipment Model

Parameter	Value		
	ART RS scenario	BRT RS scenario	Manhattan deployment scenario (optional)
	Relay Link		
RS Tx Power	36 dBm per antenna	27 dBm per antenna	36 dBm per antenna (Mandatory) 27 dBm per antenna (Optional)
Relay station antenna height	32 m	10m	10 m
Number of transmit antennas	1	2	1
Number of receive antennas	1	2	1
Antenna type	Directional	Omni in horizontal plane	Directional
Antenna gain (boresight)	20 dBi	7 dBi	20 dBi
Antenna 3-dB beamwidth	20°	N/A	20°
Antenna front-to-back power ratio	23 dB	N/A	23 dB
Antenna spacing	N/A	2λ	N/A
Antenna orientation	Antenna array broadside pointed to BS direction	Antenna array broadside pointed to BS direction	Antenna array broadside pointed to the link's source direction (BS or another RS)
Noise figure	5 dB		
Cable loss	2 dB		
	Access Link		
RS Tx Power	36 dBm per antenna	27 dBm per antenna	36 dBm per antenna (Mandatory) 27 dBm per antenna (Optional)
Relay station antenna height	32m	10m	10 m
Number of transmit antennas	2 baseline/ 4 optional		TBD
Number of receive antennas	2 baseline/ 4 optional		TBD
Number of sectors	1		4 oriented along the streets (or less)
Antenna type	Omni in horizontal plane		Directional
Antenna gain (boresight)	7 dBi		TBD
Antenna 3-dB beamwidth	N/A	N/A	TBD
Antenna front-to-back power ratio	N/A	N/A	TBD

Antenna spacing	4λ	2λ	TBD
Antenna orientation	Antenna array broadside pointed to BS direction	Antenna array broadside pointed to BS direction	TBD
Noise figure	5 dB		
Cable loss	2 dB		

Table 49: RS Equipment Model

Refer to Table 5 for MS equipment model.

14.3. Channel Models

This section describes the channel models used to model propagation conditions between BS, RS, and MS for two the different RS deployment scenarios – ART RS and BRT RS.

The same channel models are used to model both inter-cell and intra-cell propagation conditions.

14.3.1. Pathloss Models

The following notation is used in this section: h_{BS} is the BS antenna height, h_{RS} is the RS antenna height and h_{MS} is the MS antenna height.

14.3.1.1. ART RS Scenario

Pathloss models for the ART RS scenario are defined in Table 50.

Link	Pathloss model
BS-MS and RS-MS	Baseline test scenario (Mandatory) (Refer to Section 3.2.3.8)
	Urban Macrocell test scenario (Optional) (Refer to Section 3.2.3.1).
	Suburban Macrocell test scenario (Optional) (Refer to Section 3.2.3.2)
BS-RS and RS-RS	802.16j EVM Type D (Mandatory) [83]

Table 50: Pathloss models for the ART Relay Scenario

14.3.1.1.1. BS-MS and RS-MS links

The BS-MS and RS-MS links for the ART RS scenario are typical ART to BRT links. The mandatory pathloss models for the baseline and the optional Urban Macrocell and Suburban Macrocell test scenarios are described in Section 3.2.3 and used for BS-MS and RS-MS link simulations without any modifications.

14.3.1.1.2. BS-RS and RS-RS links

BS-RS and RS-RS links are assumed to be LOS ART to ART links and propagation conditions will significantly differ from the BS-MS and RS-MS links. Since there are no

suitable channel model scenarios defined in Section 3, the pathloss models described in the 802.16j EVM [81] is used.

IEEE 802.16j EVM Type D pathloss model

This model [81] is a modified IEEE 802.16 pathloss model. It is equal to the free space pathloss up to a breakpoint distance, which is determined by the transmission frequency and the RS antenna height. Beyond the breakpoint, the pathloss exponent increases. This increase is to account for the fact that LOS probability will decrease with distance from the BS. This factor is also important for multi-cell simulations for interference calculations. The pathloss is defined by:

$$PL[dB] = \begin{cases} 20 \log_{10} \left(\frac{4\pi d[m]}{\lambda[m]} \right) & \text{for } d \leq d_0' \\ A + 10\gamma \log_{10} \left(\frac{d[m]}{d_0[m]} \right) + \Delta PL_f + \Delta PL_h & \text{for } d > d_0' \end{cases}$$

where $A = 20 \log_{10}(4\pi d_0'[m]/\lambda)$; $d_0 = 100 \text{ m}$; breakpoint distance $d_0' = d_0[m] 10^{-\frac{\Delta PL_f + \Delta PL_h}{10\gamma}}$;

$\gamma = a - b h_{BS}[m] + \frac{c}{h_{BS}[m]}$ with parameters $a = 3.6$; $b = 0.005$; $c = 20$;

$\Delta PL_f = 6 \log_{10} \left(\frac{f_c[MHz]}{2000} \right)$;

$\Delta PL_h = \begin{cases} -10 \log_{10}(h_{RS}[m]/3) & \text{for } h_{RS} \leq 3 \text{ m} \\ -20 \log_{10}(h_{RS}[m]/3) & \text{for } h_{RS} > 3 \text{ m} \end{cases}$;

This model applicability range is from 100 m to 8 km.

14.3.1.2. BRT RS Scenario

The pathloss models for the BRT RS scenario are defined in Table 51.

Link	Pathloss model
BS-MS	Baseline test scenario pathloss model (Mandatory) (Refer to Section 3.2.3.8)
	Urban Macrocell test scenario pathloss model (Optional) (Refer to Section 3.2.3.1)
	Suburban Macrocell test scenario (Optional) pathloss model (Refer to Section 3.2.3.2)
BS-RS	Modified Baseline test scenario pathloss model (Mandatory) [83]
	Modified Urban Macrocell test scenario pathloss model (Optional) [83]
	Modified Suburban Macrocell test scenario pathloss model (Optional) [83]
RS-MS	Urban Microcell propagation: Urban Microcell COST-Walfish-Ikegami pathloss model (Mandatory) [5][18] Urban Microcell test scenario pathloss model (Optional) (Refer to Section 3.2.3.3)
	Outdoor to Indoor propagation: Outdoor to Indoor test scenario pathloss model (Optional) (Refer to Section 3.2.3.6)
RS-RS	Urban Microcell COST -Walfish-Ikegami pathloss model [5][18]
	Urban Microcell test scenario pathloss model (Optional) (Refer to Section 3.2.3.3)

Table 51: Path loss models for BRT RS Scenario

14.3.1.2.1. BS-MS link

The BS-MS link in the BRT RS scenario is a typical ART to BRT link. The mandatory pathloss models for the baseline and optional Urban Macrocell and Suburban Macrocell test scenarios are described in Section 3.2.3 and used for the BS-MS link simulations without any modifications.

14.3.1.2.2. BS-RS link

The BS-RS link in the BRT RS scenario is an ART to BRT link. The pathloss models for the mandatory Baseline and optional Urban Macrocell and Suburban Macrocell test scenarios (Section 3.2.3) are almost suitable for BS-RS link simulations, but it is obvious that the propagation conditions for the BS-RS link should be less severe than the ones for the BS-MS links. The following approach for the pathloss propagation calculation is proposed. First, the pathloss is calculated for the BS-RS link using one of the specified models using the assumption that $h_{RS} = h_{MS}$. Second, the pathloss is adjusted based on the h_{RS} value according to the formula

$$PL[dB] = PL(h_{RS} = h_{MS}) - \text{Height_gain} = PL(h_{RS} = h_{MS}) - 0.7h_{RS}[m]$$

An example of such an adjustment is defined in the WINNER B5d channel model [83]. The WINNER B5d channel model is defined for the NLOS stationary feeder and above

rooftop to street-level propagation. This model is almost identical to the WINNER C2 Urban Macrocell NLOS model. The only difference is that in the B5d model a small adjustment to the pathloss model is made considering that the RS is located higher than the MS:

$$PL_{B5d}[dB] = PL_{C2NLOS} - Height_gain = PL_{C2NLOS} - 0.7h_{RS}[m]$$

14.3.1.2.3. RS-MS link

Two propagation sub-scenarios for RS-MS links are considered – the Urban Microcell propagation scenario, where MSs are located outdoors, and the Outdoor to Indoor propagation scenario, where MSs are located inside the buildings.

In the case when MSs are located outdoors, the RS-MS link propagation conditions in the BRT RS scenario may be described by a typical Urban Microcell propagation scenario with both RS and MS antennas located BRT [82]. In the RS-MS link, both LOS and NLOS propagation conditions may occur and LOS/NLOS transition conditions need to be introduced for this link.

Two Urban Microcell pathloss models for the RS-MS link are defined for the RS-MS link.

The first is the pathloss model for the Urban Microcell test scenario described in Section 3.2.3.3. This model is quite complicated, topology dependent, and designed for fixed values of antenna heights. Therefore, it is reasonable to use a simplified model with generalized topology impact on the performance and more suitable for implementation in SLS tools.

The second model is the COST-Walfish-Ikegami pathloss model [5], [83]. It is recommended to be used for RS-MS link simulations as the mandatory model.

- **802.16m EMD Urban Microcell pathloss model (Optional)**

For a detailed description of this model, see Section 3.2.3.3. The main disadvantage of this model is that it is intended for simulations specifically for Manhattan-grid topologies. This model was designed for fixed values of $h_{RS} = 12.5m$ and $h_{MS} = 1.5m$ and the final pathloss equation does not consider changing those values. Because of these restrictions, this model cannot be used for different values of antenna heights. The LOS model might be applied for frequencies from ultra-high-frequency to microwave bands and distances up to 5 km [18]. No model assumptions for the NLOS case are provided in section 3.2.3.3.

- **Walfish-Ikegami pathloss model (Mandatory)**

The proposed pathloss model is based on the COST-Walfish-Ikegami LOS and NLOS models [5][18] which are defined for cases of TX antennas located ART and BRT. The following set of Walfish-Ikegami model parameters is proposed to be used: Building height 15m, building to building distance 50m, street width 25m, orientation 30° for all paths, and selection of metropolitan center. This model is designed for the following

assumptions: Carrier frequency is 800 – 2000 MHz, hBS/RS is 4 – 50 m, hMS is 1 – 3 m and distance between nodes is 0.02 – 5 km. For a more detailed description of the COST-Walfish-Ikegami pathloss model the reader is referred to [18].

Both LOS and NLOS propagation transmissions might occur in the RS-MS link. Therefore, the LOS probability needs to be defined. We set the LOS probability according to the 3GPP SCM Urban Microcell model [5] where the probability of LOS is defined to be unity at zero distance, and decreases linearly until a cutoff point at $d=300\text{m}$, where the LOS probability is zero:

$$P(LOS) = \begin{cases} (300 - d) / 300, & 0 < d \leq 300 \text{ m} \\ 0, & d > 300 \text{ m} \end{cases}$$

In the case when MSs are located indoors the optional Outdoor to Indoor test scenario pathloss model (Section 3.2.3.6) can be used for RS-MS links by the proponents that want to simulate this scenario. Also the same pathloss model shall be used for BS-MS interference calculation.

14.3.1.2.4. RS-RS link

The RS-RS link is a BRT to BRT link with both antennas located at the same level above ground, which is supposed to be high enough relative to the MS location. In the RS-RS link, both LOS and NLOS propagation conditions might occur and LOS/NLOS transition conditions need to be introduced for this link.

Although it is obvious that the RS-RS link propagation conditions can be less severe than in the RS-MS links (depending on the RS-to-RS distance as well as obstructions), current investigations have not discovered any proper models for describing the RS-RS link propagation conditions in the Urban Microcell environment.

The Urban Microcell pathloss model based on the COST-Walfish-Ikegami LOS and NLOS models [5][18] is proposed to be temporarily used. This model is valid for receiver station height less than 3 m but it is currently used assuming 10 m receiver height.

Both LOS and NLOS propagation transmissions might occur over the RS-RS link. Therefore, the LOS probability needs to be defined. The LOS probability model is proposed to be similar to the RS-MS link with cutoff point at $d = 700\text{m}$ due to the increased RS height relative to the MS location.

The optional Urban Microcell test scenario pathloss model (Section 3.2.3.3) can also be used as described in the Section 14.3.1.2.3.

14.3.1.2.5. Comparison of Pathloss Models

The pathloss for default antenna heights, $f_c = 2.5\text{GHz}$, and the BS-MS Baseline, modified Baseline, RS-MS with COST Walfish-Ikegami Urban Microcell LOS and NLOS, and RS-RS LOS WINNER B5b models is shown in Figure 36. Free space pathloss is also shown in Figure 36 for reference.

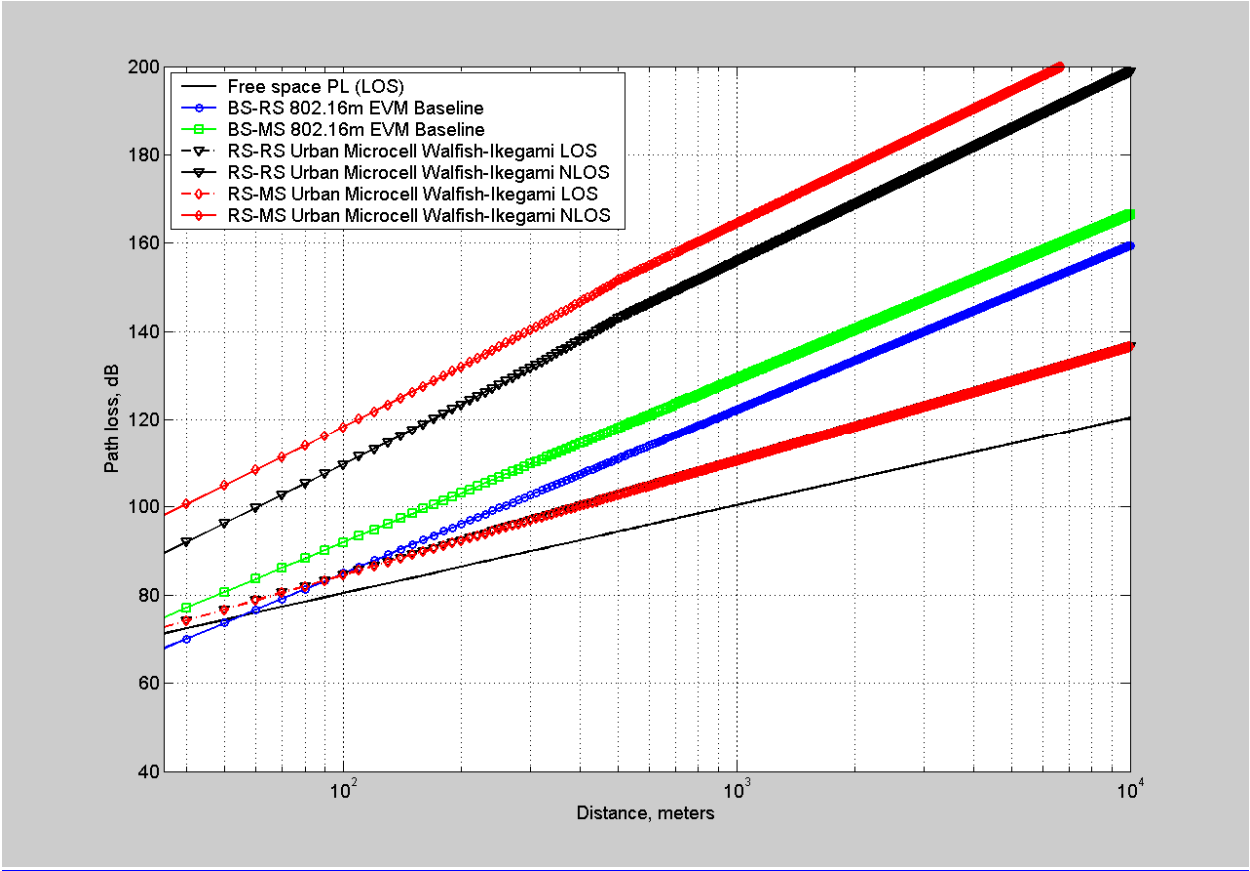


Figure 36: BRT RS Pathloss Models

14.3.1.3. Manhattan deployment scenario (optional)

The pathloss models for the Manhattan deployment scenario are defined in Table 52.

Link	Pathloss model
BS-MS and RS-MS	Urban Microcell propagation: Urban Microcell test scenario pathloss model (Mandatory) (Refer to Section 3.2.3.3) WINNER B1 Urban Microcell pathloss model (Optional) [82]
	Outdoor to Indoor propagation: Outdoor to Indoor test scenario pathloss model (Optional) (Refer to Section 3.2.3.6).
BS-RS and RS-RS	Urban Microcell test scenario pathloss model (Mandatory) (Refer to Section 3.2.3.3) WINNER B1 Urban Microcell pathloss model (Optional) [82]

Table 52: Pathloss models for the Manhattan deployment scenario

14.3.1.3.1. BS-MS and RS-MS links

Two propagation sub-scenarios for BS-MS and RS-MS links are considered – the Urban Microcell propagation scenario where MSs are located outdoors, and the Outdoor to Indoor propagation scenario where MSs are located inside buildings.

In the case when MSs are located outdoors, the BS-MS and RS-MS link propagation conditions in the BRT RS scenario may be described by a typical Urban Microcell propagation scenario with both BS/RS and MS antennas located BRT [82]. The Urban Microcell test scenario pathloss model is described in Section 3.2.3.3 and is based on the assumption of the Manhattan grid topology can be used for simulations of these links as the mandatory model. Optionally, WINNER B1 Urban Microcell pathloss model [82] can be used.

In the case when MSs are located indoors the optional Outdoor to Indoor test scenario pathloss model (Section 3.2.3.6) can be used for BS-MS and RS-MS links simulations.

14.3.1.3.2. BS-RS and RS-RS links

The BS-RS and RS-RS links are BRT to BRT links with both antennas located at almost the same level above ground, which is supposed to be high enough relative to the MS location.

Although it is obvious that the BS-RS and RS-RS links propagation conditions can be less severe than in the BS-MS and RS-MS links, current investigations have not discovered proper models for describing this type of propagation conditions in the Urban Microcell environment. The most part of the models assume that the second station is located at the typical MS height of 1.5 m.

The Urban Microcell test scenario pathloss model (Section 3.2.3.3) can be used for BS-RS and RS-RS links simulations as the mandatory. Optionally, WINNER B1 Urban Microcell pathloss model [82] can be used. Modifications of these models are FFS.

14.3.2. Spatial channel models

14.3.2.1. ART RS scenario

The spatial channel models for the ART RS scenario are defined in Table 53.

Link	Spatial channel model
BS-MS and RS-MS	Baseline test scenario (Mandatory)
	Urban Macrocell test scenario (Optional)
	Suburban Macrocell test scenario (Optional)
BS-RS and RS-RS	WINNER B5a [82][83]

Table 53: Spatial channel models for the ART RS scenario

14.3.2.1.1. BS-MS and RS-MS links

The mandatory baseline and optional Urban Macrocell and Suburban Macrocell test scenario spatial channel models described in Section 3 are used for BS-MS and RS-MS link simulations without any modifications.

14.3.2.1.2. BS-RS and RS-RS links

The WINNER B5a clustered delay-line (CDL) model is used as the spatial channel model for BS-RS and RS-RS links. Table 54 and Table 55 provide a short summary of the parameters associated with this channel model.

Parameter	Value
Power-delay profile	Exponential (non-direct paths).
Delay-spread	40 ns
K-factor	10 dB
XPR	30 dB
Doppler	A peak centered around zero Hz with most energy within 0.1 Hz.
Angle-spread of non-direct components	Gaussian distributed clusters with 0.5 degrees intra angle spread. Composite angle-spread 2 degrees. Same in both Ends.

Table 54: WINNER B5a CDL channel model parameters

Cluster #	Delay [ns]	Power [dB]	AoD [°]	AoA [°]	K-factor [dB]	Cluster ASBS= 0.5	Cluster ASRS= 0.5
1	0	-0.39	0.0	0.0	21.8		
2	10	-20.6	0.9	0.2	- Inf		
3	20	-26.8	0.3	1.5			
4	50	-24.2	-0.3	2.0			
5	90	-15.3	3.9	0.0			
6	95	-20.5	-0.8	3.6			
7	100	-28.0	4.2	-0.7			
8	180	-18.8	-1.0	4.0			
9	205	-21.6	5.5	-2.0			
10	260	-19.9	7.6	-4.1			

Table 55: WINNER B5a CDL channel model for clusters

14.3.2.2. BRT RS scenario

The spatial channel models for the BRT RS scenario are defined in Table 56.

Link	Spatial channel model
BS-MS and BS-RS	Baseline test scenario model (Mandatory) (Refer to Section 3.2.9)
	Urban Macrocell test scenario model (Optional) (Refer to Section 3.2.5.1)
	Suburban Macrocell test scenario model (Optional) (Refer to Section 3.2.5.2)
RS-MS	Urban Microcell test scenario model (Mandatory) (Refer to Section 3.2.5.3)
	Outdoor to Indoor test scenario model (Optional) (Refer to Section 3.2.5.6)
RS-RS	Modified Urban Microcell test scenario model

Table 56: Spatial Channel Models for the BRT RS Scenario

14.3.2.2.1. BS-MS and RS-MS links

In this scenario, the propagation conditions of the BS-MS and BS-RS links are assumed to be the same. The mandatory baseline and optional Urban Macrocell and Suburban Macrocell test scenario spatial channel models described in Section 3 are used for BS-MS and BS-RS link simulations without any modifications.

14.3.2.2.2. RS-MS links

The mandatory Urban Microcell and the optional Outdoor to Indoor spatial channel models described in Section 3 can be used for RS-MS link simulations without any modifications.

14.3.2.2.3. RS-RS links

The modified Urban Microcell spatial channel model (Section 3.2.5.3) is used in this case. The model parameters are modified in order to ensure symmetry in characteristics of received and transmitted signals: (1) modified per-tap mean angles of arrival are set equal to per-tap mean angles of departure of the initial model; (2) the modified arrival angular spread is set be equal to the departure angular spread of the initial model.

14.3.2.3. Manhattan deployment scenario (optional)

The spatial channel models for the Manhattan deployment scenario are defined in Table 57.

Link	Spatial channel model
BS-MS and RS-MS	Urban Microcell test scenario model (Mandatory) (Refer to Section 3.2.5.3)
	Outdoor to Indoor test scenario model (Optional) (Refer to Section 3.2.5.6)
BS-RS and RS-RS	Modified Urban Microcell test scenario model

Table 57: Spatial channel models for the Manhattan deployment scenario

14.3.2.3.1. BS-MS and RS-MS links

The mandatory Urban Microcell and the optional Outdoor to Indoor spatial channel models described in Section 3 can be used for BS-MS and RS-MS links simulations without any modifications.

14.3.2.3.2. BS-RS and RS-RS links

The modified Urban Microcell spatial channel model (Section 3.2.5.3) can be used for simulations of these links. The model parameters are modified in order to ensure symmetry in characteristics of received and transmitted signals: 1) modified per-tap mean angles of arrival are set equal to per-tap mean angles of departure of the initial model; 2) the modified arrival angular spread is set be equal to the departure angular spread of the initial model.

14.3.3. Shadowing models

The shadowing factor (SF) has a log-normal distribution with a standard deviation that is different for different scenarios as shown in Table 58. The values specified in Table 55 have been derived based on the baseline model in this document, 802.16j EVM [81], SCM, and WINNER models.

In the ART RS scenario for BS-MS and RS-MS links, the shadowing standard deviation is 8 dB according to Section 3.2.4. For BS-RS and RS-RS links, the shadowing standard deviation is 3.4 dB according to the 802.16j EVM Type D [81] and WINNER B5a channel models [82].

In the BRT RS scenario for the BS-MS link the shadowing standard deviation is 8 dB according to Section 3.2.4. For the BS-RS link “pre-planned” RS placement by operators is assumed so the shadowing standard deviation is set to 6 dB and the mean value of the shadowing factor is set to 2 dB providing a positive shift in log-normal curve. This ensures better propagation conditions than for typical BS-MS links in which MSs are assumed to be randomly located. For the RS-MS (in the Urban Microcell scenario) and RS-RS links, the shadowing standard deviation is 4 dB for NLOS and 3 dB for LOS propagation according to Section 3.2.4 and the WINNER Urban Microcell channel models [82]. For the Outdoor-to-Indoor test scenario RS-MS link shadowing standard deviation is 7 dB according to Section 3.2.4.

In the Manhattan deployment scenario for the BS-MS, RS-MS links with Urban Microcell propagation conditions and BS-RS, RS-RS links, the shadowing standard deviation is 4 dB for NLOS and 3 dB for LOS propagation according to Section 3.2.4 and the WINNER models [82]. For the BS-MS and RS-MS links with Outdoor-to-Indoor propagation conditions shadowing standard deviation is 7 dB according to Section 3.2.4.

	BS-RS	BS-MS	RS-RS	RS-MS
ART RS	3.4 dB	8 dB	3.4 dB	8 dB
BRT RS	6 dB and 2 dB mean value positive shift	8 dB	NLOS: 4 dB LOS: 3 dB	Urban Microcell propagation: NLOS: 4 dB LOS: 3 dB
				Outdoor to Indoor propagation (Optional): 7 dB
Manhattan deployment scenario (optional)	NLOS: 4 dB LOS: 3 dB	Urban Microcell propagation: NLOS: 4 dB LOS: 3 dB	NLOS: 4 dB LOS: 3 dB	Urban Microcell propagation: NLOS: 4 dB LOS: 3 dB
		Outdoor to Indoor propagation (Optional): 7 dB		Outdoor to Indoor propagation (Optional): 7 dB

Table 58: Shadowing standard deviation

The correlation model for shadow fading is the same as the one described in this document, but the correlation distance for shadowing is corrected according to Table 59. The parameters in Table 59 have been derived based on the baseline model in this document, 802.16j EVM [81], SCM, and WINNER models.

In the ART RS scenario for BS-MS and RS-MS links, the shadowing correlation distance is chosen to be 50 m according to Section 3.2.4. For the BS-RS and RS-RS links, the shadowing correlation distance is chosen to be 100 m according to typical values of the LOS channel correlation distance.

In the BRT RS scenario for the BS-MS and BS-RS links, the shadowing correlation distance is chosen to be 50 m according to Section 3.2.4. For the RS-RS and RS-MS links, the shadowing correlation distance is chosen to be 12 m for NLOS and 14 m for LOS conditions according to typical values of correlation distance given in WINNER [82] for Urban Microcell scenarios. For the RS-MS links in Outdoor to Indoor propagation conditions the shadowing correlation distance is chosen to be 7 m according to WINNER [82].

In the Manhattan deployment scenario, for the BS-RS, RS-RS links and BS-MS, RS-MS links with Urban Microcell propagation conditions, the shadowing correlation distance is chosen to be 12 m for NLOS and 14 m for LOS conditions according to typical values of correlation distance given in WINNER [82]. For the BS-MS, RS-MS links with Outdoor to Indoor propagation conditions the shadowing correlation distance is chosen to be 7 m according to WINNER [82].

1

	BS-RS	BS-MS	RS-RS	RS-MS
ART RS	100 m	50 m	40 m	50 m
BRT RS	50 m	50 m	NLOS: 12 m LOS: 14 m	Urban Microcell propagation NLOS: 12 m LOS: 14 m
				Outdoor to Indoor propagation (Optional): 7 m
Manhattan deployment scenario (optional)	NLOS: 12 m LOS: 14 m	Urban Microcell propagation: NLOS: 12 m LOS: 14 m	NLOS: 12 m LOS: 14 m	Urban Microcell propagation: NLOS: 12 m LOS: 14 m
		Outdoor to Indoor propagation (Optional): 7 m		Outdoor to Indoor propagation (Optional): 7 m

Table 59: Correlation distance for shadowing

2
3

4 The shadow fading cross correlation properties for all types of links are summarized in
 5 Table 60 for the ART RS scenario. Table 61 describes the cross correlation values for
 6 the BRT RS scenario. Table 62 describes the cross correlation values for the Manhattan
 7 deployment scenario.

8

Link 1	Link 2	Correlation between Links 1 and 2
$BS \rightarrow MS_{(i)}$	$BS \rightarrow MS_{(j)}$	Derived from distance between MSs (correlation distance - 50 m)
$MS \rightarrow BS_{(i)}$	$MS \rightarrow BS_{(j)}$	0.5
$BS \rightarrow RS_{(i)}$	$BS \rightarrow RS_{(j)}$	0 (due to large distance between different RSs)
$RS \rightarrow BS_{(i)}$	$RS \rightarrow BS_{(j)}$	0 (due to large distance between different BSs)
$RS \rightarrow MS_{(i)}$	$RS \rightarrow MS_{(j)}$	Derived from distance between MSs (correlation distance – 50 m)
$MS \rightarrow RS_{(i)}$	$MS \rightarrow RS_{(j)}$	0.5 (similar to BS-MS links)
$MS \rightarrow BS_{(i)}$	$MS \rightarrow RS_{(j)}$	0.5 (similar to BS-MS links)
$RS \rightarrow RS_{(i)}$	$RS \rightarrow RS_{(j)}$	0 (because distance between RSs is much larger than correlation distance equal to 40 m)

Table 60: Shadow fading correlation in ART RS scenario

9
10
11
12
13
14

Link 1	Link 2	Correlation between Links 1 and 2
BS→MS(i)	BS→MS(j)	Derived from distance between MSs (correlation distance – 50 m)
MS→BS(i)	MS→BS(j)	0.5
BS→RS(i)	BS→RS(j)	0 (because distance between RSs is much larger than correlation distance equal to 50m)
RS→BS(i)	RS→BS(j)	0.5 (similar to BS-MS links)
RS→MS(i)	RS→MS(j)	Derived from distance between MSs (correlation distance – LOS 14 m, NLOS- 12 m for Urban Microcell propagation scenario, and 7 m for Outdoor to Indoor propagation scenario)
MS→RS(i)	MS→RS(j)	0 (due to large distance between different BRT RSs and independency of different MS-RS links)
MS→BS(i)	MS→RS(j)	0 (due to large distance between different BRT RSs and BSs and independency of MS-RS and MS-BS links)
RS→RS(i)	RS→RS(j)	0 (because distance between RSs is much larger than correlation distance equal to 12 – 14 m)

Table 61: Shadow Fading Correlation in BRT RS Scenario

Link 1	Link 2	Correlation between Links 1 and 2
BS→MS(i)	BS→MS(j)	Derived from distance between MSs (correlation distance – LOS 14 m, NLOS- 12 m for Urban Microcell scenario, and 7 m for Outdoor to Indoor scenario)
MS→BS(i)	MS→BS(j)	0 (due to large distance between different BRT BSs and independency of different MS-BS links)
BS→RS(i)	BS→RS(j)	0 (because distance between BSs and RSs is much larger than correlation distance equal to 12 – 14 m)
RS→BS(i)	RS→BS(j)	0 (because distance between BSs and RSs is much larger than correlation distance equal to 12 – 14 m)
RS→MS(i)	RS→MS(j)	Derived from distance between MSs (correlation distance – LOS 14 m, NLOS- 12 m for Urban Microcell scenario, and 7 m for Outdoor to Indoor scenario)
MS→RS(i)	MS→RS(j)	0 (due to large distance between different BRT RSs and independency of different MS-RS links)
MS→BS(i)	MS→RS(j)	0 (due to large distance between different BRT RSs and BSs and independency of MS-RS and MS-BS links)
RS→RS(i)	RS→RS(j)	0 (because distance between RSs is much larger than correlation distance equal to 12 – 14 m)

Table 62: Shadow fading correlation in the Manhattan deployment scenario

14.3.4. Summary

BS-RS link	ART RS scenario	BRT RS scenario	Manhattan deployment scenario
Penetration Loss	0dB	0 dB	0 dB
Pathloss Model	IEEE 802.16j EVM Type D pathloss model (Mandatory)	Modified Baseline Model (Mandatory) Modified Urban and Suburban Macrocell (Optional)	Urban Microcell pathloss model (Mandatory) (To be further modified) WINNER B1 Urban Microcell pathloss model (Optional) (To be further modified)
Lognormal Shadowing Standard Deviation	3.4dB	6 dB and 2 dB mean value positive shift	NLOS: 4dB LOS: 3dB
Correlation Distance for Shadowing	100m	50m	NLOS: 12m LOS: 14m
Channel Mix	Single static channel	Single static channel	Single static channel
Spatial Channel Model	WINNER B5a	Baseline Model (Mandatory) Urban and Suburban Macrocell (Optional)	Modified Urban Microcell
RS-RS link			
Penetration Loss	0dB	0 dB	0 dB
Pathloss Model	IEEE 802.16j EVM Type D pathloss model (Mandatory)	Walfish-Ikegami LOS and NLOS pathloss models (Mandatory) (To be further modified) Urban Microcell (Optional) (To be further modified)	Urban Microcell pathloss model (Mandatory) (To be further modified) WINNER B1 Urban Microcell pathloss model (Optional) (To be further modified)
Lognormal Shadowing Standard Deviation	3.4dB	NLOS: 4dB LOS: 3dB	NLOS: 4dB LOS: 3dB
De-correlation Distance for Shadowing	40m	NLOS: 12m LOS: 14m	NLOS: 12m LOS: 14m

Channel Mix	Single static channel	Single static channel	Single static channel
Spatial Channel Model	WINNER B5a	Modified Urban Microcell	Modified Urban Microcell
RS-MS link			
Penetration Loss	10dB	Urban Microcell propagation: LOS: 0 dB NLOS: 10 dB Outdoor to Indoor propagation: 0 dB	Urban Microcell propagation: LOS: 0 dB NLOS: 10 dB Outdoor to Indoor propagation: 0 dB
Pathloss Model	Baseline Model (Mandatory) Urban and Suburban Macrocell (Optional)	COST Walfish-Ikegami LOS and NLOS pathloss models (Mandatory) Urban Microcell (Optional) Outdoor to Indoor (Optional)	Urban Microcell pathloss model (Mandatory) WINNER B1 Urban Microcell pathloss model (Optional) Outdoor to Indoor pathloss model (Optional)
Lognormal Shadowing Standard Deviation	8dB	Urban Microcell propagation: NLOS: 4dB LOS: 3dB Outdoor to Indoor propagation: 7 dB	Urban Microcell propagation: NLOS: 4dB LOS: 3dB Outdoor to Indoor propagation: 7 dB
Correlation Distance for Shadowing	50m 50% BSs, RSs correlation	Urban Microcell propagation: NLOS: 12m LOS: 14m Outdoor to Indoor propagation: 7 m	Urban Microcell propagation: NLOS: 12m LOS: 14m Outdoor to Indoor propagation: 7 m
Channel Mix	ITU Pedestrian B and Vehicular A channel models ITU PB 3kmph - 60%	Urban Microcell propagation: 3kmph – 60% 60kmph – 30%	Urban Microcell propagation: 3kmph – 60% 60kmph – 30%

	ITU VA 30kmph - 30% ITU VA 120kmph – 10%	120kmph – 10% Outdoor to Indoor propagation: TBD	120kmph – 10% Outdoor to Indoor propagation: TBD
Spatial Channel Model	Baseline model (Mandatory) 802.16m EMD Urban and Suburban Macrocell (Optional)	Urban Microcell (Mandatory) Outdoor to Indoor (Optional)	Urban Microcell (Mandatory) Outdoor to Indoor (Optional)
BS-MS link			
Penetration Loss	10dB	10dB	Urban Microcell propagation: LOS: 0 dB NLOS: 10 dB Outdoor to Indoor propagation: 0 dB
Pathloss Model	Baseline model (Mandatory) Urban and Suburban Macrocell (Optional)	Baseline model (Mandatory) Urban and Suburban Macrocell (Optional)	Urban Microcell pathloss model (Mandatory) WINNER B1 Urban Microcell pathloss model (Optional) Outdoor to Indoor pathloss model (Optional)
Lognormal Shadowing Standard Deviation	8dB	8dB	Urban Microcell propagation: NLOS: 4dB LOS: 3dB Outdoor to Indoor propagation: 7 dB
Correlation Distance for Shadowing	50m 50% BSs correlation	50m 50% BSs correlation	Urban Microcell propagation: NLOS: 12m LOS: 14m Outdoor to Indoor propagation: 7 m

Channel Mix	802.16m ITU Pedestrian B and Vehicular A channel models ITU PB 3kmph - 60% ITU VA 30kmph - 30% ITU VA 120kmph – 10%	802.16m ITU Pedestrian B and Vehicular A channel models ITU PB 3kmph - 60% ITU VA 30kmph - 30% ITU VA 120kmph – 10%	Urban Microcell propagation: 3kmph – 60% 60kmph – 30% 120kmph – 10% Outdoor to Indoor propagation: TBD
Spatial Channel Model	Baseline model (Mandatory) Urban and Suburban Macrocell (Optional)	Baseline model (Mandatory) Urban and Suburban Macrocell (Optional)	Urban Microcell (Mandatory) Outdoor to Indoor (Optional)
Error Vector Magnitude (EVM)	Ideal	Ideal	Ideal

Table 63: Summary of pathloss and channel models

14.4. Relaying Model

A default relaying model is specified to provide a common starting point for relay simulations. This model is intended to emulate the simplest form of multihop relay and should be sufficient to allow the evaluation and comparison of most relay techniques. The default model may be changed by proponents of relay techniques as long as the changes are described in sufficient detail that allows other participants to implement the modifications in order to verify and compare results.

The default relaying model is defined as follows:

- RSs follow a decode, store, encode, forward model. It is assumed that data transmitted on a relay link is decoded and potentially stored until a later frame. It is then encoded and transmitted on the next hop.
- For simulations in which MSs are static (do not move), MS associations are static for the duration of a trial. An MS is assigned to associate with one or more of the BS and RSs in a sector and this association is not changed during a trial.
- Access link transmissions from/to the BS and RSs within a sector can occur simultaneously (in time/frequency) or within time/frequency partitions dedicated to individual stations (BS and RSs). The scheduler decides for specific transmissions what occurs in parallel and what occurs sequentially in the case of centralized scheduling. In the case of distributed scheduling the scheduler RS may use different zones to avoid such interference for specific set of mobiles which needs to be specified with the simulation results.

- Transmissions from/to MSs which are associated with an RS are performed hop-by-hop. It is assumed that a relay link / access link transmission is received with some probability of error and potentially retransmitted. After successful reception the data is scheduled on the next hop.

14.5. Simulation Procedure and Flow

The simulation procedure of the 16m system with relays is based on the simulation procedure described in Section 11. In this section we highlight the areas in which this procedure is amended to support relay.

- Deployment
 - RSs are placed within each sector in accordance with the selected deployment scenario (refer to Section 14.1).
 - MSs are dropped according to the specification in Section 11.
 - Pathloss, shadow fading, and antenna patterns are calculated for all possible links between MSs, RSs, and BSs.
- MS Association
 - MSs are associated with BSs and RSs as described in Section 14.6.
- Scheduling
 - The generic proportional fair scheduler specified in appendix F, is used for allocation of the resources.
 - The access link is simulated explicitly for all test scenarios.
 - The resources used for relay link transmissions are determined as part of the scheduling of each RS access link transmission. The relay link resources that can be used within each frame are limited by the size of the zone in which relay transmissions are performed. If the relay zone resources are used up, no additional RS access link transmissions can be scheduled in that frame. Proponents should specify the average relay link spectral efficiency that was assumed for a given simulation.
 - For test scenarios in which a static relay link is assumed, the average relay link spectral efficiency shall be used to calculate the relay link resources for all transmissions.
 - For test scenarios in which a dynamic relay link is assumed the spectral efficiency of the relay link is calculated explicitly for each transmission by determining the appropriate MCS and corresponding packet error rate. This spectral efficiency is used to calculate the amount of allocated for relay link resources for the given transmission. The relay link spectral efficiency is calculated to take into account the PER of the relay link:

$$SE = SE_{MCS}(1 - PER)$$

where SE_{MCS} is the spectral efficiency of the selected modulation coding scheme and PER the packet error rate.

For evaluation of HARQ protocols the HARQ process is simulated

explicitly on each hop. The procedure as well as details of the HARQ simulation model (queuing, buffer size, etc) need to be specified by proponent in sufficient detail in order to allow other members to recreate the simulation in order to verify the results.

14.6. MS Association

MS association is the procedure of selecting the BS or RS with which each MS within the desired sectors will associate. A default procedure is specified here. Other MS association procedures may be used to investigate advanced relay modes for which the default procedure is not appropriate. Proponents must describe the MS association procedure that was used in their simulation.

The default MS association procedure uses a one or two step association process. In the first step, SNR is used to determine an initial association. SNR is estimated between each MS and each of the BS sectors and RSs. Each MS is associated with the BS or RS to which it has highest SNR. The second step is optional. In the second step effective capacity is calculated between each MS and the BS and RSs within the sector to which the MS was assigned. The effective capacity calculation may take into account SINR at the MS, relay link overhead and the possibility of resource reuse by BS and RSs. The MS is assigned to the BS or RS with which it has the highest value of effective capacity. MS Association and the details of the procedure need to be described by the proponent in sufficient detail in order to allow other members to duplicate the simulation in order to verify the results.

14.7. Scheduling

The generic proportional fair scheduler specified Appendix F is used for allocation of the resources. The number of active users and partitions is adjusted to better model the interactions between the BS and RSs. Distributed and centralized scheduling models are defined.

14.7.1. Frame partitioning

The number of partitions and active users should be increased for the case of relay (above the 5 partitions and 10 users used for the baseline case). The number of partitions and users may depend on the number of relays used within a sector. Proponents should specify the number of partitions and active users along with the partition size and downlink control overhead that is assumed in the simulation.

In order to make comparison of results easier, the following numbers of partitions and users are suggested for the following number of RSs per sector. Proponents are encouraged to use these values, but proponents may choose to use different numbers.

- 2 RSs per sector: 10 partitions and 20 active users.
- More than 2 RSs per sector: 20 partitions and 40 active users.

14.7.2. Distributed scheduling

When distributed scheduling is used, the DL or UL access zones are partitioned into sub-zones which are assigned to the BS and RSs. Sub-zones may overlap, allowing simultaneous transmissions to/from BS and the RSs using the same resources.

MSs associated with the BS are scheduled by the BS within the sub-zone assigned to the BS transmissions. MSs associated with each RS are scheduled by each RS within the sub-zone assigned to that RS. Scheduling of the subscribers associated with the BS and each of the RSs is performed independently by independent scheduler instances.

The size of the sub-zones should remain constant for the duration each simulation run. Proponents should specify the size of the sub-zones and the amount of overlap between sub-zones assigned to the BS and RSs.

14.7.3. Centralized scheduling

When centralized scheduling is used, the resources in the entire DL and UL access zones of the BS and RSs within the sector are scheduled by the BS scheduler. The BS scheduling algorithm allocates resources on a per-frame basis to the MSs taken from the common pool in each sector. It is assumed that the scheduling algorithm realized at the BS has access to channel state information (CSI) for each MS. The CSI should be delayed by a few frames to indicate the frame exchange delay. Proponents should specify the delay that was used in their simulation. Extra scheduling margin should be used to accommodate the CQI delay. A value of 2dB should be used for simulations of 2 hop topologies. For topologies with 3 or more hops, proponents should specify the margin (in dB) which was used in their simulations.

14.7.4. Relay HARQ

HARQ transmissions are scheduled in the same way as usual packet transmissions. The route for the HARQ retransmissions is determined by the scheduler (either distributed or centralized).

For distributed scheduling, delays for HARQ retransmissions and acknowledgements for relay HARQ should be the same as delays for retransmissions for conventional HARQ schemes.

For centralized scheduling, delays should be increased in accordance to the number of hops between the BS and MS, since decision about HARQ retransmission is performed at the BS side.

14.8. Performance metrics

Most of the performance metrics proposed in Section 13 can be applied to the relay case without any additions, since they are derived from the user data throughput (Section 13.2.1.1). The users are scheduled on a per-frame basis; the resources of each frame are distributed between access (BS-MS, RS-MS) and relay (BS-RS) links. The relay link overhead is automatically taken into account in a user data throughput metric since part of frame resources are given to a BS-RS link by the scheduler.

Therefore, definition of the basic performance metrics, such as user throughput and sector throughput are the same as in Section 13.

14.8.1. System performance metrics

14.8.1.1. Spectral efficiency and aggregate sector throughput

Spectral efficiency metrics and cell/sector throughput metrics should be considered in the sense of aggregate sector throughput going through the BS (including useful traffic from all RSs in the sector).

14.8.1.2. Combined coverage and capacity index

The Combined Coverage and Capacity index (cc) is the number of simultaneous users per sector that can be supported achieving a target information throughput R_{min} with specified coverage reliability ($x\%$, 95% by default). The definition of this metric is based on the “Combined Coverage and Capacity Index Metric, Method One” as specified in section 4.2.2. of the IEEE 802.16j EVM [81].

The metric is calculated individually within each zone of the frame structure and the individual values are summed as shown in the formula below. Assume that N MSs are dropped uniformly in the service area. For the MSs assigned to each zone, the simulator calculates the achievable data rate r_i , based on the assigned MCS and available time-frequency resources within the zone. All MSs are sorted in descending order and only the top $x\%$ of the MSs are considered for further calculations. If k is the number of MSs that were selected for consideration, then Combined Coverage and Capacity index is:

$$cc = \sum_{zones} \frac{1}{\frac{1}{k} \sum_{i=1}^k \frac{R_{min}}{r_i}}$$

If $\min(r_i) < R_{min}$, then $cc = 0$ and service with R_{min} throughput cannot be provided with the required coverage, regardless the number of users.

For large N , coverage and capacity index cc approaches the expected value of the number of users that can be supported by the system for service requiring R_{min} throughput with the given $x\%$ coverage.

14.8.2. Relay specific performance metrics

The described relay evaluation methodology requires introducing several associated performance metrics in addition those defined for non-relay case.

14.8.2.1. Relay link overhead percentage

The Relay overhead is defined as the average number of additional slots required to transmit data from BS to RS for further distribution to MS associated with the RS relative to the total number of slots in a frame. Since the overhead is defined with respect to the time and frequency slots (not the amount of data), it reflects the efficiency

of BS to RS links and takes into account possible spatial multiplexing of BS to different RS stations that may be exploited.

14.8.2.2. Relay link average SE

This metric characterizes the BS-RS link quality in terms of spectral efficiency. This is an important characteristic of the relay system and should be used for relay link overhead calculation, along with Relay link PER. Relay link average SE is measured in the same way as access link average SE as described in Section 13.

14.8.2.3. Relay link PER

Packet error rate for the BS-RS and RS-RS links defined as the ratio of the successfully received relay link packets to the total number of transmitted relay links packets. Relay link PER is measured in the same way as access link PER, as described in Section 13.

15. Template for Reporting Results

Relevant system performance metrics for partial and complete technical proposals should be generated and included in the evaluation report as specified in the following table. For relative performance metrics, results for the reference system should be included. Models and assumptions should be aligned with those listed in this document. Additional assumptions and deviations from required assumptions should be specified.

System Level results such as the cdf of normalized throughput and Link Level results that are required for performance evaluation should be shown in separate figures.

Performance Metric	Value : 802.16m	Value : 802.16e Reference System
Peak Data Rate DL / UL (bps/Hz)		
Maximum Data Latency DL / UL (ms)		
State Transition Latency (ms)		
Maximum Intra-frequency handover interruption time (ms)		
Maximum Inter-frequency handover interruption time (ms)		
Average User Throughput * DL / UL (bps/Hz)		
Cell Edge User Throughput * DL / UL (bps/Hz)		
Sector Throughput * DL / UL (bps/Hz)		

VoIP Capacity ** DL / UL (Active Users/MHz/sector)		
MBS Spectral Efficiency *** 0.5 km site-to-site distance (bps/Hz)		
MBS Spectral Efficiency 1.5 km site-to-site distance (bps/Hz)		
Estimated Layer 1 Overhead DL / UL (%)		
Estimated Layer 2 Overhead DL / UL (%)		

Table 64: Evaluation report

* Applies to full buffer data traffic for all active users

** Applies to VoIP traffic for all active users

*** All configuration baseline parameters defined in Section 2 apply to site-to-site distance of 0.5 km

1
2
3
4

Appendix A: Spatial Correlation Calculation

In order to compute the spatial correlation, two methods can be considered here:

Method-1: Using 20 subpaths to approximate the Laplacian PDF

For each path, generate 20 subpaths with some angular offsets from the per-path AoD_n and AoA_n. The angular offsets of the k-th (k=1..20) subpath are determined by (the offsets are the same for all paths)

$$\psi_{k,BS} = \Delta_k * AS_{BS,Path}$$

$$\psi_{k,MS} = \Delta_k * AS_{MS,Path}$$

where the values of Δ_k are given below.

Sub-path number k	Δ_k
1,2	± 0.0447
3,4	± 0.1413
5,6	± 0.2492
7,8	± 0.3715
9,10	± 0.5129
11,12	± 0.6797
13,14	± 0.8844
15,16	± 1.1481
17,18	± 1.5195
19,20	± 2.1551

Table 65: Value of Δ_k

Derive the antenna spatial correlation at the BS and MS between the p-th and q-th antenna as:

$$r_{n,BS}(p,q) = \frac{1}{20} \sum_{k=1}^{20} \exp \left\{ j \frac{2\pi d_{BS}}{\lambda} (p-q) \sin(AOD_n + \psi_{k,BS} + \theta_{BS}) \right\}$$

$$r_{n,MS}(p,q) = \frac{1}{20} \sum_{k=1}^{20} \exp \left\{ j \frac{2\pi d_{MS}}{\lambda} (p-q) \sin(AOA_n + \psi_{k,MS} + \theta_{MS}) \right\}$$

where d_{BS} (d_{MS}) is the antenna spacing at BS (MS) and λ is the wavelength.

Method-2: Pre-compute the correlation values with quantized AoA, AoD

Pre-calculate the BS spatial correlation matrices for a set of

$AOD \in \{-90^\circ, -80^\circ, \dots, 0^\circ, \dots, 80^\circ, 90^\circ\}$ and the MS spatial correlation matrices for a set of

$AOA \in \{-90^\circ, -80^\circ, \dots, 0^\circ, \dots, 80^\circ, 90^\circ\}$

$$R_{BS}(m, p, q) = \int_{-\infty}^{\infty} f(\alpha) \exp \left\{ j \frac{2\pi d_{BS}}{\lambda} (p-q) \sin(AOD[m] + \alpha + \theta_{BS}) \right\} d\alpha$$

$$R_{MS}(m, p, q) = \int_{-\infty}^{\infty} f(\beta) \exp \left\{ j \frac{2\pi d_{MS}}{\lambda} (p-q) \sin(AOA[m] + \beta + \theta_{MS}) \right\} d\beta$$

where m is the quantization step index, α , β are the angular offset at BS and MS, respectively with Laplacian PDF as defined in 3.2.8.

Assuming omni directional antennas and the incoming rays within $\pm\Delta$ of the mean angle of arrival or departure (i.e. the Laplacian PAS is defined over $[\phi_0 - \Delta, \phi_0 + \Delta]$) an exact expression to calculate the spatial correlation coefficient is given by [1]

$$\Re[R_{BS}(m, p, q)] = J_0(D(p-q)) + 2 \sum_{r=1}^{\infty} \frac{J_{2r}(D(p-q))}{\left(\frac{\sqrt{2}}{\sigma_\phi^2}\right)^2 + (2r)^2} (\cos(2r\phi_0)) \left\{ \frac{\sqrt{2}}{\sigma_\phi^2} + \exp\left(-\frac{\Delta\sqrt{2}}{\sigma_\phi^2}\right) \left[2r \sin(2r\Delta) - \frac{\sqrt{2}}{\sigma_\phi^2} \cos(2r\Delta) \right] \right\}$$

$$\Im[R_{BS}(m, p, q)] = 2 \sum_{r=0}^{\infty} \frac{J_{2r+1}(D(p-q))}{\left(\frac{\sqrt{2}}{\sigma_\phi^2}\right)^2 + (2r+1)^2} \sin((2r+1)\phi_0) \left\{ \frac{\sqrt{2}}{\sigma_\phi^2} - \exp\left(-\frac{\Delta\sqrt{2}}{\sigma_\phi^2}\right) \left[(2r+1) \sin((2r+1)\Delta) + \frac{\sqrt{2}}{\sigma_\phi^2} \cos((2r+1)\Delta) \right] \right\}$$

Where $D = \frac{2\pi d_{BS}}{\lambda}$, $\sigma_\phi = AS_{BS,Path}$, $J_x(\cdot)$ is the x -th order Bessel function of the first kind and ϕ_0 is the AOD. Similarly the expressions for the $R_{MS}(m, p, q)$ can be written with $D = \frac{2\pi d_{MS}}{\lambda}$, and $\sigma_\phi = AS_{MS,Path}$. The infinite sums are truncated at $\frac{(r+1) - \text{th term}}{\text{Sum of first } r \text{ terms}} = 0.1\%$.

For each path, determine the index m_{BS} corresponding to AoD_n ,

$$m_{BS} = \left\lfloor \frac{AOD_n}{10} \right\rfloor$$

and the index m_{MS} corresponding to AoA_n

$$m_{MS} = \left\lfloor \frac{AOA_n}{10} \right\rfloor$$

The spatial correlation matrix for this path is then

$$r_{n,BS}(p, q) = R_{BS}(m_{BS}, p, q)$$

$$r_{n,MS}(p, q) = R_{MS}(m_{MS}, p, q)$$

Appendix B: Polarized Antenna

Correlation between polarized antennas results from the cross polarization power ratio (XPR). The polarization matrix is given by:

$$\mathbf{S} = \begin{bmatrix} S_{vv} & S_{vh} \\ S_{hv} & S_{hh} \end{bmatrix},$$

where v denotes vertical and h horizontal polarization, the first index denoting the polarization at BS and the second the polarization at MS. The example below assumes -8 dB per-tap power ratio between vertical-to-horizontal and vertical-to-vertical polarisations (also $P_{hv}/P_{hh} = -8\text{dB}$). But the actual XPR value for each scenario should follow the specification in respective CDL model. The -8dB value was adopted from reference [24]. The following derivation of antenna correlation due to polarization with -8dB XPR can also be found in [24]. This results in the following mean power per polarization component

$$p_{vv} = E\{|s_{vv}|^2\} = 0 \text{ dB} = 1$$

$$p_{vh} = E\{|s_{vh}|^2\} = -8 \text{ dB} = 0.1585$$

$$p_{hv} = E\{|s_{hv}|^2\} = -8 \text{ dB} = 0.1585$$

$$p_{hh} = E\{|s_{hh}|^2\} = 0 \text{ dB} = 1$$

If the MS polarizations are assumed to be vertical and horizontal, but the BS polarizations are slant $+45^\circ$ and -45° . The MS and BS polarization matrices \mathbf{P}_{MS} and \mathbf{P}_{BS} respectively are rotation matrices, which map vertical and horizontal polarizations to MS and BS antenna polarizations.

$$\mathbf{P}_{MS} = \begin{bmatrix} 1 & 0 \\ 0 & 1 \end{bmatrix}$$

$$\mathbf{P}_{BS} = \frac{1}{\sqrt{2}} \begin{bmatrix} 1 & 1 \\ 1 & -1 \end{bmatrix}$$

The total channel is the matrix product of the BS polarization, the channel polarization, and the MS polarization:

$$\mathbf{Q} = \mathbf{P}_{BS} \mathbf{S} \mathbf{P}_{MS} = \frac{1}{\sqrt{2}} \begin{bmatrix} S_{vv} + S_{hv} & S_{vh} + S_{hh} \\ S_{vv} - S_{hv} & S_{vh} - S_{hh} \end{bmatrix}$$

The covariance matrix of the channel is

$$\begin{aligned}
\Gamma &= E\{vec(\mathbf{Q}) \cdot vec(\mathbf{Q})^H\} \\
&= E\left\{\frac{1}{2} \begin{bmatrix} (s_{vv} + s_{hv})(s_{vv} + s_{hv})^* & (s_{vv} + s_{hv})(s_{vv} - s_{hv})^* & (s_{vv} + s_{hv})(s_{vh} + s_{hh})^* & (s_{vv} + s_{hv})(s_{vh} - s_{hh})^* \\ (s_{vv} - s_{hv})(s_{vv} + s_{hv})^* & (s_{vv} - s_{hv})(s_{vv} - s_{hv})^* & (s_{vv} - s_{hv})(s_{vh} + s_{hh})^* & (s_{vv} - s_{hv})(s_{vh} - s_{hh})^* \\ (s_{vh} + s_{hh})(s_{vv} + s_{hv})^* & (s_{vh} + s_{hh})(s_{vv} - s_{hv})^* & (s_{vh} + s_{hh})(s_{vh} + s_{hh})^* & (s_{vh} + s_{hh})(s_{vh} - s_{hh})^* \\ (s_{vh} - s_{hh})(s_{vv} + s_{hv})^* & (s_{vh} - s_{hh})(s_{vv} - s_{hv})^* & (s_{vh} - s_{hh})(s_{vh} + s_{hh})^* & (s_{vh} - s_{hh})(s_{vh} - s_{hh})^* \end{bmatrix}\right\} \\
&= \frac{1}{2} \begin{bmatrix} p_{vv} + p_{hv} & p_{vv} - p_{hv} & 0 & 0 \\ p_{vv} - p_{hv} & p_{vv} + p_{hv} & 0 & 0 \\ 0 & 0 & p_{vh} + p_{hh} & p_{vh} - p_{hh} \\ 0 & 0 & p_{vh} - p_{hh} & p_{vh} + p_{hh} \end{bmatrix}
\end{aligned}$$

Here the property of uncorrelated fading between different elements in \mathbf{S} (i.e. $E\{s_{ij}s_{kl}^*\} = 0, i \neq k, j \neq l$) has been used to simplify the expressions. Plugging the numerical example of -8dB XPD, we have

$$\Gamma = \frac{1}{2} \begin{bmatrix} 1+0.1585 & 1-0.1585 & 0 & 0 \\ 1-0.1585 & 1+0.1585 & 0 & 0 \\ 0 & 0 & 0.1585+1 & 0.1585-1 \\ 0 & 0 & 0.1585-1 & 0.1585+1 \end{bmatrix} = \begin{bmatrix} 0.5793 & 0.4208 & 0 & 0 \\ 0.4208 & 0.5793 & 0 & 0 \\ 0 & 0 & 0.5793 & -0.4208 \\ 0 & 0 & -0.4208 & 0.5793 \end{bmatrix}$$

When all of the diagonal elements are equal, the covariance matrix can be further normalised to correlation matrix:

$$\Gamma = \begin{bmatrix} 1 & \gamma & 0 & 0 \\ \gamma & 1 & 0 & 0 \\ 0 & 0 & 1 & -\gamma \\ 0 & 0 & -\gamma & 1 \end{bmatrix}$$

The value of γ depends only on XPR and it is obtained from the previous matrix after the normalization of the diagonal values to "1". With different orientations of MS and BS antenna polarizations, also the covariance matrix structure will be different.

Appendix C: LOS Option with a K-factor

A single-tap MIMO channel can be added to the TDL channels in this case and then modify the time-domain channels as:

$$\mathbf{H}_n = \begin{cases} \sqrt{\frac{1}{K+1}}\mathbf{H}_n + \sqrt{\frac{K}{K+1}}\mathbf{H}^{LOS} & n = 1(\text{first tap}) \\ \sqrt{\frac{1}{K+1}}\mathbf{H}_n & n \neq 1 \end{cases}$$

where the K-factor is in decimal and the LOS component is defined as, between p-th BS antenna and q-th MS antenna

$$\mathbf{H}^{LOS}(p, q) = \exp\left(j \frac{2\pi d_{BS}(p-1)}{\lambda} \sin(\theta_{BS})\right) \times \exp\left(j \frac{2\pi d_{MS}(q-1)}{\lambda} \sin(\theta_{MS})\right)$$

where d_{BS} and d_{MS} are antenna spacing at the BS and MS, respectively, assuming uniform linear array in this case.

Appendix D: Antenna Gain Imbalance and Coupling

Overall receive correlation matrix is

$$\mathbf{H}'_n = \begin{bmatrix} \sqrt{\frac{1}{c+1}} & \sqrt{\frac{c}{c+1}} \\ \sqrt{\frac{c}{c+1}} & \sqrt{\frac{1}{c+1}} \end{bmatrix} \begin{bmatrix} 1 & 0 \\ 0 & \sqrt{a} \end{bmatrix} \mathbf{H}_n$$

where antenna-1 to antenna-2 coupling coefficient (leakage of ant-1 signal to ant-2) is “c” (linear) and the antenna-1 and antenna gain ratio is “a” (linear).

Appendix E: WINNER Primary Model Description

This appendix describes the primary model from which the CDL models were derived. The primary model is an accurate representation of the true MIMO radio channel. The CDL modes are a simplification of the primary model in order to save simulation time. The use of the primary model is optional but encouraged for further simulation.

The primary model is a double-directional model. Geometric based modeling of the radio channel enables separation of propagation parameters and antennas.

The channel parameters for individual snapshots are determined stochastically, based on statistical distributions extracted from channel measurement. Antenna geometries and field patterns can be defined properly by the user of the model. Channel realizations are generated with geometrical principle by summing contributions of rays (plane waves) with specific small scale parameters like delay, power, angle-of-arrival (AoA) and angle-of-departure (AoD). Superposition results to correlation between antenna elements and temporal fading with geometry dependent Doppler spectrum.

A number of rays constitute a cluster. In the terminology of this document we equate the cluster with a propagation path diffused in space, either or both in delay and angle domains. For a discussion of the word cluster, refer to Section 3.2.5.

The WINNER generic model is a system level model, which can describe an infinite number of propagation environment realizations. The generic model can describe single or multiple radio links for all the defined scenarios and arbitrary antenna configurations. This is done by applying different parameter sets to a single common mathematical framework. The generic model is a stochastic model with two (or three) levels of randomness. The first level, known as large scale (LS), parameters like Shadow fading, delay and angular spreads are drawn randomly from tabulated distribution functions. LS parameters have cross-correlation between different parameters and auto-correlation between different transceiver locations. Next, the small scale parameters like delays, powers and directions arrival and departure are drawn randomly according to tabulated distribution functions and the random LS parameters (second moments). At this stage the geometric setup is fixed and the only free variables are the random initial phases of the scatterers. By picking (randomly) different initial phases, an infinite number of different realizations of the model can be generated. When the initial phases are also fixed, there is no further randomness.

Channel segment (drop) represents period of quasi-stationarity in which probability distributions of low-level parameters are not changed. During this period all large-scale control parameters, as well as velocity and direction-of-travel for mobile station (MS), are held constant. Motion within a segment is only virtual and causes fast fading and the Doppler effect by superposition of rotating phasors, rays. To be physically feasible, the channel segment must be relatively confined in distance. The size depends on the environment, but it can be at maximum few meters. Although the large scale

- 1 parameters can be correlated between the channel segments, the radio channel is
- 2 discontinuous from segment to segment.
- 3 A detailed description of the WINNER model is given in [13]. An implementation of the
- 4 primary model is available in [25].

Appendix F: Generic Proportionally Fair Scheduler for OFDMA

The proportionally fair scheduler (PFS), in its simplest form, computes a metric for all active users at for a given scheduling interval. The user with the highest metric is allocated the resource available in the given interval, the metrics for all users are updated before the next scheduling interval, and the process repeats. To adapt this simple algorithm for OFDMA systems, the definition of scheduling interval and scheduling resource must be extended to apply to a two-dimensional OFDMA frame resource. Furthermore, this PFS applies only to baseline full buffer traffic simulations and zones which use a distributed subcarrier permutation such as PUSC.

For OFDMA systems, the scheduling interval is typically a frame, and multiple users may be allocated in the same frame. Therefore, in the simplest extension to OFDMA systems, two modifications must be made to the PFS: (i) Frames must be equi-partitioned into regular, fixed scheduling resources that must be scheduled sequentially until all available resources are assigned. (ii) The metric must be updated after scheduling each partition. Note that the number of resources eventually allocated to a user depends on the metric update process, and does not preclude a single user from getting multiple or all the resources in a frame. For system simulations with an assumption of fixed overhead allowing for up to $N_{partition}$ resource partitions, each partition assignment should be considered as a separate packet transmission.

To promote fair comparison, each proponent should evaluate system performance with full-buffer traffic using this generic PFS. If this scheduler is not used, the proponent must justify the use of an alternate scheduler, and describe the algorithm in detail. The number of partitions, $N_{partition}$, the time constant of the filter used in the metric computation, and number of active users are all simulation parameters that must be specified by the proponent.

For informative purposes, the metric for a simple proportionally fair scheduler, in which a single user is scheduled in a given scheduling interval, is described in the remainder of this appendix.

At any scheduling instant t , the scheduling metric $M_i(t)$ for subscriber i used by the proportional fair scheduler is given by

$$M_i(t) = \frac{T_inst_i(t)}{[T_average_i(t)]^\alpha}$$

where $T_inst_i(t)$ is the data rate that can be supported at scheduling instant t for subscriber i , $T_inst_i(t)$ is a function of the CQI feedback, and consequently of the modulation and coding scheme that can meet the PER requirement. $T_average_i(t)$ is throughput smoothed by a low-pass filter at the scheduling instant t for user i . α is a

1 fairness exponent factor with default value 1. For the scheduled subscriber,
 2 $T_average_i(t)$ is computed as

$$T_average_i(t) = \frac{1}{N_{PF}} * T_inst_i(t) + (1 - \frac{1}{N_{PF}}) * T_average_i(t-1)$$

7 and for unscheduled subscriber,

$$T_average_i(t) = (1 - \frac{1}{N_{PF}}) * T_average_i(t-1)$$

11 The latency scale of the PF scheduler, N_{PF} , is given by

$$N_{PF} = T_{PF} N_{Partitions} / T_{Frame}$$

15 where T_{PF} represents the latency time scale in units of seconds and T_{Frame} is the frame
 16 duration of the system.

18 In some implementations, the scheduler may give priority to HARQ retransmissions.

Appendix G: 19 Cell Wrap Around Implementation

G-1. Multi-Cell Layout

In Figure 37, a network of cells is formed with 7 clusters and each cluster consists of 19 cells. Depending on the configuration being simulated and required output, the impact of the outer 6 clusters may be neglected. In such cases, only 19 cells of the center cluster may be modeled.

For the cases where modeling outer-cells are necessary for accuracy of the results, the wrap around structure with the 7 cluster network can be used. In the wrap around implementation, the network is extended to a cluster of networks consisting of 7 copies of the original hexagonal network, with the original hexagonal network in the middle while the other 6 copies are attached to it symmetrically on 6 sides, as shown in Figure 37. The cluster can be thought of as 6 displacements of the original hexagon. There is a one-to-one mapping between cells/sectors of the center hexagon and cells/sectors of each copy, so that every cell in the extended network is identified with one of the cells in the central (original) hexagonal network. Those corresponding cells have thus the same antenna configuration, traffic, fading etc. except the location. The correspondence of those cells/sectors is illustrated in Figure 38.

An example of the antenna orientations in case of a sectorized system is defined in Figure 38. The distance from any MS to any base station can be obtained from the following algorithm: Define a coordinate system such that the center of cell 1 is at (0,0). The path distance and angle used to compute the path loss and antenna gain of a MS at (x,y) to a BS at (a,b) is the minimum of the following:

- a. Distance between (x,y) and (a,b);
- b. Distance between (x,y) and $(a + 3R, b + 8\sqrt{3}R/2)$;
- c. Distance between (x,y) and $(a - 3R, b - 8\sqrt{3}R/2)$;
- d. Distance between (x,y) and $(a + 4.5R, b - 7\sqrt{3}R/2)$;
- e. Distance between (x,y) and $(a - 4.5R, b + 7\sqrt{3}R/2)$;
- f. Distance between (x,y) and $(a + 7.5R, b + \sqrt{3}R/2)$;
- g. Distance between (x,y) and $(a - 7.5R, b - \sqrt{3}R/2)$,

Where, R is the radius of a circle which connects the six vertices of the hexagon.

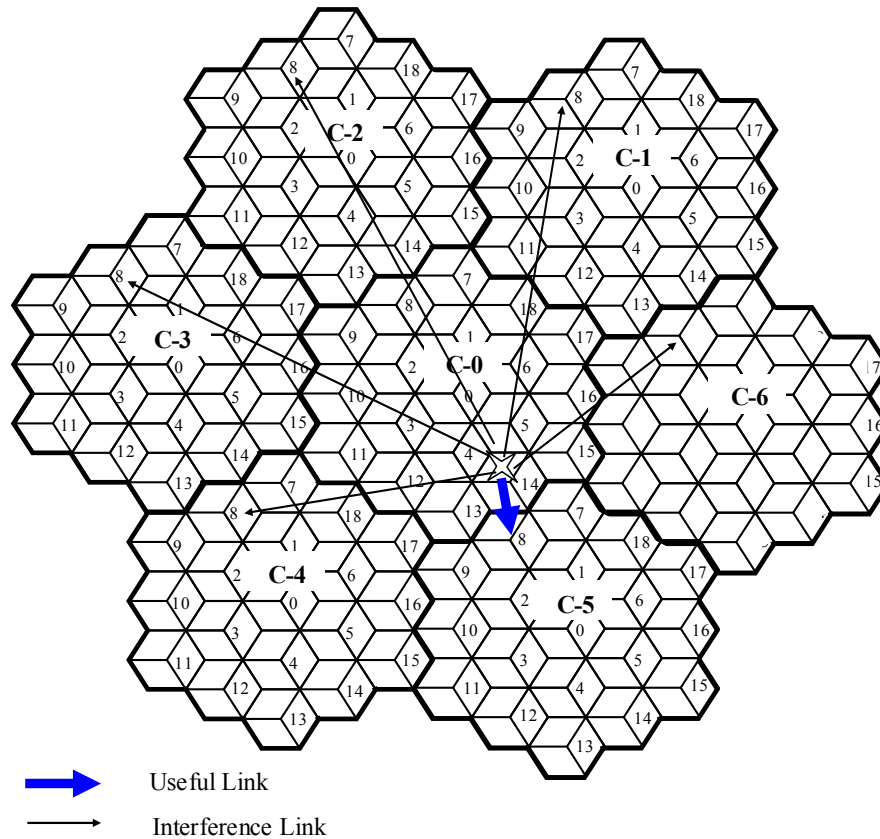


Figure 37: Multi-cell layout and wrap around example

G-2. Obtaining virtual MS locations

The number of MSs is predetermined for each sector, where each MS location is uniformly distributed. The MS assignment is only done for the cluster-0 from where the decided MSs are replicated in the other six clusters. The purpose to employ this wrap-around technique, as will be discussed in later section, is to easily model the interferences from other cells.

G-3. Determination of serving cell/sector for each MS in a wrap-around multi-cell network

The determination of serving cell for each MS is carried out by two steps due to the wrap-around cell layout. The first step is to determine the 19 shortest distance cells for each MS from all seven logical cells clusters, and the second step is to determine the serving cell/sector among the nearest 19 cells for each MS based on the strongest link according to the path-loss and shadowing.

To determine the shortest distance cell for each MS, the distances between the target MS and all logical cell clusters should be evaluated and the 19 cells with a shortest distance in all 7 cell clusters should be selected. Figure 37 illustrates an example for determination of the shortest distance cell for the link between MS and cell-8. It can be

seen that the cell-8 located in cluster-5 generates the shortest distance link between MS and cell-8.

To determine the serving cell for each MS, we need to determine 19 links, whereby we may additionally determine the path-loss, shadowing and transmit/receive antenna gain in consideration of antenna pattern corresponding to the nearest 19 cells/sectors. The serving cell for each MS should offer a strongest link with a strongest received long-term power. It should be noted that the shadowing experienced on the link between MS and cells located in different clusters is the same.

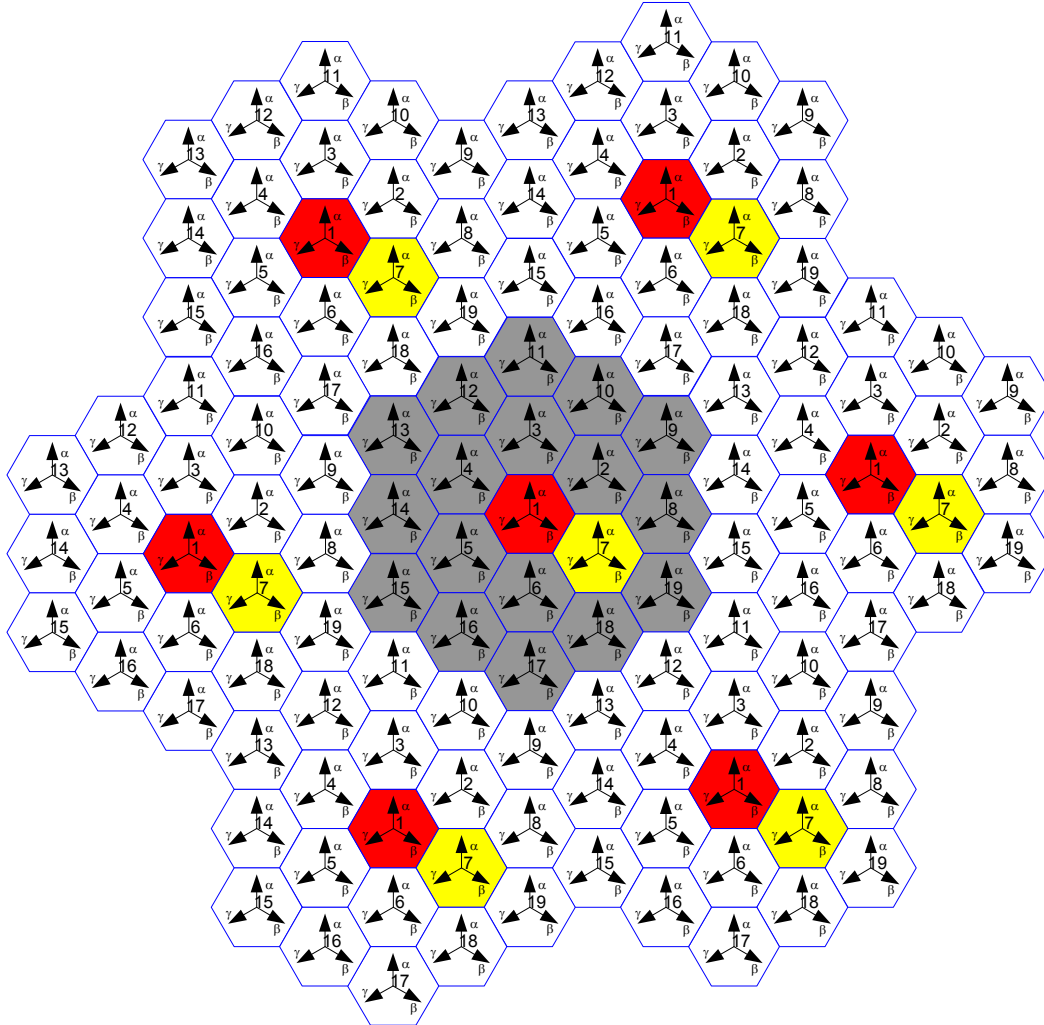


Figure 38: Antenna orientations for a sectorized system in wrap around simulation *

* The arrows in the figure show the directions that the antennas are pointing

Appendix H: Path Loss Calculations

The modified COST231 Hata model define the following pathloss

$$PL[dB] = (44.9 - 6.55 \log_{10}(h_{bs})) \log_{10}\left(\frac{d}{1000}\right) + 45.5 + (35.46 - 1.1h_{ms}) \log_{10}(f) - 13.82 \log_{10}(h_{bs}) + 0.7h_{ms} + C$$

where 'd' is expressed in meters and that 'f' is expressed in MHz. The constant C = 3 dB for urban macro.

Assuming MS height of 1.5m and at f=2GHz carrier frequency, the model becomes

$$PL = (44.9 - 6.55 \log_{10}(h_{BS})) \log_{10}(d) + 26.46 + 5.83 \log_{10}(h_{BS})$$

In addition, a frequency scaling factor of $26 \log_{10}(f_c)$ is used to account for the path loss change according to the carrier frequency. The frequency correction factor was taken from some work done by Jakes and Reudink [17] where they used measurement data taken in New Jersey at frequencies of 450MHz, 900MHz, 3.7GHz, and 11.2GHz. They showed a frequency dependence for path loss of $f^{2.6}$, which is larger than the frequency correction being employed by the WINNER models (f^2). Note that the original Hata model has a frequency dependence of $(26.16 - 1.1h_{ms} + 1.56) \log(f)$ (=26.07 when $h_{ms}=1.5m$), which is very close to the dependence found by Jakes and Reudink. So the proposed path loss model becomes

$$PL = (44.9 - 6.55 \log_{10}(h_{BS})) \log_{10}(d) + 26.46 + 5.83 \log_{10}(h_{BS}) + 26 \log_{10}(f[GHz]/2)$$

with $50m < d < 5km$ $h_{BS} > 30m$ $f = 2...6GHz$

With both a default BS and MS heights 32m and 1.5 respectively, the model reduces to

$$PL = 35.2 + 35 \log_{10}(d) + 26 \log_{10}(f[GHz]/2)$$

For the COST 231 Hata suburban path loss model the path loss equation is identical to that of the urban macro model in (ref except for a C=0dB correction factor instead of 3dB. However, this offset itself is somewhat contradictory with the suburban offset used in the original Hata model derived for 150-1500MHz. The original Hata offset for suburban areas was [19]. The offset between urban and suburban path loss models applies to 2.5 GHz only.

$$PL_{Suburban} = PL_{Urban} - 2 \left[\log \left(\frac{f(MHz)}{28} \right) \right]^2 - 5.4$$

Since the original Hata offset matches well with the experiments reported in the Erceg model [3], it is adopted here. Again, a frequency scaling factor of $26 \log_{10}(f_c)$ is used to account for the path loss change according to the carrier frequency.

The recommended urban microcellular LOS path loss model is the following [20]:

$$\frac{P_r(r)}{P_t} = -20 \log \left(\frac{e^{sr} 4\pi r D(r)}{\lambda} \right)$$

where,

P_t = Transmit Power

$P_r(r)$ = Received power

r = Distance between Tx and Rx antennas

e^{sr} = Visibility factor ($s = 0.002$)

λ = Wavelength

$$D(r) = \begin{cases} 1 & \text{if } r \leq r_{bp} \\ \frac{r}{r_{bp}} & \text{if } r > r_{bp} \end{cases}$$

$$r_{bp} = \frac{4(h_t - h_0)(h_r - h_0)}{\lambda} = \text{breakpoint distance}$$

h_t = Height of transmit antenna above the road

h_r = Height of receive antenna above the road

h_0 = Effective road height = 1.0m

This is effectively a two ray model, which has an effective road height to account for the effect of traffic on the ground reflected ray. It also includes a visibility factor, which adds additional path loss at longer ranges as visibility in the street becomes more obscured. The model has been validated by measurements at several frequencies in Japan [20].

The WINNER path loss model for this case assumes that the dominant propagation path is around the streets, and therefore only has a 'round-the-streets' component. However, in practice there is also an over-the-rooftop component, as given in the ETSI model for UMTS in [21]. The ETSI model combines a round-the-streets model (Berg model) with an over-the-rooftop model, taking the minimum of these two models at any given mobile location. The ETSI model was modified to include the advanced LOS model [20].

Appendix I: Modeling Control Overhead and Signalling (Informative)

I-1. Overhead Channels

I-1.1. Dynamic Simulation of the Downlink Overhead Channels

Dynamic simulation of the overhead channels is essential to capture the dynamic nature of these channels. The simulations should be done as follows:

The performance of the overhead channels shall be included in the system level simulation results unless the overhead channel is taken into account as part of fixed overhead e.g., if an overhead channel is time division multiplexed, and takes all the bandwidth, the percentage of time used translates into the same percentage decrease in throughput.

There are two possible types of overhead channels depending on the proposal: static and dynamic. A static overhead channel requires fixed base station power and bandwidth. A dynamic overhead channel requires dynamic base station power and (or) bandwidth.

Layer 1 (L1) and Layer 2 (L2) overhead should be accounted for in time and frequency for the purpose of calculation of system performance metrics such as spectral efficiency, user throughput, etc. Examples of L1 overhead include synchronization, guard and DC subcarriers, guard/switching time (in TDD systems), pilots and cyclic prefix. Examples of L2 overheads include common control channels, HARQ ACK/NACK signaling, channel feedback, random access, packet headers and CRC. It must be noted that in computing the overheads, the fraction of the available physical resources used to model control overhead in L1 and L2 should be accounted for in a non-overlapping way. Power allocation/boosting should also be accounted for in modeling resource allocation for control channels.

The demodulation performance (i.e., frame error rate) of the downlink control channel could be assessed using the link abstraction method used to model traffic channels, with proper modifications, if necessary, to reflect any difference in the transmission or coding format of the control channel.

The system level simulations need not directly include the coding and decoding of overhead channels. The link level performance should be evaluated off-line by using separate link-level simulations. The link level performance is characterized by curves of detection, miss, false alarm, and error probability (as appropriate).

For static overhead channels, the system simulation should compute the received SINR and predict the demodulation performance.

For dynamic modeling of overhead channels with open-loop control (if used), the simulations should take into account the required downlink power or bandwidth for

transmission of the overhead channels. During the reception of overhead information, the system simulation should compute the received SINR.

Once the received SINR is obtained and the frame error rate is predicted, then the impact of the detection, miss, false alarm, error probability should be appropriately taken into account in system-level simulation.

All overhead channels should be modeled or accounted for. If a proposal adds messages to an existing channel (for example sending control on a data channel), the proponent shall justify that this can be done without creating undue loading on this channel. The system level and link level simulation required for this modified overhead channel as a result of the new messages shall be performed.

I-1.2. Uplink Modeling in Downlink System Simulation

The proponents shall model feedback errors (e.g. power control, acknowledgements, rate indication, etc.) and measurements (e.g. C/I measurement). In addition to supplying the feedback error rate average and distribution, the measurement error model and selected parameters, the estimated power level required for the physical reverse link channels shall be supplied.

I-1.3. Signaling Errors

Signaling errors shall be modeled and specified as in the following table.

Signaling Channel	Errors	Impact
ACK/NACK channel (if proposed)	Misinterpretation, missed detection, or false detection of the ACK/NACK message	Transmission (frame or encoder packet) error or duplicate transmission
Explicit Rate Indication (if proposed) / mode selection	Misinterpretation of rate / mode selection	One or more Transmission errors due to decoding at a different rate (modulation and coding scheme) or selection of a different mode
User identification channel (if proposed)	A user tries to decode a transmission destined for another user; a user misses transmission destined to it.	One or more Transmission errors due to HARQ/IR combining of wrong transmissions
Rate or C/I feedback channel(if proposed)	Misinterpretation of rate or C/I	Potential transmission errors
Transmit sector indication, transfer of HARQ states etc.(if proposed)	Misinterpretation of selected sector; misinterpretation of frames to be retransmitted.	Transmission errors

Table 66: Signaling errors

Proponents shall quantify and justify the signaling errors and their impacts in the evaluation report.

Appendix J: Transmit Power and EVM

Different modulation methods may have different PAPR and spectral characteristics, affecting the maximum transmit output power. Table 3 specifies the baseline output power and EVM values for the BS and MS, which are applicable for OFDM transmission. This section may be used for evaluating the proposed techniques affecting maximum output power such as PAPR and spectral characteristics

In the case that a proposed modulation method yields different PAPR and/or different spectral characteristics which affect the maximum output power, these numbers shall be calibrated accordingly. Table 67 contains the reference parameters required for calibration.

Parameter	Value	Notes
PA model	RAPP-2 ($s=2$)	AM/AM compression model. See below.
Spectral masks	FCC	Refer to Appendix M
EVM (error vector magnitude)	To be specified in the proposal	May be chosen to optimize performance per MCS
Over sampling	≥ 4	
RBW (resolution bandwidth)	1% of signal bandwidth (100Khz for 10Mhz BW)	For emission measurement. Refer to Appendix M
Reference OFDM transmission	Full bandwidth UL/DL PUSC	

Table 67: Reference parameters for transmit power calibration

Equation (111) defines the RAPP model. $x(t)$, $y(t)$ are the complex baseband representations of the PA input and output respectively, and the parameter s controls the smoothness of the curve. A value of $s=2$ will be used by default. It is also recommended to supply results for $s=30$ to represent a linearized PA. C is the saturation amplitude of the PA.

$$y(t) = \frac{x(t)}{\left(1 + \left|\frac{x(t)}{C}\right|^{2s}\right)^{1/2s}} \quad (111)$$

The proponents should provide simulation results where the modulated signal is passed through a PA compression model and the spectral masks and EVM are computed. The maximum transmit power is the maximum power which meets the spectral masks and the required EVM. The maximum transmit power of flat, full bandwidth modulated OFDM reference signal shall be compared with the maximum effective transmit power of the proposed modulation (with the same PA and mask parameters), and the

1 difference (power gain or loss) will be added to the BS/MS transmit power as defined in
2 Table 3. The saturation power C shall be set so that the maximum power that the
3 reference OFDM system can transmit is according to the power defined in Table 3. The
4 EVM may be chosen per MCS/mode and results in potentially different maximum
5 transmit power per MCS. The EVM required for the reference OFDM system is as
6 defined in Table 3. Effective transmit power and EVM are defined below.
7

8 EVM is defined as the ratio between the effective transmit power and the power of the
9 error vector, both described below. Error vector power is measured over all
10 subchannels, including unmodulated sub-channels. Sub-carriers which do not carry
11 information for any user (guard, DC sub-carriers, and reserved sub-carriers for PAPR
12 reduction) are not included (neither for the error calculation nor for the power
13 calculation). The error signal may be computed using pilot based equalization (as
14 described in [67] 802.16e-2005, subclause 8.4.12.3), or by comparing the transmitted
15 signal with an undistorted (but possibly filtered) signal. In the second case since the
16 distortion error is correlated with the signal, a suitable gain should be applied to
17 undistorted signal such that the error signal becomes uncorrelated with the undistorted
18 signal (and the error vector could be abstracted as additive uncorrelated noise).
19

20 The effective transmit power is defined as the power of the distorted signal which is
21 correlated to the ideal signal (so that the power does not include either the error vector
22 or any extra energy for PAPR reduction).
23

24 The error vector power and effective transmit power are accumulated in linear domain
25 and their ratio is converted to dB. The EVM is accumulated over a single transmission
26 time interval. In case the EVM varies between different cases in the same transmission
27 mode (e.g. between different sub-channels), the 10% percentile shall be used.
28
29

Appendix K: TCP Modeling (Informative)

The widespread use of TCP as a transport protocol in the internet requires an accurate model of TCP behavior to better characterize traffic flow. The major behaviors that need to be accounted for in the TCP model are the session establishment and release and TCP slow start.

K-1. TCP Session Establishment and Release

TCP uses a 3-way handshake to establish and release a TCP session. The sequences of establishing and releasing a TCP session on the downlink and the uplink are shown in Figure 39 and Figure 40 respectively.

A TCP session is established by the transmitter sending a 40 byte SYNC control segment to the remote server. In response, the server sends a 40 byte SYNC/ACK control segment. The final acknowledgement is sent by the transmitter by setting the ACK flag in the first TCP segment of the TCP session, which is then started in slow start mode [60].

The TCP session is released by the transmitter setting the FIN flag in the last TCP segment. In response, the receiver sends by a FIN/ACK control segment. The session is concluded by the transmitter sending a final ACK message [60].

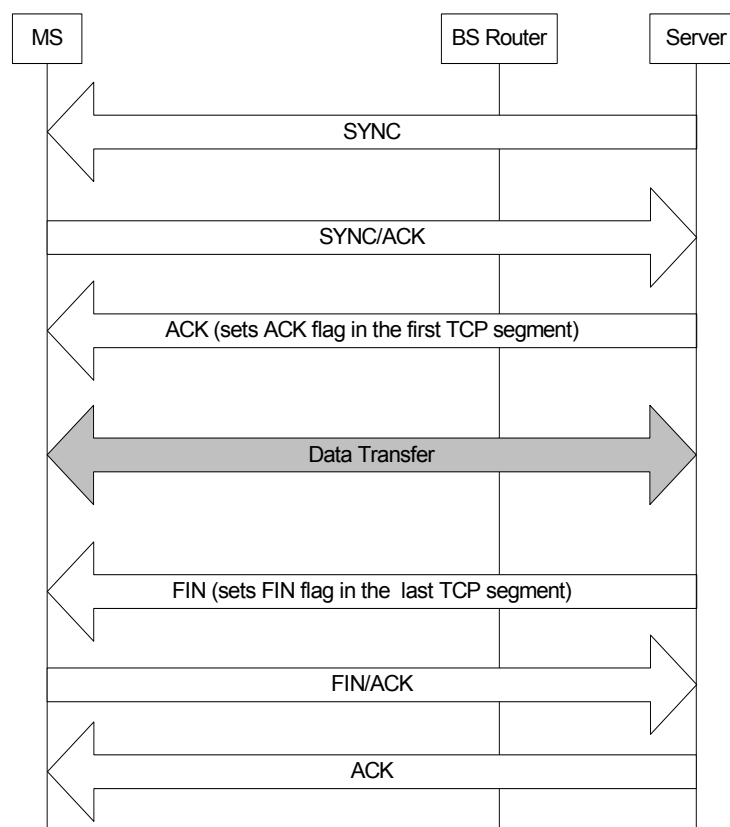


Figure 39: TCP connection establishment and release on the downlink

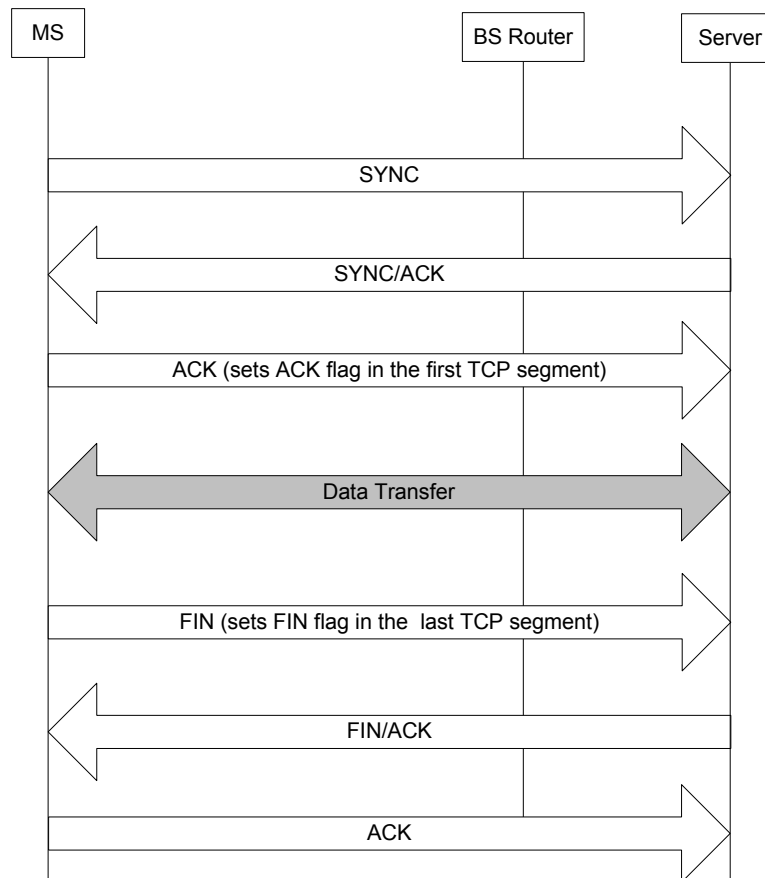


Figure 40: TCP connection establishment and release on the uplink

K-2. TCP Slow Start Modeling

TCP slow start is part of the congestion control mechanism implemented in the TCP protocol. Congestion control is implemented using a window flow control mechanism, which tracks the maximum amount of unacknowledged or outstanding data at the transmitter.

The amount of outstanding data that can be sent without receiving an acknowledgement (ACK) is determined by the minimum of the congestion window size and the receiver window size. After the TCP session is established, the transfer of data starts in slow-start mode with an initial congestion window size of 1 segment. The congestion window size is subsequently increased by one with each arriving ACK for a successfully received packet. This increase occurs regardless of whether the packet is correctly received or not, and regardless of whether the packet is out of order or not. This results in an exponential growth of the congestion window.

Figure 41 explains the packet transmission sequence in a TCP session. The round trip time (RTT) for the TCP slow start model consists of:

$$RTT = \tau_1 + \tau_2$$

1 where:

2
3 τ_1 : Time taken by an ACK packet to travel from the client (server) to Base Station +
4 Time taken by an ACK packet to travel from Base Station to server (client) + Time taken
5 by TCP segment to travel from server (client) to Base Station.
6

7 τ_2 : Time taken by ACK segment to travel from Base Station to Client (server).
8

9 τ_1 is assumed to be a random variable of exponential distribution, while τ_2 is
10 determined by the air link throughput. This model only accounts for the slow start
11 process, while congestion control and avoidance have not been modeled. Additionally,
12 the receiver window size is assumed to be large, and thus not a limiting factor.

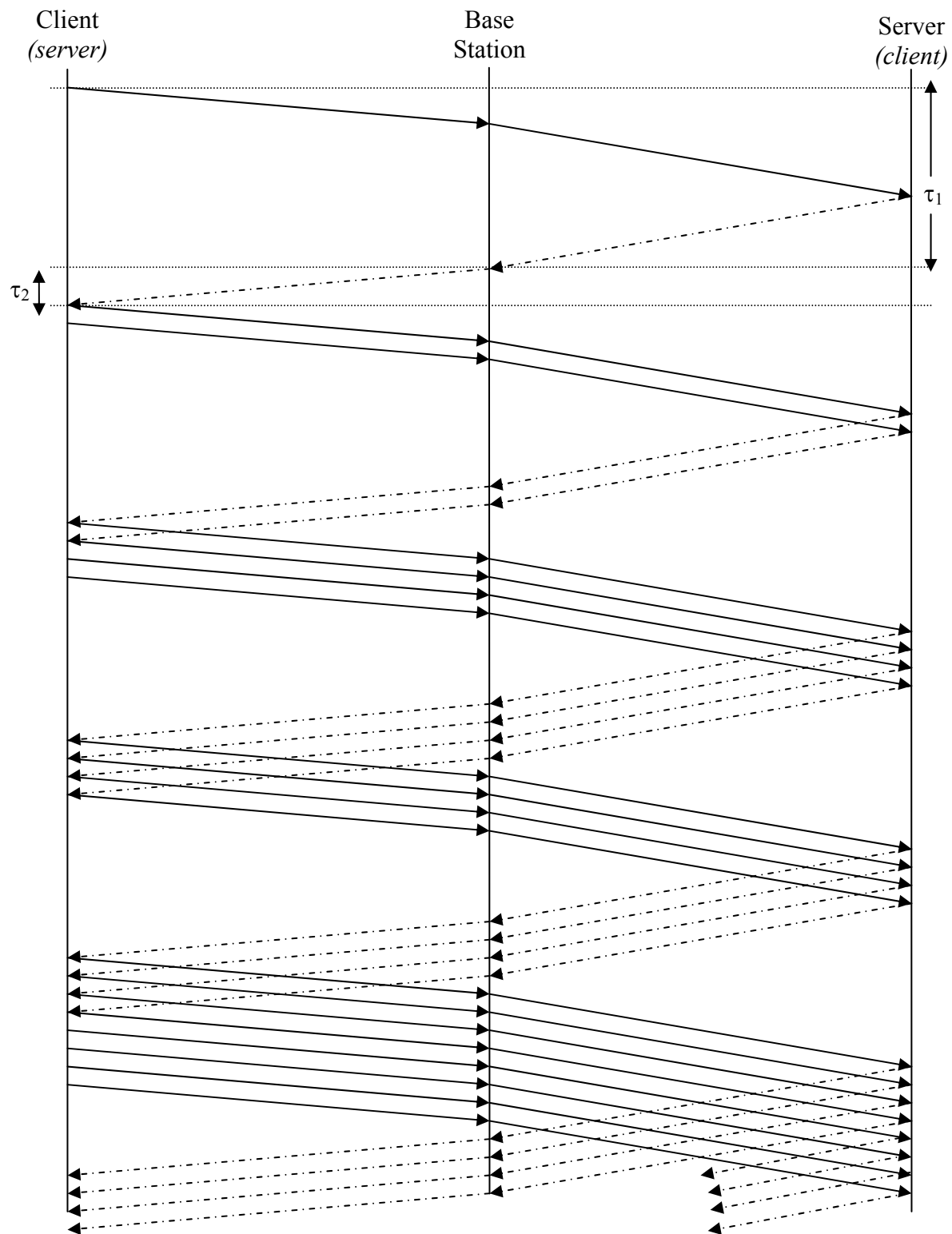


Figure 41: TCP slow start process

Appendix L: Trace Based Model for Streaming Video (Informative)

There is no silver bullet on the synthetic traffic generation for streaming video. Multiple analytical algorithms are proposed but no single reference algorithm is ideal for the task. Generally, long range dependency is recognized for the probability distributions of frame sizes. By using self-similar traffic generator, some of the characteristics of the streaming video traffic can be reproduced. However, the synthetic video traces generated by the analytical model are so different from the reference traces that it is difficult to convince people that synthetic traces have captured the core characteristics of the streaming video traffic.

Since streaming video traces are easy to obtain and they are easy to use in the simulation environment, a trace based streaming video traffic model is recommended. In this model, a set of 12 MPEG4 traces are selected from the ASU video library. They are representative of the typical mix supported in the network. Among the 12 traces, 6 of them are from the major movie genre, such as drama, action, SciFi, and cartoon; 2 of them are from major sport events; 1 is from MTV, 2 are from talk show with and without commercial, and 1 is from TV sitcom. For a simulation run, each user with video traffic is randomly assigned one video trace out of the 12 available traces. The first packet in the trace is not limited to the start of the trace but is picked at random. Starting from this packet, the trace should continue to evolve sequentially to the end and then wrap around from the beginning back to this starting point. The key characters of these streaming video traces are listed in Table 68.

MPEG4 Video Library*

	Name	Hurst Parameter	Mean Bit Rate (Kbps)	Quantization (I-P-B)	CBR/VBR
Movie					
1	Citizen Kane	0.84	52	30-30-30	VBR
2	Citizen Kane		128		CBR
3	Die Hard	0.72	70	30-30-30	VBR
4	Jurassic Park	0.61	78.5	24-24-24	VBR
5	Star War IV	0.78	65	24-24-24	VBR
6	Aladdin	0.86	91	30-30-30	VBR
Sports					
7	Football With Commercials	0.74	267.5	24-24-24	VBR
8	Baseball With Commercials	0.58	74.2	30-30-30	VBR
MTV					
9	MTV	0.85	212.4	24-24-24	VBR
Talk Show					
10	Tonight Show With Commercials (Jay Leno)	0.8	482	24-24-24	VBR
11	Tonight Show Without Commercials (Jay Leno)	0.93	55	24-24-24	VBR
Sitcom					
12	Friends vol4	0.77	53	24-24-24	VBR

* From ASU video library. URL: <http://trace.eas.asu.edu/>

Table 68: MPEG4 video library

- 1
- 2 A user is defined in outage for streaming video service if the 98th percentile video frame
- 3 delay is larger than 5 seconds. The system outage requirement is such that no more
- 4 than 2% of users can be in outage.

Appendix M: FCC Spectral Mask (Informative)

The following table specifies FCC spectral mask regulations for mobile stations taken from [62].

Frequency band	Maximum signal power	RBW
First 1 MHz from channel edge	-13 dBm/RBW,	1% of signal BW, for example 100 KHz for 10 MHz signal
1 MHz to 5.5 MHz from channel edge	-13 dBm/RBW	1 MHz
5.5 MHz or more from edge	-25 dBm/RBW	1 MHz

Table 69: FCC spectral mask

Appendix N: Per-tone Post Processing SINR for MISO and MIMO with CDD (Informative)

Cyclic delay diversity (CDD) is a technique that transforms spatial diversity into frequency diversity. The new effective CDD or composite channel frequency response that incorporates the physical channel gains $H_m^{(0)}(n)$ and the artificially induced frequency selectivity associated with a CDD cyclic shifts $e^{-j2\pi\delta_m/N}$ is given by

$$\tilde{H}^{(0)}(n) = \frac{1}{\sqrt{N_T}} \sum_{m=0}^{N_T-1} H_m^{(0)}(n) e^{-j2\pi\delta_m/N}$$

where $\delta_m = m$, $m = 0, 1, 2, \dots, N_T - 1$ is the delay applied to the m -th antenna, with $\delta_0 = 0$ is assumed to be the reference antenna in a CDD implementation.

For MISO (multi-input, single-output) and MIMO proposals with CDD implementations the effective CDD or composite channel gains should be used for per tone SINR computations. For example, the n -th tone post processing SINR for a MISO system with a CDD implementation may be defined as

$$SINR^{(0)}(n) = \frac{P_{tx}^{(0)} P_{loss}^{(0)} |\tilde{H}^{(0)}(n)|^2}{\sigma^2 + \sum_{j=1}^{N_T} P_{tx}^{(j)} P_{loss}^{(j)} |H^{(j)}(n)|^2}.$$

Appendix O: Updated HTTP Traffic Model (Informative)

Recent measurement and analysis for web page structures can be found in [75]. These measurements have been performed using a recent online-traffic analysis provided by market research firm ComScore Media Metrix, which examined the number of visitors among the top 50 Web sites on January 2007 [76]. The paper [75], includes web page sizes and compositions of the 50 top web sites after analyzing 25000 measurements, and each web site has been visited 500 times for three weeks from April 7 to April 23 in 2007. Web site visits are about one minute apart, and visits to the same website are about an hour apart. Table 70 provides the updated model parameters for HTTP traffic for downlink and uplink connections based on the measurements in [76] and the model in [48],[49].

Component	Distribution	Parameters		PDF
		Downlink	Uplink	
Main object size (SM)	Truncated Lognormal	Mean = 52390bytes SD= 49591bytes Min = 1290bytes Max = 0.25Mbytes $\sigma = 0.8, \mu = 10.55$	Mean = 9055 bytes SD = 13265 bytes Min = 100 bytes Max = 100 Kbytes $\sigma = 1.37, \mu = 8.35$	$f_x = \frac{1}{\sqrt{2\pi}\sigma x} \exp\left[-\frac{(\ln x - \mu)^2}{2\sigma^2}\right], x \geq 0$ if $x > \max$ or $x < \min$, discard and generate a new value for x
Embedded object size (SE)	Truncated Lognormal	Mean = 8551bytes SD = 59232bytes Min = 5bytes Max = 6Mbytes $\sigma = 1.97, \mu = 7.1$	Mean = 5958 bytes SD = 11376 bytes Min = 50 bytes Max = 100 Kbytes $\sigma = 1.69, \mu = 7.53$	$f_x = \frac{1}{\sqrt{2\pi}\sigma x} \exp\left[-\frac{(\ln x - \mu)^2}{2\sigma^2}\right], x \geq 0$ if $x > \max$ or $x < \min$, discard and generate a new value for x
Number of embedded objects per page (Nd)	Truncated Pareto	Mean = 51.1 Max. = 165 $\alpha = 1.1, k = 2, m = 55$	Mean = 4.229 Max. = 53 $\alpha = 1.1, k = 2, m = 55$	$f_x = \frac{\alpha k}{x^{\alpha+1}}, k \leq x < m$ $f_x = \left(\frac{k}{m}\right)^{\alpha}, x = m$ Subtract k from the generated random value to obtain Nd if $x > \max$, discard and regenerate a new value for x

Reading time (Dpc)	Exponential	Mean = 30 sec	Mean = 30 sec $\lambda = 0.033$	$f_x = \lambda e^{-\lambda x}, x \geq 0$
Parsing time (Tp)	Exponential	Mean = 0.13 sec	Mean = 0.13 sec $\lambda = 7.69$	$f_x = \lambda e^{-\lambda x}, x \geq 0$

Table 70: HTTP parameters for updated model.

Appendix P: Derivations and Details for RBIR Metric (Informative)

P-1. Derivation of the AVE and VAR for RBIR

Given the channel matrix $H = \begin{bmatrix} H_1 & H_2 \end{bmatrix} = \begin{bmatrix} h_{11} & h_{12} \\ h_{21} & h_{22} \end{bmatrix}$ and SNR for each sub-carrier, the LLR distribution parameter pair (AVE, VAR) can be obtained for MIMO SM 2x2 as specified below.

The mean of the LLR for the 1st stream is

$$AVE_1 = \frac{d^2(|h_{11}|^2 + |h_{21}|^2)}{\sigma^2} - E\{K_1\}$$

where 'd' indicates the minimum distance in QAM constellation, for example, QPSK: $d = \sqrt{2}$; 16QAM: $d = 2/\sqrt{10}$; 64QAM: $d = 2/\sqrt{42}$ and the mean $E\{K_1\}$ is defined by

$$E\{K_1\} = \int_{-\infty}^{\infty} \frac{1}{\sqrt{2\pi} \frac{d|H_1|}{\sigma}} e^{\frac{-x^2}{2d^2 \frac{|H_1|^2}{\sigma^2}}} \log_e \left(2e^{-x} + e^{\frac{-d^2|H_1|^2}{\sigma^2}} e^{-2x} \right) dx$$

where H_1 is the first column vector.

The variance of the LLR for the 1st stream can be written as

$$VAR_1 = E\{K_1^2\} - E^2[K_1]$$

where

$$E\{K_1^2\} = \int_{-\infty}^{\infty} \frac{1}{\sqrt{2\pi} \frac{d|H_1|}{\sigma}} e^{\frac{-x^2}{2d^2 \frac{|H_1|^2}{\sigma^2}}} [\log_e (2e^{-x} + e^{\frac{-d^2|H_1|^2}{\sigma^2}} e^{-2x})]^2 dx$$

From the above formulae the numerical integral results for (AVE, VAR) are shown in Table 26.

P-2. Search for the Optimal 'a' Value

The procedure used to obtain the parameter a [77] can be described as follows:

Step 1: From the AWGN SINR-to-BLER curve, calculate $SNR_{AWGN}(BLER)$ from the measured BLER.

Step 2: For a particular value of a , calculate the RBIR metric for a given channel matrix 'H' and SINR and then compute the effective SINR_{eff} value from the SINR to RBIR mapping in Table 26.

Step 3: Repeat the process over different values of a and choose the value of 'a' which results in the smallest gap over all values of BLER between the interpolated SNR (step 1) and effective SNR (step 2).

$$a = \min_a |SNR_{AWGN}(BLER) - SINR_{eff}(BLER)|^2$$

$\forall BLER$ and $\forall H$ which corresponding to a particular range of k and $\lambda_{min} dB$.

P-3. Search for the Optimal Values of p_1 and p_2

The procedure used to obtain the parameter p_1 and p_2 [77] can be described as follows:

Step 1: From the AWGN SINR-to-BLER curve, calculate the $SINR_{AWGN}(BLER)$ from the measured BLER.

Step 2: Calculate the corresponding RBIR metric over the two streams for a given channel matrix 'H', SINR and parameter 'a' determined from Table 27.

Step 3: Calculate the average RBIR metric as a weighted sum of ' p_1 ' and ' p_2 ' and then calculate the effective $SINR_{eff}$ value using the averaged RBIR from the SINR to RBIR mapping in Table 25.

Step 4: Find the parameters p_1 and p_2 which result in the smallest gap over all values of BLER between the interpolated SINR (step 1) and effective SNR (step 3).

$$p = \min_{(p_1, p_2)} |SINR_{AWGN}(BLER) - SINR_{eff}(BLER)|^2$$

$\forall BLER$ and $\forall H$ which belongs to a particular range of k and $\lambda_{min} dB$.

Note that the search for parameters p_1 and p_2 can be simplified by setting $p_1 + p_2 = 1$.